(12)

ARL-AERO-REPORT-157

AR-002-925

DEPARTMENT OF DEFENCE SUPPORT

DEFENCE SCIENCE AND TECHNOLOGY ORGANISATION

AERONAUTICAL RESEARCH LABORATORIES

MELBOURNE, VICTORIA

AERODYNAMICS REPORT 157

POWER EFFECTS ON THE LONGITUDINAL CHARACTERISTICS OF SINGLE-ENGINE PROPELLER-DRIVEN AIRCRAFT

by

C. A. MARTIN

Approved for Public Release

FEBRUARY 1983

AR-002-925

DEPARTMENT OF DEFENCE SUPPORT
DEFENCE SCIENCE AND TECHNOLOGY ORGANISATION
AERONAUTICAL RESEARC LABORATORIES

AERODYNAMICS REPORT 157

POWER EFFECTS ON THE LONGITUDINAL CHARACTERISTICS OF SINGLE-ENGINE PROPELLER-DRIVEN AIRCRAFT

by

C. A. MARTIN

SUMMARY

The effects of power on the longitudinal flying qualities of a single-engine propeller-driven aircraft have been investigated. The net effect is developed as the resultant of six major contributions which, in this study, have been estimated from the USAF Stability and Control Datcom. These contributions are not independent and in general are non-linear functions of both incidence and speed. It is shown that the effect on stability of the incidence-dependent terms is conveniently described by the neutral point (h_n) while the combined incidence and speed terms can be described by the static stability limit. (h_s). The effects of each power contribution on the longitudinal static and dynamic characteristics of a basic aircraft layout, termed the "standard case", have been illustrated both individually and collectively. The influence of aircraft layout and configuration has also been demonstrated with both power-off and power-on. It is shown that net power effects are sensitive to aircraft layout and can change appreciably when flaps are deflected. An instability is demonstrated which is due to power and flap effects and which is almost independent of c.g. position. The power effects for an aircraft layout typical of modern designs are also illustrated. The study is completed by a survey of research on propeller power effects which draws attention to the large amount of wind tunnel research which has been carried out from the early days of powered flight. The sources of many of the estimation methods in Datcom are identified and discussed. From the survey and from the information presented in this Report it is concluded that there exists a need for more robust theoretical and numerical design methods for most of the power effects considered and also for more comprehensive wind tunnel and flight test data regarding the effect of slipstream on tailplane lift.

POSTAL ADDRESS: Director, Aeronautical Research Laboratories,
Box 4331, P.O., Melbourne, Victoria, 3001, Australia

CONTENTS

Page No.

NOTATION

1. INTRODUCTION 1

2. LONGITUDINAL FLYING QUALITIES 2

3. METHOD OF ANALYSIS 4

4. SMALL ANGLE ASSUMPTION 10

5. DISCUSSION OF THE EFFECTS OF POWER ON LONGITUDINAL STABILITY 10

5.1 Thrust Coefficient 12

5.2 Propeller Axial Force 14

5.3 Propeller Normal Force 14

5.4 Effect of a Running Propeller on Wing–Body Aerodynamic Characteristics 17

5.5 Effect of Power on Downwash at the Tailplane 23

5.6 Effect of Power on Dynamic Pressure at the Tailplane 28

5.7 Combined Power Effects 31

6. EFFECT OF POWER ON LONGITUDINAL STABILITY WITH CHANGES IN AIRCRAFT LAYOUT AND CONFIGURATION 31

6.1 Thrust Axis Setting Angle and Vertical Position 31

6.2 Wing Setting Angle and Vertical Position 35

6.3 Tailplane Vertical and Longitudinal Position 49

6.4 Effect of Flap Deflection 56

7. EFFECT OF POWER ON "CONTROLS FREE STABILITY" 65

8. EFFECT OF POWER ON LONGITUDINAL "MANOEUVRABILITY", DYNAMIC MODES, AND RESPONSE TO CONTROLS 72

8.1 Longitudinal "Manoeuvrability" 72

8.2 Longitudinal Dynamic Modes 73

8.3 Longitudinal Response to Controls 77

9. POWER EFFECTS ON A SINGLE-ENGINE PROPELLER-DRIVEN AIRCRAFT WITH TYPICAL LAYOUT 82

10. REVIEW OF RESEARCH ON THE EFFECTS OF POWER ON PROPELLER-DRIVEN AIRCRAFT 96

11. CONCLUSIONS 98

REFERENCES

DISTRIBUTION

DOCUMENT CONTROL DATA

LIST OF TABLES

1. Details of Aircraft Design from Reference 9.

2. Typical Aircraft Thrust Coefficients

3. Breakdown of Wing–Body Contributions for $C_L = 0{\cdot}8$.

LIST OF FIGURES

1. Aircraft Layout from Reference 9.
2. "Standard Case" Aircraft Layout and Details of Single-Slotted Flap
3. Example of Slipstream Location Plots (Maximum Power)
4. Approximation Due to the Small Angle Assumption
5. C_T *v.* C_L
6. γ *v.* V
7. Effect of Propeller Axial Force
8. Effect of Propeller Normal Force
9. Effect of Power on Wing–Body C_{m_0}
10. Effect of Power on Wing–Body Lift and Pitching Moment
11. Effect of Power on Downwash
12. Effect of Power on Dynamic Pressure at the Tail
13. Combined Power Effects for the "Standard Case"
14. Accumulation of Power Effects on h_s and h_n "Standard Case"
15. Effect of Thrust Axis Setting and Vertical Position (Power On)
16. Accumulation of Power Effects on h_s and h_n—Thrust Axis—5 deg
17. Accumulation of Power Effects on h_s and h_n—Raised Thrust Axis
18. Effect of Wing Setting Angle (Power Off)
19. Effect of Wing Setting Angle (Power On)
20. Effect of Wing Vertical Position (Power Off)
21. Effect of Wing Vertical Position (Power On)
22. Effect of Tailplane Vertical Position (Power Off)
23. Effect of Tailplane Vertical Position (Power On)
24. Effect of Tail Vertical Position on Static Stability Limit
25. Accumulation of Power Effects, High Tail Position
26. Effect of Tail Longitudinal Position: Tail Volume Coefficient ($\bar{V}$) Constant, Power Off
27. Effect of Tail Longitudinal Position: Tail Volume Coefficient ($\bar{V}$) Constant, Power On
28. Effect of Tail Longitudinal Position: Tail Volume Coefficient ($\bar{V}$) Varying, Power Off
29. Effect of Tail Longitudinal Position: Tail Volume Coefficient ($\bar{V}$) Varying, Power On
30. Effect of 20 deg Flap Deflection, Power Off
31. Effect of 20 deg. Flap Deflection, Power On
32. Effect of Power on h_s for Controls Fixed and Free
33. Control Force per g: "Standard Case"

34. Control Force per g: Thrust Axis Inclined—5 deg.
35. Control Force per g: Flaps 20 deg.
36. Effect of Power on Longitudinal Dynamic Modes: Root Locus Plots—"Standard Case"
37. Effect of Power on Longitudinal Dynamic Modes: Root Locus Plots—"Flaps 20 deg."
38. Short Period Frequency Requirement, "Standard Case"
39. Short Period Frequency Requirements, "Flaps 20 deg."
40. Trim and Stability Characteristics for a Typical Aircraft Layout, Power Off
41. Trim and Stability Characteristics for a Typical Aircraft Layout, Power On
42. Trim and Stability Characteristics for a Typical Aircraft Layout, Power Off, Flaps 20 deg.
43. Trim and Stability Characteristics for a Typical Aircraft Layout, Power On, Flaps 20 deg.
44. Control Force per g: Typical Aircraft Layout, Flaps Zero
45. Control Force per g: Typical Aircraft Layout, Flaps 20 deg.
46. Effect of Power and Flaps on Longitudinal Dynamic Modes: Root Locus Plots
47. Short Period Characteristics: Typical Aircraft Layout
48. Trim Characteristics: Comparison with Flight Tests

NOTATION

b	Wing span, m
C_L	Lift coefficient
C_D	Drag coefficient
C_m	Pitching moment coefficient
C_{m_0}	Zero lift pitching moment coefficient
C_{n_p}	Propeller normal force coefficient
C_{L_e}	Equilibrium lift coefficient
C_T	Thrust coefficient based on wing area
C_H	Hinge moment coefficient
C_{L_J}	Derivative of coefficient C_L, w.r.t. J
$\bar{c}$	Mean aerodynamic chord (MAC), m
C_{δ_e}	Elevator chord, m
c.g.	Centre of gravity
D_p	Propeller diameter, m
g	Normal acceleration in gravitational units
G_{δ_e}	Elevator control gearing, rad/m
h_n	Neutral point
h_0	Static stability limit
l_T	Distance between wing and tailplane aerodynamic centres, m
N	Engine speed, rpm
n_z	Normal acceleration, g
n/α	Ratio of normal acceleration to incidence
n	Real part of complex number
P	Engine power, kW
P_{δ_e}	Elevator control force, N
P_L	Power lever setting
q	Pitch rate, rad/s
$\dot{q}_0$	Initial pitch acceleration, rad/s/s
S_w	Wing area, m²
S_p	Propeller disc area, m²
S_{δ_e}	Elevator area, m²
T	Thrust

T_C	Thrust coefficient based on propeller diameter
V	Aircraft flight path velocity, m/s
$\bar{V}$	Horizontal tail volume coefficient
W	Aircraft weight, N
x_p	Distance of propeller from aircraft c.g., m
α	Incidence angle, deg
γ	Flight path angle, deg
Γ	Dihedral angle, deg
δ_e	Elevator angle, deg
δ_t	Elevator tab angle, deg
ϵ	Downwash angle, deg
ϵ_p	Propeller downwash angle, deg
θ	Aircraft pitch attitude
η_p	Propeller efficiency
μ_1	Relative density parameter
ρ	Density of air, kg/m^3
$\omega_{n_{sp}}$	Short period frequency, rad/s
ω	Imaginary part of complex number
Suffixes	
T	Tailplane
F	Flaps
SS	Steady state
TH	Thrust
p	Propeller

1. INTRODUCTION

In this Report the effects of power on the longitudinal characteristics of single-engine propeller-driven aircraft are discussed. This topic is of interest in Australia because of the current development by the Australian aircraft industry of a basic trainer aircraft for the RAAF.

Two important phases in the study of aircraft flight dynamics are: firstly, the estimation of aerodynamic data from theoretical, empirical, wind-tunnel and flight-test sources and, secondly, the representation and interpretation of the calculated static and dynamic characteristics in terms of flying quality parameters which can be related to pilot opinion. These two phases are given particular emphasis in this Report. While the general nature of the power effects due to propellers is well known, and the net effect is known from flight measurements, there are still significant deficiencies in the accuracy of theoretical and empirical design methods. Very little published information exists on the way individual power effects accumulate to alter flying qualities for different aircraft layouts and configurations, even though the net effects may be known for particular aircraft.

In the first part of this Report, the numerous effects of power are described. The effects of aircraft layout and configuration are then discussed, both with power on and with power off. With these descriptions as a background a survey of research literature of propeller power effects is presented.

In recent years there has been a design trend towards more highly powered propeller-driven aircraft for basic military trainers, STOL transports and for fuel-efficient multi-engined transports. The trend to highly-powered basic trainer aircraft arises from the need to extend the training capability of primary trainers and also because of the attraction of fitting gas turbine engines; currently the available gas turbine engines are more powerful than alternative piston engines. An increase in the power-to-weight ratio of propeller-driven aircraft introduces handling problems similar to those exhibited by military aircraft built during the 1940s; many of those aircraft would not have satisfied current Flying Qualities Requirements.

During the 1940s a considerable amount of wind tunnel research was carried out in the UK and the USA on the effects of power on longitudinal stability. Much of this work forms the basis of current design estimation techniques, which have undergone little change since that time. Reference 1 draws attention to the lack of reliable theoretical and empirical design information for the estimation of power effects, and the need for powered-model testing to give results with engineering precision for new configurations. Even with the benefit of wind tunnel measurements, there are numerous examples of low-speed propeller-driven aircraft which have required substantial design changes, or the installation of mechanical devices such as downsprings and bobweights during flight test development, to achieve the desired design centre of gravity range and control force characteristics.

Major obstacles to the development and validation of reliable design estimation techniques are firstly, the complexity of the problem, and secondly the sensitivity of the effects of power to small changes in aircraft layout such as engine, wing and tail location. With the development of computational methods for the analysis of fluid dynamic problems of increasing complexity, the establishment of more rigorous estimation techniques can be foreseen. The survey of propeller power effects indicates that the most complete set of design estimation methods for application to conventional low-speed aircraft is contained in Datcom [Ref. 6]. These methods have been used in this Report for calculating the various effects of power on longitudinal flying qualities. The research background to the methods is discussed more fully in the review of research on the effects of power on propeller driven aircraft in Section 10.

The dynamic motion of an aircraft can be summarised in terms of performance and flying qualities parameters. For conventional low-speed, propeller-driven aircraft, satisfactory longitudinal flying qualities have generally resulted if the "static stability" requirements have been met. Consequently the topic of "static stability" including both its estimation at the design

stage, and its measurement during the flight development stage, has always been a major consideration. Furthermore, while a number of advanced methods of flight test analysis are now available, which enable the general motion of an aircraft to be described, it is still necessary, for the purpose of aircraft certification, to demonstrate stability using the "static stability" approach. The direct measurement of "trim curves" and the derivation of neutral points and static stability limits can also provide useful additional information about the longitudinal aerodynamic characteristics. Unfortunately, the analysis of trim curves can be limited, firstly by poor measurements due either to inaccurate instrumentation or to poor test technique, and secondly by deficiencies in the interpretation of results. Methods for the measurement of "static stability" are well documented in flight test manuals and in textbooks on flight mechanics. In some cases, the effects of configuration, compressibility, aeroelasticity, control system mechanical properties, and propulsion are described (e.g. Ref. 5). However, these descriptions are often quite general and not quantitative, and they are usually limited in detail. In this Report the particular effects of propulsion and configuration, for the case of a single-engine, propeller-driven aircraft are addressed. The remaining effects listed above are assumed to be absent. This is a reasonable assumption since compressibility and aeroelastic effects become significant at high speeds, where power effects are diminishing.

The concept of neutral points and of static stability limits within the theory of "static stability" provide a concise way of representing the effects of numerous contributions to longitudinal stability. However, the inclusion of power effects introduces terms which are, in general, non-linear and mutually interfering, and so the solution of the longitudinal trim equations no longer has a closed form. Therefore an iterative procedure has been used on a digital computer to solve the trim equations for steady rectilinear and steady turning flight and also to calculate flying qualities parameters. The flying qualities which are important in addition to "static stability" are the control force and deflection per g, longitudinal short period and long period characteristics, and control response parameters. These parameters are discussed in more detail in Section 2. In Sections 3 and 4 the method of analysis and the assumptions involved are discussed. In Sections 5 to 9 calculations are presented to demonstrate the influence of power effects both individually and collectively on aircraft trim in steady rectilinear and steady turning flight and on longitudinal flying qualities parameters. The effect of changes in aircraft layout and configuration are also demonstrated. In Section 10 a survey of research literature on propeller power effects is presented and the limitations of current theoretical and empirical design methods are indicated. Throughout the text the terms "aircraft velocity" or "velocity" and the term "speed" are all used to describe the aircraft velocity along the flight path. Following common usage, the choice of name is generally determined by the context of the discussion. For example, when reference is made to aerodynamic effects, the term "aircraft velocity" is generally used, and when reference is made to aircraft operations the term "speed" is generally used.

2. LONGITUDINAL FLYING QUALITIES

In the study of aircraft longitudinal flying qualities, the topic of "static stability" has always played a major role. The main reasons for this are: Firstly, "static stability" is strongly affected by changes in aircraft c.g. position; it is, therefore, a major consideration in determining the aircraft c.g. range. Secondly, for many low-speed aircraft with conventional layouts, compliance with the "static stability" requirement has produced satisfactory characteristics for most other longitudinal flying qualities.

The theory of "static stability" was first presented in Reference 2 in 1911 and is covered in detail in most textbooks dealing with flight dynamics. In its most usual form, the theory makes quite a number of assumptions in describing the longitudinal aerodynamic forces and moments acting upon an aircraft, but produces the very useful criterion that the longitudinal motion will be stable providing that the pitch stiffness term $(-C_{m_\alpha})$ is positive. Since the criterion relates to a term which is independent of motion, it has traditionally been called *static* stability. To emphasise this special qualification of stability, the term "static stability" will be enclosed in quotation marks within this Report. The theory also gives the result that pitch stiffness is a direct function

of the difference between the aircraft longitudinal c.g. position and a longitudinal position termed the neutral point (h_n), where

$$C_{m_\alpha} = C_{L_\alpha}(h - h_n). \tag{1}$$

According to this definition, when the c.g. is at the neutral point, the pitch stiffness will be zero and the aircraft will have neutral stability. Furthermore, the theory shows (e.g. Ref. 1) that, if flight measurements are made of the elevator angle (δ_e) required for trim in rectilinear flight at a series of aircraft lift coefficients (C_L), then the variation of δ_e with C_L will be proportional to the pitch stiffness. Consequently, the c.g. position giving $(d\delta_e/dC_L) = 0$ defines the aircraft neutral point (h_n). This is a very practical method for determining the neutral point from flight measurements and has provided a basis for establishing stability requirements in aircraft specifications.

For many aircraft the assumptions made in the simple theory of "static stability" cannot be supported. In particular, when compressibility, aeroelasticity and propulsion effects are significant, the "static stability" requirement for positive pitch stiffness cannot be regarded as a sufficient or a necessary condition for stability. In this more general case, the forces and moments acting on the aircraft in rectilinear flight can be non-linear functions of both the state variables, incidence (α) and velocity (V). In the simple theory, V is only a scaling factor which disappears when the equations are non dimensionalised. To describe this more general case, the extended theory of "static stability" was developed in Reference 3 in which additional velocity parameters were introduced. Reference 1 presents an alternative approach which is particularly useful for the analysis of flight results and which can be related directly to the coefficients of the general equations of unsteady motion. In this approach it is shown that the variation of elevator angle for trim with speed ($d\delta_e/dV$) is a true criterion for stability in the more general case. The c.g. position for $(d\delta_e/dV) = 0$ gives neutral stability and is called the static stability limit (h_s). When the aerodynamic forces are taken as linear functions of the state variables V and α, h_s is related to the neutral point (h_n) by:

$$h_s = h_n + \frac{C_{m_V}}{C_{L_V} + 2C_{L_e}}. \tag{2}$$

In most cases C_{m_α} is the major contribution to h_s and, because of its importance, it has been attributed the name "pitch stiffness" in Reference 1. The speed derivatives $C_{m_V} = \partial C_m/\partial V$, and $C_{L_V} = \partial C_L/\partial V$, which account for the difference between h_s and h_n, generally have a much smaller influence. The requirement for positive $(d\delta_e/dV)$, that is, increasing downward elevator for trim with increasing speed, is an important flying qualities criterion in current Airworthiness Specifications.

Because the presence of power introduces lift and pitching moment terms which are, in general, non-linear functions of the motion state variables incidence (α) and velocity (V), the use of linear methods of analysis introduces an approximation. However, the magnitude of the non-linearities is, in general, small unless very large amplitude motion is considered. Therefore for small disturbances about the trim condition, linear stability analysis, and the static stability limit concept are considered to be applicable.

It is conventional practice in the analysis of flight measurements to interpret trim and stability changes from plots of δ_e v. C_L rather than δ_e v. V since, in the absence of velocity-dependent and non-linear aerodynamic terms, the plots v. C_L are linear while those against speed are parabolic. These plots are commonly referred to as "trim curves". When these restricted assumptions do not hold, it is still more convenient to use C_L for the abscissa, since the non-linear effects can readily be observed as non-linearities in the "trim curves", and the curves are still good, if not absolute, indicators of stability; furthermore the trim capability of the elevator is still clearly evident from the curves. The interpretation of "trim curves" is an important analytical technique used during flight test development. It is, therefore, a major objective of this Report to present the various effects of power in a manner which will assist this interpretation.

The theory of "manoeuvrability" which is often closely associated with "static stability", concerns the aircraft trim conditions in steady trims or in a steady pull-up. Again quotation marks are used to indicate this restricted use of the term manoeuvrability. The additional aerodynamic terms to consider are those due to pitch rate which, for a conventional aircraft, are mainly due to an increase in local incidence at the tail. The manoeuvres are assumed to occur at constant velocity and the main flying qualities parameters of interest are the elevator control

force and elevator control angle per g. The effect of engine power on these parameters has been determined in this Report and is displayed with the trim information for rectilinear flight. These results are discussed in detail in Section 8.

For a stable conventional aircraft layout, the unsteady longitudinal motion following a disturbance is the sum of two oscillatory modes, the phugoid and the short period mode. The frequency and damping of these modes are required by Flying Qualities Specifications to lie within given ranges. Values for these parameters have been determined assuming a linear variation of the lift and pitching moment with the longitudinal state variables V, α, q and θ at each trim condition. The effect of power on these parameters is calculated and is discussed in Section 8.

For an aircraft to possess good longitudinal flying qualities, it is also necessary for the unsteady response to pilot control inputs to have specific characteristics. A number of handling qualities parameters have been proposed as measures of control response. In Reference 4, the ratio of normal acceleration to incidence change (n_z/α), calculated for the response when steady, is used as well as the ratio of initial pitch acceleration to steady state normal acceleration $(\dot{q}_0/n_{z_{ss}}) \equiv (\omega_n{}^2{}_{sp}/n_{z_\alpha})$. The left-hand side of the equivalence expression, which is developed in Reference 1, is often called the control anticipation parameter (CAP). For aircraft with manual controls, the ratio of initial control force to steady normal acceleration $P_{\delta_e}(0)/n_{z_{ss}}$ is also an important characteristic, as discussed in Reference 17. This parameter should be included in the consideration of longitudinal response. However, such considerations are outside the scope of this Report.

3. METHOD OF ANALYSIS

A considerable amount of computation is required to determine the flying qualities parameters described in Section 2 for a range of power effects and flight conditions with different aircraft layouts. For this purpose, the general unsteady equations of motion of an aircraft have been programmed on a digital computer. The program is capable of providing the following information:

(*a*) trim conditions in steady rectilinear flight with either constant engine power or power for level flight;

(*b*) trim conditions in steady turns;

(*c*) position of the neutral point (h_n) controls fixed and controls free;

(*d*) position of the static stability limit (h_s) controls fixed and controls free;

(*e*) elevator control deflection and elevator control force per g in steady turns;

(*f*) natural frequency, damping and eigenvalues for the longitudinal modes of motion;

(*g*) flying qualities parameters n_z/α and $(\dot{q}_0/n_{z_{ss}})$;

(*h*) diagram of the propeller slipstream location in relation to aircraft geometry;

(*i*) time histories of aircraft response to controls.

To facilitate program development, individual contributions to the forces and moments acting on the aircraft are calculated in separate subroutines. The aerodynamic information is derived either from empirical design estimates using the methods of Reference 6 or, if available, from wind tunnel or flight test measurements. Performance characteristics for a propeller in take-off, climbing, and cruising conditions have been represented from the charts given in Reference 7. The empirical methods given in Reference 6 are used to estimate the effects of power on lift, drag and pitching moment. Selections can be made to allow the individual power effects to be included separately or in any combination. Calculation of the propeller slipstream locus follows the approach used in Reference 6. The slipstream is assumed to be cylindrical with diameter equal to the propeller diameter; that is, neither contraction of the slipstream nor distortion due to the body or wing is represented. The accuracy of this level of representation is not indicated in Reference 6 and would be difficult to establish from available information.

Trimming of the equations of motion in steady level or steady turning flight is performed by the subroutine POWIT. This procedure is described in Reference 8 and is an application of Powell's "direct search" method for the solution of non-linear algebraic equations. The Newton–Raphson minimisation method is used to determine the static stability limit (h_s) and the neutral

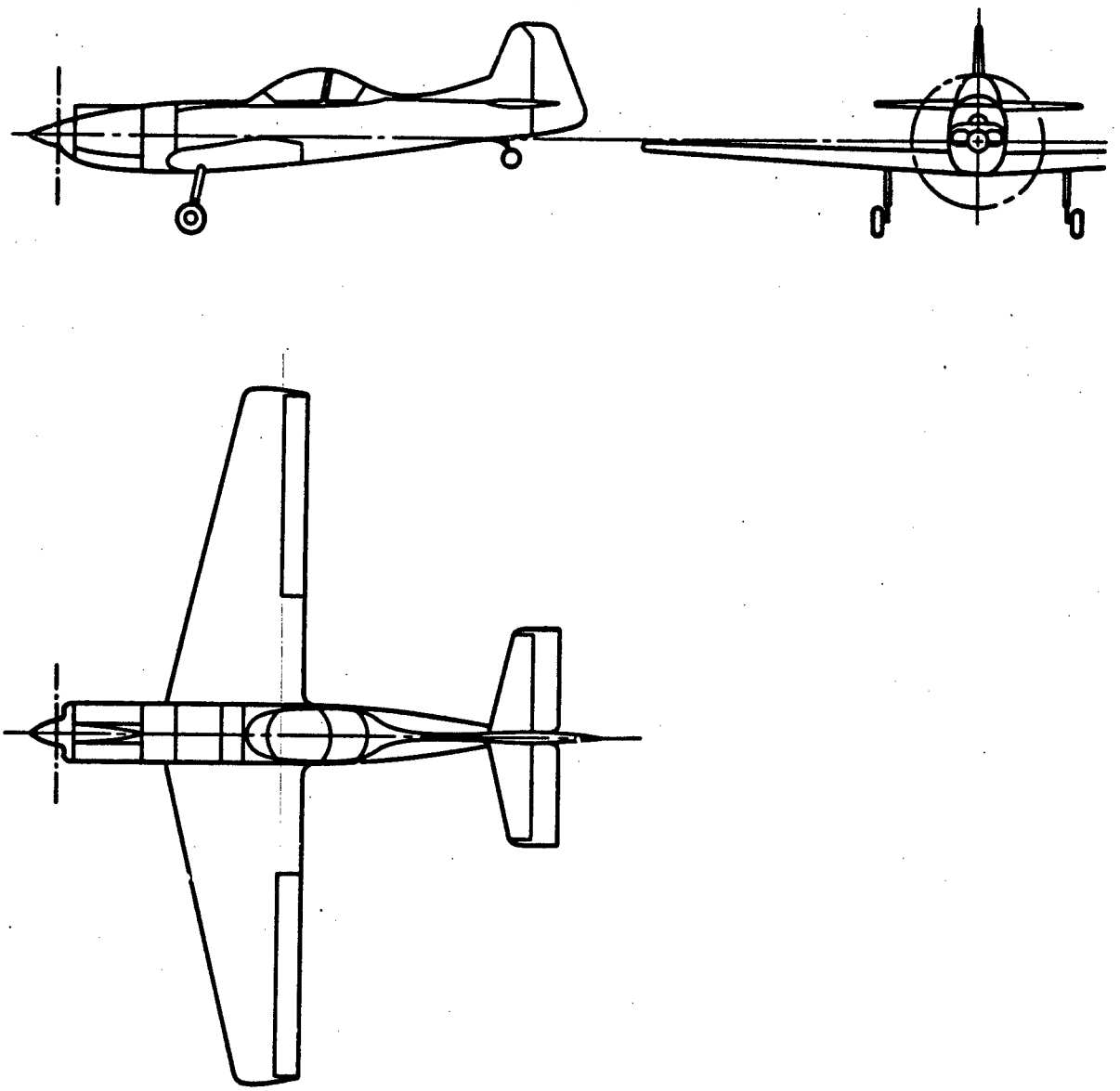

FIG. 1 AIRCRAFT LAYOUT FROM REF. 9

point (h_n) according to the requirements for $(d\delta_e/dV) = 0$ and $(dC_m/d\alpha) = 0$ respectively. The corresponding control free values are determined from the requirements for $(d\delta_t/dV) = 0$ and $(dC_m/d\alpha)\delta_{e,\text{FREE}} = 0$ respectively.

Dynamic mode characteristics are determined using the linear small disturbance non-dimensional longitudinal equations (5.13.19) of Reference 1. The aerodynamic derivatives depending upon α and V are determined numerically by assuming local linear variation about the trim points using the full set of dynamic equations.

The aircraft design used for the study of power effects is shown in Figure 1 and geometric details are given in Table 1. This design was selected because of its moderately high power-to-weight ratio and because aerodynamic design estimates are available in Reference 9, and flight measured data are available in Reference 10. For the investigation a base line layout shown in Figure 2*a* was defined and termed the "standard case". This differs from the aircraft in Reference 9 in that the thrust axis is set at zero degrees to the aircraft horizontal reference line and the engine, wing and tailplane are all located on the horizontal reference line. All power-on results presented in the Report are based on a power of 156 kW and an aircraft mass of 1250 kg. This gives a mass-to-power ratio of 8 kg/kW (13 lb/hp) and a wing loading of 819 N/m² (17·1 lbf/ft²). As shown in Table 2, the associated thrust coefficient (C_T) at $C_L = 1{\cdot}0$ is comparable with, though slightly lower than, the other aircraft listed, and the wing loading approaches that of current military training aircraft.

TABLE 1

Details of Aircraft Design from Reference 9

Wing: Span	10 m
Area	15 m²
Aspect ratio	6·7
Mean aerodynamic chord (MAC)	1·57 m
Tail: Span	3·11 m
Area	2·72 m²
Arm	4·33 m
Fin: Area	2 m²
Arm	4·31 m
A.U.W.	866 kg f
c.g. (typical aerobatic configuration)	26·3%MAC
Inertias: Pitch	2466 kg/m²
Roll	1355 kg/m²
Yaw	3586 kg/m²

The "standard case" layout is used to illustrate the individual effects of power and also the following effects of changing aircraft layout both with power on and power off:

(*a*) thrust axis setting angle and vertical position;

(*b*) wing setting angle and vertical position;

(*c*) tailplane vertical and longitudinal position;

(*d*) flap deflections of 0 and 20 deg.

The aircraft of Reference 9 did not possess wing flaps and so for the purpose of this study, the single slotted flap shown in Figure 2*b* was defined. Its aerodynamic characteristics were determined from Reference 6 for deflections of 0 and 20 deg.

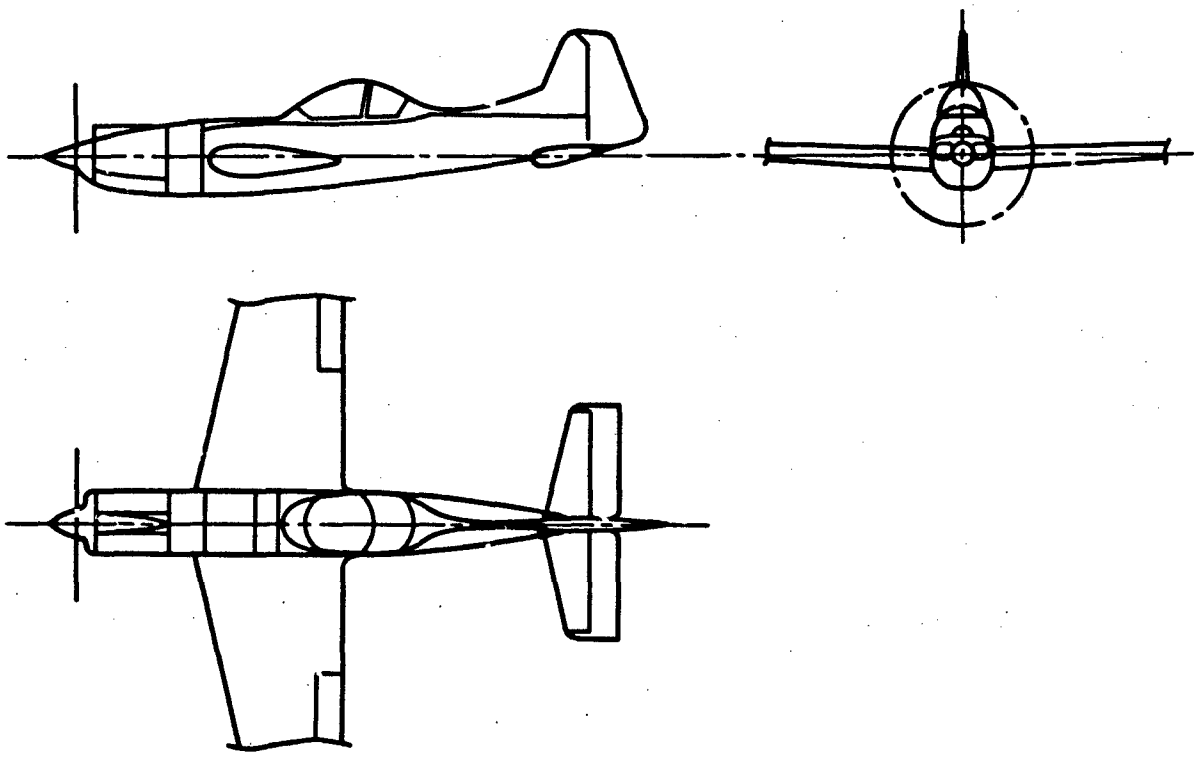

FIG. 2(a) 'STANDARD CASE' AIRCRAFT LAYOUT

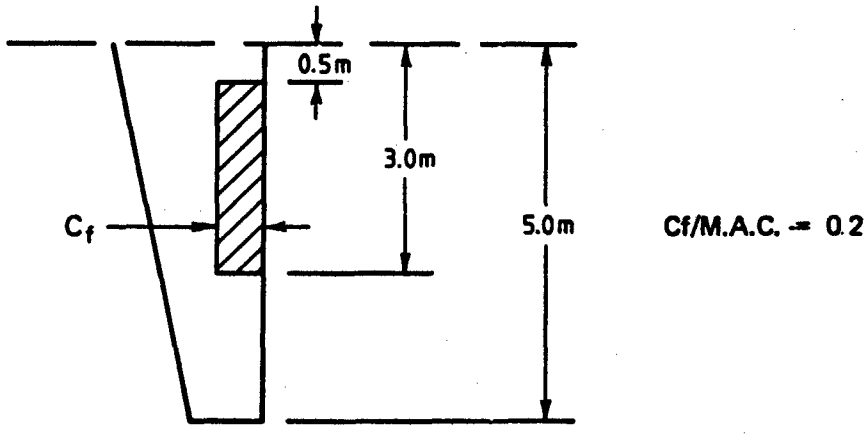

FIG. 2(b) DETAILS OF SINLGE-SLOTTED FLAP

TABLE 2

Typical Aircraft Thrust Coefficients

$T_C = T/\rho V^2 D_p^2$ (Equation (4)); $C_T = T/\frac{1}{2}\rho V^2 S_w$ (Equation (3))
Thrust is calculated assuming a propeller efficiency of 0·6 at low speeds.

Aircraft	Weight	Power	Wing loading	Power loading	Values at $C_L = 1{\cdot}0$		
	(lb.f) (kg.)	(hp) (kW)	(lb.f/ft²) (N/m²)	(lb.f/hp) (N/kW)	V (kn)	T_C	C_T
Tempest	13250 6010	2520 1879	44·00 2107	5·26 31·00	113	0·30	0·33
Spitfire	9950 4513	1490 1111	41 1963	6·67 40·00	110	0·19	0·27
Hurricane	7014 3181	1185 883	27·2 1302	5·91 35·30	89	0·30	0·37
P-40K	7740 3510	1000 745·7	32·0 1532	7·74 46·20	97	0·25	0·26
A1 [Ref. 10]	1950 884	210 156	12·1 580	9·30 55·50	60	0·73	0·35
Modern military trainer	4409 2000	550 410	20·5 981	8·02 47·90	78	0·60	0·31
"Standard case" aircraft (this Report)	2756 1250	210 156	17·1 819	13·10 78·10	71	0·44	0·21

The effects of power for an aircraft layout typical of modern designs have also been calculated and these are discussed separately in Section 9.

To aid comparisons between different power effects and different aircraft layouts, a standard presentation has been adopted. Trim and stability characteristics have been calculated at a series of speeds for c.g. positions of 25·1%$\bar{c}$ (forward c.g.), 32·3%$\bar{c}$ (mid c.g.) and 39·6%$\bar{c}$ (aft c.g.). The aft c.g. coincides with power-off values for h_0 and h_n assuming a linear model, and the forward c.g. is chosen to give an elevator trim range with power off, of 10 deg.

The presentation of trim characteristics is typical of that used in the flight technique for the determinations of "static stability" and so discrete data points are plotted. However, the results are theoretical values and do not contain any errors other than those associated with the resolution selected for the trimming and minimisation algorithms and those associated with the graphical representation of basic data charts.

Solid lines are used in the presentation for the characteristics of the "standard case" layout with power off and propeller stopped. In this case, the aerodynamic characteristics are linear and the results are calculated using the simple theory of "static stability" and the small angle approximation.

Manoeuvre characteristics are shown, firstly, as plots of control force *v.* g, to illustrate the variation with incidence at a constant speed of 120 kn, and, secondly, as control force per g at each trim condition to show the variation with speed. The manoeuvre characteristics which are presented alongside of the "static stability" data are summarised and discussed separately in Section 8.1.

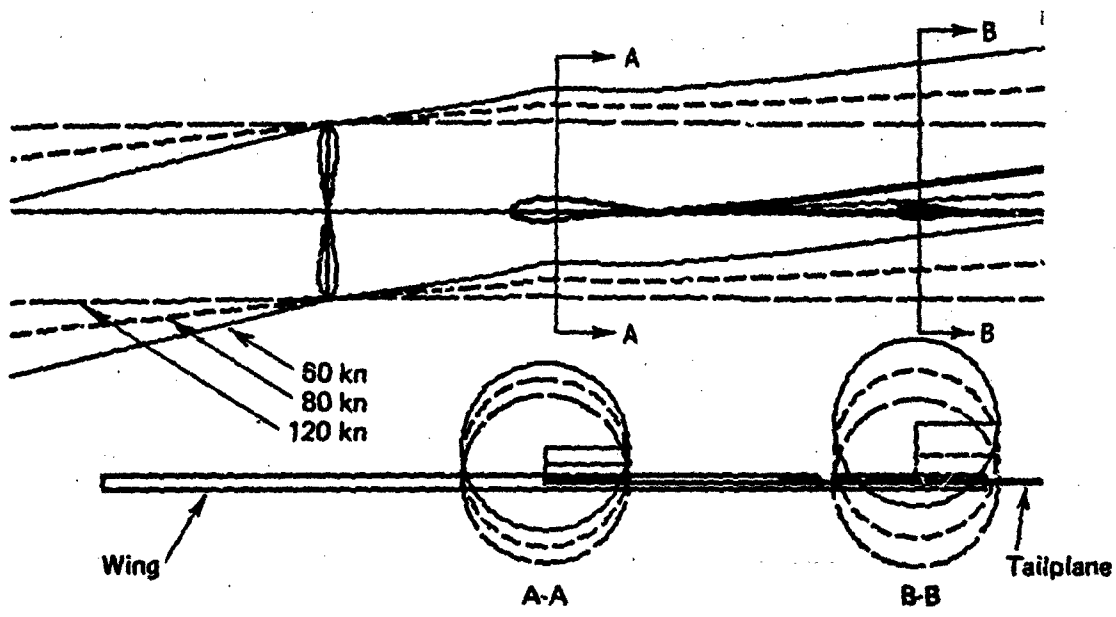

FIG. 3 EXAMPLE OF SLIPSTREAM LOCATION PLOTS (MAX'MUM POWER)

The standard presentation is completed by a diagram of the slipstream location for the low-speed case with high thrust coefficient. Figure 3 shows an example of the slipstream location plots for three speeds. The areas of wing and tailplane shown immersed within the slipstream are used in calculating the effects of power on lift, drag and pitching moment.

4. SMALL ANGLE ASSUMPTION

For the analysis of aircraft stability it has generally been found that satisfactory results can be obtained by representing the aerodynamic characteristics by linear approximations. Therefore, in the development and use of "static stability" theory, it is usual to define a linear representation of the aerodynamic forces acting over a small range of the system state variables. In this study, in which the effects of engine power are investigated, it is assumed that all power-off aerodynamic forces are linear functions of the motion state variables and control deflections and that the following effects, which can cause non-linear variations in the aerodynamics, are absent:

(*a*) Reynolds number;

(*b*) compressibility;

(*c*) aeroelasticity.

Furthermore, it is assumed that the tail lift due to elevator deflection, is represented by a change in lift coefficient at the tail aerodynamic centre with zero change in zero lift pitching moment. However, the small angle assumption regarding wing and tail incidence is *not* made in this study; hence the lift and drag forces are taken to act normal and parallel to the mean local flow directions respectively.

Figure 4 shows that, for the "standard case", when the small angle assumption is not invoked, the changes in the trim curves and static stability limit (h_n) are very small compared with the linear model. This result does not apply, as shown later in Section 6.2, when the vertical distance between wing aerodynamic centre and aircraft c.g. position is non-zero.

The assumptions listed above ensure that, for the "standard case", power off and propeller stopped, the "static stability" characteristics are substantially linear. The effects of power can then be compared to a base line configuration which has linear characteristics.

5. DISCUSSION OF THE EFFECTS OF POWER ON LONGITUDINAL STABILITY

The power effects on propeller-driven aircraft can be divided into the following main components:

(1) Propeller axial force—This force contributes a lift component when it is not coincident with the velocity vector and a pitching moment if its line of action does not pass through the aircraft c.g.

(2) Propeller normal force, when the propeller is at incidence to the velocity vector—This effect contributes a lift force, a small thrust force, and a pitching moment about the aircraft c.g.

(3) Increase in dynamic pressure and change in local wing–body incidence due to the propeller slipstream and normal force respectively—These effects result in changes to wing–body lift, drag and pitching moment.

(4) Increase in downwash behind the wing due to propeller normal force and slipstream effects on the centre portion of the wing and fuselage.

(5) Increase in dynamic pressure at the tailplane.

The distribution of dynamic head and downwash and the effects of slipstream swirl at the tailplane are not represented in the model. Only the mean effective values for these quantities are computed from the empirical estimation methods.

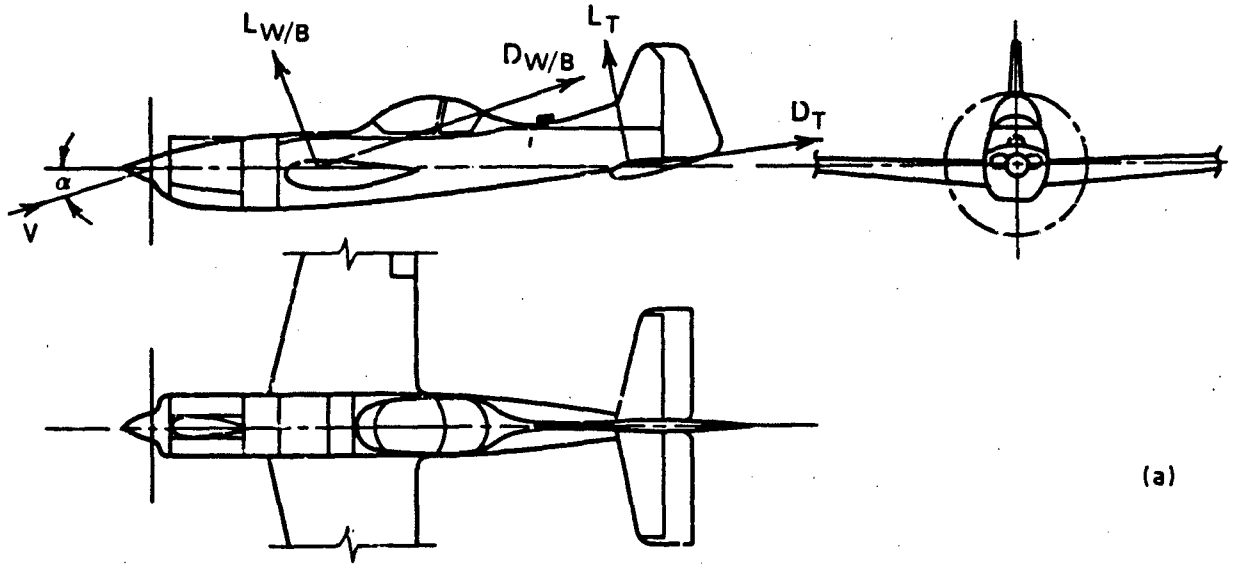

(a)

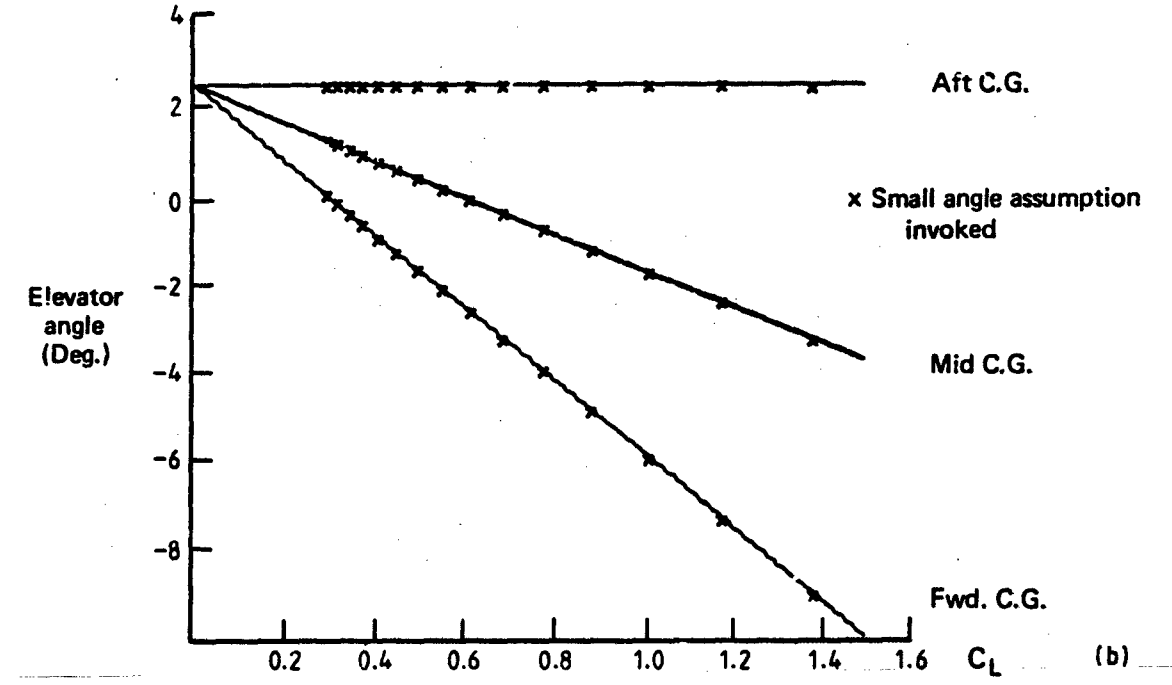

(b)

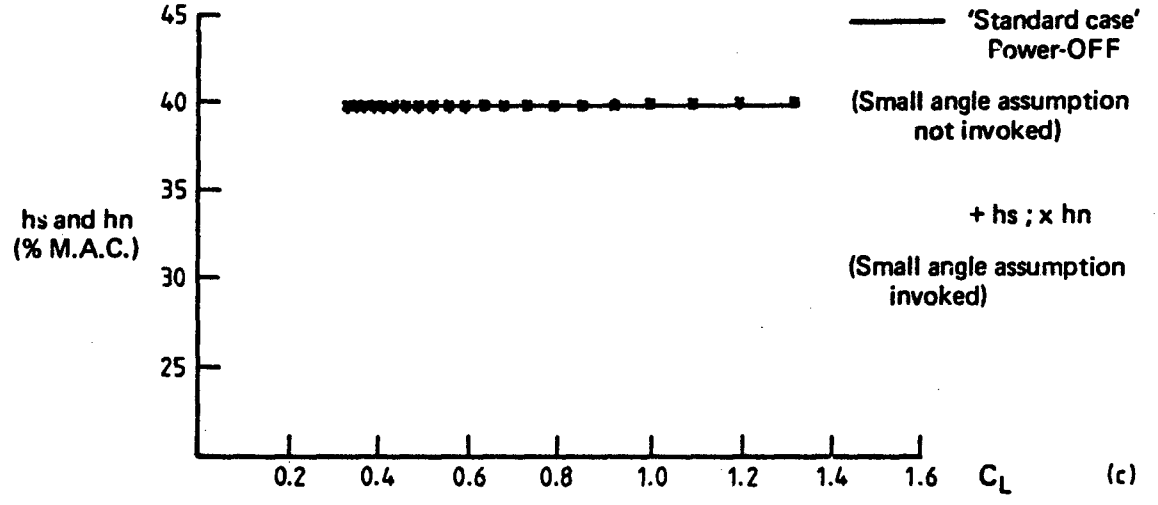

(c)

FIG. 4 APPROXIMATION DUE TO THE SMALL ANGLE ASSUMPTION

5.1 Thrust Coefficient

Since the main force produced by the propeller is the axial thrust force, it is useful to define a thrust coefficient with which to characterise the power effects.

The thrust force is normally non-dimensionalised using wing area in order that it should be directly comparable with the drag coefficient, i.e.

$$C_T = T/\tfrac{1}{2}\rho V^2 S_w. \tag{3}$$

In the theory and measurement of propeller performance it is more usual to define a thrust coefficient based on propeller diameter (D_p) and rpm (N), i.e. for the static case

$$T_C = T/\rho N^2 D_p^4, \tag{4}$$

or for the forward speed case

$$T_C' = T/\rho V^2 D_p^2. \tag{5}$$

For the testing of powered models in wind tunnels, it is necessary, as discussed in Reference 10, to reproduce the thrust coefficient exactly, and the most appropriate coefficient to use is C_T.

Since the propeller efficiency is given by:

$$\eta_p = TV/P \tag{6}$$

then thrust (T) can be written as a function of velocity(V)

$$T = \eta_p P/V \tag{7}$$

so that

$$C_T = \eta_p P/\tfrac{1}{2}\rho V^3 S_w. \tag{8}$$

The effects of power on stability are usually greatest where the thrust coefficient, and hence the axial velocity of the slipstream, is greatest. Equation (8) shows that these effects will be largest at low speeds, assuming η_p and P are reasonably constant.

It is useful for the wind tunnel representation of power and for flight test analysis to determine C_T as a function of trimmed lift coefficient (C_L). For an aircraft in steady rectilinear flight,

$$V = (W \cos\gamma/\tfrac{1}{2}\rho S_w C_L)^{1/2}. \tag{9}$$

Assuming that the flight path angle (γ) is small, then C_T can be approximated for the purpose of this discussion by:

$$C_T = \left(\frac{\rho}{2}\right)^{1/2} \eta_p \frac{P}{W} \frac{C_L^{3/2}}{(W/S_w)^{1/2}}. \tag{10}$$

For constant-speed propellers, the power remains approximately constant, and blade angle varies such that propeller efficiency tends to increase with speed, i.e. decrease with trim C_L. Therefore, C_T increases at less than the three-halves power of C_L (as shown in Fig. 5) and is inversely proportional to the square root of the wing loading. Equation 10 shows that the power effects, for a given power-to-weight ratio in trimmed flight, will be greatest for high lift coefficients and low wing loading and for sea level conditions; that is, conditions necessary for flight at low speeds.

Table 2 shows a comparison of the thrust coefficient for a number of single-engine aircraft. It is noteworthy that, although the fighter aircraft of the 1940s had large power-to-weight ratios, their high wing loadings gave lower in-flight thrust coefficients than current basic training aircraft. However, large power effects occurred during take-off because of the associated low speeds.

The effects of power would only satisfy the assumptions in the simple theory of "static stability" if they resulted in lift forces and pitching moments which were linear functions of incidence. However, as shown above, the power effects and consequently their effect on lift and pitching moment also change with velocity (V). In general the power effects are non-linear functions of the longitudinal motion state variables: velocity (V), incidence (α), pitch rate (q) and also of the control variables power lever setting (P_L), rpm setting and elevator position (δ_e). These variations are reflected in non-linearities in the trim curves of δ_e $v.$ C_L and in the manoeuvre characteristics, control force and control deflection per g.

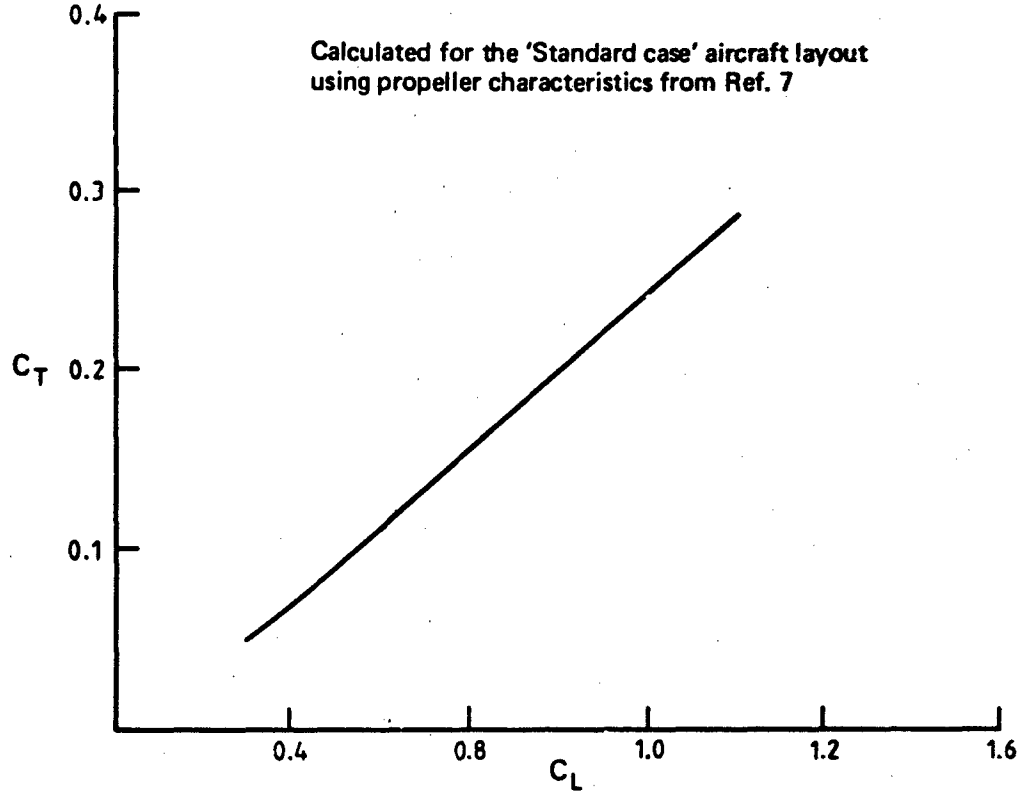

FIG. 5 THRUST COEFFICIENT VS LIFT COEFFICIENT
STEADY RECTILINEAR FLIGHT – MAXIMUM POWER

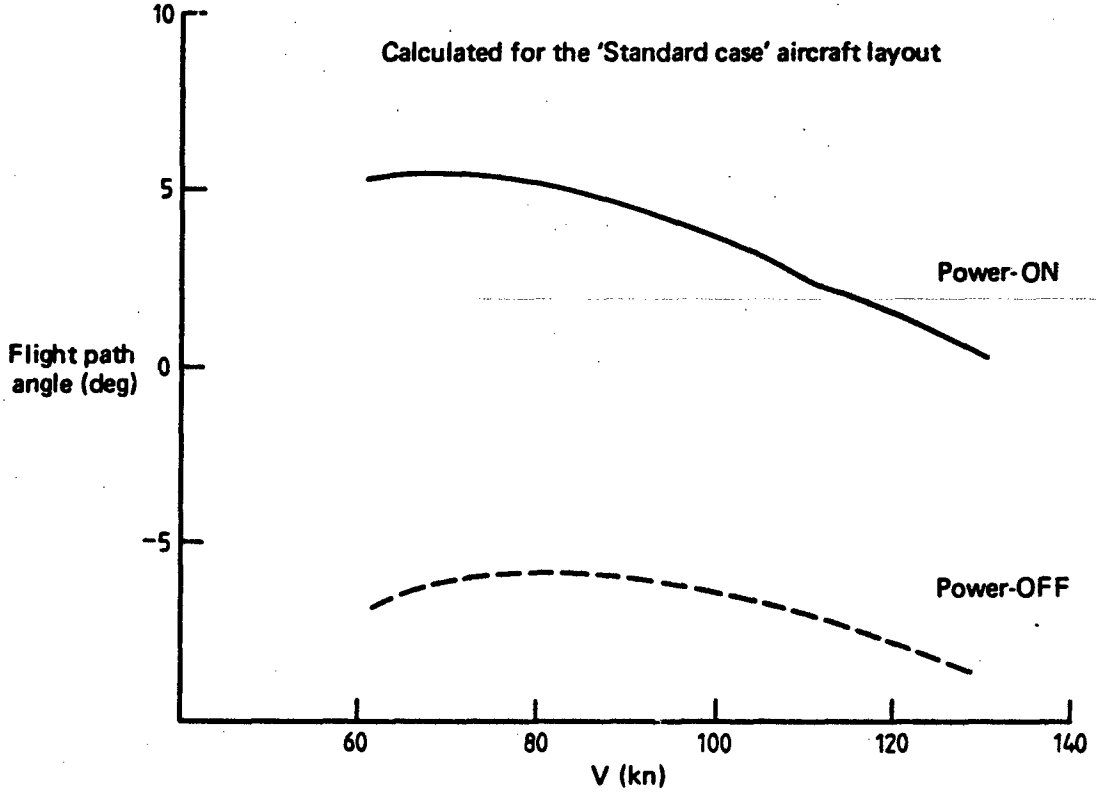

FIG. 6 FLIGHT-PATH ANGLE VS SPEED

In Sections 5.2–5.7 the nature and magnitude of the individual power effects will be described and their effect on longitudinal trim, stability and "manoeuvre" characteristics will be illustrated. The individual effects cannot be summed algebraically since many of the effects interact. For example, the change in slipstream locus due to propeller normal force alters the slipstream effect on the wing and tail contribution. In Section 5.7 the combined effects of power are illustrated and also the result of accumulating the power effects in the order listed in Section 5 is presented.

5.2 Propeller Axial Force

The forces acting on a propeller are generally presented in terms of the axial force (or thrust), the normal force, and a moment. Reference 11 shows that these forces can be represented by a lift and a drag force acting at an aerodynamic centre slightly forward of the propeller disc. For the case in which the thrust axis acts through the aircraft c.g., e.g. the "standard case", the aircraft trim characteristics will be altered by the propeller axial force in two ways:

(*a*) The axial force will contribute a lift component normal to the velocity vector given by

$$\Delta C_L = C_T \sin \alpha_{TH}. \tag{11}$$

Since α_{TH} and C_L are approximately linearly related in trimmed rectilinear flight and C_T and C_L are approximately linearly related, as shown in Figure 5, then ΔC_L will tend towards a parabolic variation with C_L.

(*b*) The component of axial force parallel to the velocity vector will alter the net longitudinal force and hence, will change the flight path angle (γ) compared with the value in power-off flight.

Using the standard equations for trimmed rectilinear flight:

$$\tan \gamma = \frac{C_T \cos \alpha_{TH} - C_D}{C_T \sin \alpha_{TH} + C_L}. \tag{12}$$

The change in flight path angle due to power is shown in Figure 6 as a function of velocity V for the "standard case" aircraft layout.

Component (*a*) contributes an incremental lift force at a given aircraft velocity and hence, a reduction in incidence is required to maintain rectilinear flight, and a smaller negative elevator angle will be required to maintain trim. However, since the axial force passes through the c.g., it does not contribute a pitching moment and so the relationship between pitching moment and the state variables α and V remains unchanged, and hence, "static stability" is not changed.

Component (*b*) produces a similar effect in that, for a given aircraft velocity, the C_L required for rectilinear flight varies with flight path angle. Aircraft incidence and elevator angle are adjusted accordingly, but "static stability" is not changed.

In both cases the changes in trim angle are related to the pitch stiffness ($-C_{m_\alpha}$) and so are greatest at forward c.g. as shown in Figure 7*b*, while h_n and h_s remain unchanged as shown in Figure 7*c*. When the propeller thrust line does not pass through the aircraft c.g., substantial changes in stability can occur, as will be shown in Section 6.1.

5.3 Propeller Normal Force

A running propeller produces a normal force (N_p) which depends upon the incidence of the flow to the propeller and on the thrust. The estimation of N_p in this study is taken from Reference 6 and is based on the results presented in Reference 31 (1944). This Reference shows that, for small incidence angles, the propeller normal force coefficient may be represented as:

$$C_{n_p} = (\partial C_{n_p}/\partial \alpha_p)\alpha_p \tag{13}$$

where C_{n_p} is based on propeller disc area. $\partial C_{n_p}/\partial \alpha_p$ is presented in Reference 6 as a function of propeller characteristics and thrust coefficient.

The contribution to lift will have a small but similar effect to the lift component of axial force, but there will also be a significant pitching moment contribution which will affect trim and stability.

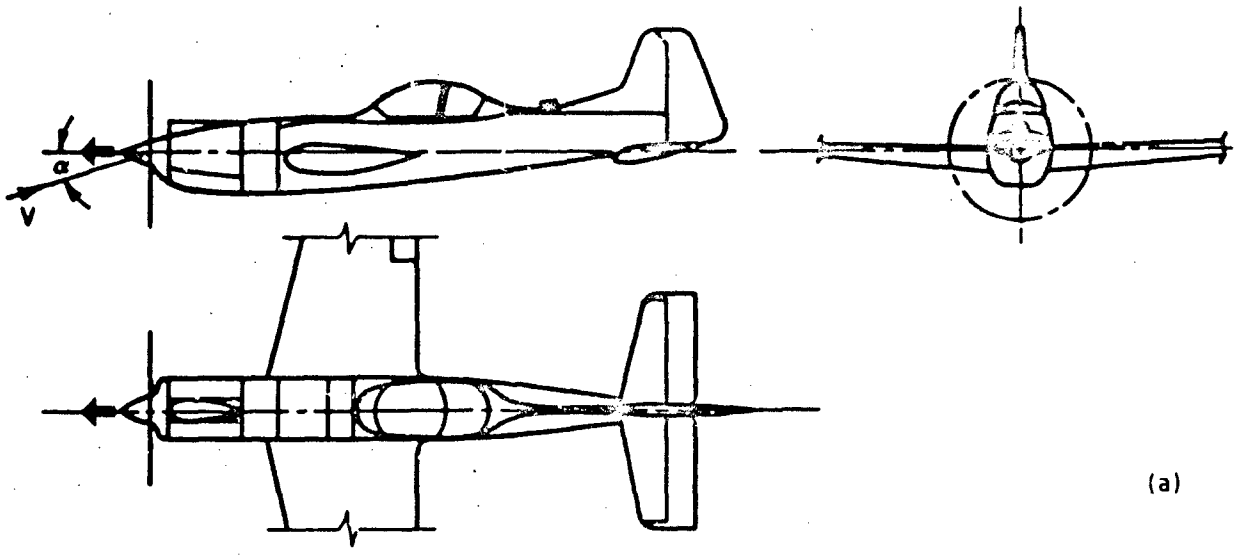

(a)

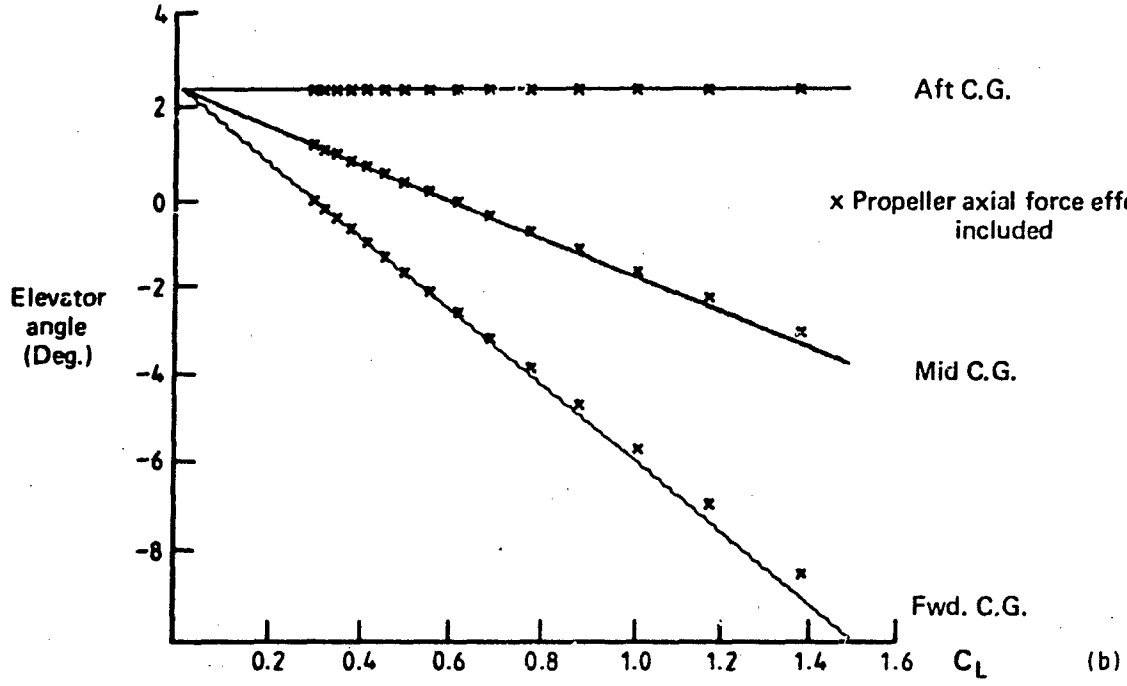

(b)

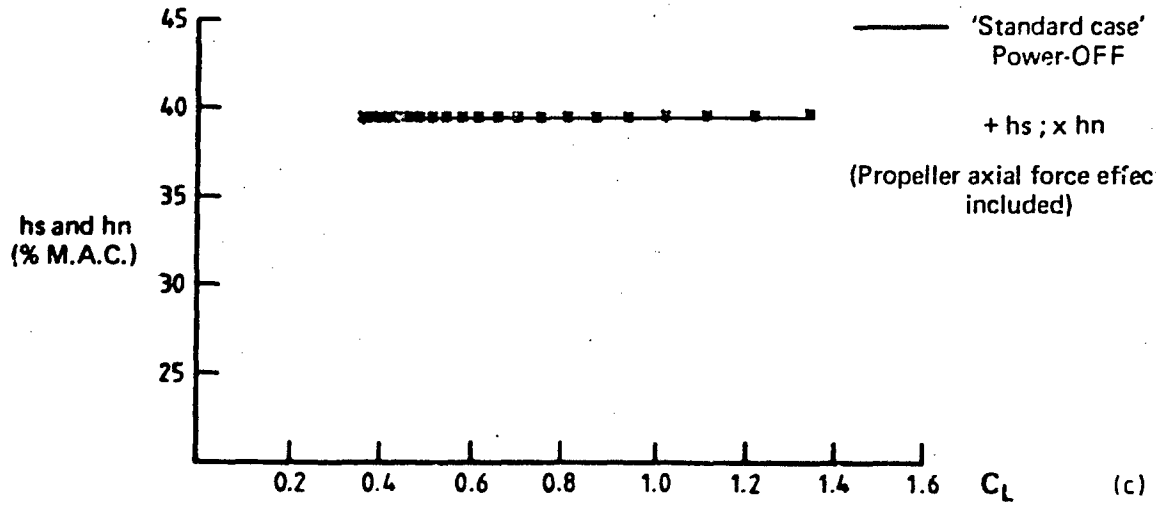

(c)

FIG. 7 EFFECT OF PROPELLER AXIAL FORCE

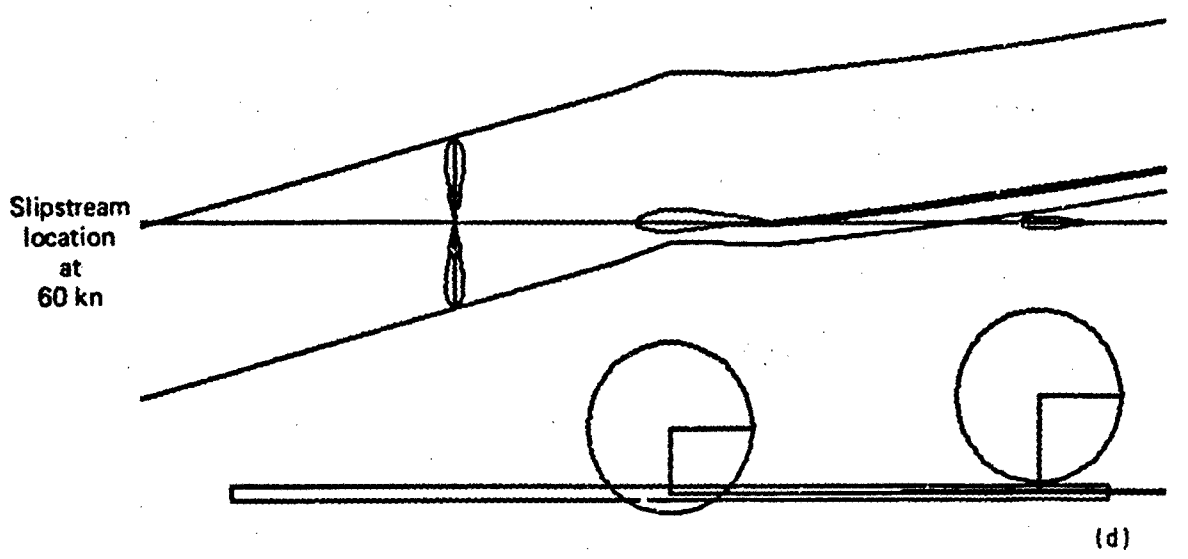

(d)

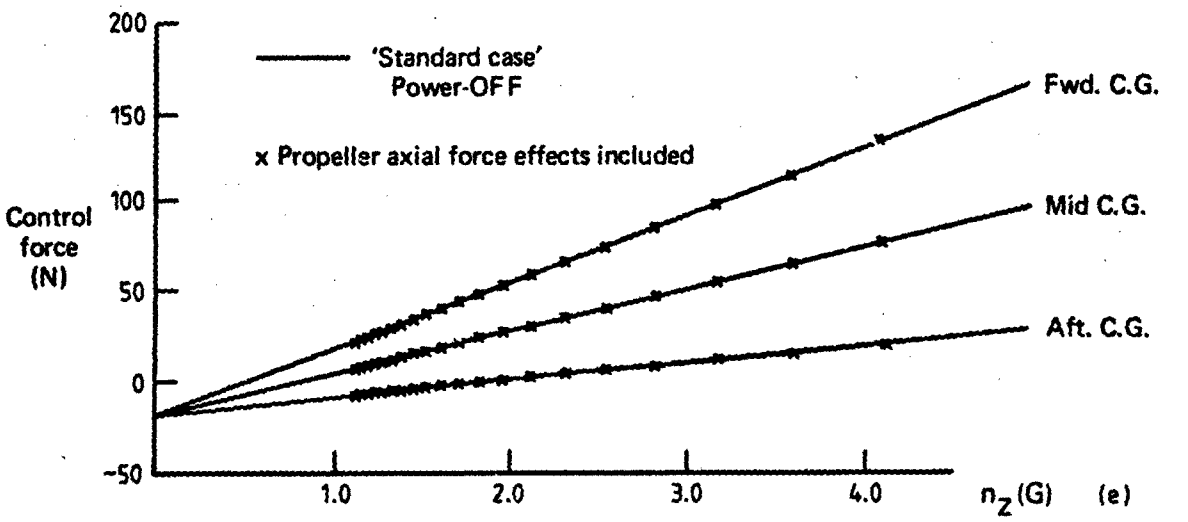

(e)

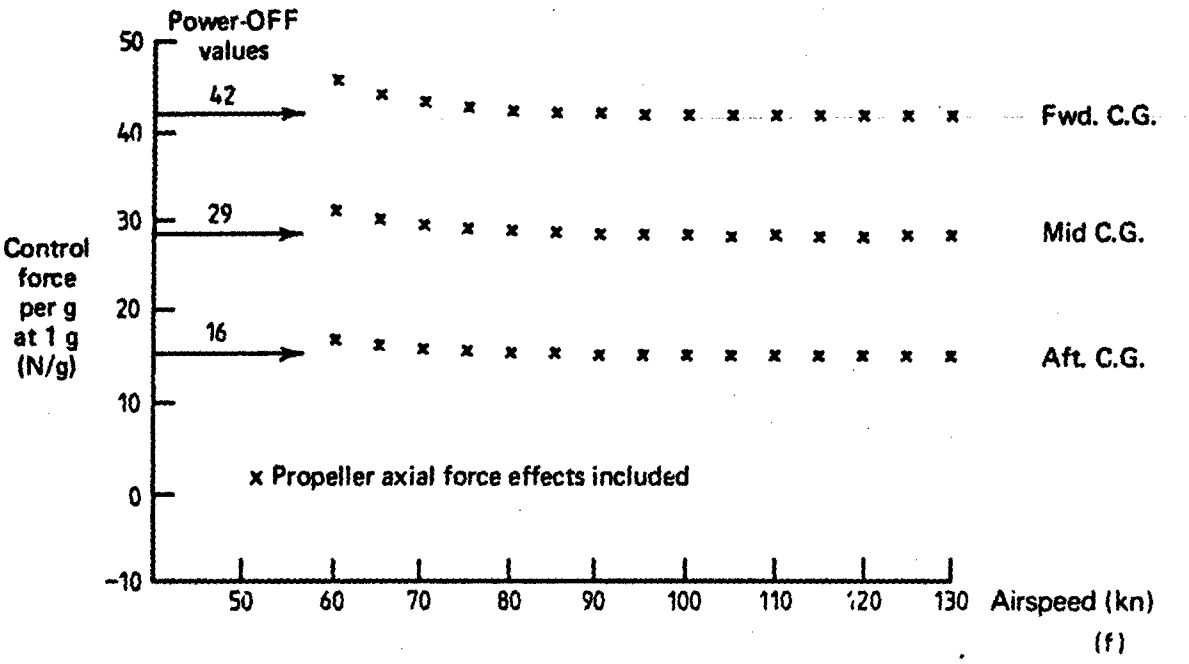

(f)

FIG. 7 EFFECT OF PROPELLER AXIAL FORCE

For a propeller with aerodynamic centre distance x_p ahead of the aircraft c.g., the propeller pitching moment coefficient is given by

$$C_{m_p} = \frac{S_p}{S_w}\frac{x_p}{\bar{c}} C_{n_p}. \tag{14}$$

If the propeller is mounted close to the wing, the propeller incidence will be modified by wing upwash, so that:

$$\alpha_p = \alpha + \epsilon_p. \tag{15}$$

The pitching moment due to propeller normal force is then given by:

$$C_{m_p} = \frac{S_p}{S_w}\frac{x_p}{\bar{c}}\frac{\partial C_{n_p}}{\partial \alpha_p}(\alpha+\epsilon_p). \tag{16}$$

Since $\partial C_{n_p}/\partial \alpha_p$ is a function of C_T, then in rectilinear flight, Equation (16) shows that C_{m_p} is a function of both state variables V and α, and so will produce a pitching moment variation with trim C_L tending towards parabolic. This variation is reflected in the "trim curves" presented in Figure 8*b*. The slopes of the "trim curves" are a good guide to the level of longitudinal stability, and as Figure 8*b* shows, propeller normal force produces a reduction in trim curve slope at high C_L's, indicating a reduction in stability. However, this information does not permit incidence or aircraft velocity effects to be distinguished. Assuming linear characteristics about each trim point, as discussed in Section 2, the propeller normal force contribution to pitch stiffness is given by:

$$-(\partial C_{m_p}/\partial \alpha) = \frac{-S_p}{S_w}\frac{x_p}{\bar{c}}\frac{\partial C_{n_p}}{\partial \alpha_p}(1+\partial \epsilon_p/d\alpha). \tag{17}$$

All terms on the right-hand side of Equation (17) excepting x_p are positive. Therefore propeller normal force produces a reduction in pitch stiffness, which is largest at large values of $\partial C_{n_p}/\partial \alpha_p$, i.e. large C_T, which is given by large power at low speeds. For the "standard case" this reduction leads to a forward movement of h_n of 2%$\bar{c}$ at high speeds and 3%$\bar{c}$ at low speeds as shown in Figure 8*c*. The derivative $(\partial C_{n_p}/\partial \alpha_p)$ increases with increasing C_T, therefore the propeller normal force will produce negative values for the derivatives C_{m_V} and C_{L_V}. For the "standard case" these speed effects lead to a static stability limit (h_s) 0·5%$\bar{c}$ ahead of h_n, as shown in Figure 8*c*.

In summary, for a propeller located at a distance ahead of the c.g. and supplying large thrust, there is a significant change in trim, and a reduction in stability due to the propeller normal force. This reduction is primarily an incidence rather than a speed effect.

With power off but with the propeller windmilling, a normal force is produced which leads to a similar, but smaller reduction in stability, as shown in Figures 8*g–i*.

5.4 Effect of a Running Propeller on the Wing–Body Aerodynamic Characteristics

A running propeller ahead of the wing–body combination causes the following effects to occur:

(*a*) An increase in the effective zero lift pitching moment (C_{m_0}) due to, increased dynamic pressure, and to changes in the flow characteristics over the portion of the wing and body affected by the slipstream.

(*b*) A reduction in the local incidence due to the downwash associated with the propeller normal force.

(*c*) An increase in lift due to increased dynamic pressure over the portion of the wing and body affected by the slipstream.

The estimation of contributions (*a*) to (*c*) is from Reference 6 which uses information from Reference 14. In this study the change in effective C_{m_0} is assumed to be due to the change in dynamic pressure alone, since the estimation of the effect of changes in flow pattern due to propeller slipstream generally requires wind tunnel measurements to give reliable results. For a normal wing–body combination C_{m_0} is negative, so the effect of the slipstream is to introduce an increasing nose-down moment as C_T increases with decreasing aircraft velocity (V). This

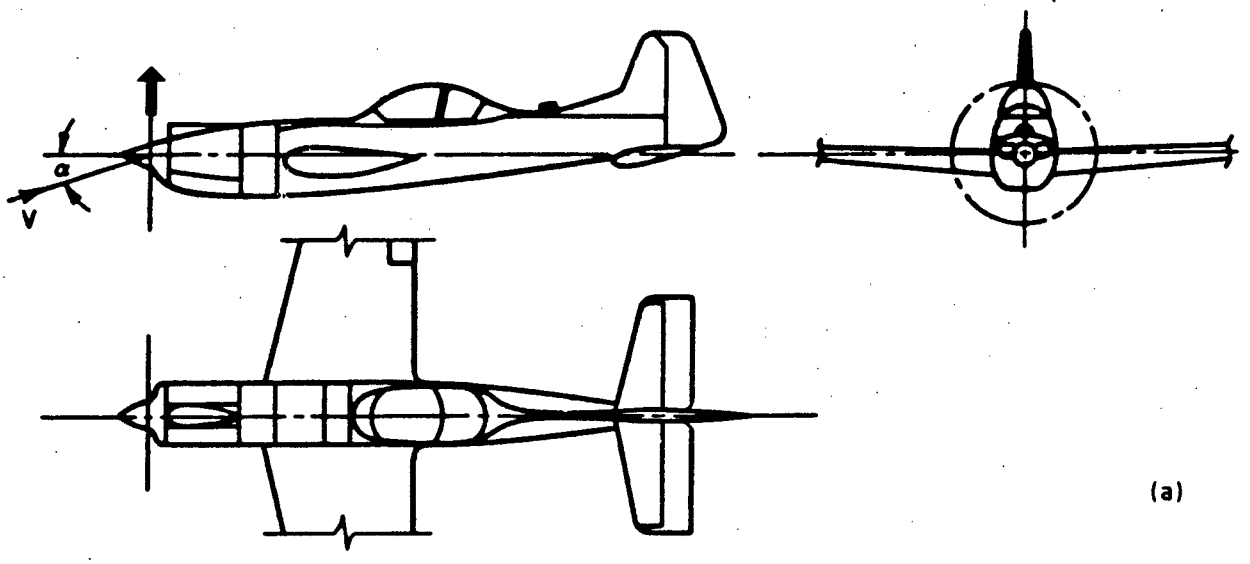

(a)

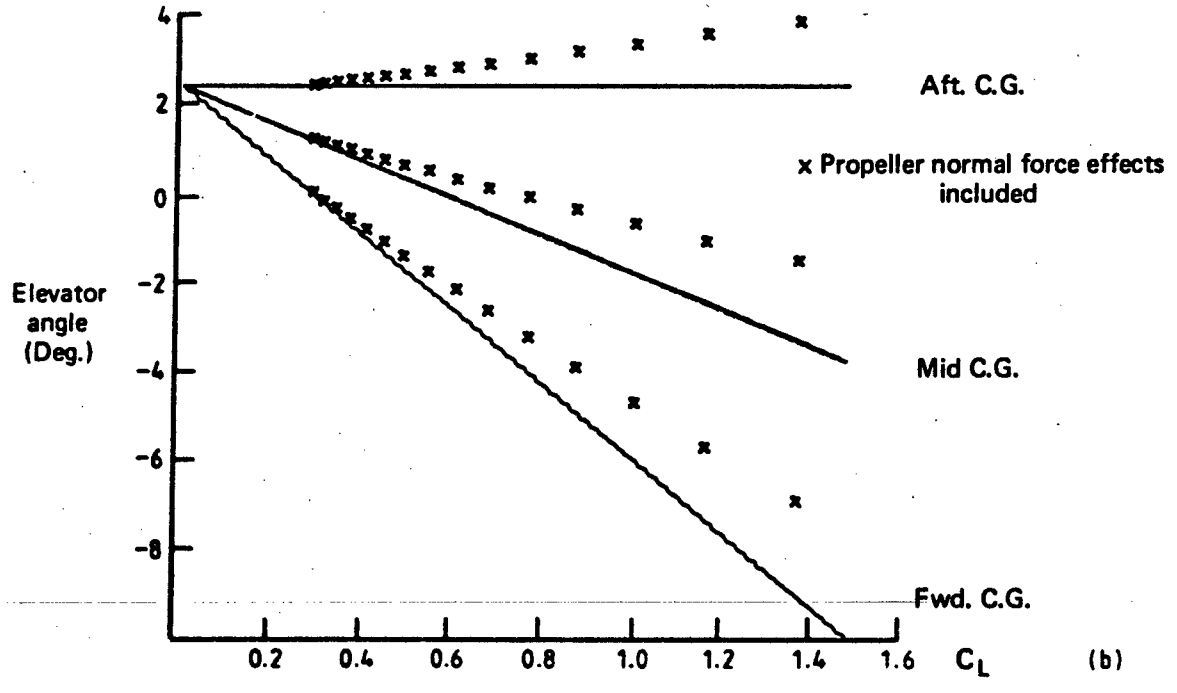

(b)

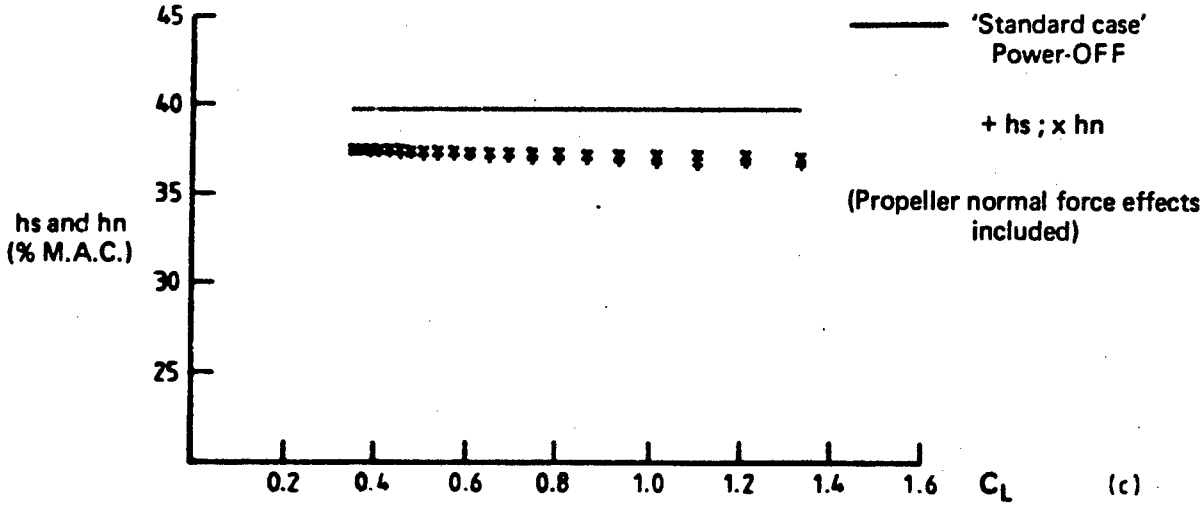

(c)

FIG. 8 EFFECT OF PROPELLER NORMAL FORCE

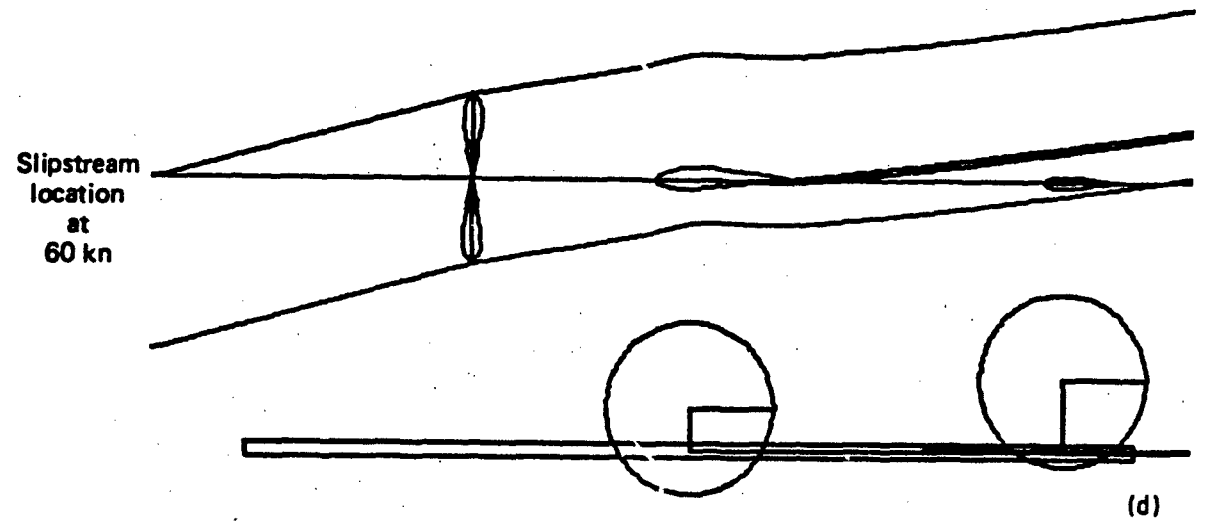

(d)

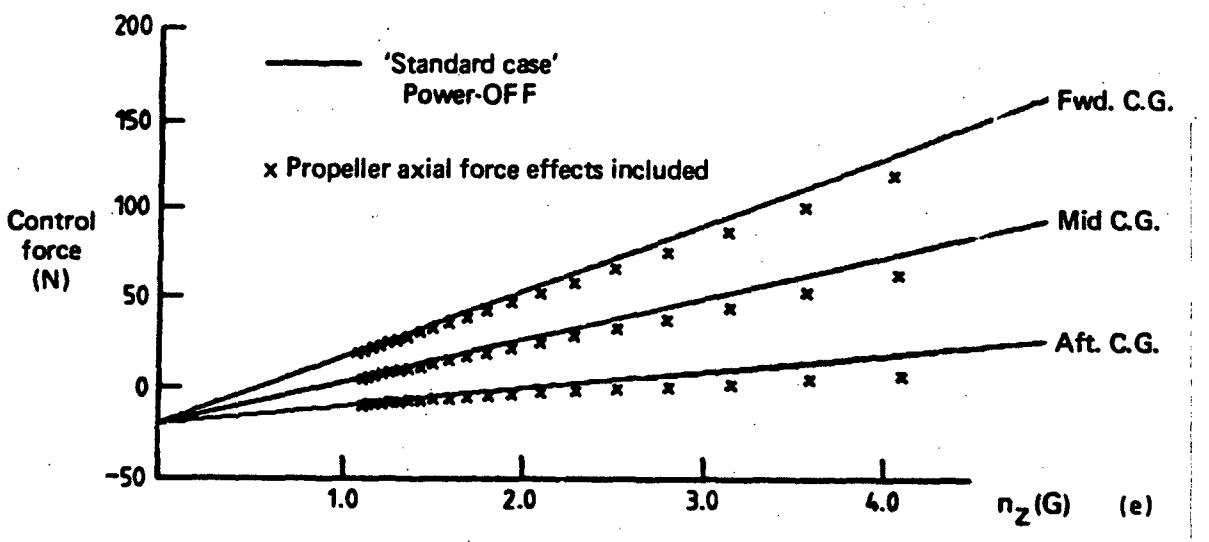

(e)

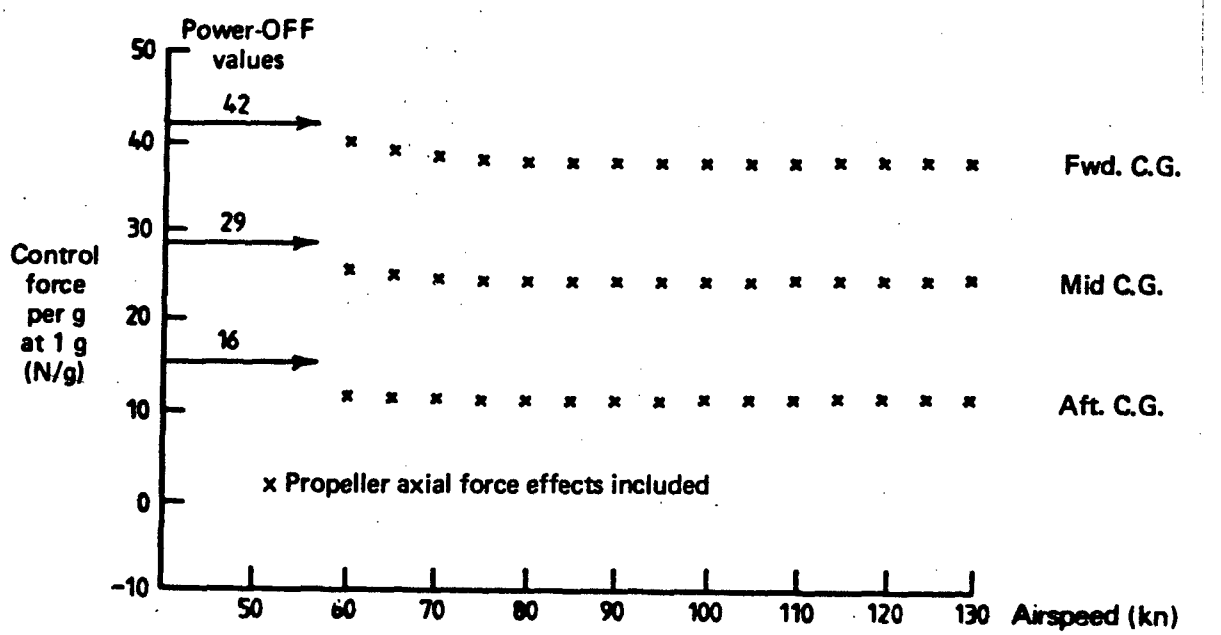

(f)

FIG. 8 EFFECT OF PROPELLER NORMAL FORCE

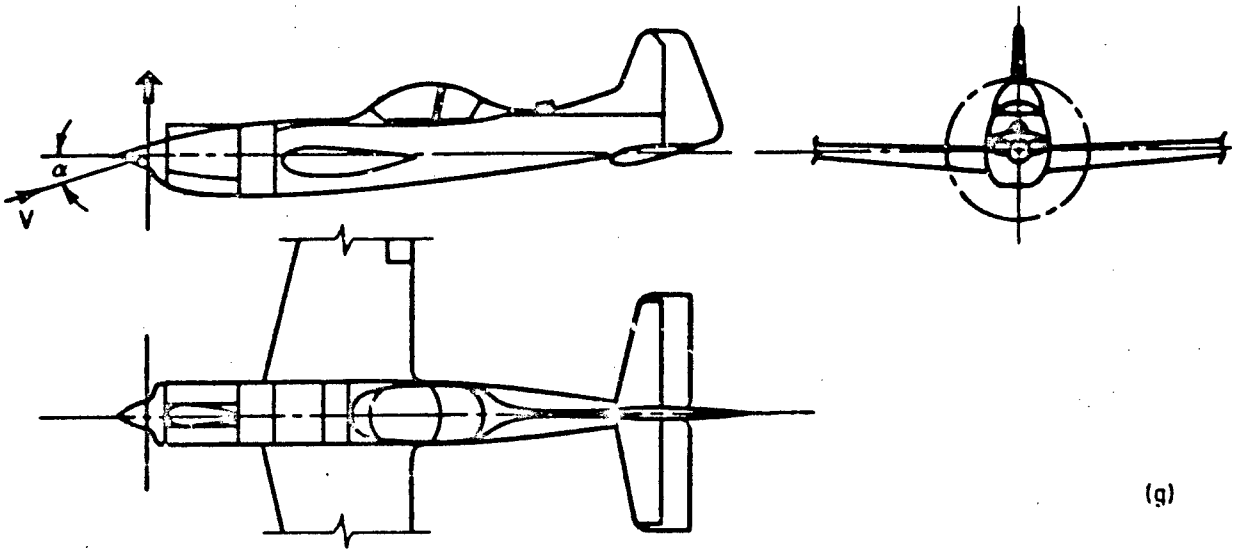

(g)

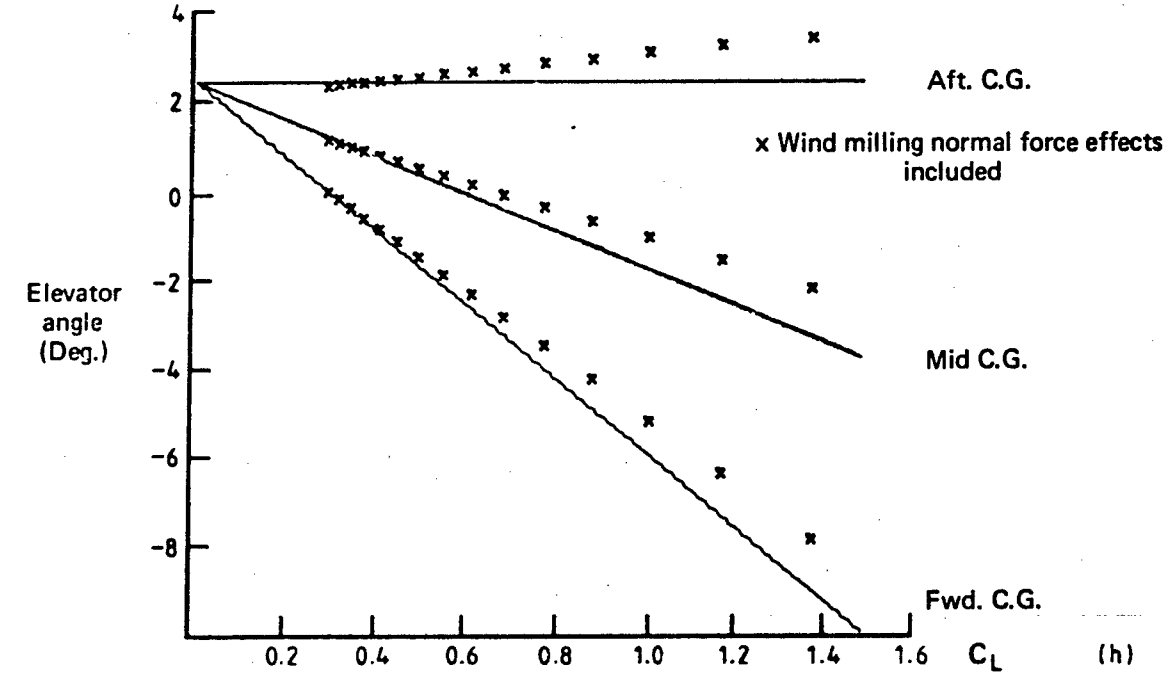

(h)

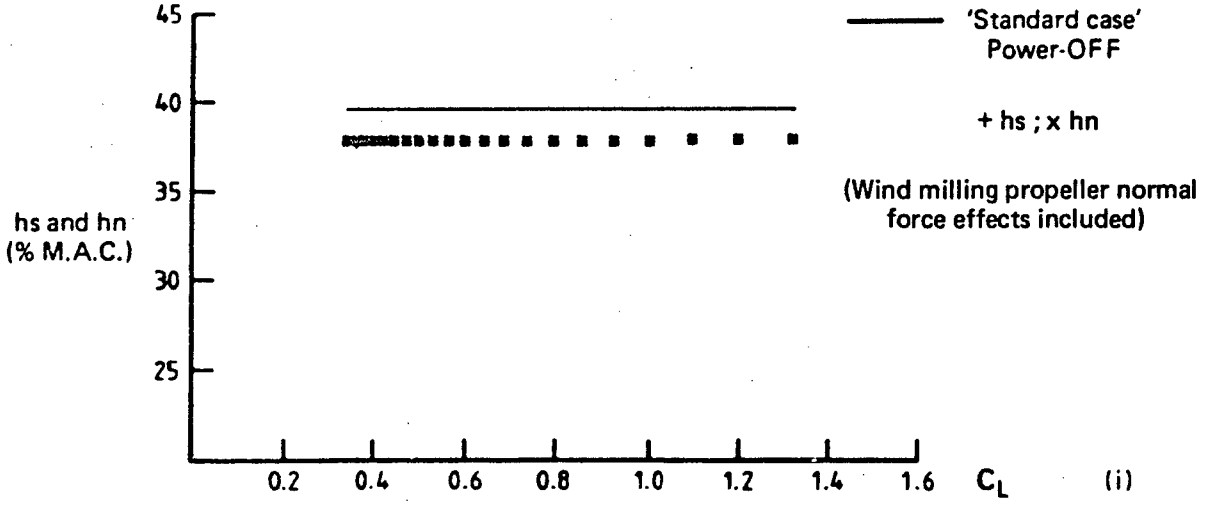

(i)

FIG. 8 EFFECT OF PROPELLER NORMAL FORCE (WINDMILLING PROPELLER)

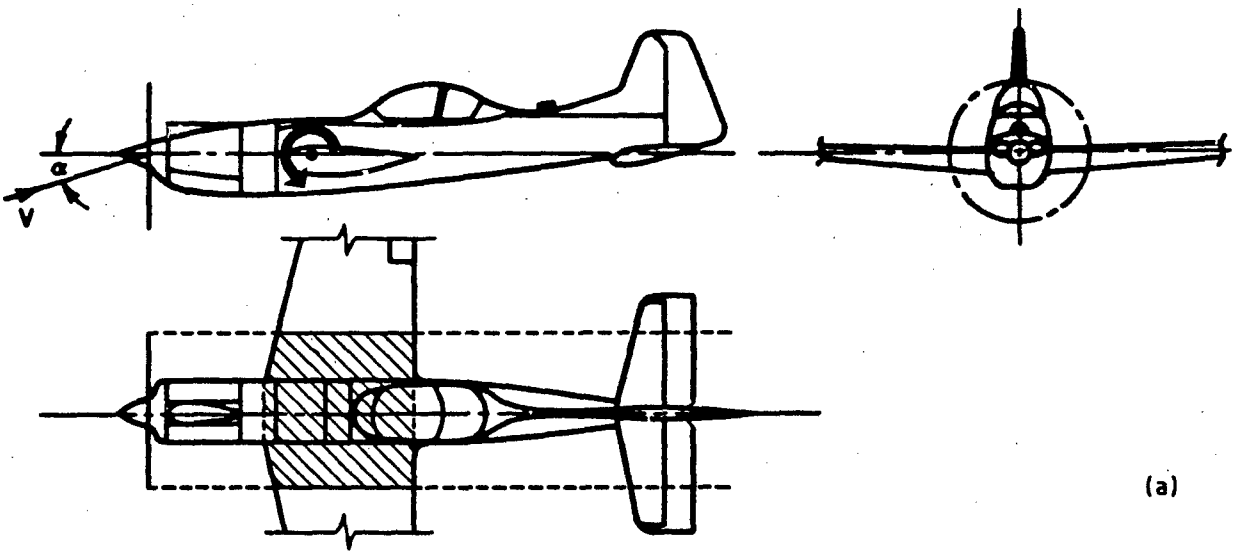

(a)

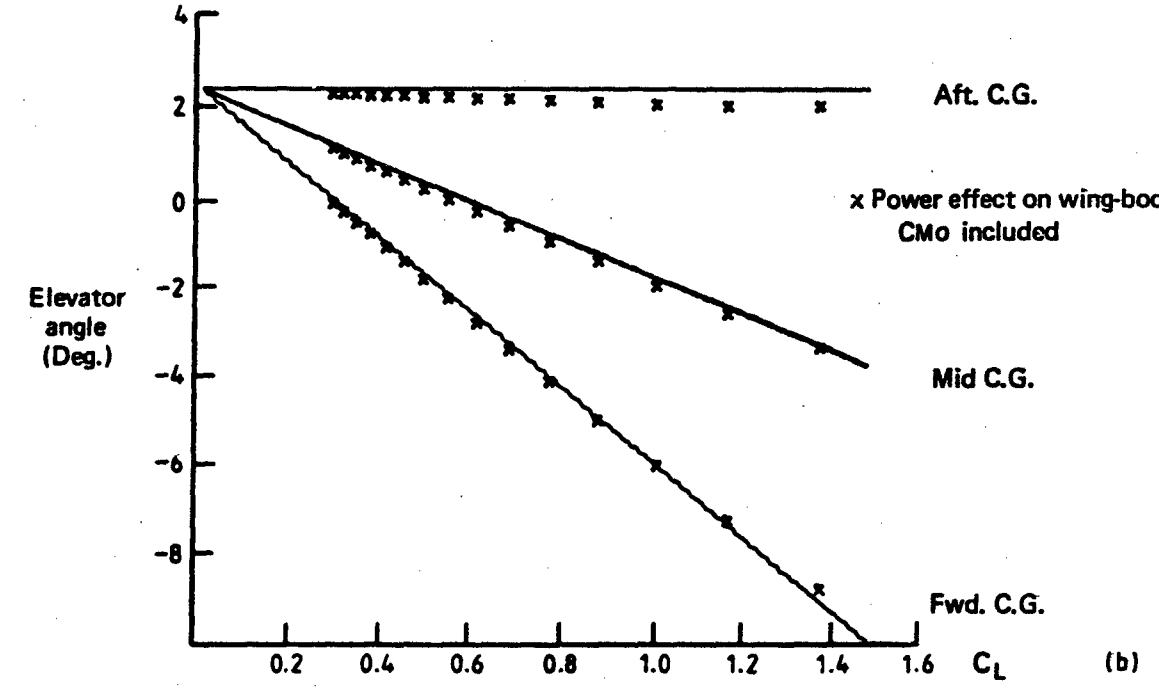

(b)

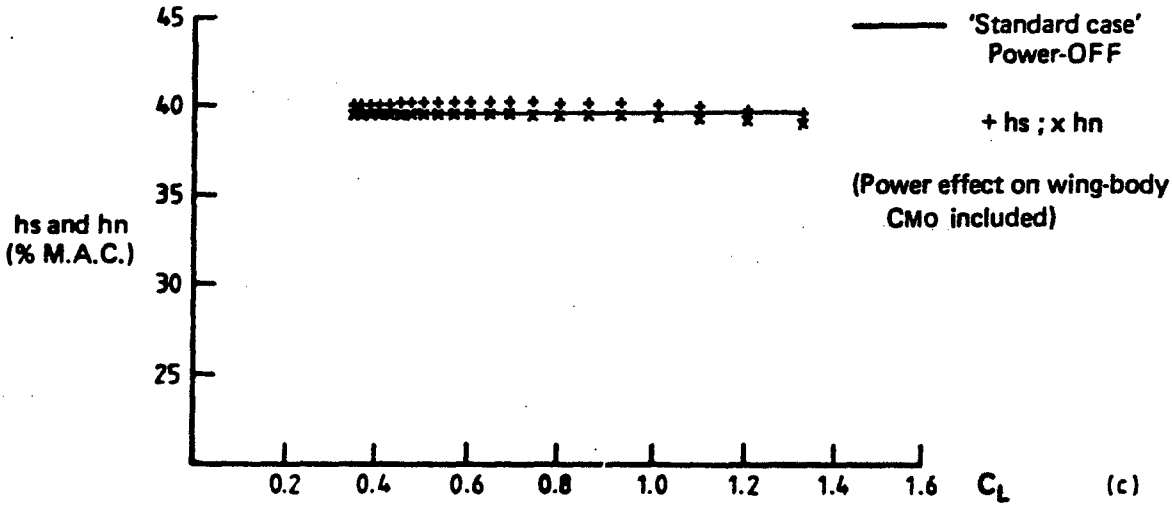

(c)

FIG. 9 EFFECT OF POWER ON WING-BODY C_{M_o}

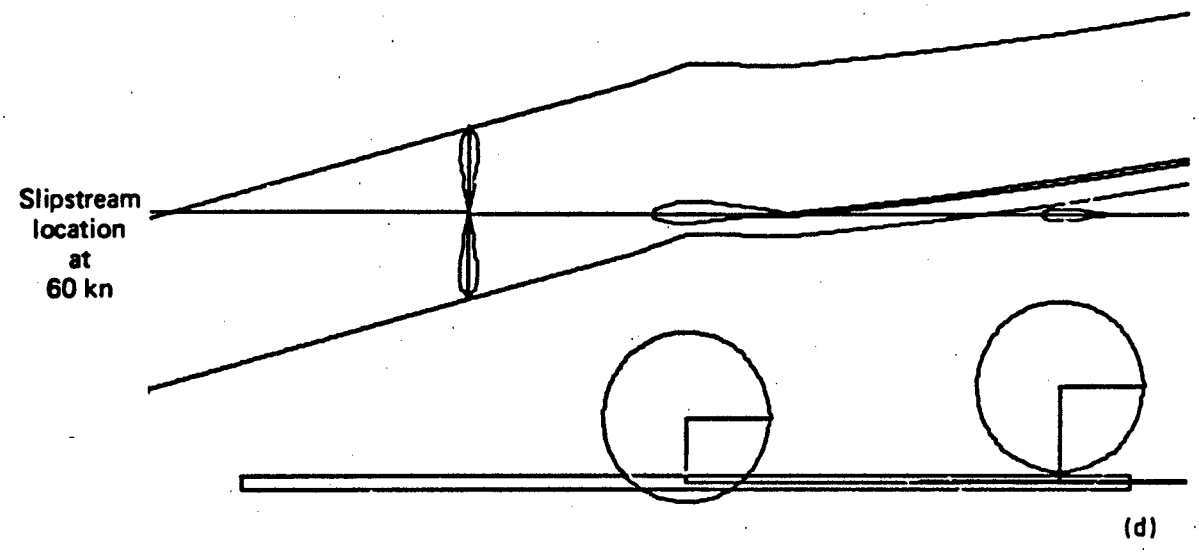

(d)

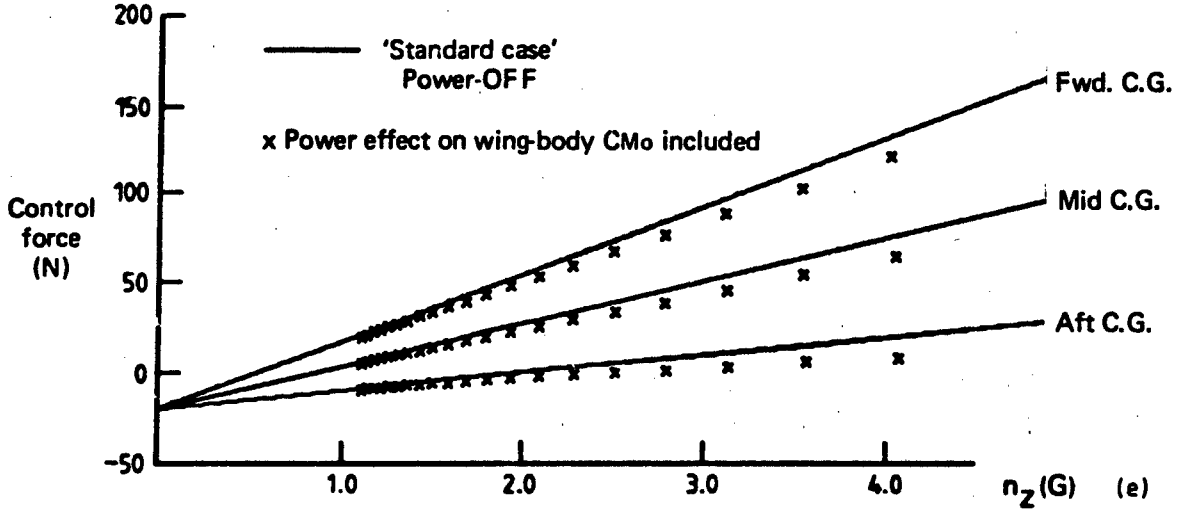

(e)

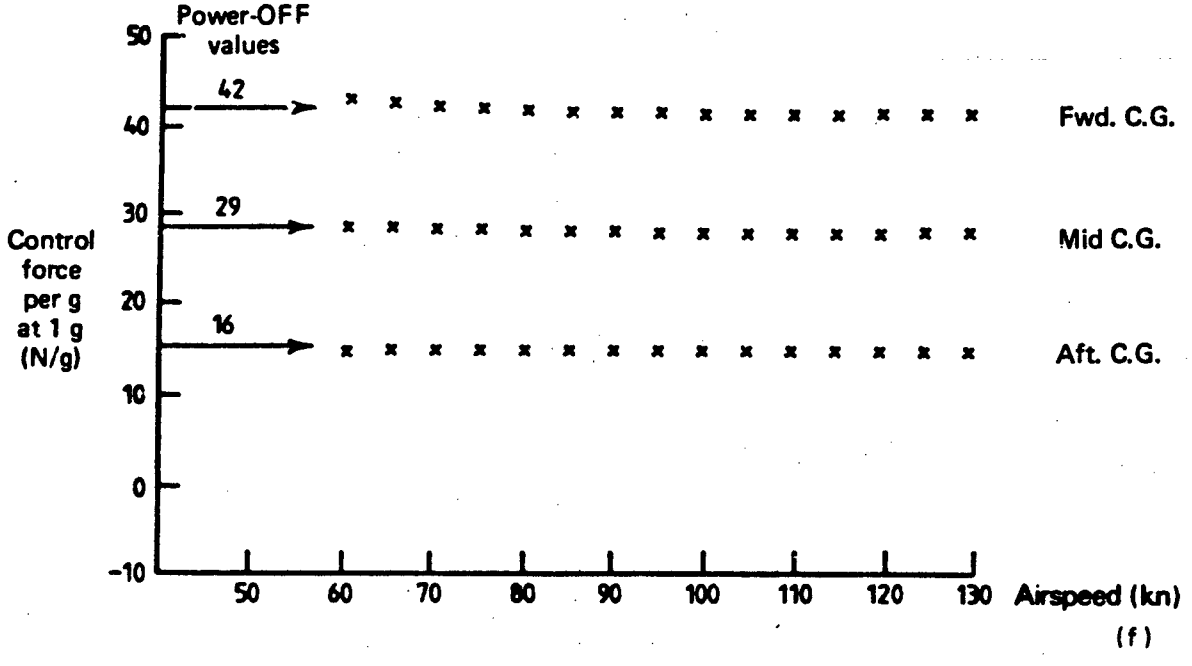

(f)

FIG. 9 EFFECT OF POWER ON WING-BODY CMo

results in a positive value of C_{m_V} and an increase in stability as shown by the increase in h_s in Figure 9*c*. The pitch stiffness and hence h_n are not altered.

Effect (*b*) may be interpreted in two ways: Firstly, from consideration of the simple theory of "static stability", the neutral point is defined as the c.g. position for zero pitch stiffness and is given by:

$$h_n = h_0 + \bar{V} C_{L_{\alpha_T}} / C_{L_\alpha} (1 - \partial\epsilon/\partial\alpha) \qquad (18)$$

where h_0 is the wing–body aerodynamic centre. Effect (*b*) reduces the change in local lift for a given change in incidence and so effectively decreases the wing–body lift curve slope C_{L_α}. This will lead to an increase in h_n, as shown by Equation (18) and hence, to an increase in h_s. In the second interpretation, it may be considered that to achieve a given change in lift, a greater incidence change is required; hence a greater restoring moment will be provided by the tailplane. Since propeller normal force also depends upon C_T then local wing incidence will also vary with aircraft velocity (V). The variation leads to positive values for C_{L_V} and C_{m_V} which give an increase in the static stability limit (h_s).

Effect (*c*) results in similar changes to effect (*b*) but with opposite signs. The increase in dynamic head over the portion of the wing and body affected by the slipstream, results in an *increase* in wing–body lift curve slope C_{L_α}. This leads to a decrease in h_n, as shown by Equation (18), and also to further decreases in h_s since the contributions to C_{L_V} and C_{m_V} are negative.

The net effect of (*a*), (*b*) and (*c*) is illustrated in Figure 10. Both h_n and h_s are decreased; the reductions due to velocity exceeding those due to incidence.

A further effect, which is configuration-dependent, is caused by the change in the area of wing and body immersed within the slipstream as the trim condition changes. For a low-wing aircraft with a forward-mounted propeller for example, the effect of dynamic head on C_{m_0} and C_L will change as the wing emerges from the slipstream. The magnitudes of the individual changes to h_n and h_s due to the wing–body effects identified, are given in Table 3 for the "standard case" for $C_L = 0{\cdot}8$. For this condition, the rate of change of immersed wing and body area with incidence is small. Considered individually, certain wing–body power effects are large, but the net change in stability, for the "standard case" considered, is small. These increments are determined in the presence of propeller axial and normal force effects, and are shown in context later as the change from Curve 2 to Curve 4 in Figures 14*a* and 14*b*.

TABLE 3

Breakdown of Wing–Body Contributions for $C_L = 0{\cdot}8$

"Standard case", maximum power, $C_L = 0{\cdot}8$

Individual wing body effects	Δh_n % $\bar{c}$	Δh_s % $\bar{c}$
(*a*) Change in effective C_{m_0} due to dynamic head	0	+1·0
(*b*) Change in local incidence due to propeller "normal" force	+1·75	+2·5
(*c*) Change in effective C_{L_α} due to dynamic head	−2·5	−5·25
Net effect	−0·75	−1·75

5.5 Effect of Power on Downwash at the Tailplane

The downwash at the tailplane, and its rate of change with incidence and with aircraft velocity, all change with power. The changes are caused firstly, by the lift generated by the propeller, as discussed in Sections 5.3 and 5.4, and secondly by the changes in lift on the wing and body described in items (*b*) and (*c*) of Section 5.4. For single-engine aircraft, a substantial portion of the tailplane lies within this modified downwash field. This results in changes to both incidence (α), and aircraft velocity ($\bar{V}$), dependent pitching moments. The change in downwash with power is estimated from Reference 6 as a change in the mean effective downwash acting on the tailplane. The downwash distribution, which can vary significantly across the span, is not

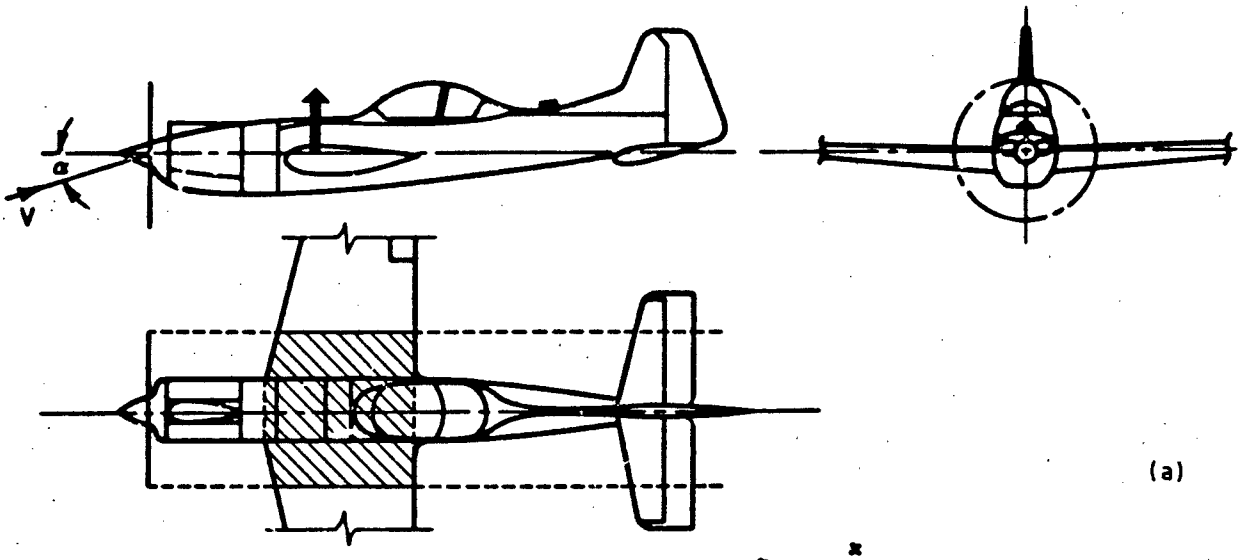

(a)

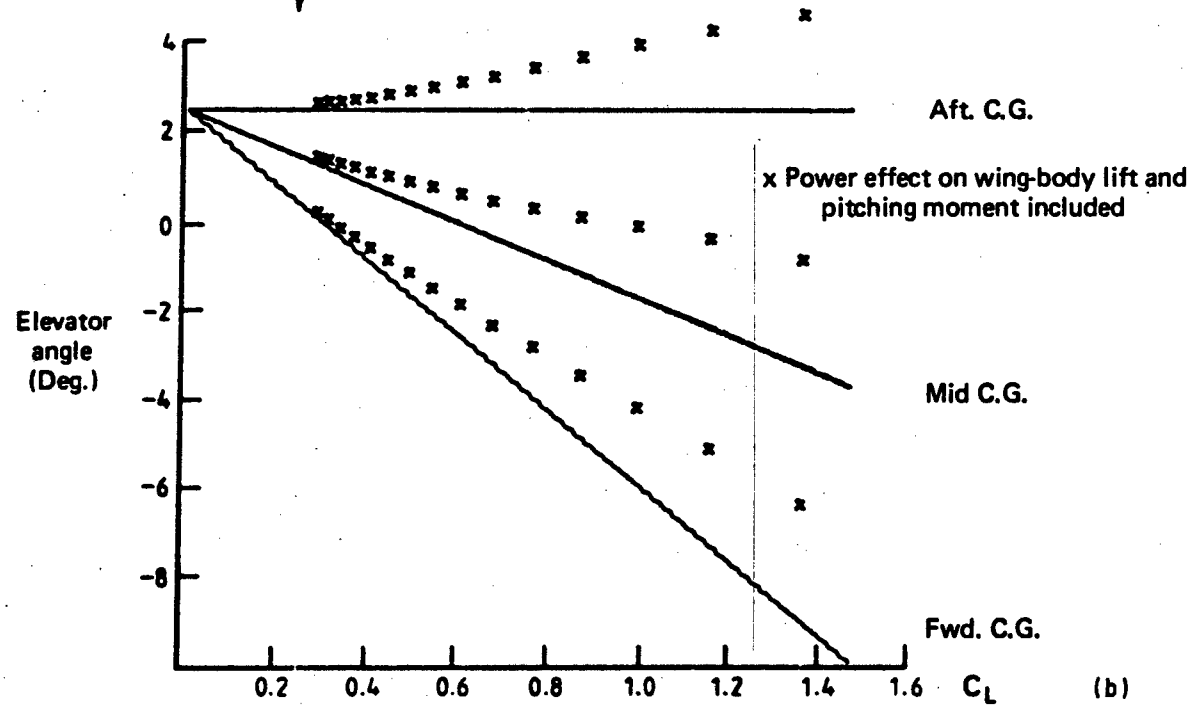

(b)

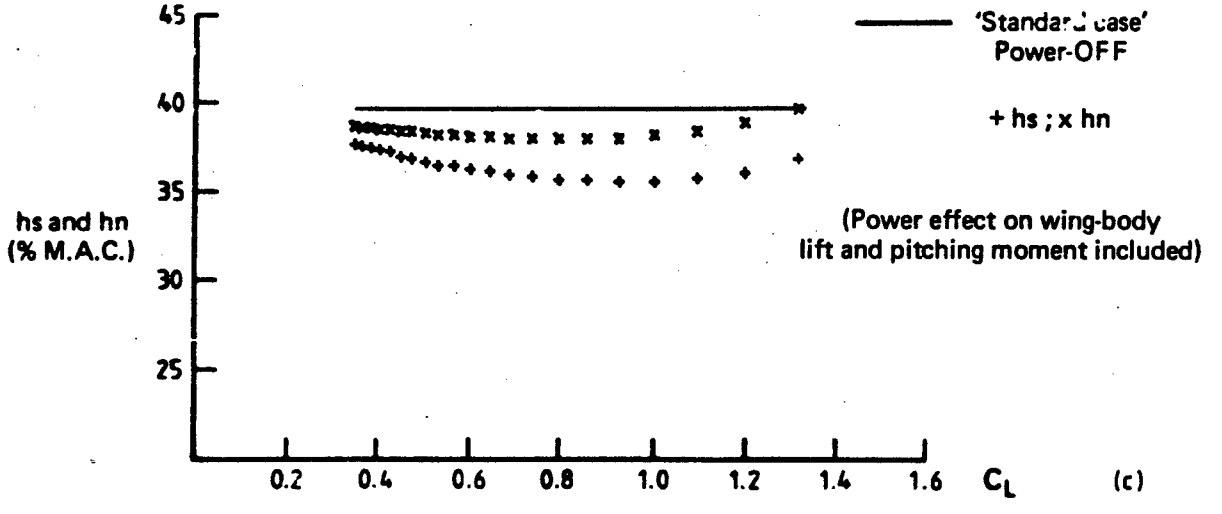

(c)

FIG. 10 EFFECT OF POWER ON WING-BODY LIFT AND PITCHING MOMENT

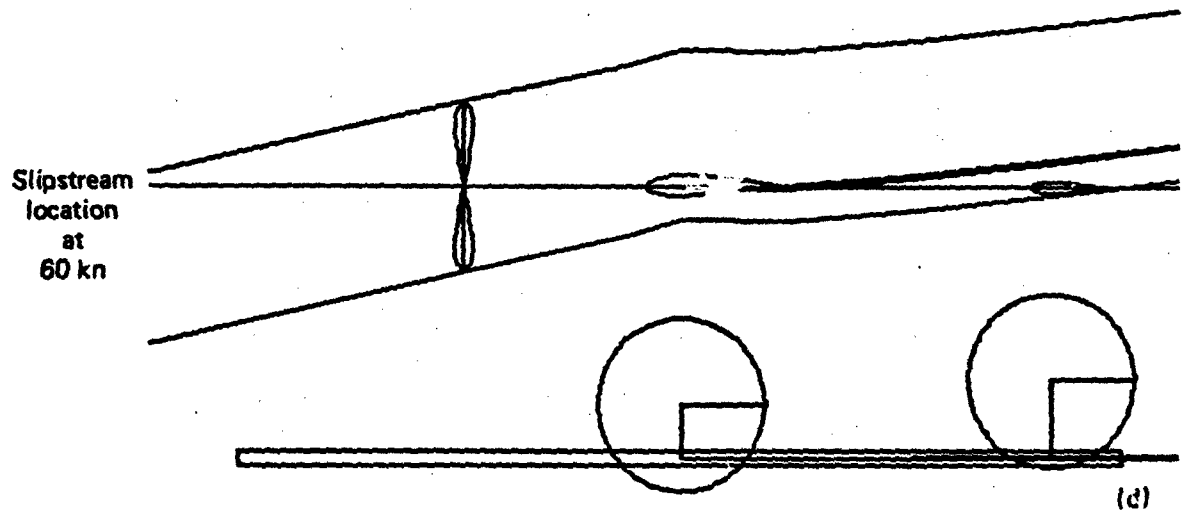

(d)

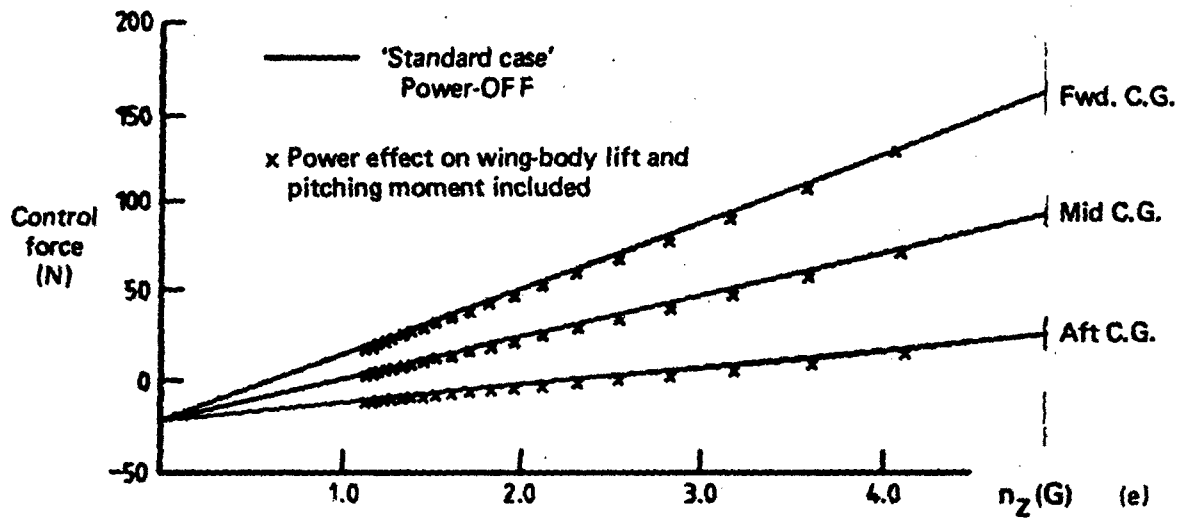

(e)

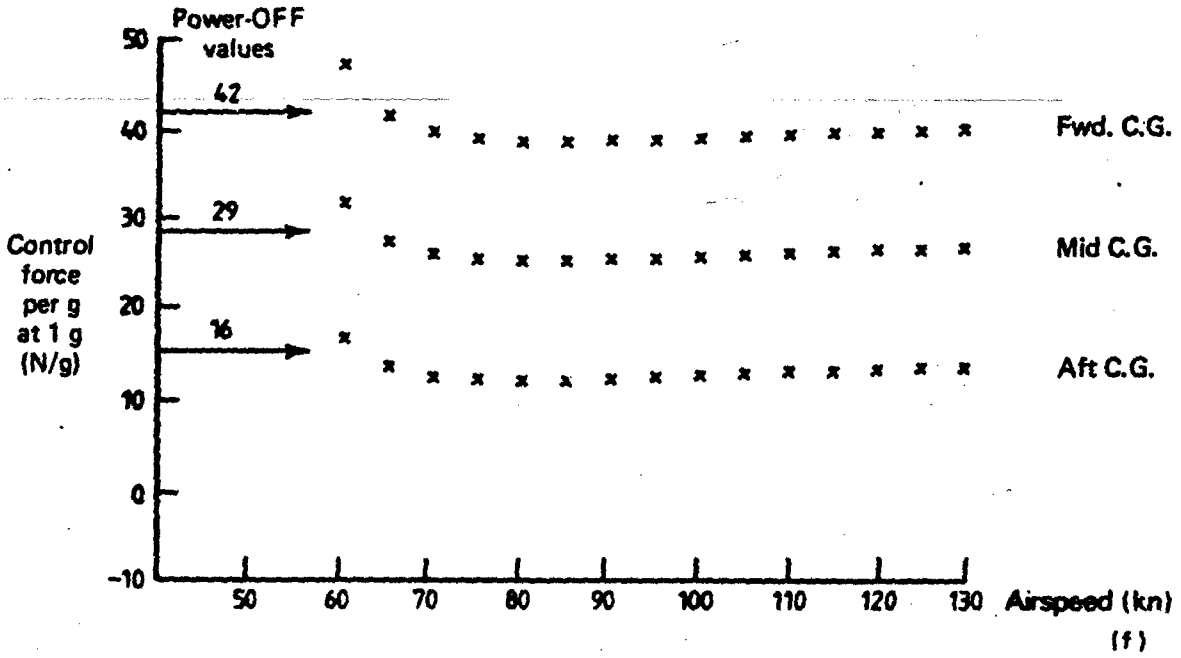

(f)

FIG. 10 EFFECT OF POWER ON WING-BODY LIFT AND PITCHING MOMENT

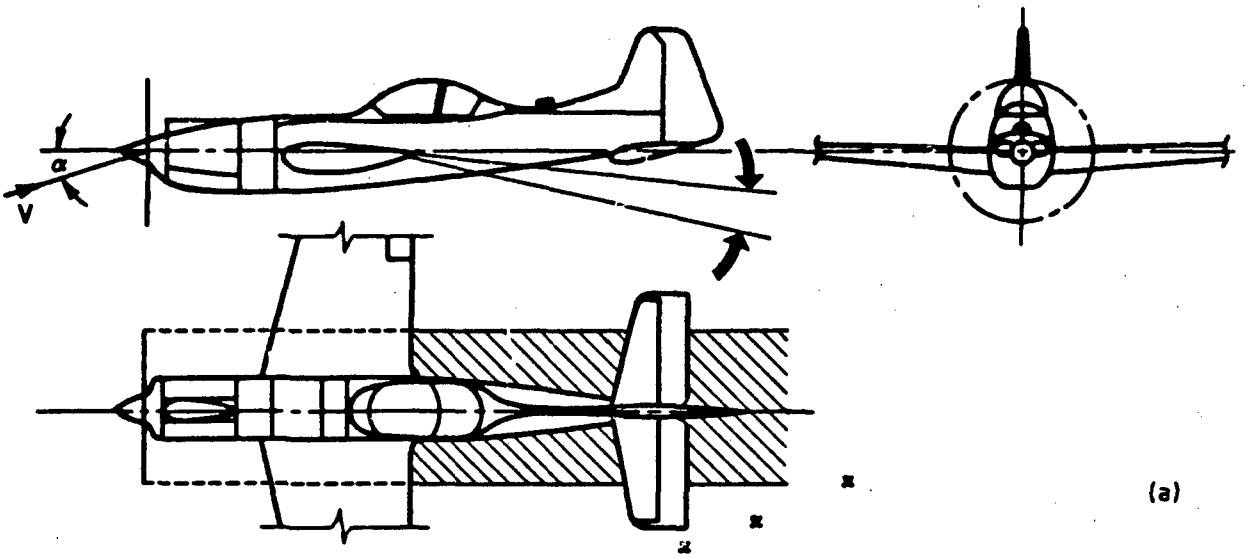

(a)

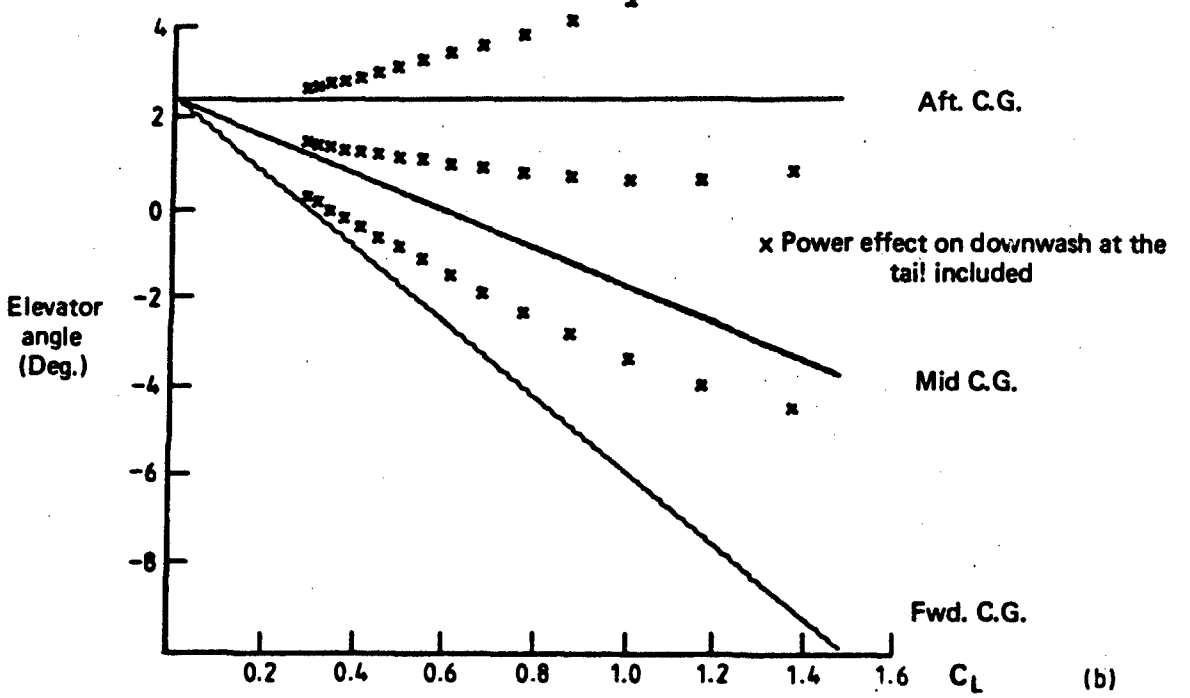

(b)

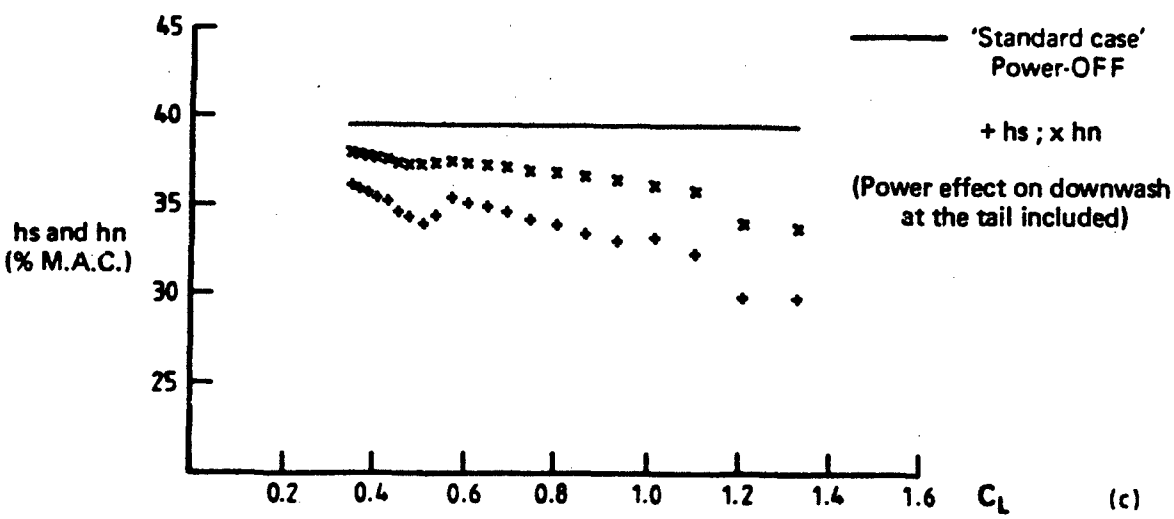

(c)

FIG. 11 EFFECT OF POWER ON DOWNWASH

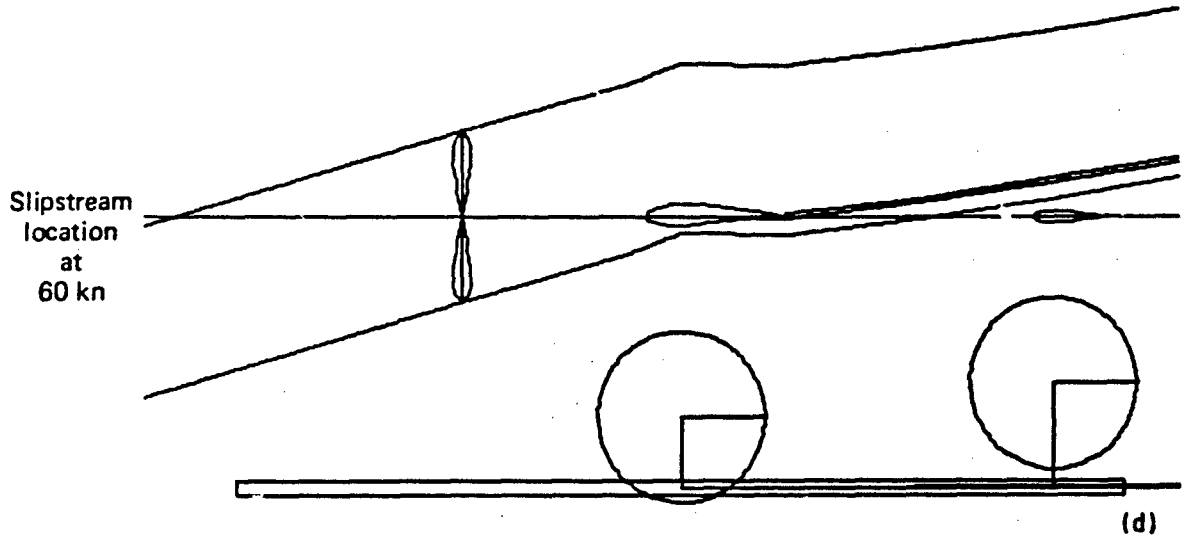

(d)

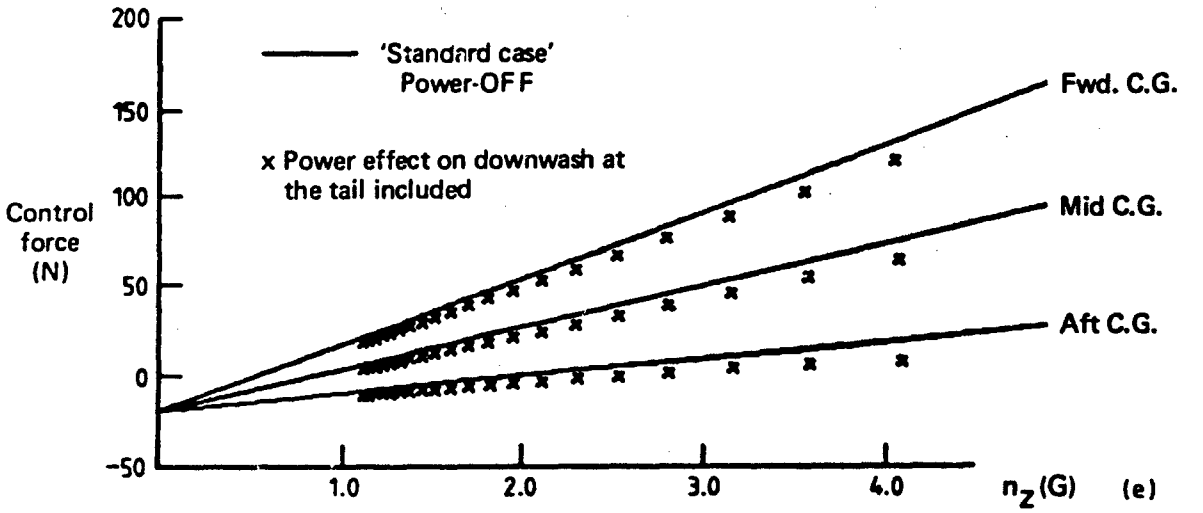

(e)

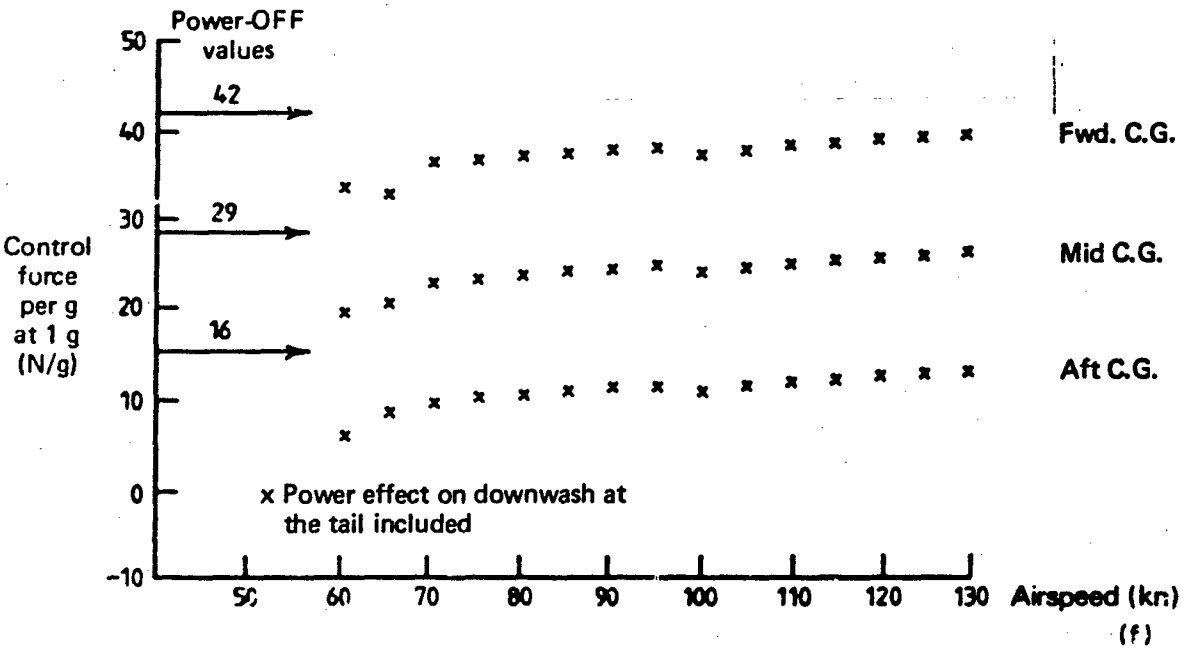

(f)

FIG. 11 EFFECT OF POWER ON DOWNWASH

represented. The accuracy of the technique for estimating downwash is not indicated in Reference 6. To obtain estimates with engineering accuracy, it is usually necessary to carry out powered model tests.

The effect of power is to increase the rate of change of mean effective downwash with incidence ($\partial\epsilon/\partial\alpha$), which decreases pitch stiffness and results in a forward movement of h_n as shown in Figure 11*c*.

The increase in C_T with decrease in V results in an increase in lift coefficient on the wing and body and hence an increase in downwash. This effect produces a negative increment in C_{m_V} and a small positive increment in C_{L_V} which results in a substantial reduction in h_s as shown in Figure 11*c*. For trimmed rectilinear flight, the downwash changes with incidence, and with aircraft velocity, give trim curves with a gentle curvature, as shown in Figure 11*b*.

It is shown later (in Figures 14*a* and 14*b*) that the increase in downwash is one of the main destabilising power effects, and is a major cause of the "flattening" of the trim curves at high C_L, a characteristic which is common in flight measurements.

For the "standard case", the results show that the aircraft velocity-related (V) effects are as significant as the incidence-related (α) effects. Consequently "static stability" will be degraded more than "manoeuvrability" by this effect.

The irregular variation in the h_s curve at $C_L = 0{\cdot}55$ (and to a lesser extent in the h_n curve) arises from a small discontinuity in the slopes of the thrust curves from Reference 7, where the data changes from climb to cruise conditions. These discontinuities are magnified when the derivatives associated with h_s and h_n are calculated numerically.

5.6 Effects of Power on Dynamic Pressure at the Tailplane

For the portion of the tailplane within the propeller slipstream, there is a net increase in the dynamic pressure with increasing power. In practice this increase will not be uniform because of non-uniformity of the flow leaving the propeller, of swirl in the slipstream, and the presence of the wing and body. As discussed in Section 3, this level of detail is not included in the estimation methods.

Assuming linear aerodynamic characteristics, the tailplane lift characteristics, which are discussed in this Section, and the hinge moment characteristics, which are discussed in Section 7, can be expressed as:

$$\left.\begin{aligned} C_{L_T} &= C_{L_{T_0}} + \frac{\partial C_{L_T}}{\partial \alpha_T}.\alpha_T + \frac{\partial C_{L_T}}{\partial \delta_e}.\delta_e + \frac{\partial C_{L_T}}{\partial \delta_t}.\delta_t \\ C_H &= C_{H_0} + \frac{\partial C_H}{\partial \alpha_T}.\alpha_T + \frac{\partial C_H}{\partial \delta_e}.\delta_e + \frac{\partial C_H}{\partial \delta_t}.\delta_t \end{aligned}\right\} \qquad (19)$$

where $\alpha_T = \alpha + i_T - \epsilon$,

and i_T = tailplane setting angle,

δ_e = elevator angle,

δ_t = trim tab angle.

Estimates for the effects of power, which are taken from Reference 5, assume that the aerodynamic coefficients in Equation (19) are all increased in proportion to the mean effective dynamic pressure ratio. Little information is available on the accuracy of this assumption.

The present discussion is confined to controls fixed stability; the case with the elevator free to float under the action of the hinge moments, i.e. the controls free case, is treated separately in Section 7. Since the dynamic pressure ratio acts as a multiplier to Equation (19), the tailplane lift will depend upon the magnitude of the dynamic pressure, and will change as the dynamic pressure changes with aircraft velocity (V) and incidence (α). The effective tailplane lift curve slope, $C_{L_{T\alpha_T}}$, is proportional to the dynamic pressure ratio, and so an increase in power will give an increase in tail effectiveness and, hence, an increase in pitch stiffness. As aircraft velocity (V) decreases and C_T increases, the total lift force on the tail will alter in proportion to the increase in dynamic pressure. If the net tailplane lift is upwards, then decreasing V will result in a nose-down pitching moment, giving a positive C_{m_V} increment, which as discussed in Section 2, is stabilising. Conversely if the net tailplane lift is downwards, the C_{m_V}

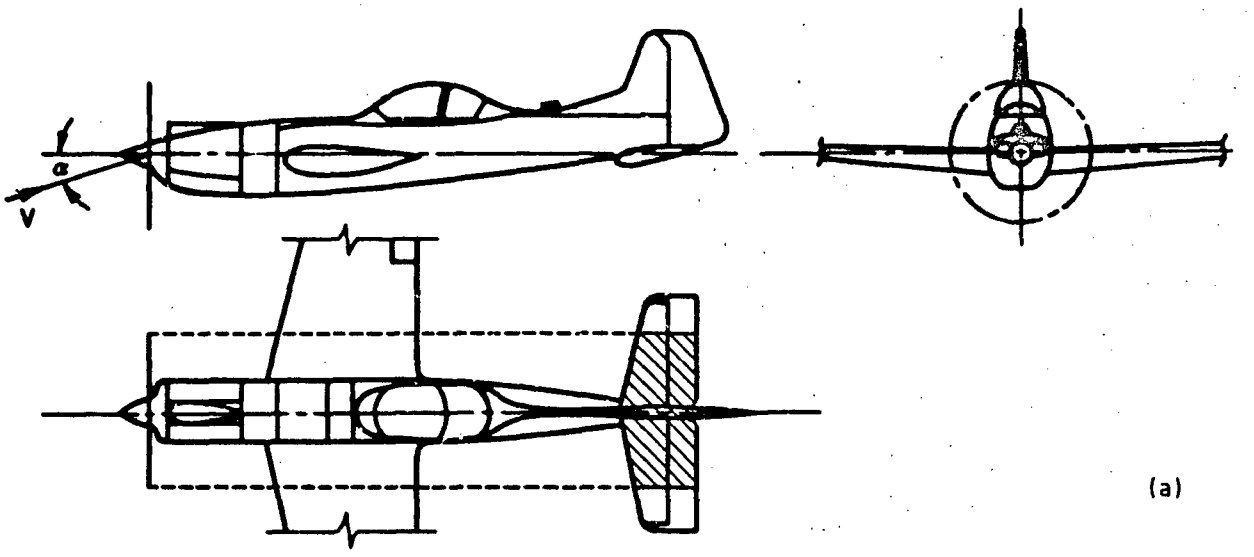

(a)

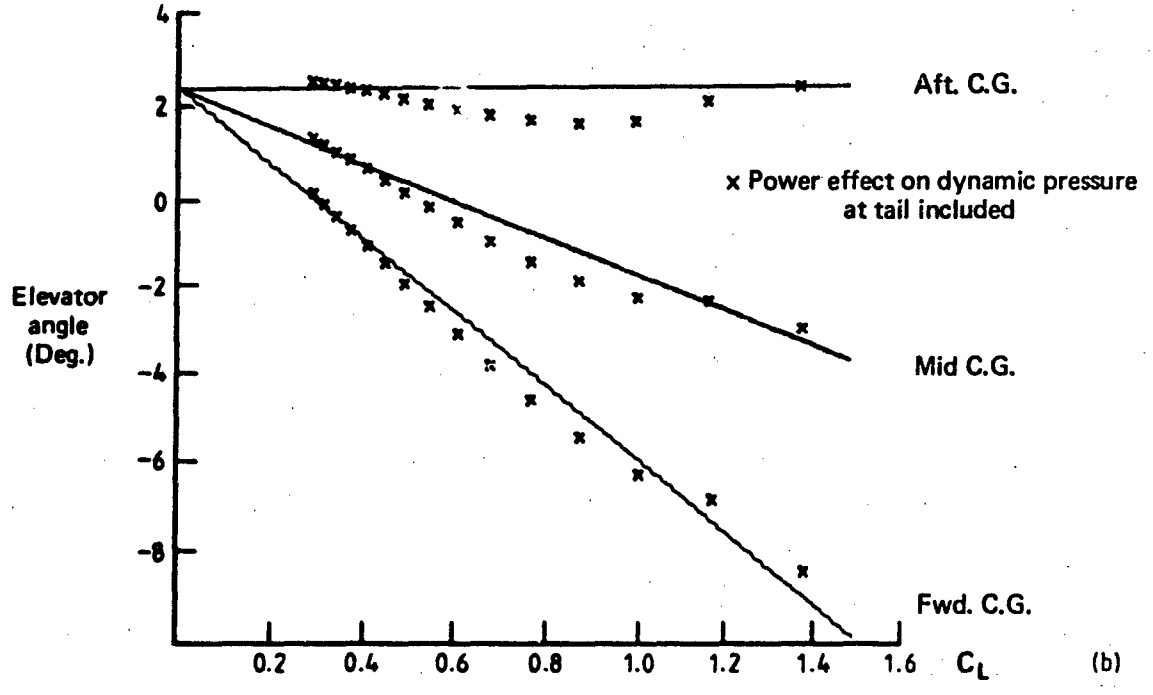

(b)

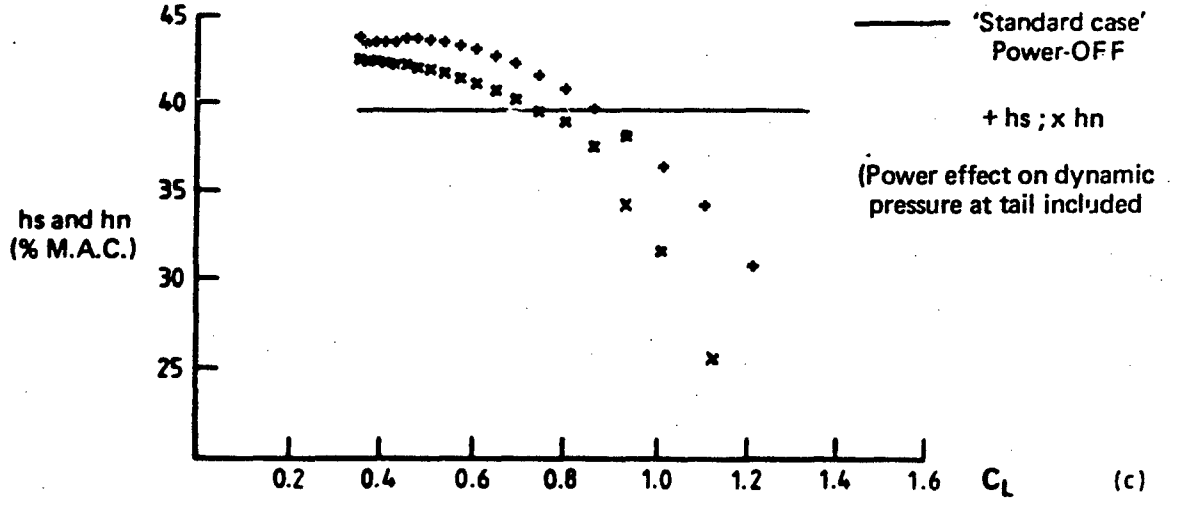

(c)

FIG. 12 EFFECT OF POWER ON DYNAMIC PRESSURE AT THE TAIL

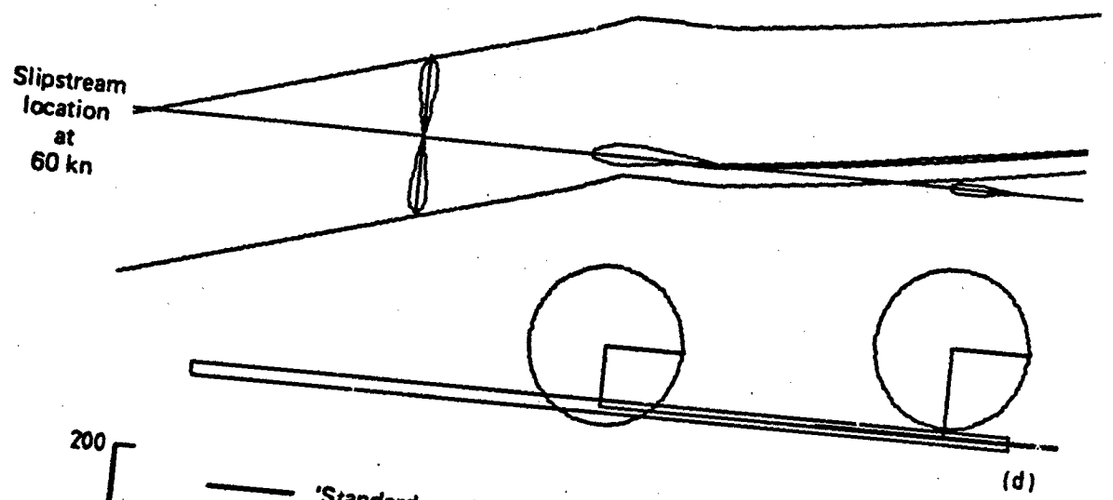

(d)

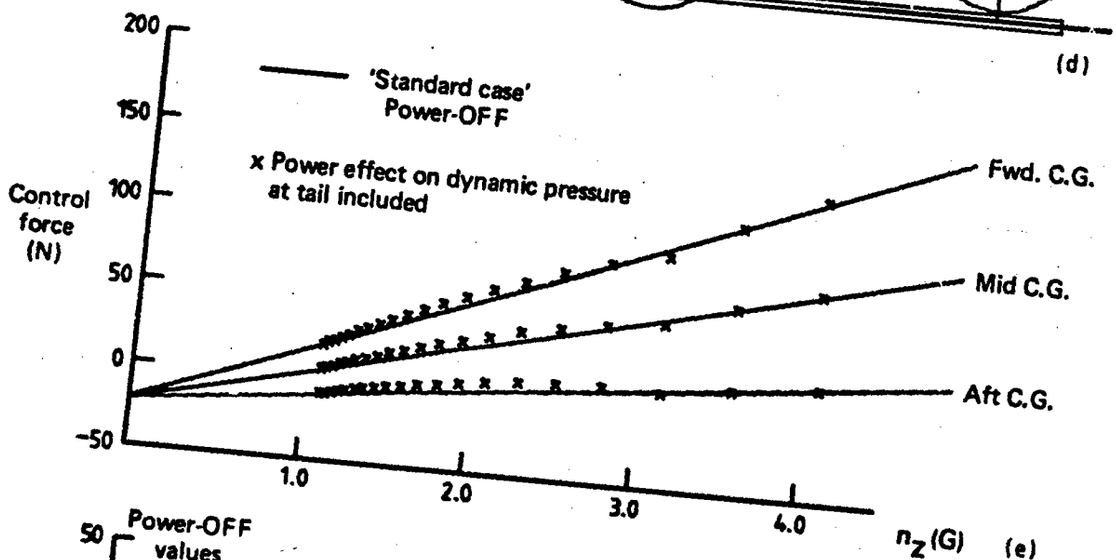

(e)

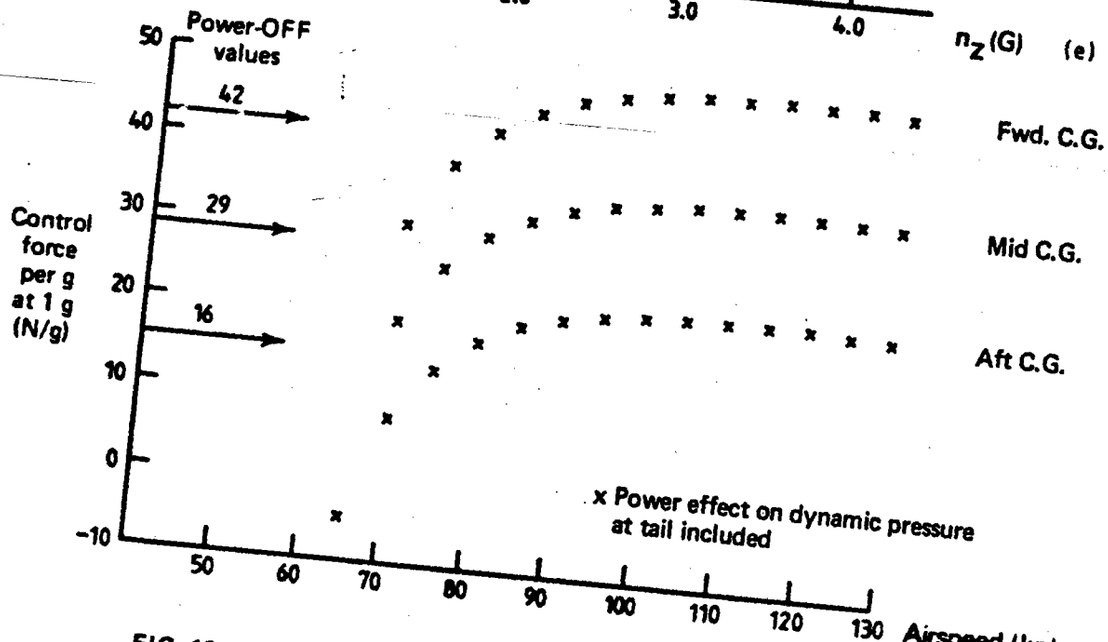

(f)

FIG. 12 EFFECT OF POWER ON DYNAMIC HEAD AT THE TAIL

contribution will be negative and hence destabilising. With flaps zero, most conventional aircraft experience a down tail load only at high speeds where power effects are small. With flaps deflected, the tailplane may carry a download at all speeds, and in this case, the destabilising effect of aircraft velocity on dynamic pressure ratio may be substantial.

Depending upon the relative positions of the tailplane and slipstream, it is possible for the mean effective dynamic pressure ratio to vary also with changes in incidence. For example, if the tailplane enters the slipstream as aircraft incidence is increased to maintain rectilinear flight, and the tailplane is carrying a download, then pitch stiffness, and hence stability will be reduced. The influence of tailplane location in the presence of power and with wing flaps deflected is discussed in Section 6, and an example of the destabilising effect of dynamic pressure is given in Section 9.

For the "standard case", the tailplane load becomes negative only at high speeds. At these speeds, the increase in effective tail lift curve slope more than compensates for the destabilising effects due to tailplane download, as shown in Figure 12*c*. At low speeds the tailplane load is upwards but, as Figure 12*d* shows, the tailplane emerges from the slipstream at these speeds and so causes a substantial reduction in stability (as shown in Figure 12*c*).

Because the accuracy of the slipstream representation used in this Report is difficult to establish, the magnitude of the changes, demonstrated in Figure 12*c*, should only be regarded as indicative of the nature of the changes that could occur in practice.

5.7 Combined Power Effects

The summation of the power effects previously described, is shown in Figure 13 for the "standard case" aircraft layout. The results are characterised by a substantial decrease in the static stability limit (h_s) with power at low speeds. The effects are larger than the flight-measured effects shown in Reference 56 for several single-engine propeller-driven aircraft. However, as will be indicated in Section 9, this is partly due to the rather unusual layout of the "standard case" aircraft in which propeller, wing, and tail, are located at the same height.

At maximum power and maximum C_L, the reduction in h_s, compared with the power-off case, is 13%$\bar{c}$ while the reduction in h_n is 11%$\bar{c}$. The reduction in stability is also reflected in the trim curves as an upwards divergence from the power-off case as C_L increases. As illustrated in the previous Sections, the major causes of the reduction in stability are, in order of severity, the effect of power on: (i) downwash, (ii) dynamic head at the tailplane, (iii) propeller normal force and (iv) wing–body characteristics. These contributions are illustrated in Figures 14*a* and 14*b* which show the change in h_s and h_n as the power effects are accumulated in the order discussed in Sections 5.2–5.6. For the "standard case", the normal beneficial effect of power on tailplane dynamic head is not sustained at high C_L because of the emergence of the tailplane from the slipstream as incidence increases.

Although the net difference between h_s and h_n is only approximately 2%$\bar{c}$, it can be seen from Figures 14*a* and 14*b* that larger differences occur in the individual effects. This observation is emphasized by the results for the wing–body effects, which were presented in Table 3 in Section 5.3.

The loss in pitch stiffness with increasing incidence is also evident in the control force per g measurements. The control force decreases with increasing g as shown in Figure 13*e* for $V = 120$ kn, and the 1g control force per g values decrease with decreasing trim speed, as shown in Figure 13*f*.

Because of the idealised representation of the slipstream used in this Report, and the particular features of the "standard case" layout, the net power effects demonstrated are larger than is usually experienced. Results for a more typical aircraft layout are presented and discussed in Section 9.

6. EFFECT OF POWER ON LONGITUDINAL STABILITY WITH CHANGES IN AIRCRAFT LAYOUT AND CONFIGURATION

6.1 Thrust Axis Setting Angle and Vertical Position

A common method of increasing longitudinal stability power on, is to incline the thrust axis nose down, so that the moment arm about the aircraft c.g. gives an increasing nose-down pitching moment with increasing thrust coefficient, C_T. Therefore, for rectilinear flight, a positive increment in C_{m_T} is produced which moves h_s rearwards. This direct effect produces no change

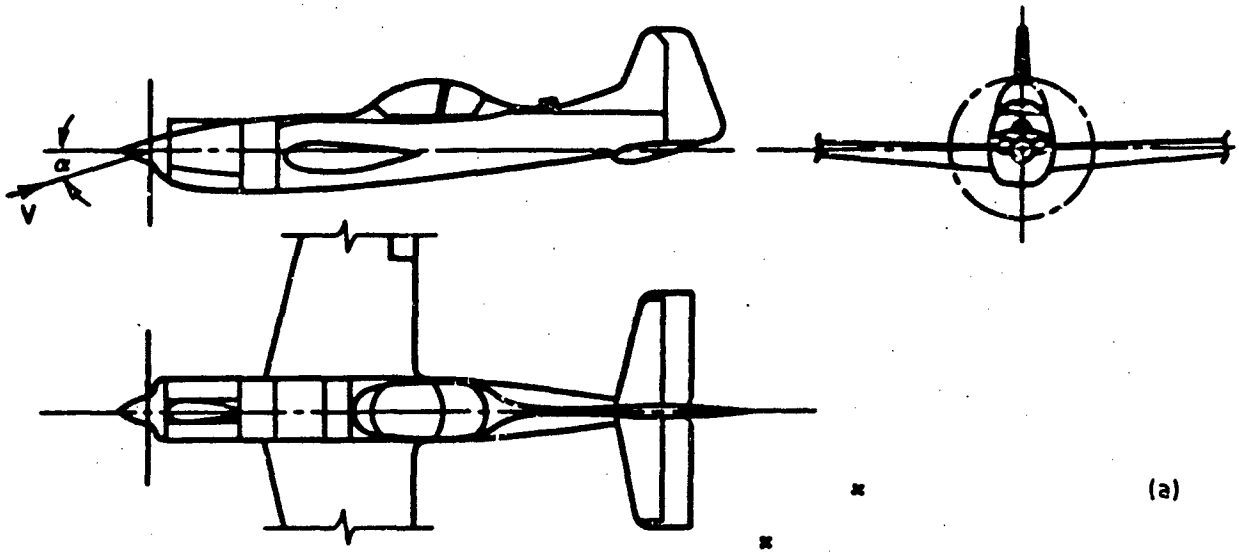

(a)

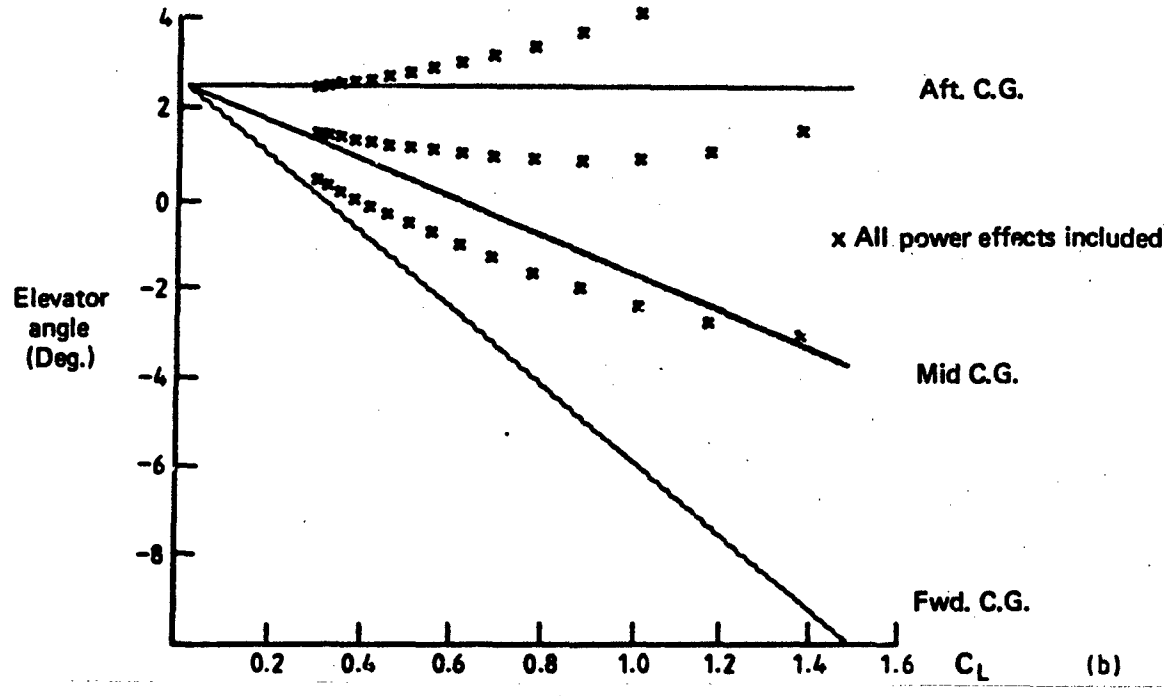

(b)

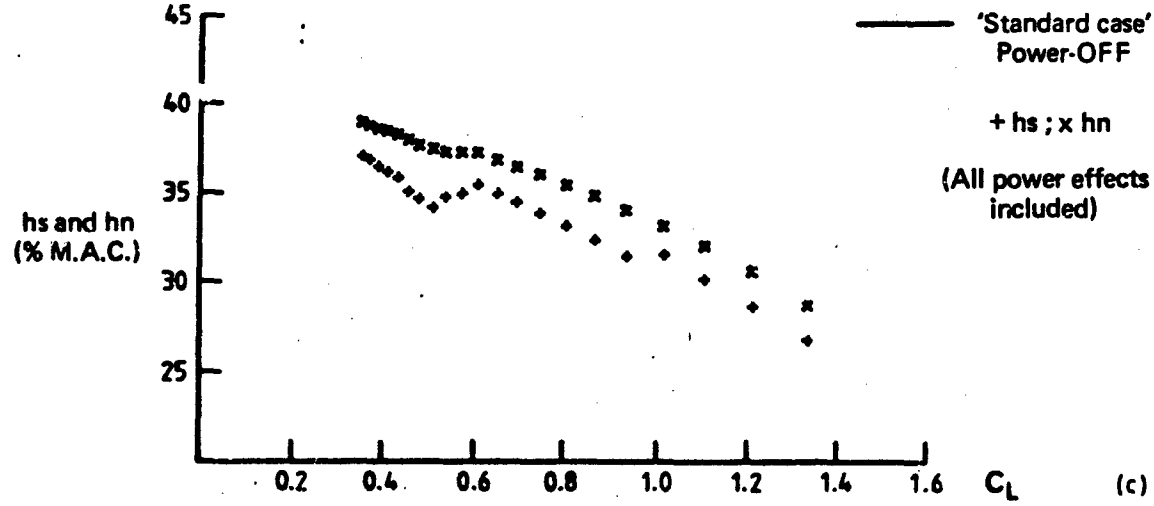

(c)

FIG. 13 COMBINED POWER EFFECTS FOR THE 'STANDARD CASE'

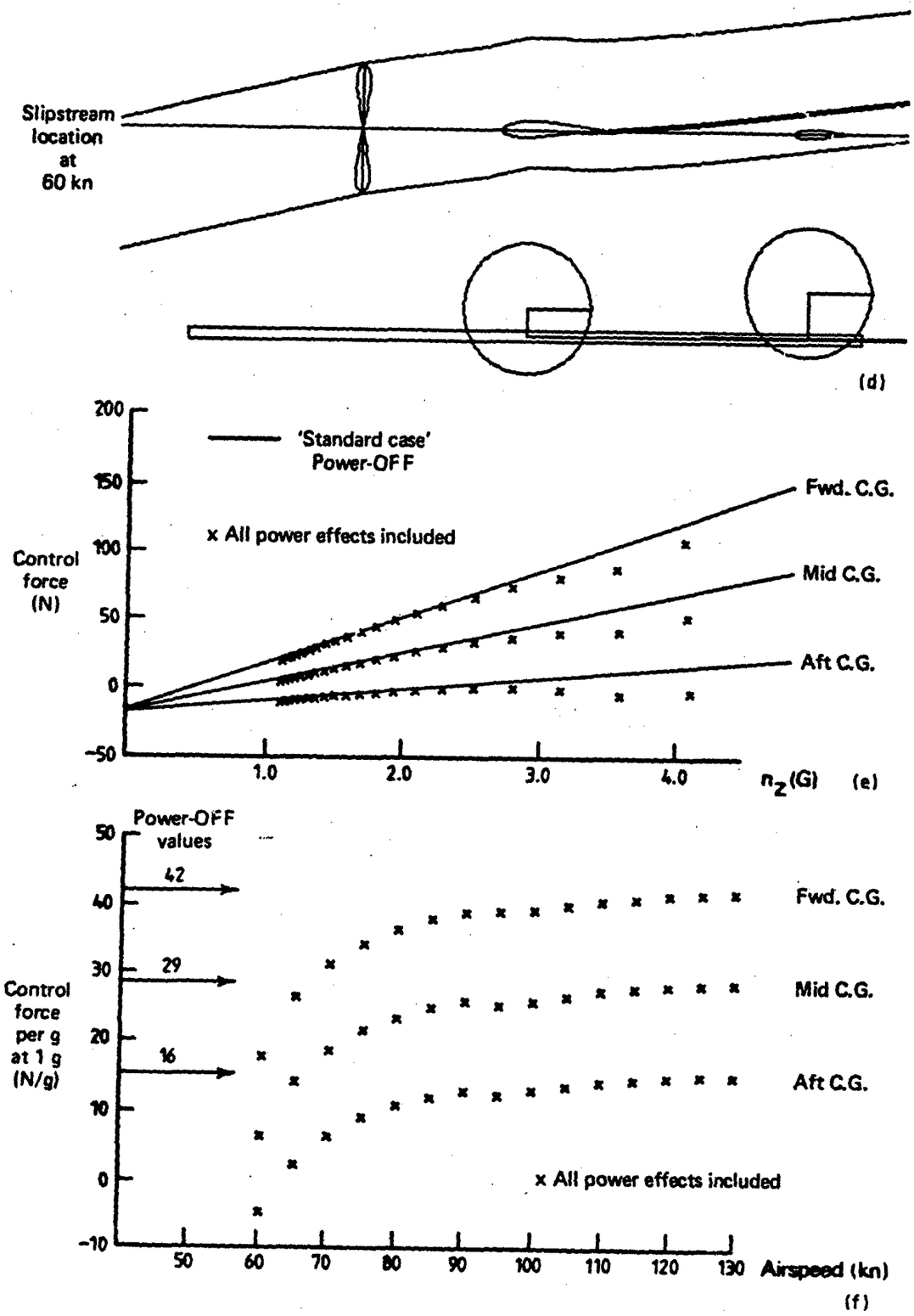

FIG. 13 COMBINED POWER EFFECTS FOR THE 'STANDARD CASE'

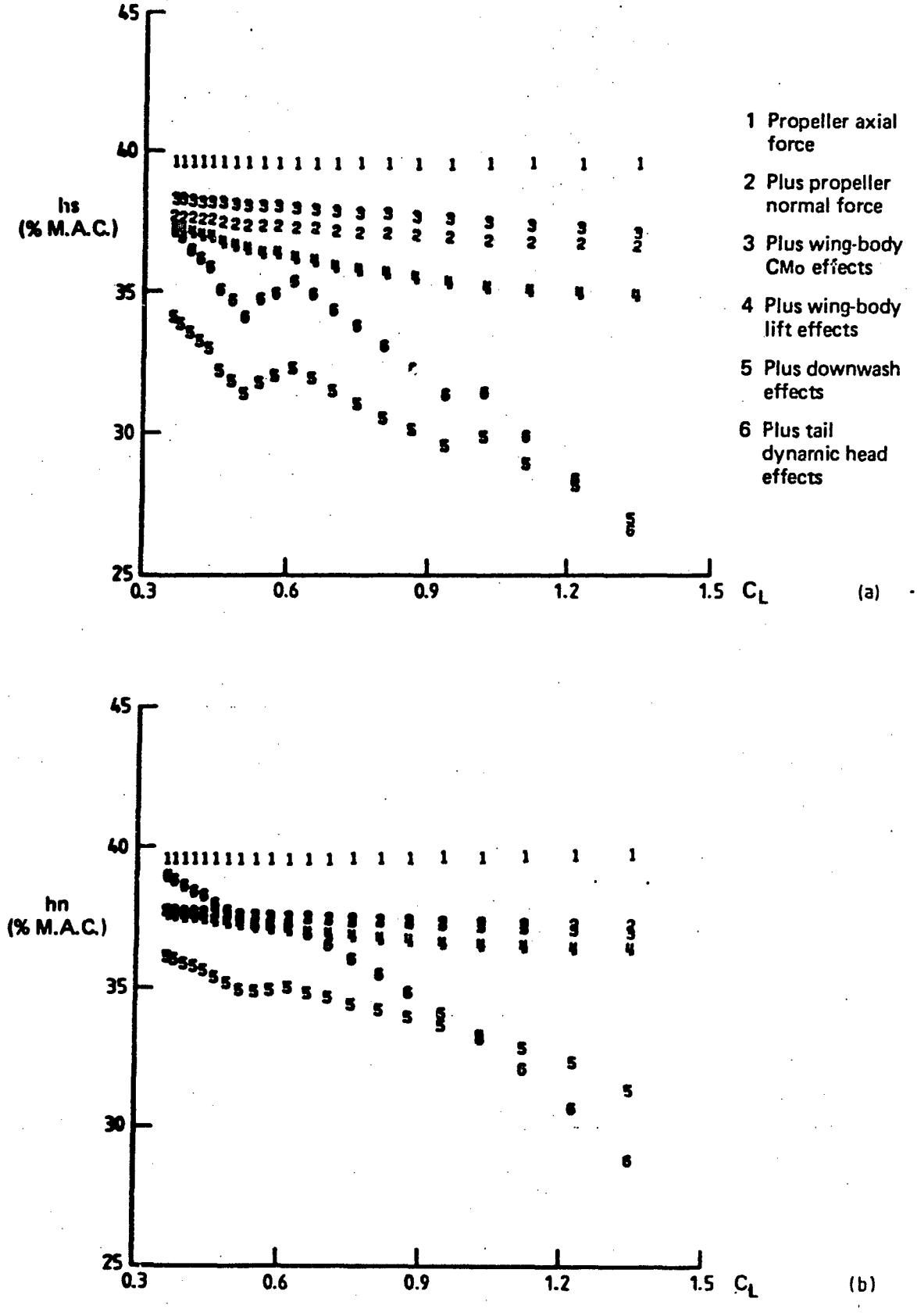

FIG. 14 ACCUMULATION OF POWER EFFECTS ON hs AND hn 'STANDARD CASE'

in pitch stiffness and hence none in h_n. This design capability may be useful where there is a need to increase "static stability" without changing "manoeuvrability".

Because of secondary effects, the expected improvement in "static stability" may not be realised. To illustrate these secondary effects, calculations have been made for two cases: In the first case (Figs 15 and 16), the thrust line is inclined 5 deg. nose down to the horizontal body reference line and, in the second case (Figs. 15 and 17), the thrust axis is raised 0·235 m to give the same thrust moment arm as the first case, for a c.g. location of 40%$\bar{c}$. The power-off effects due to these changes are negligible and so are not presented. Figure 15*d* shows that the net effect of inclining the thrust axis 5 deg. is to increase h_n by approximately 3½%$\bar{c}$ at all speeds, while the net effect of raising the thrust line is to increase h_n by 1%$\bar{c}$ at high speeds and 2%$\bar{c}$ at low speeds. In both cases, the direct thrust effect in isolation will increase h_n by 2½%$\bar{c}$ at high speeds and 3½%$\bar{c}$ at low speeds with maximum power. The net changes due to secondary effects arise from small changes in the different power effects discussed in Section 5. These are mainly caused by the difference in slipstream loci as shown in Figure 15*f*. For the raised thrust line, the slipstream locus is simply displaced. For the inclined thrust line, the propeller normal force variation is displaced with respect to incidence, compared with the "standard case". Consequently the deflection of the slipstream through the propeller at a given incidence will be different. The resulting changes to the various power effects, though small, are detailed below.

As discussed in Section 5.3, the variation of propeller normal force with C_L in rectilinear flight is approximately parabolic. With the thrust axis inclined downwards 5 deg. the propeller operates over a lower incidence range and the maximum reduction due to this effect is 0·5%$\bar{c}$ less than for the "standard case", as shown by comparison of Figures 14*a* and 16*a*. For the raised thrust line, the propeller normal force contribution does not change.

As discussed in Section 5.4, the downwash due to propeller normal force results in an increase in stability due to its influence on wing–body lift-curve slope. Because of the lower propeller normal force with the inclined thrust axis, this increase will be less. Comparison of Figures 14*c* and 16*a* indicates that the net reduction in h_n due to the propeller plus wing–body effect, is 1%$\bar{c}$ less than for the "standard case". Very little change would be expected from the effect of dynamic pressure on wing–body C_{m_0} and C_{L_α} since Figure 15*f* shows that, the area immersed within the slipstream has hardly changed. Consequently, most of the change is attributed to propeller normal force and associated downwash. Comparison of Figures 14*a* and 17*a* shows that, for the raised thrust line, the reduction in h_n due to propeller and wing–body effects is 0·5%$\bar{c}$ less than for the "standard case" at a trim C_L of 0·8. This can be attributed to the smaller area of wing and body immersed within the slipstream, as shown in Figure 15*f*.

Comparison of Figures 16*a* and 17*a* with Figure 14*a* shows that, with both the inclined thrust axis and the raised thrust axis, the effect of power on downwash, as indicated by the difference between curves 4 and 5, is virtually the same as for the "standard case". However, the effect of power on tailplane dynamic head, indicated by the difference between curves 5 and 6, is virtually unchanged for the inclined thrust case, but reduces h_n compared with the "standard case" when the thrust axis is raised.

In summary, for the aircraft layout considered, the expected improvement in "static stability" due to inclining the thrust axis is modified only slightly due to secondary power effects. For the raised thrust line, only 50% of the expected improvement is realised at low speeds, due to a less favourable slipstream location at the tailplane.

6.2 Wing Setting Angle and Vertical Position

Wing setting angle is determined by general design considerations such as ensuring minimum drag in the cruise, providing good pilot visibility for landing, or, in the case of passenger aircraft, maintaining the fuselage approximately horizontal in cruising flight. Normally the wing setting angle lies in the range 1 to 3 deg.

In the simple theory of "static stability", wing setting angle by itself does not affect pitch stiffness and hence does not change longitudinal stability. The main design consideration is the maintenance of a satisfactory elevator operating range, usually by adjustment of tailplane setting angle. In practice, both trim and stability characteristics are altered both with power off and power on. These effects are illustrated in Figures 18 and 19 for the "standard case" using wing setting angles from 1 to 3 deg.

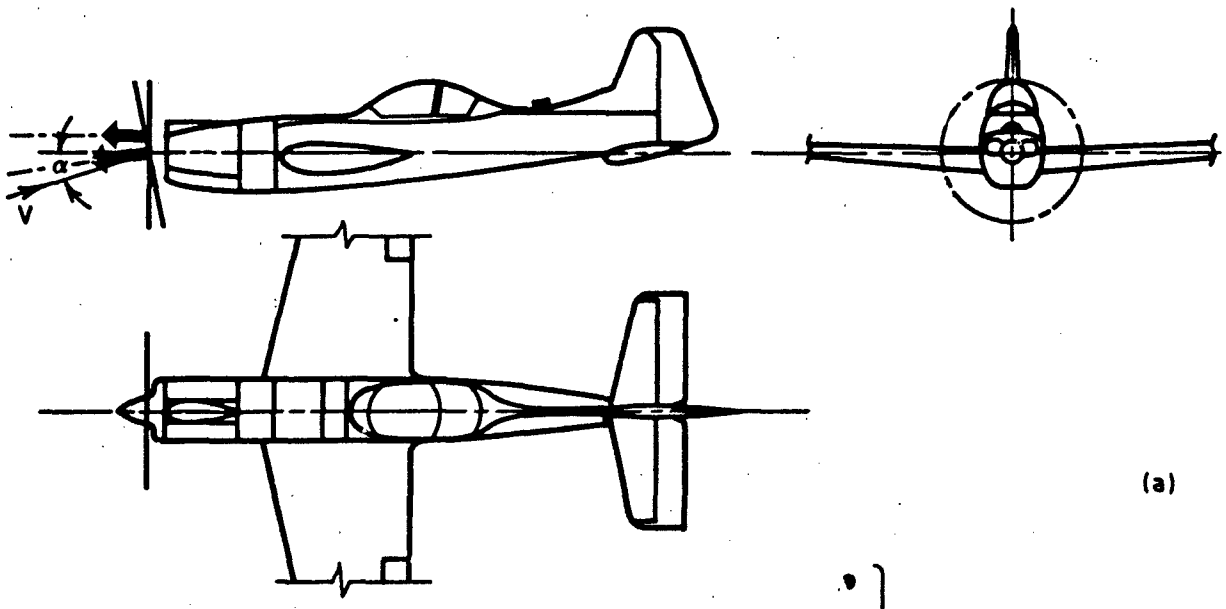

(a)

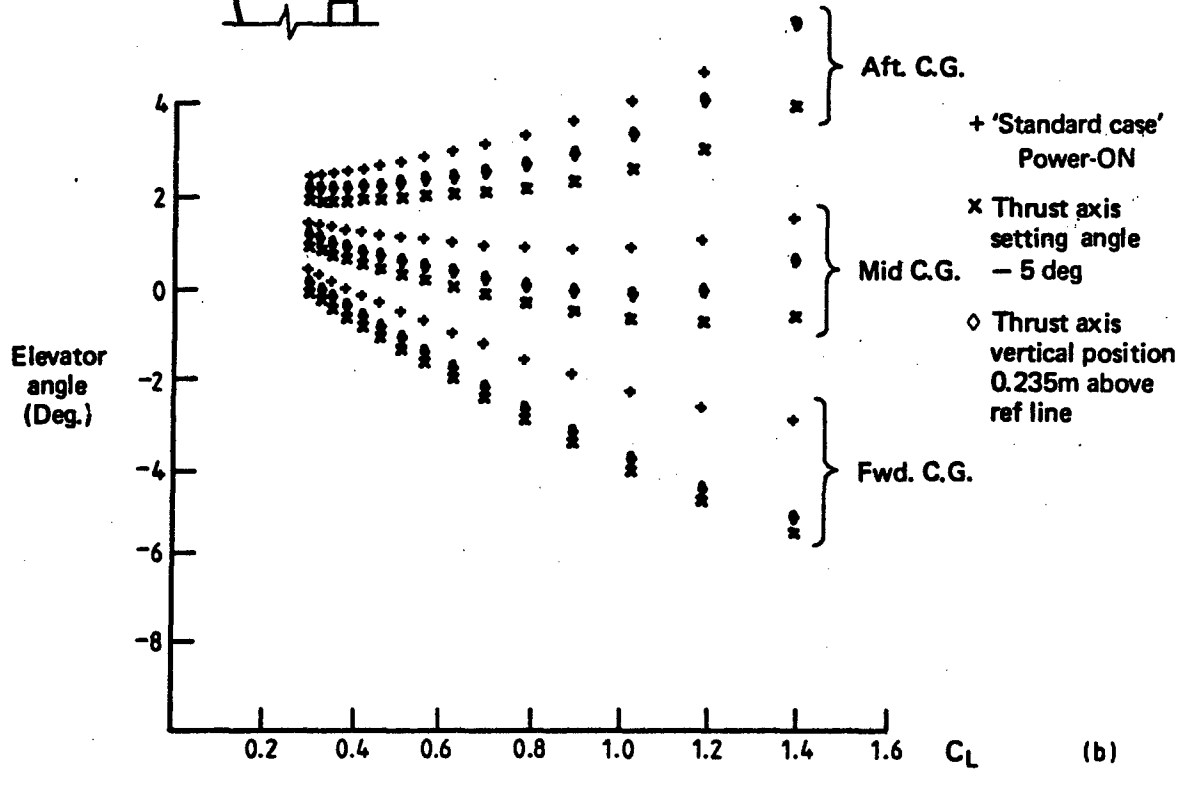

(b)

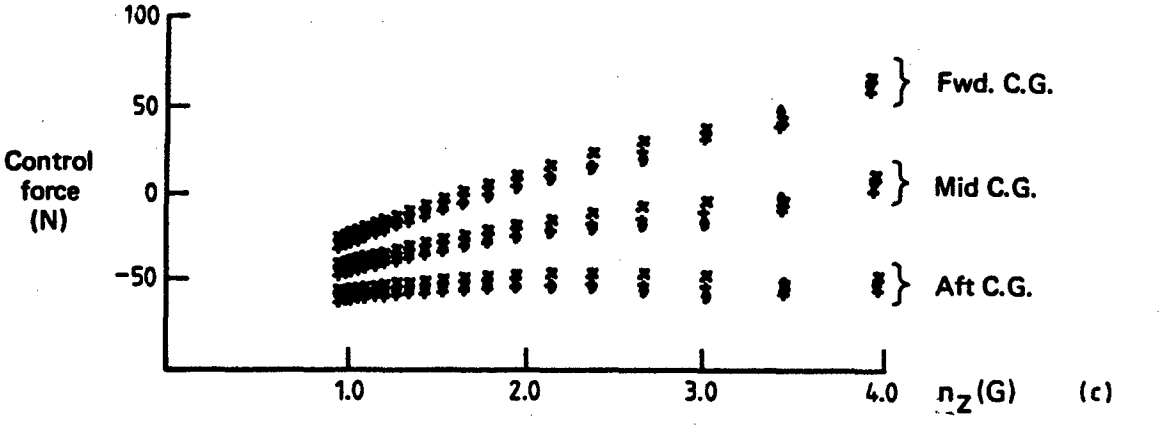

(c)

FIG. 15 THRUST AXIS SETTING ANGLE AND VERTICAL POSITION (POWER-ON)

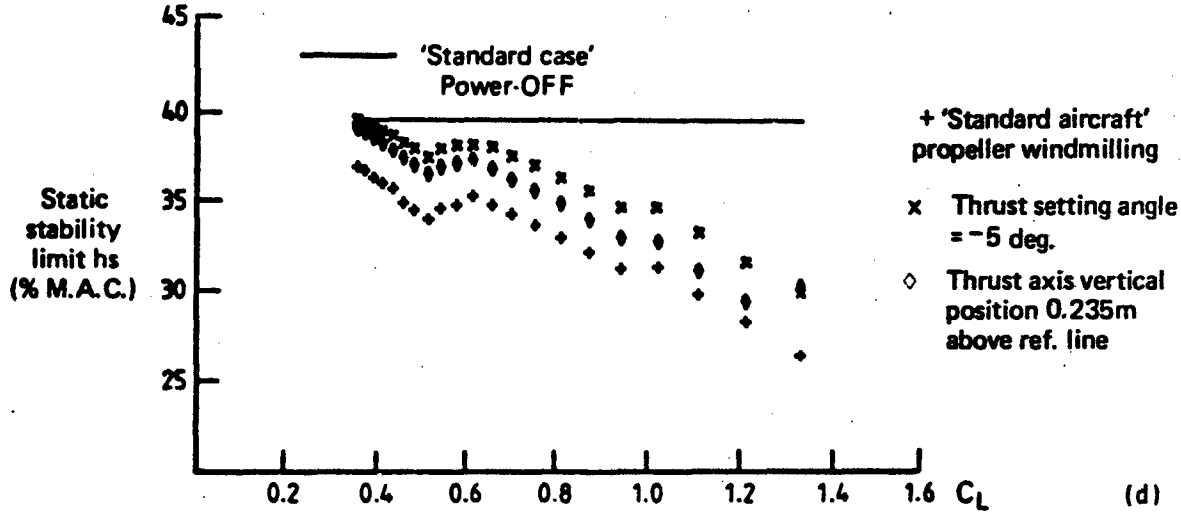

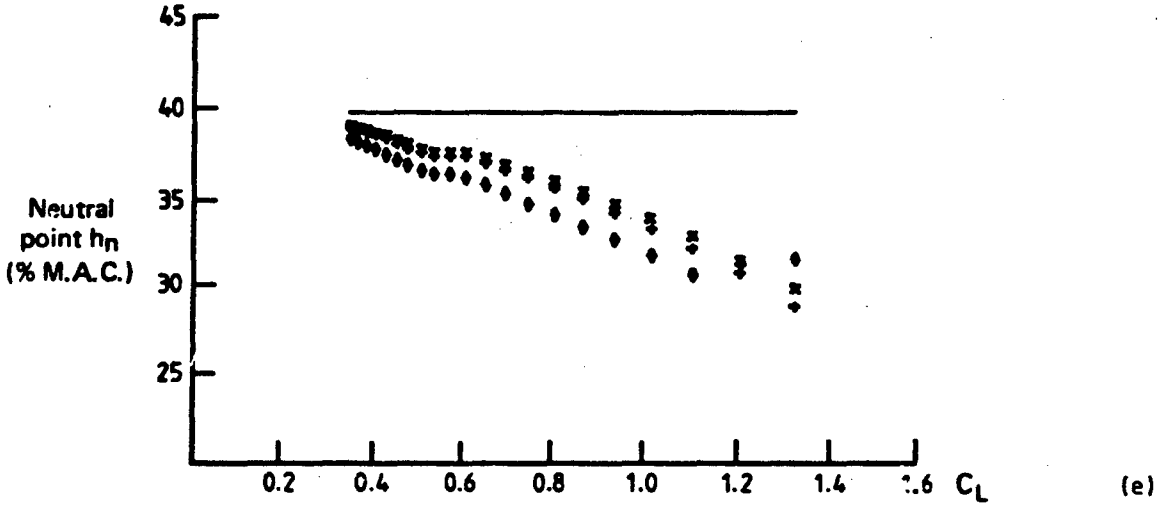

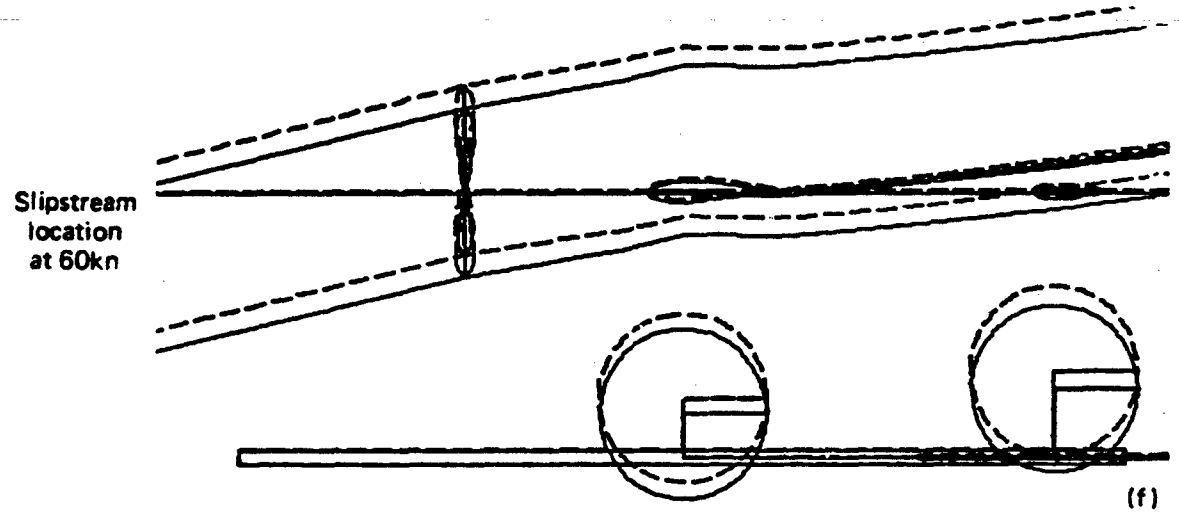

FIG 15 THRUST AXIS SETTING ANGLE AND VERTICAL POSITION (POWER-ON)

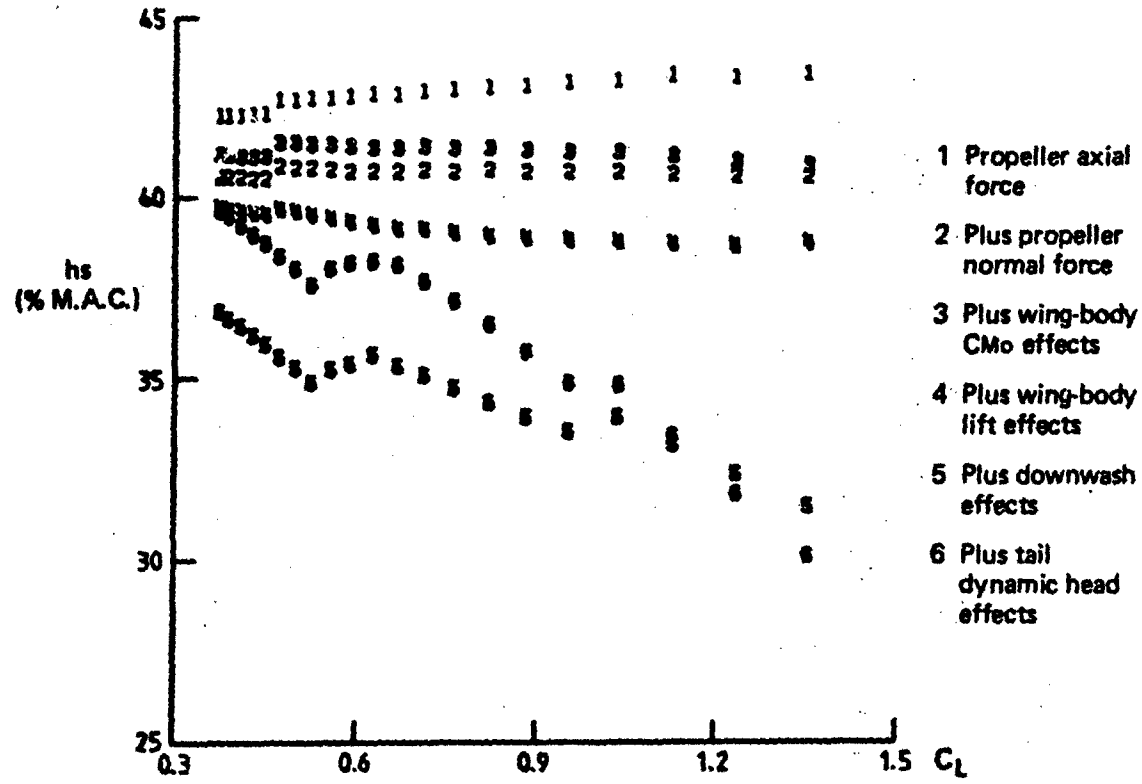

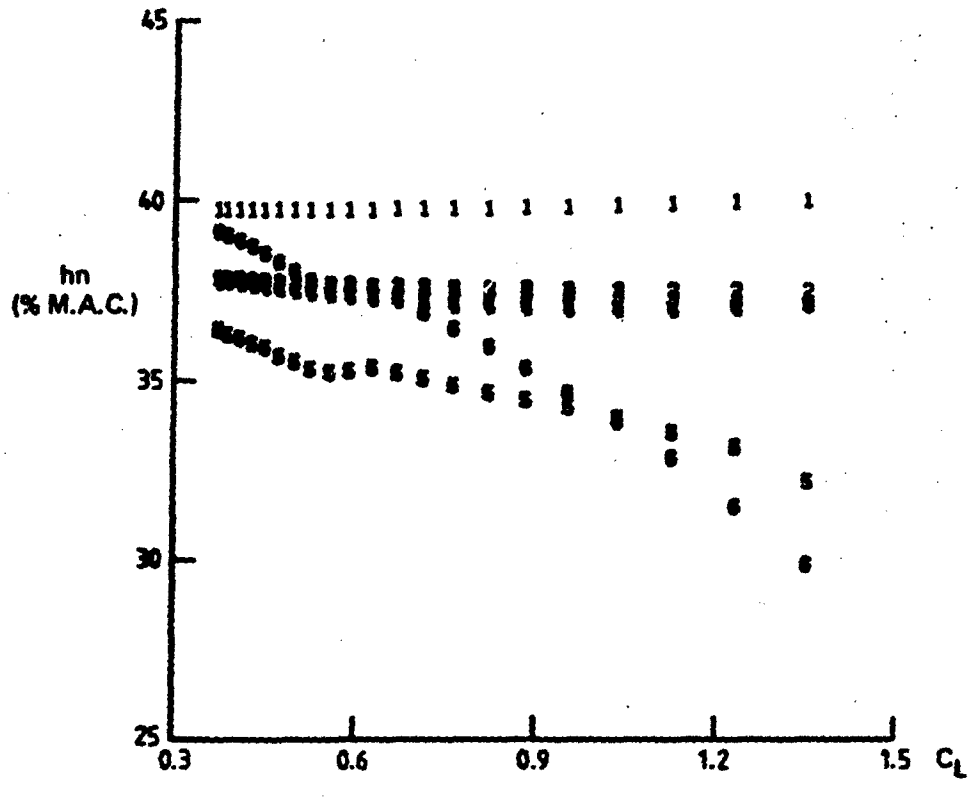

FIG. 16 ACCUMULATION OF THRUST EFFECTS ON hs AND hn THRUST AXIS = −5 DEG.

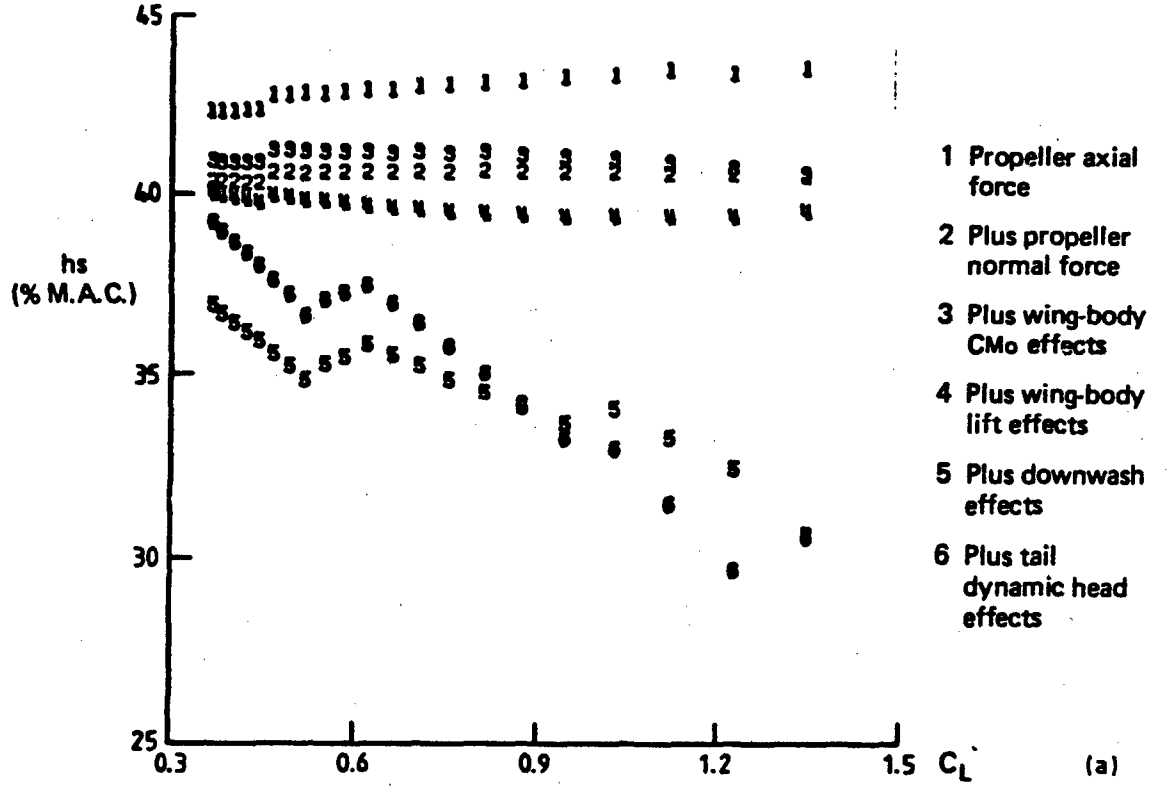

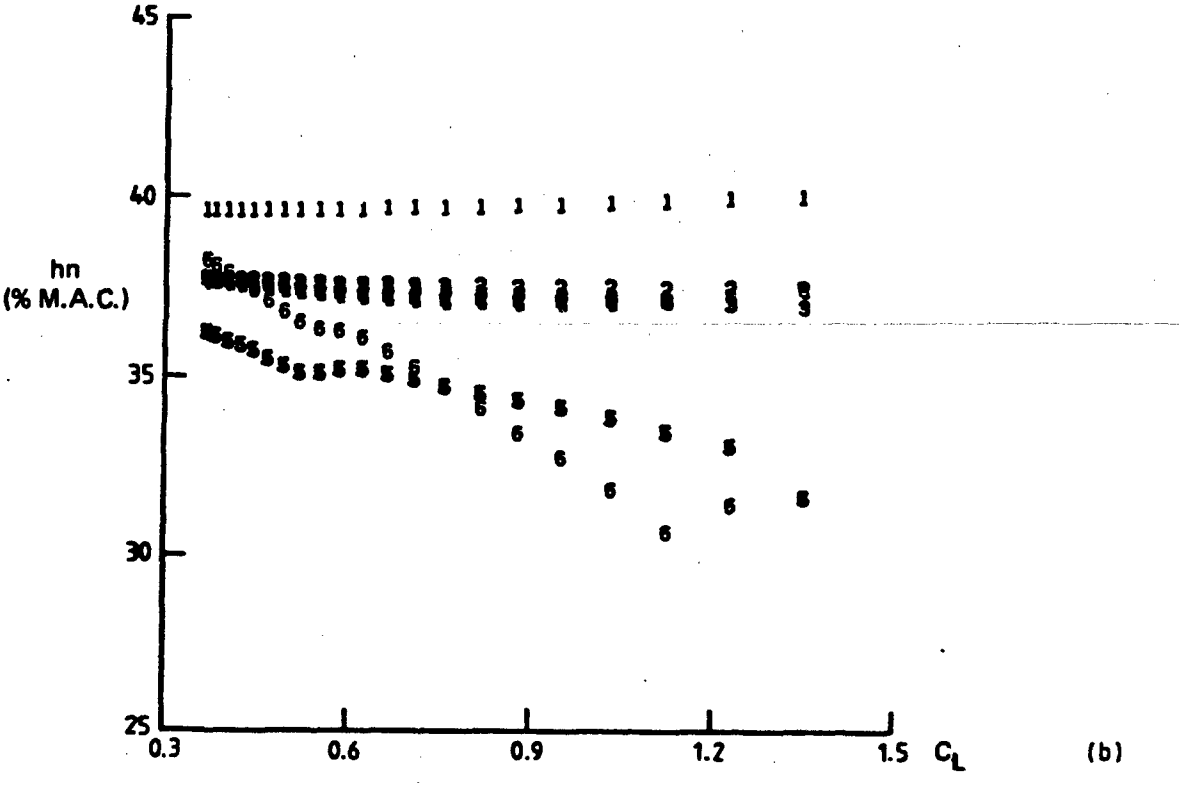

FIG. 17 ACCUMULATION OF POWER EFFECTS ON hs AND hn THRUST AXIS RAISED .235M

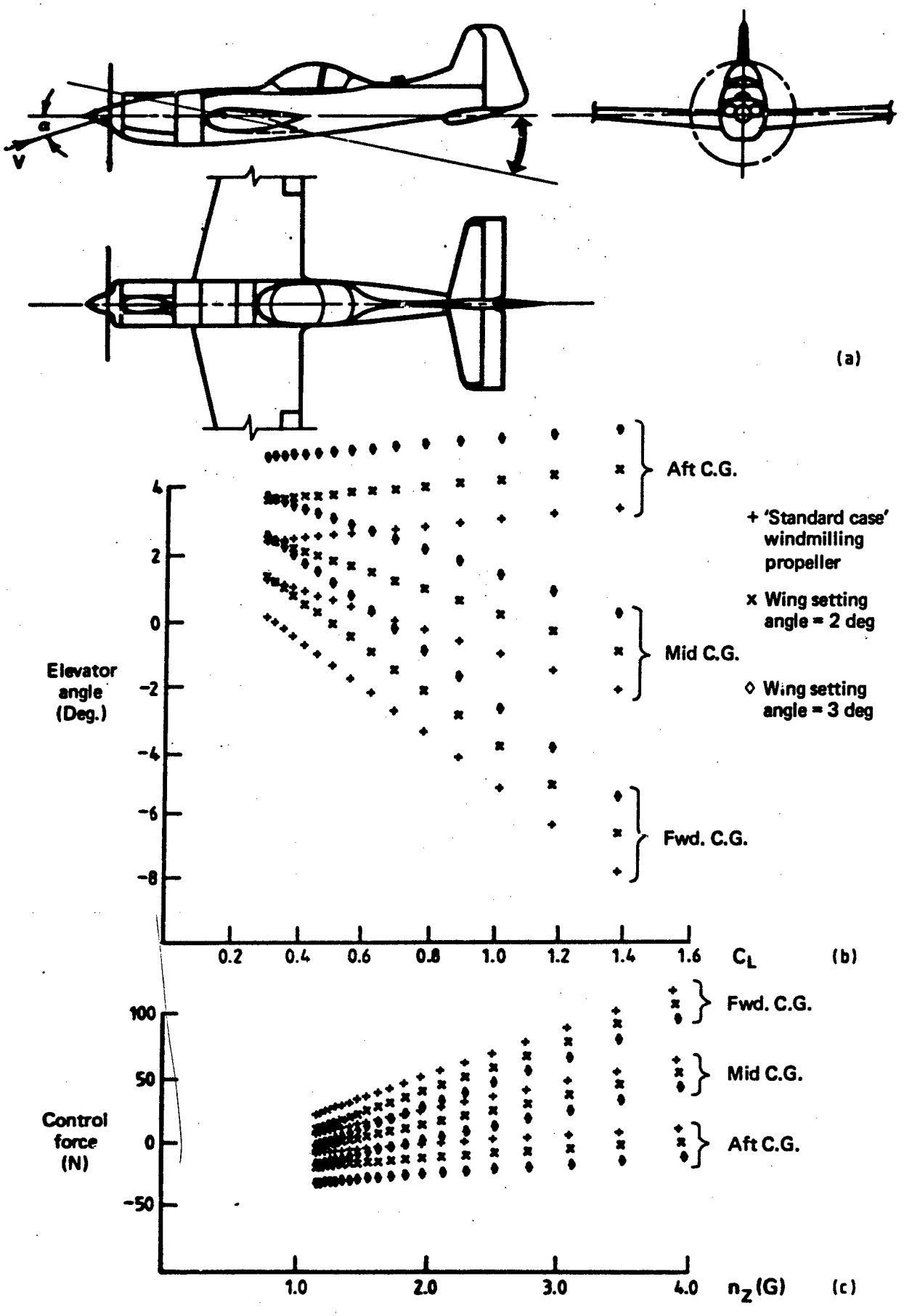

FIG. 18 EFFECT OF WING SETTING ANGLE (POWER-OFF)

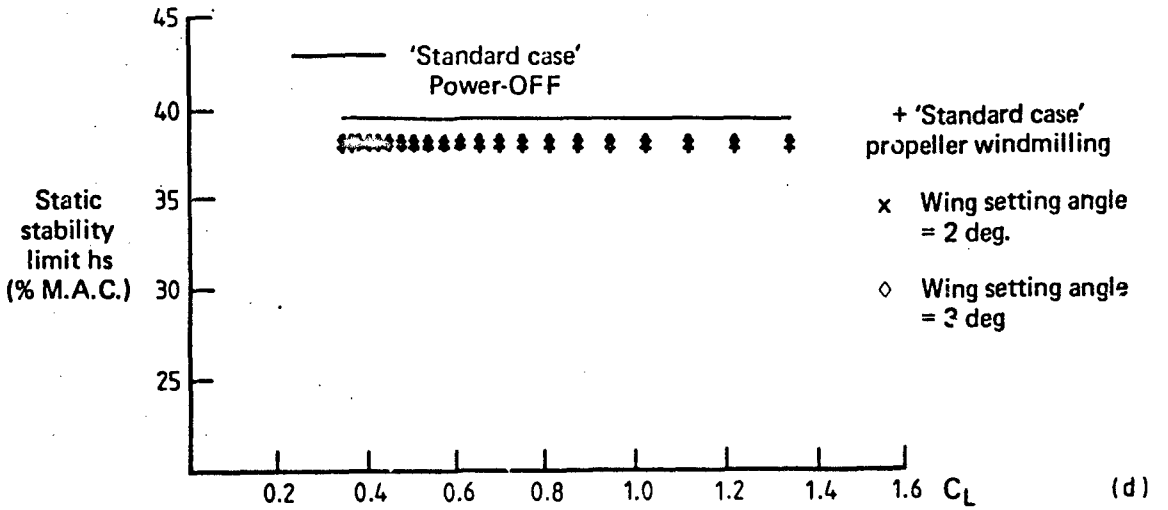

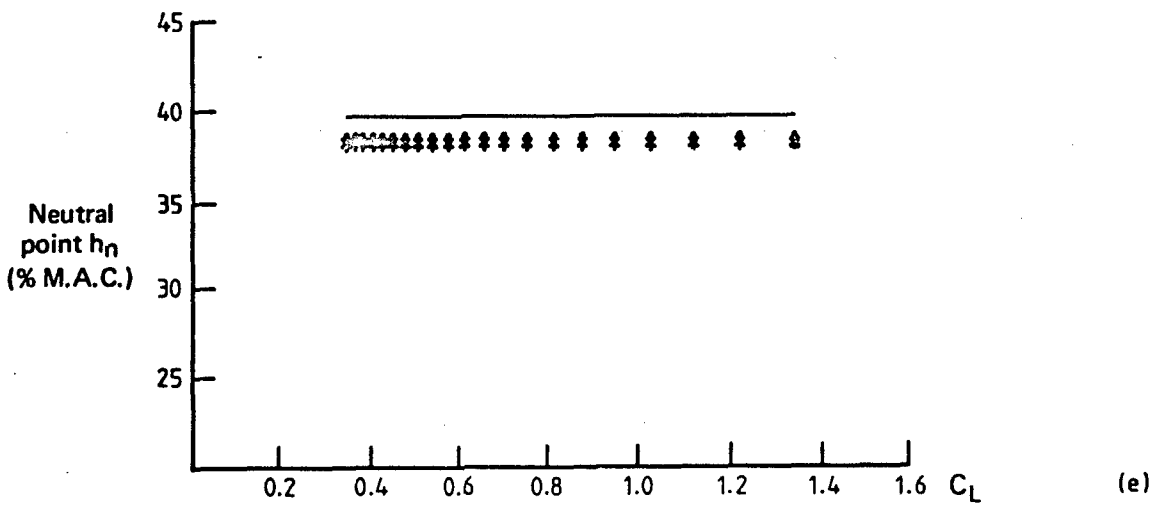

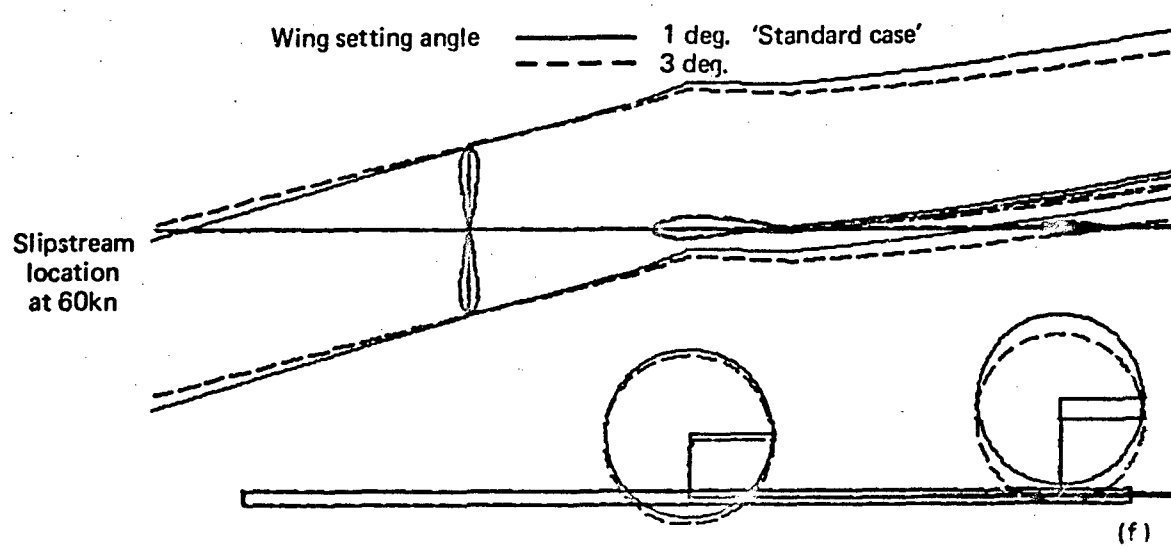

FIG. 18 EFFECT OF WING SETTING ANGLE (POWER-OFF)

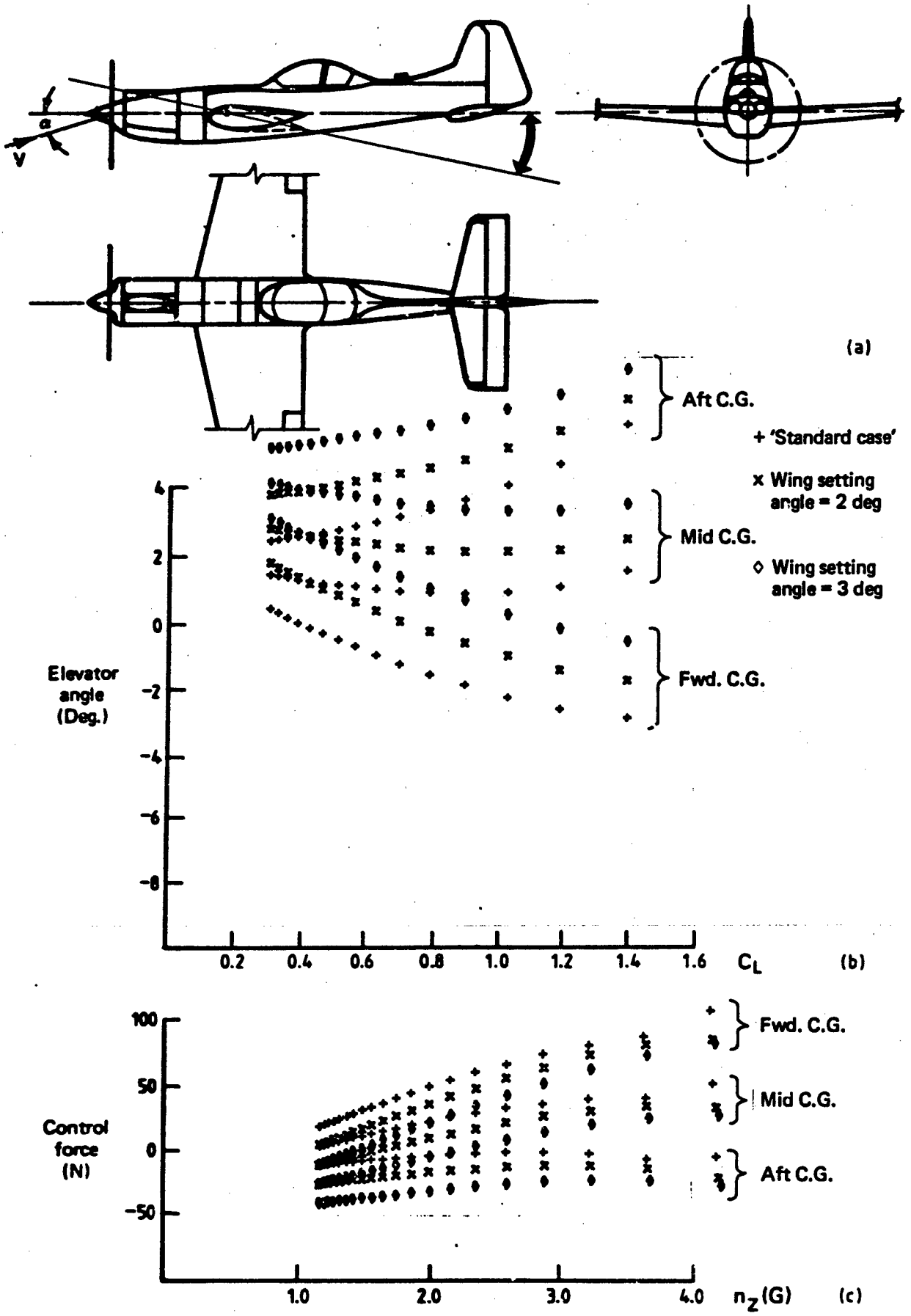

FIG. 19 EFFECT OF WING SETTING ANGLE (POWER-ON)

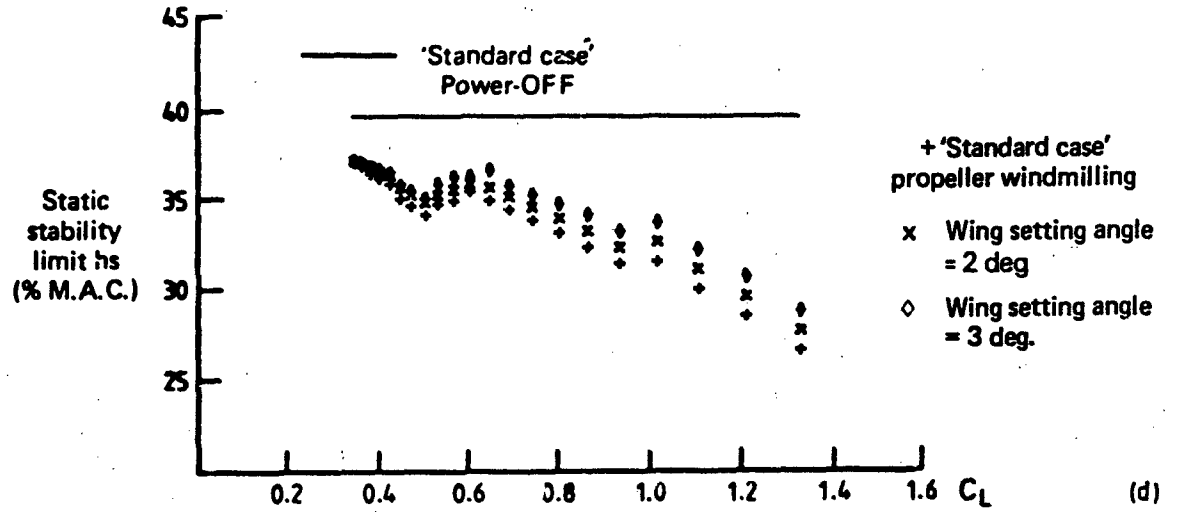

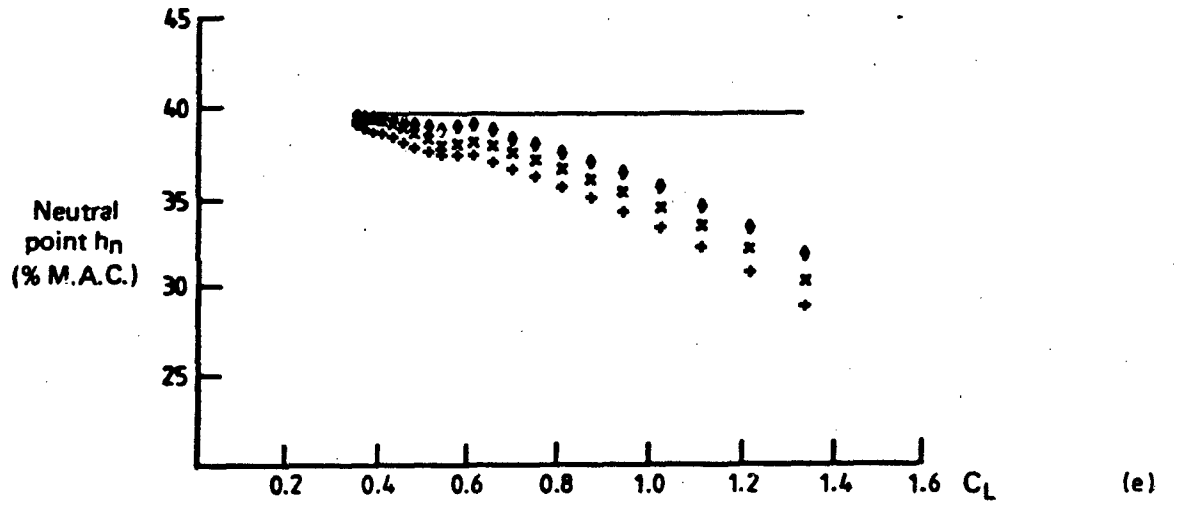

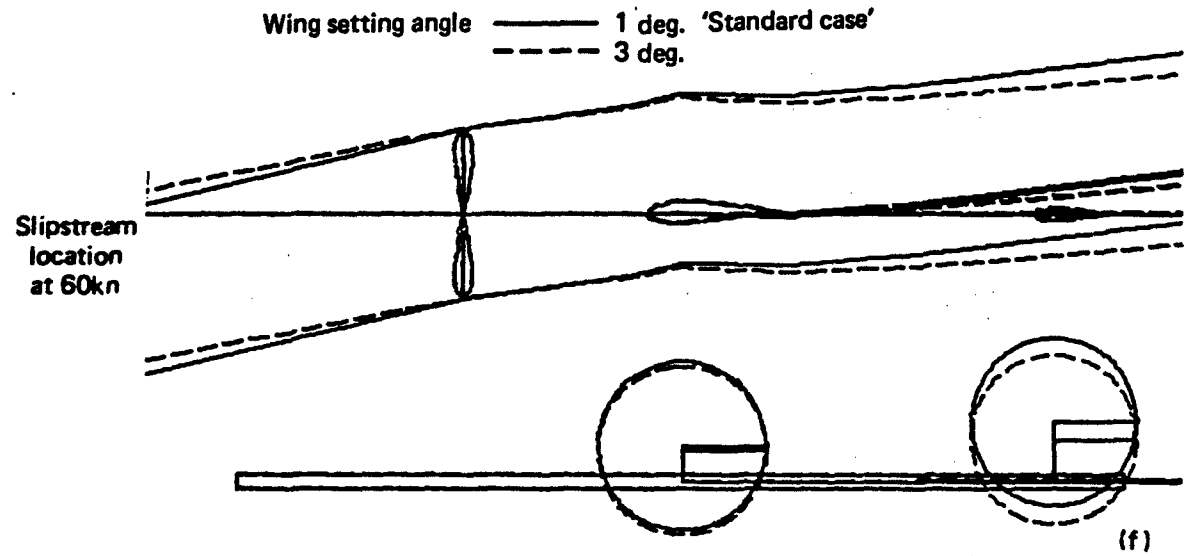

FIG. 19 EFFECT OF WING SETTING ANGLE - POWER ON

Figures 18*f* and 19*f* show that, with different wing setting angles, the tailplane is placed in a different location relative to both wing-wake and downwash field. With power off, the larger setting angle gives a slightly smaller downwash gradient giving an increase in h_n of $0{\cdot}25\%\bar{c}$, as shown in Figure 18*e*. With power on, additional stability changes occur as detailed below, when wing setting angle is increased.

(*a*) At a given C_L, the propeller incidence will be lower and, as described in 6.1 for the inclined thrust axis, this alters the propeller and wing–body contributions slightly. However, the net effect of these changes for the "standard case" is small and h_n is increased by less than $0{\cdot}25\%\bar{c}$.

(*b*) The increase in wing setting angle will increase the combined wing–body zero lift pitching moment (C_{m_0}). This will increase the derivative C_{m_V} and increase h_n as discussed in Section 5.4. However, the increase in C_{m_0} due to an increase in wing setting angle of 2 deg. is calculated (from Ref. 6) to be only $7{\cdot}5\%$. Calculations, not plotted, show that this increase gives a negligibly small increase in h_n.

(*c*) The effect of power-on downwash is calculated in Reference 6 as a function of the power-off downwash. Therefore, the slightly more favourable tail location with the 3 deg. wing setting will lead to a smaller power effect on downwash. As with power effects (*a*) and (*b*), these changes are not significant for the "standard case", giving less than $0{\cdot}25\%\bar{c}$ increase in h_n.

(*d*) The only significant change with power results from the increased area of the tailplane immersed within the slipstream as shown in Figure 19*f*. This contribution increases h_n by $2\%\bar{c}$ at low speed, reducing to zero at 100 kn and above, as shown in Figure 19*d*.

The relative position of the slipstream and vertical tailplane location will be shown (in Section 6.3) to result in large changes in stability with power. Changing wing setting angle does give a limited capability to alter this relationship even though it may be an unattractive design option.

Of more importance than wing setting angle is the vertical position of the wing in relation to the aircraft thrust line, vertical c.g. location, and tailplane height. As will be demonstrated, significant stability changes occur both with power off and power on.

The power-off effects are greatest at low speeds and were clearly described in Reference 14 in 1938. When the wing aerodynamic centre is displaced vertically from the aircraft c.g., an additional pitching moment arises due to the change in the wing lift moment arm with changes in incidence (α). Since lift is proportional to incidence and the moment arm is proportional to $\sin\alpha$, the total effect results in a parabolic variation of pitching moment with incidence. For a low wing the effect is destabilising, while the reverse is true for a high wing. Figure 20 shows the results for a wing positioned plus and minus 0·3 m about the "standard case" position. The trim curves in Figure 20*b* show clearly the characteristic upward curvature for low wings and the downward curvature for high wings. Figures 20*d* and 20*e* show that h_n and h_m are identical, indicating that the change in stability is entirely due to changes in pitch stiffness. For the "standard case" with a low wing, h_n is decreased by zero at high speed, to $7\%\bar{c}$ at low speed. For low wing aircraft with low wing sweep, lateral-directional flying qualities requirements generally lead to aircraft designs with significant wing dihedral. Assuming elliptical spanwise wing loading then the height of the wing aerodynamic centre above the wing root is given as a function of dihedral angle by

$$z_L = \tfrac{3}{8}(b/\pi)\tan\Gamma. \tag{20}$$

For the low wing case considered above, a dihedral angle of 5 deg. and the associated change in vertical c.g. would reduce the vertical moment arm and the calculated changes in h_n by approximately 40%.

The aircraft drag force will also contribute a moment about the aircraft c.g. However, since the drag moment arm is proportional to $\cos\alpha$, the variation of moment with incidence is small compared with that due to lift. For the low wing configuration considered above, the drag component is stabilising but increases h_m and h_n by less than $0{\cdot}2\%\bar{c}$.

The downwash field at the tailplane is also altered by a change in wing height. For the low wing considered, the associated downwash field gives a value of h_n which is $1\%\bar{c}$ larger than for the "standard case".

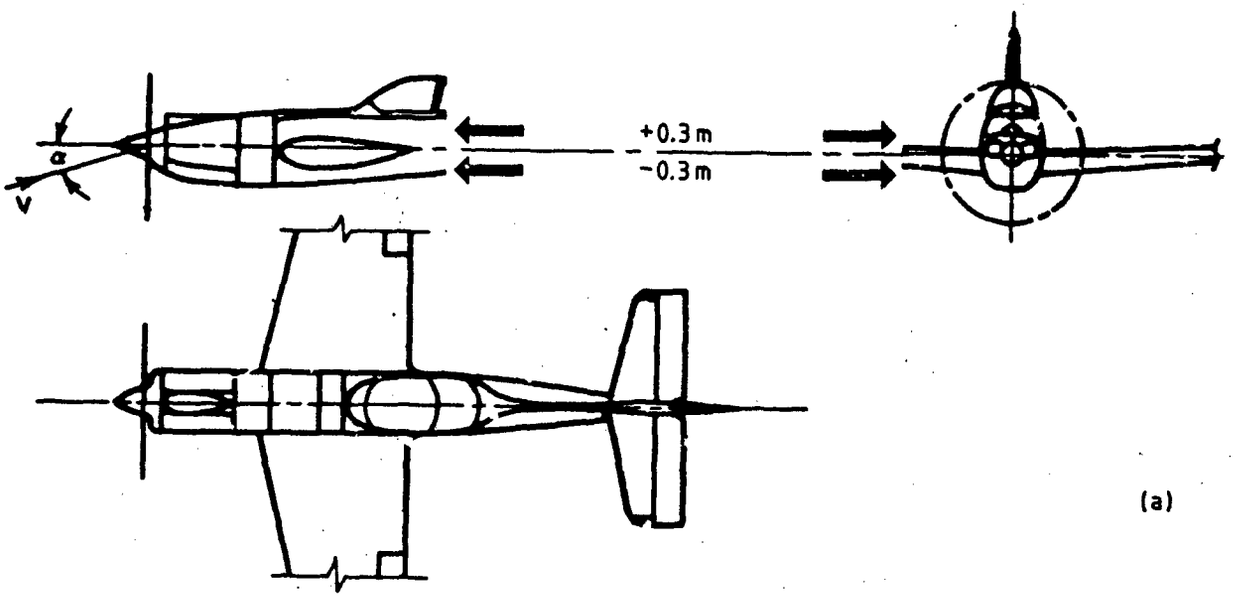

(a)

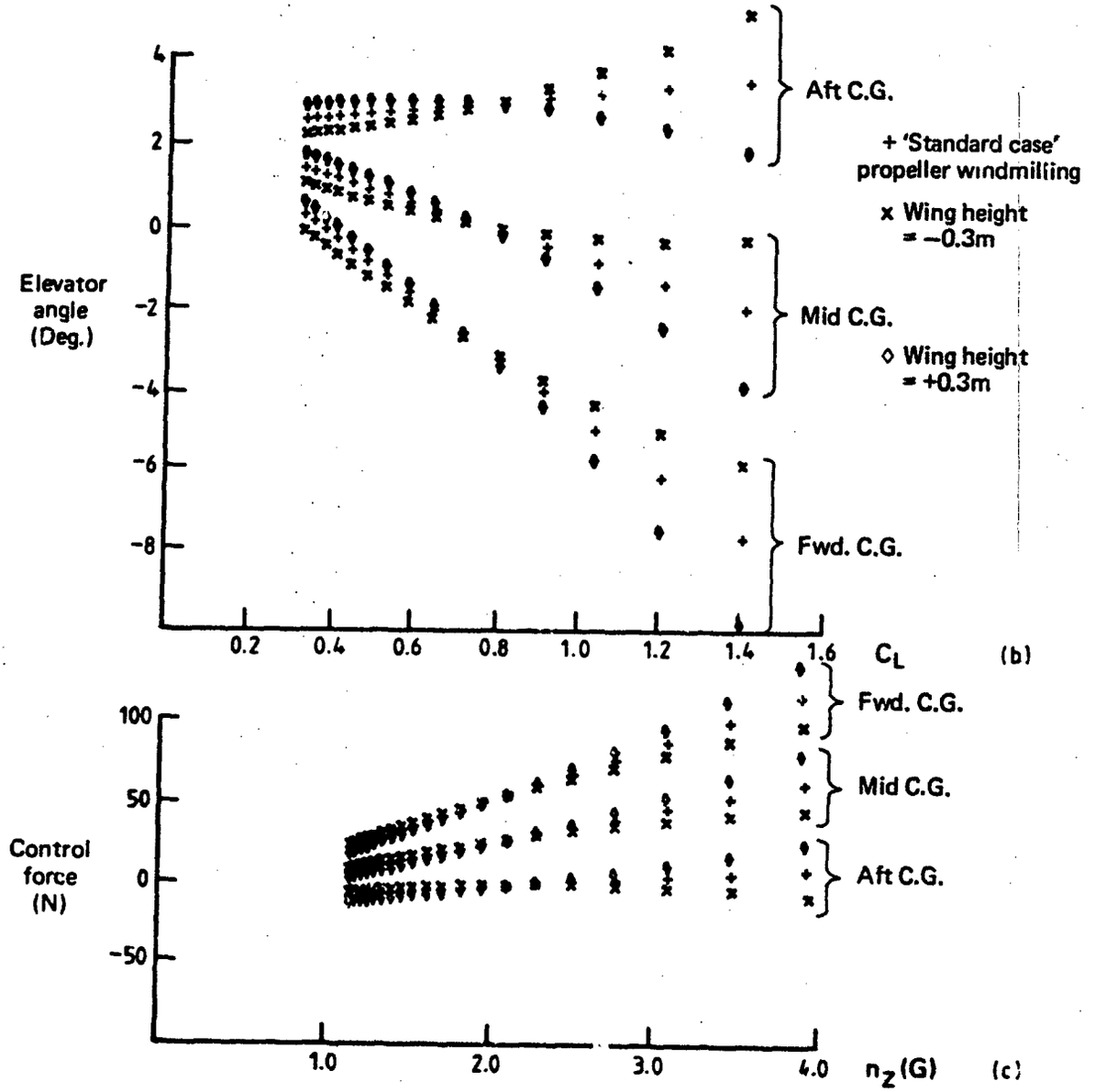

FIG. 20 EFFECT OF WING VERTICAL POSITION (POWER-OFF)

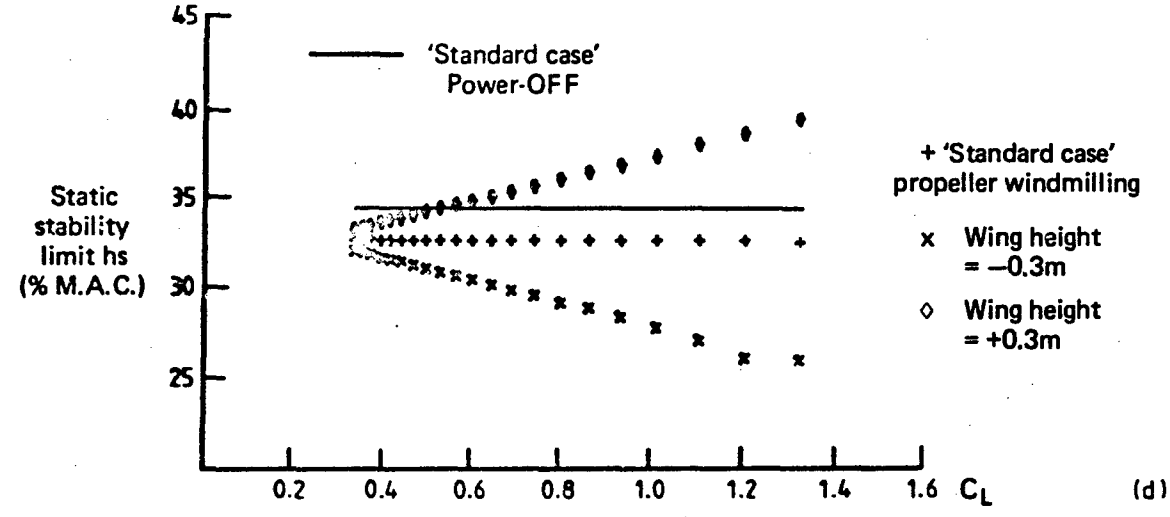

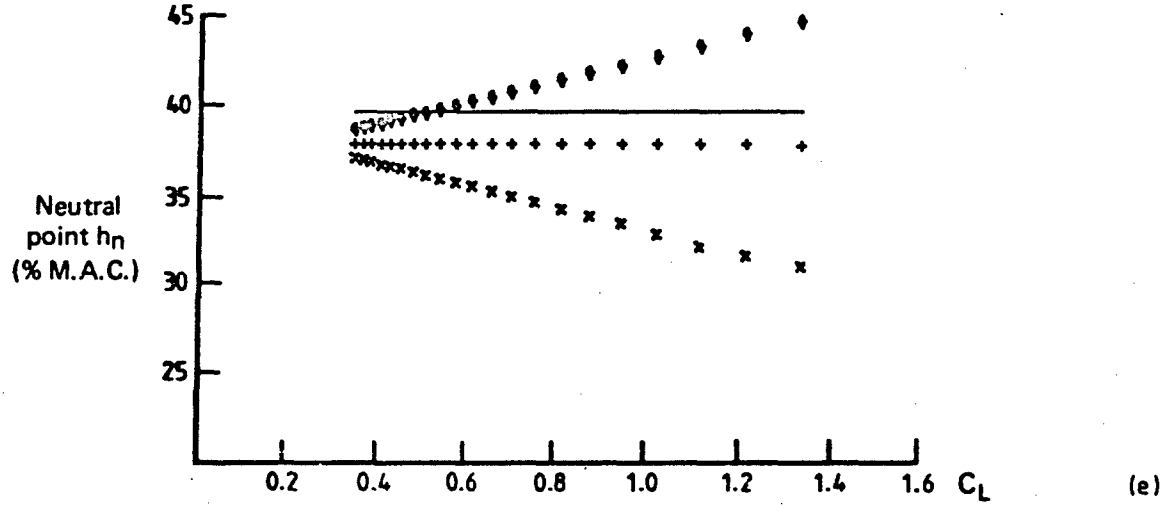

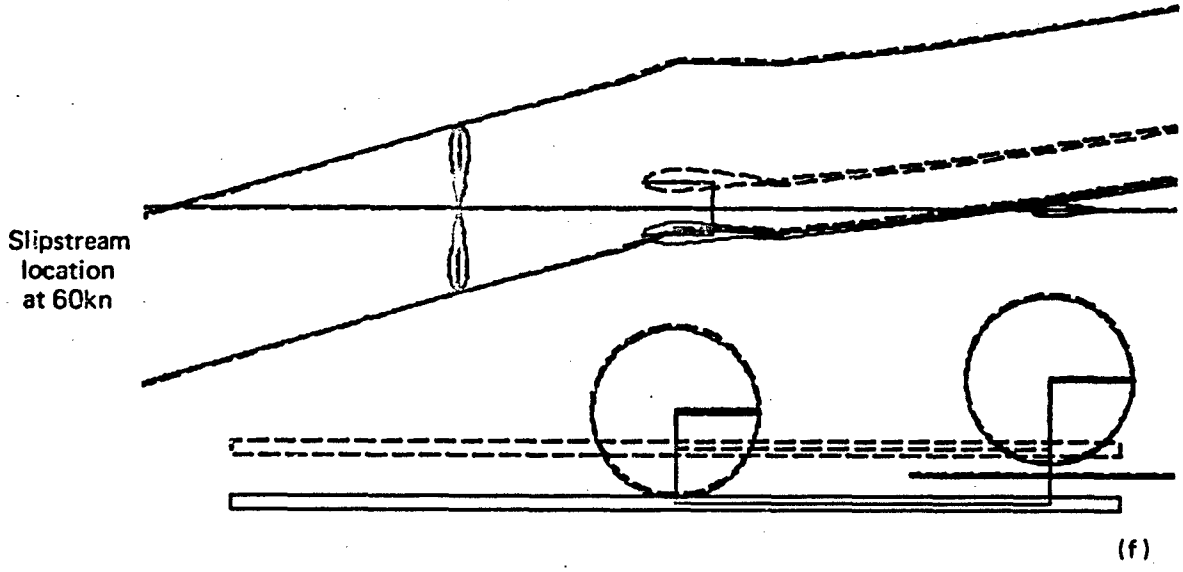

FIG. 20 EFFECT OF WING VERTICAL POSITION (POWER-OFF)

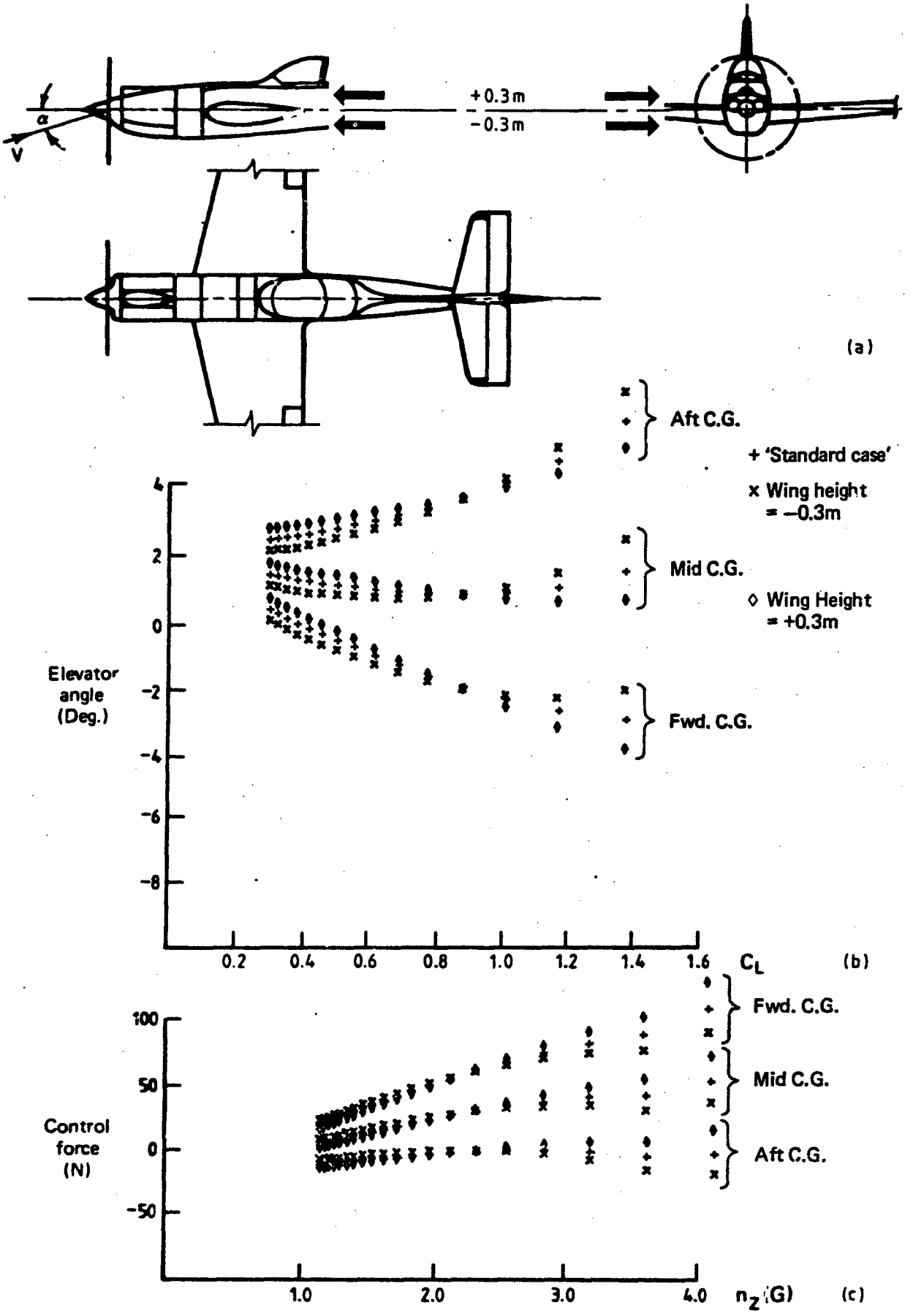

FIG. 21 EFFECT OF WING VERTICAL POSITION (POWER-ON)

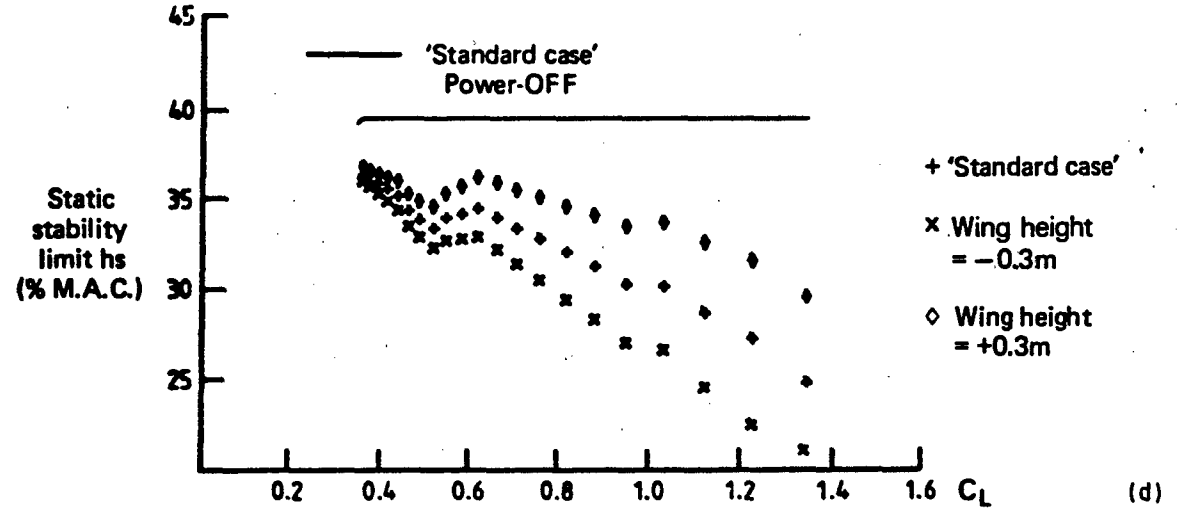

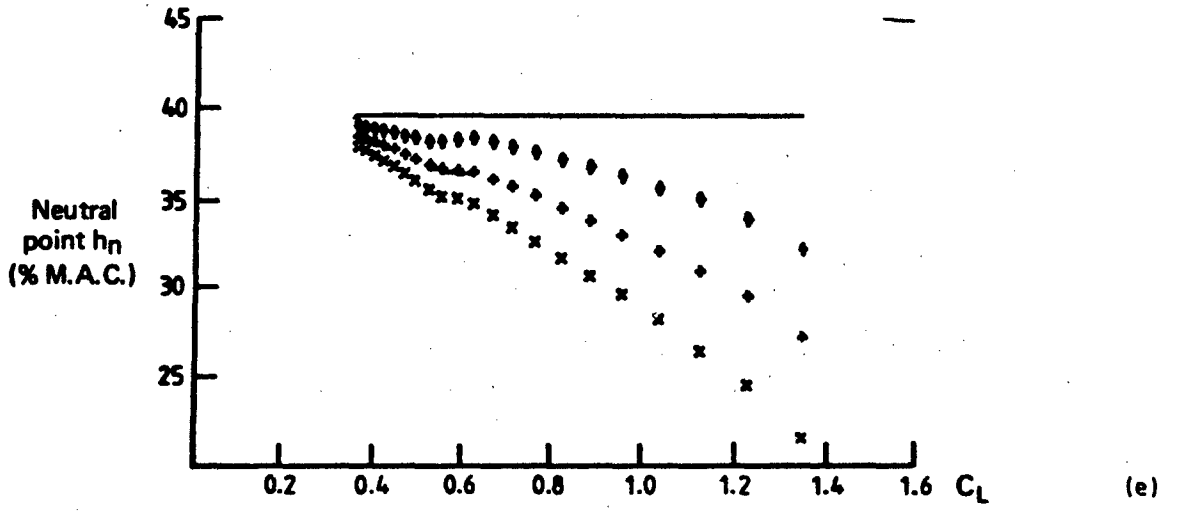

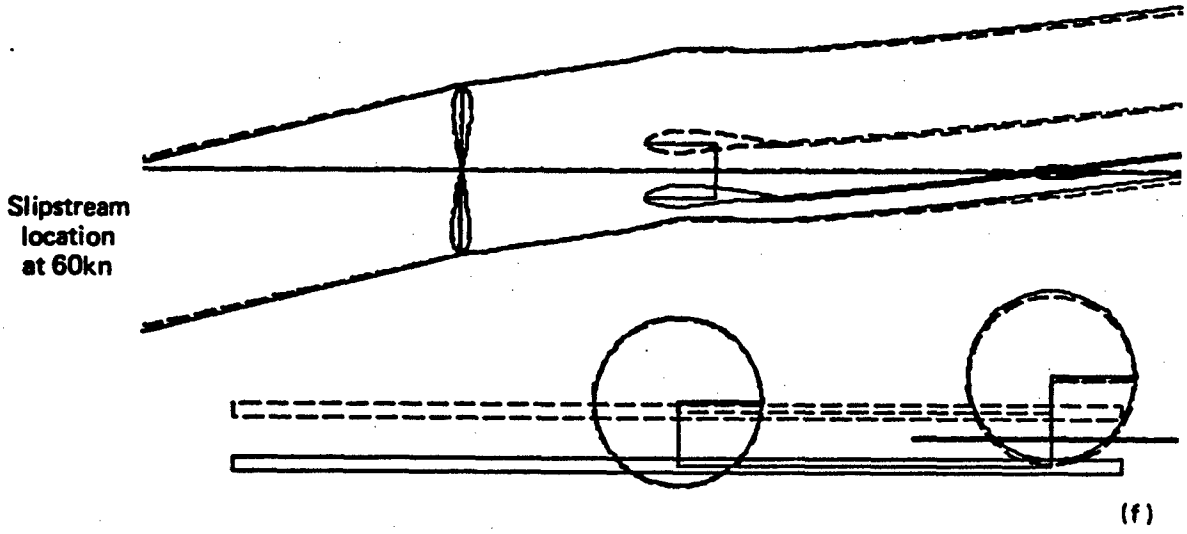

FIG. 21 EFFECT OF WING VERTICAL POSITION (POWER-ON)

With power on, the only significant change in stability associated with the low wing, is a reduction in the wing–body destabilizing effect arising from the smaller areas of wing and body immersed within the slipstream, as shown in Figure 21*f*. The change in downwash gradient with power is the same as that for the "standard case" and, since the slipstream location is not significantly altered, the effect of dynamic head at the tailplane is little different from the "standard case". The net effects of power for the low-wing layout are shown in Figure 21*d*. At low speeds, power reduces h_n by $9\%\bar{c}$ compared with a $10\%\bar{c}$ reduction for the "standard case". The large changes in h_n for this layout are unlikely to occur in practice, since dihedral angle will attenuate the low-wing effect and a more typical tailplane location, as considered in Section 9, will reduce the effects of power on stability.

6.3 Tailplane Vertical and Longitudinal Position

The effect of downwash and slipstream dynamic head at the tailplane has been shown in Section 5 to produce significant changes in longitudinal stability. Consequently, the vertical location of the tailplane in relation to the downwash field and to the slipstream, is an important design parameter. Reference 15 gives a striking example of an aircraft, which when initially tested, had a power-on neutral point forward of the aircraft forward c.g. limit of $20\%\bar{c}$. The tailplane was then moved out of the slipstream, by giving it 13 deg. of dihedral with the result that the aircraft became stable at the aft c.g. limit of $38\%\bar{c}$.

To aid the following discussions, the variations in downwash and dynamic head with tailplane position, as predicted by the estimation methods of Reference 6, are summarised below.

(*a*) With power off, a reduction in downwash results when the tail arm increases, or when the normal distance between the tailplane and the extended wing chord line increases; the method assumes no change with tailplane span.

(*b*) The incremental increase in downwash with power decreases, when the power-off downwash decreases, or when the normal distance between the tailplane and the extended thrust line increases.

(*c*) The incremental change in lift due to slipstream dynamic head decreases when the distance between the tailplane and the slipstream centreline increases, and when the area of tailplane immersed within the slipstream decreases.

Figures 22 and 23 show the effect of changing the tailplane height $\pm 0{\cdot}5$ m about the "standard case" location. With power off, the high tail gives an increase in h_n of $2\frac{1}{2}\%\bar{c}$ at high speeds and $3\frac{1}{2}\%\bar{c}$ at low speeds, compared with the low tail. This increase is due to the reduction in downwash gradient ($\partial\epsilon/\partial\alpha$) as tail height increases. With power on, the tail height has a major influence on h_n, as shown in Figures 23 and 24. For tail positions including that of the "standard case" and below, power produces a reduction in h_n of between $2\%\bar{c}$ and $4\%\bar{c}$ at high speeds, and of $11\%\bar{c}$ at low speeds. The composition of these net effects has been described in detail in Section 5. For tailplane locations above the "standard case" location, the reduction in h_n with power becomes progressively less as height is increased. For the highest position considered, that is 0·6 m above the "standard case", the net reduction in h_n due to power is $2\%\bar{c}$ at high speeds and zero at low speeds. The composition of these changes is illustrated in Figure 25, in which the accumulated results of the power effects (taken in the order listed in Section 5) are presented. With power off, the high tail gives an increase in h_n of approximately $1\%\bar{c}$ at all speeds, due to reduce downwash gradient compared with the "standard case". With power on, the direct propeller and wing–body contributions are unchanged from the "standard case". The change in downwash gradient due to power is less for the high tail, and increases h_n by $1\%\bar{c}$ at almost all speeds compared with the "standard case". By far the largest change in h_n arises from the increase in effectiveness of the high tail at low speeds, due to its location at the centre of the slipstream, as shown in Figure 23*f*. In contrast with the "standard case", the tailplane does not emerge from the slipstream at low speeds, but provides an increase in h_n of up to $7\frac{1}{2}\%\bar{c}$.

In summary, the large reduction in stability with power for the "standard case" aircraft layout is removed when the tailplane is raised 0·5 m. This is due primarily to an increase in tailplane effectiveness, because of its more favourable location within the slipstream, and to a less extent, to a reduction in downwash gradient. In practice the downwash and dynamic head distri-

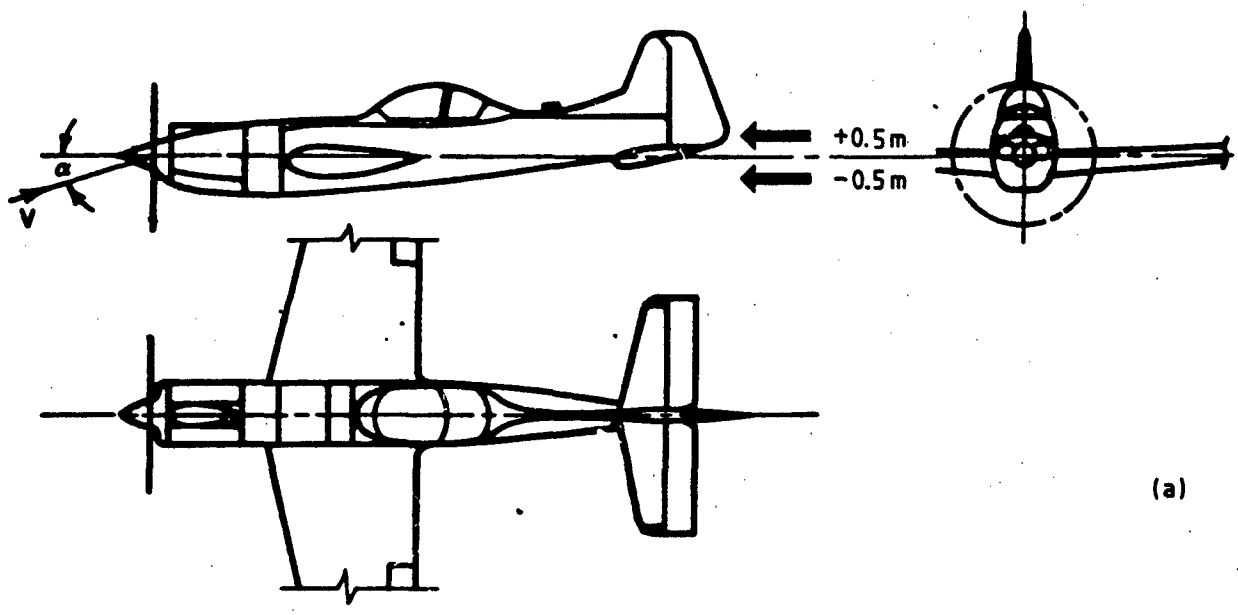

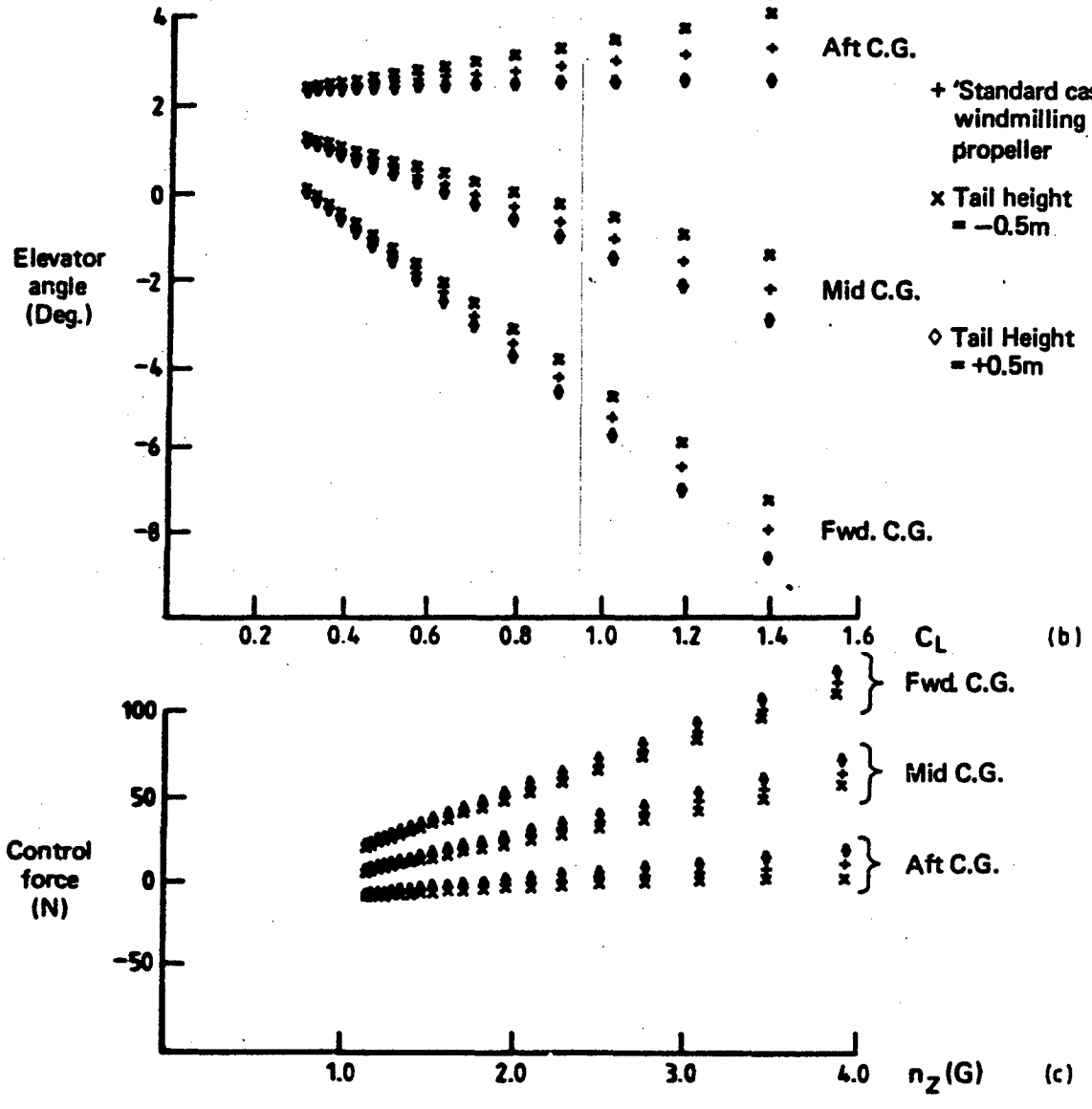

FIG. 22 EFFECT OF TAILPLANE VERTICAL POSITION (POWER-OFF)

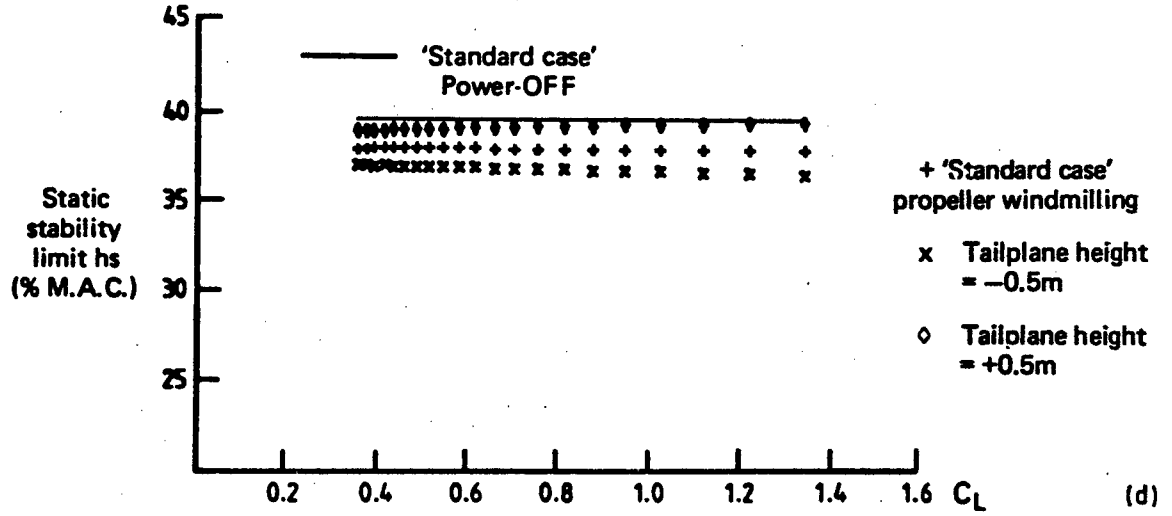

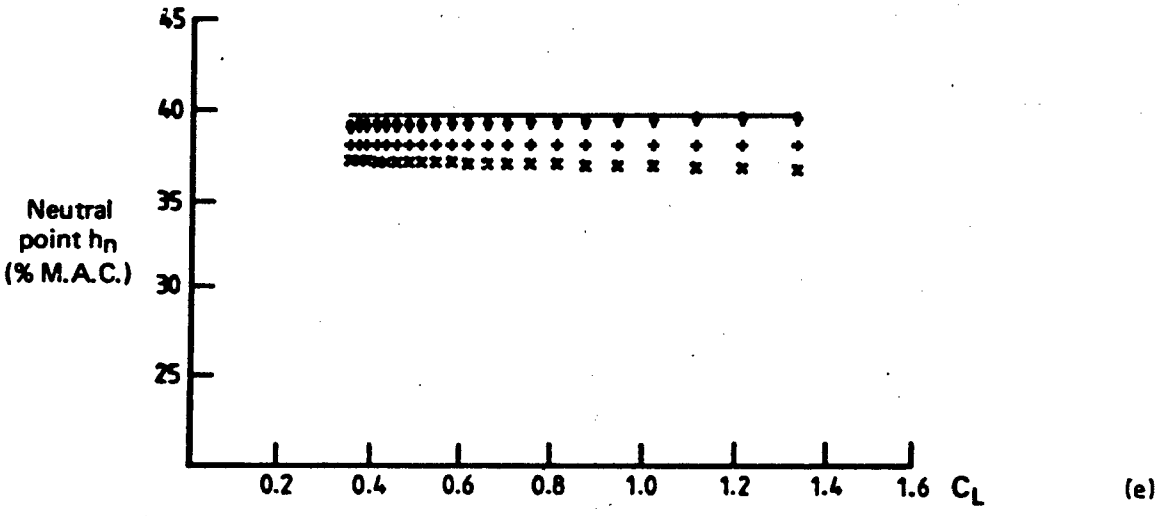

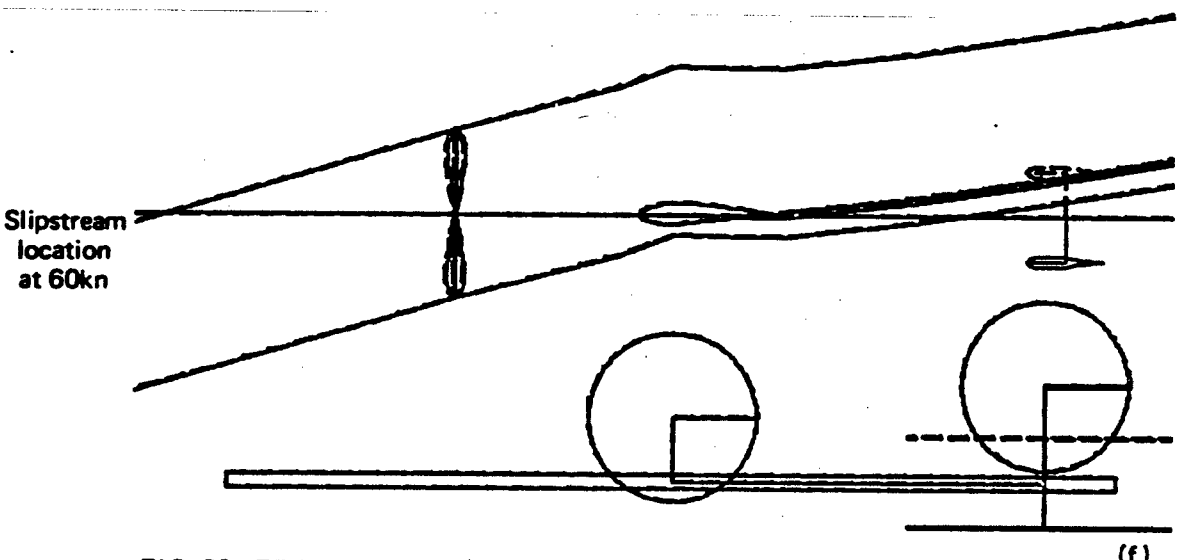

FIG. 22 EFFECT OF TAILPLANE VERTICAL POSITION (POWER-OFF)

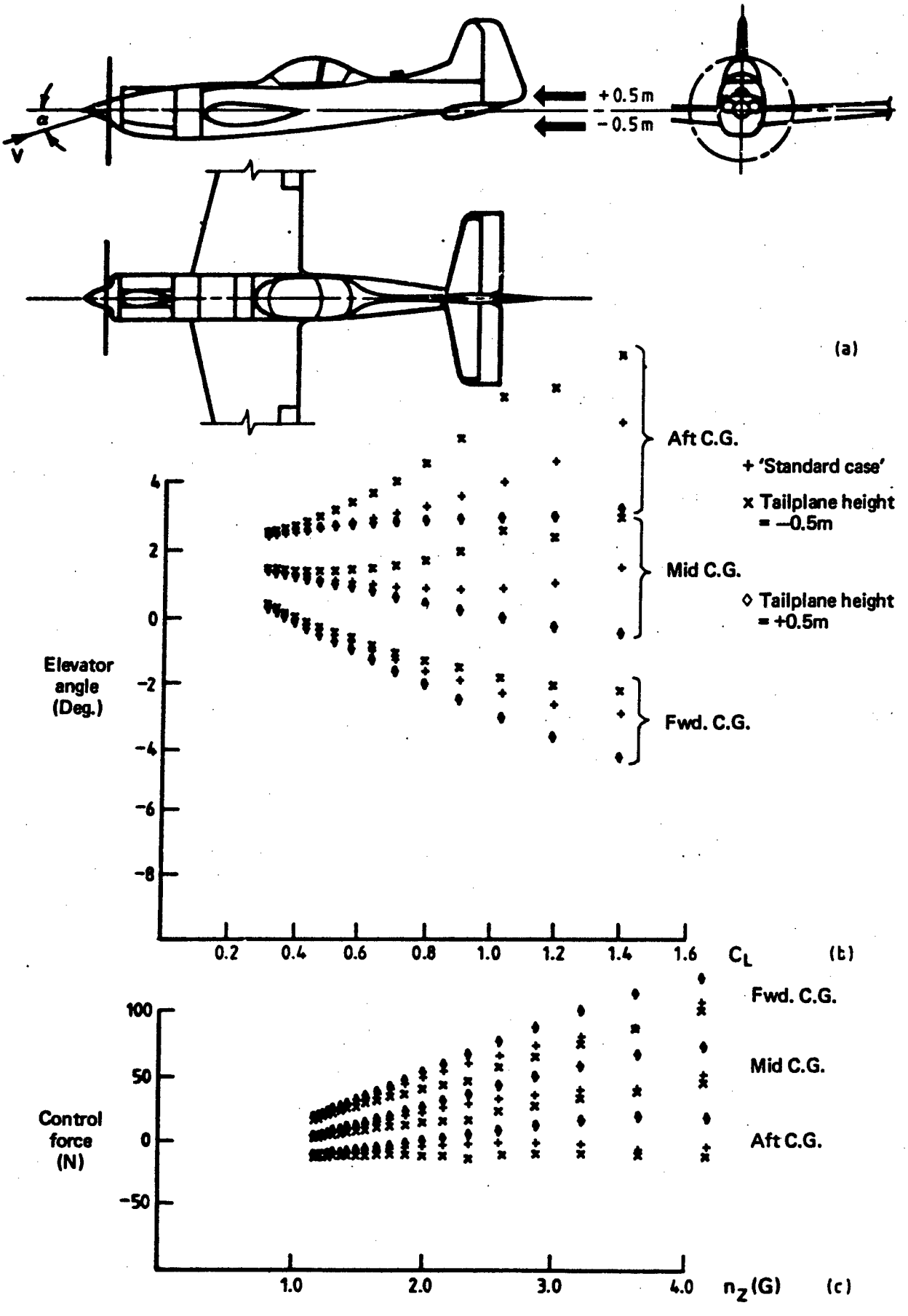

FIG. 23 EFFECT OF TAILPLANE VERTICAL POSITION (POWER-ON)

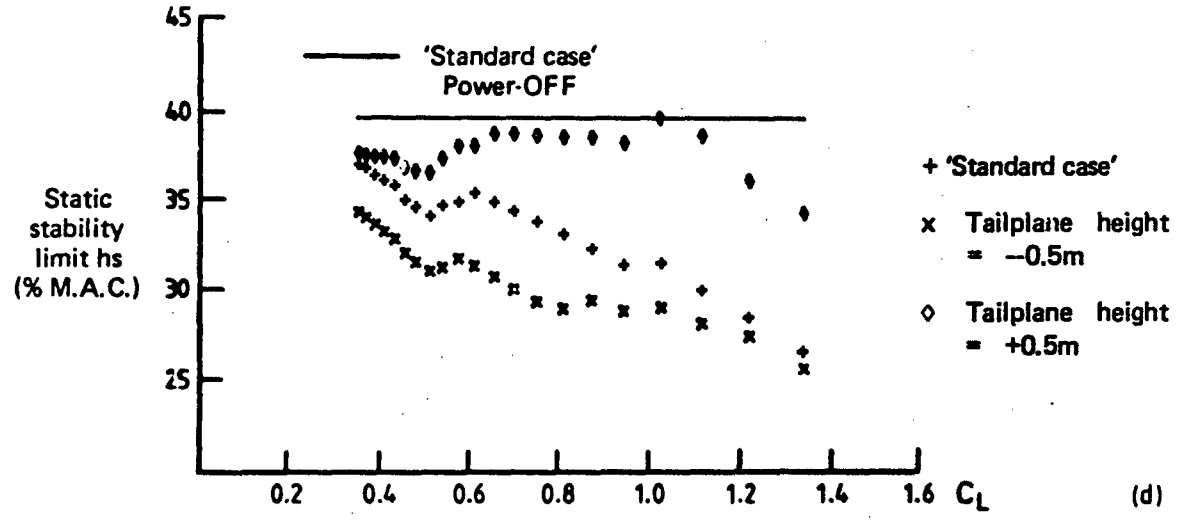

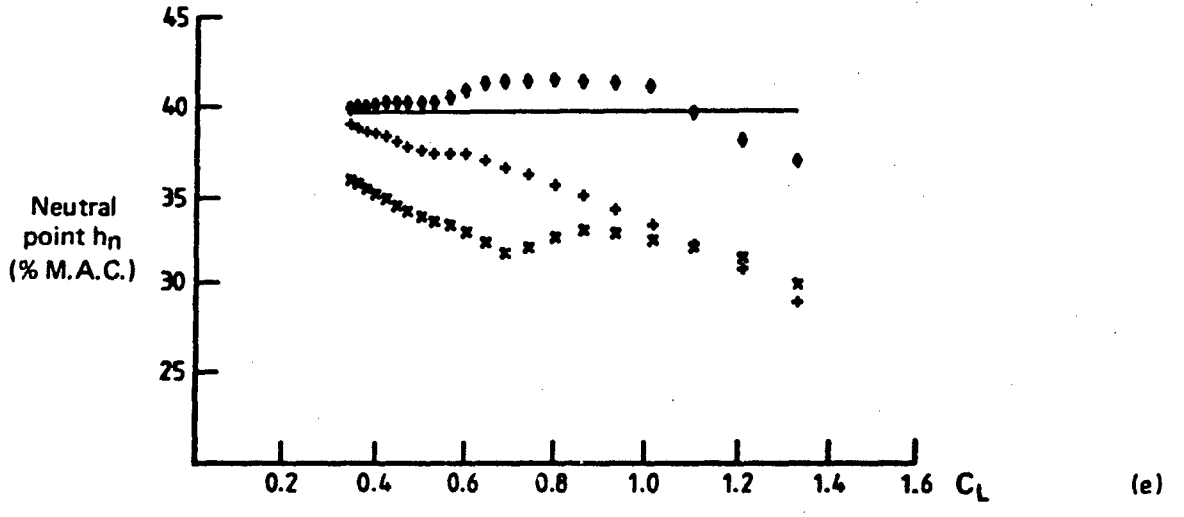

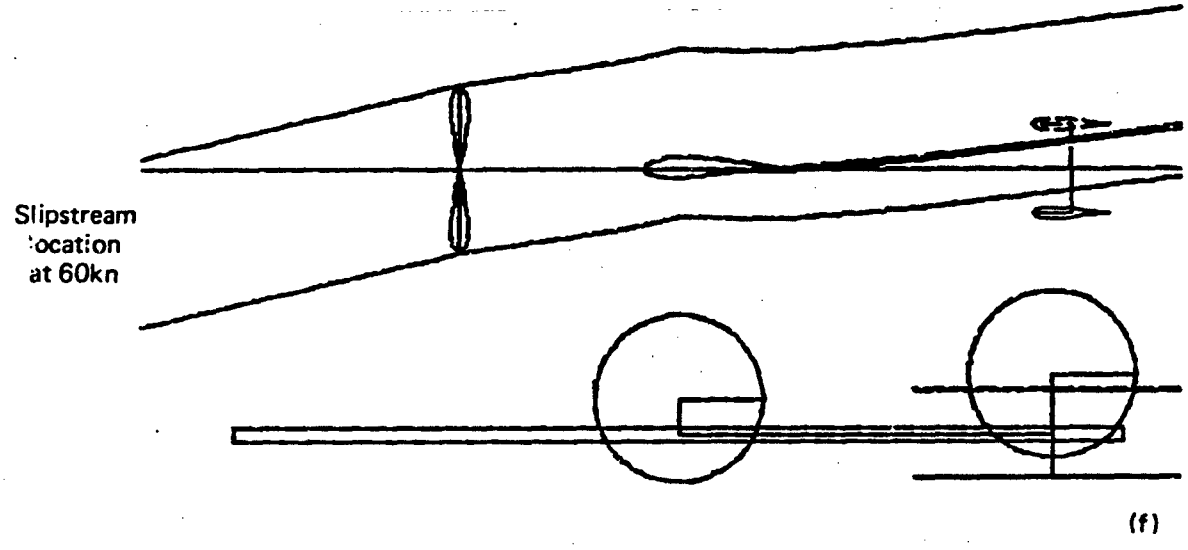

FIG. 23 EFFECT OF TAIL VERTICAL POSITION (POWER-ON)

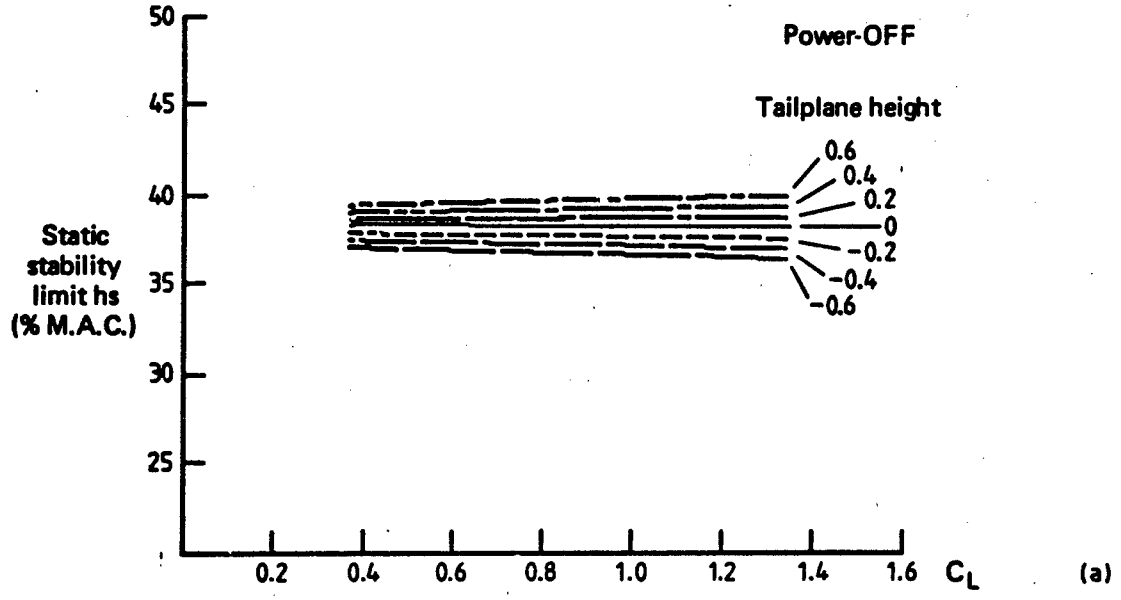

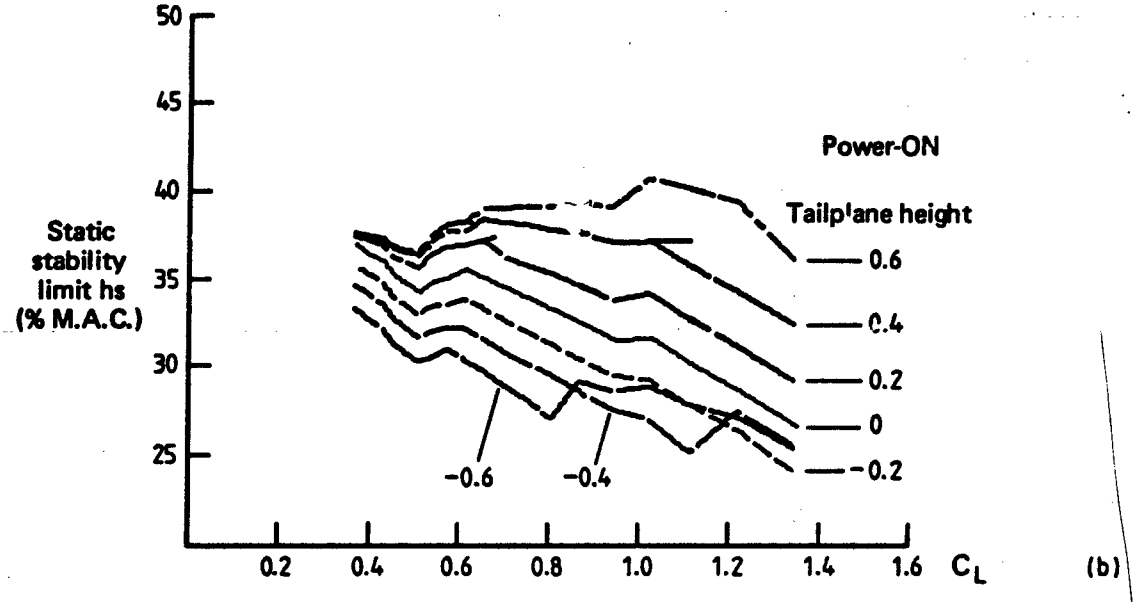

FIG. 24 EFFECT OF TAIL VERTICAL POSITION ON STATIC STABILITY LIMIT

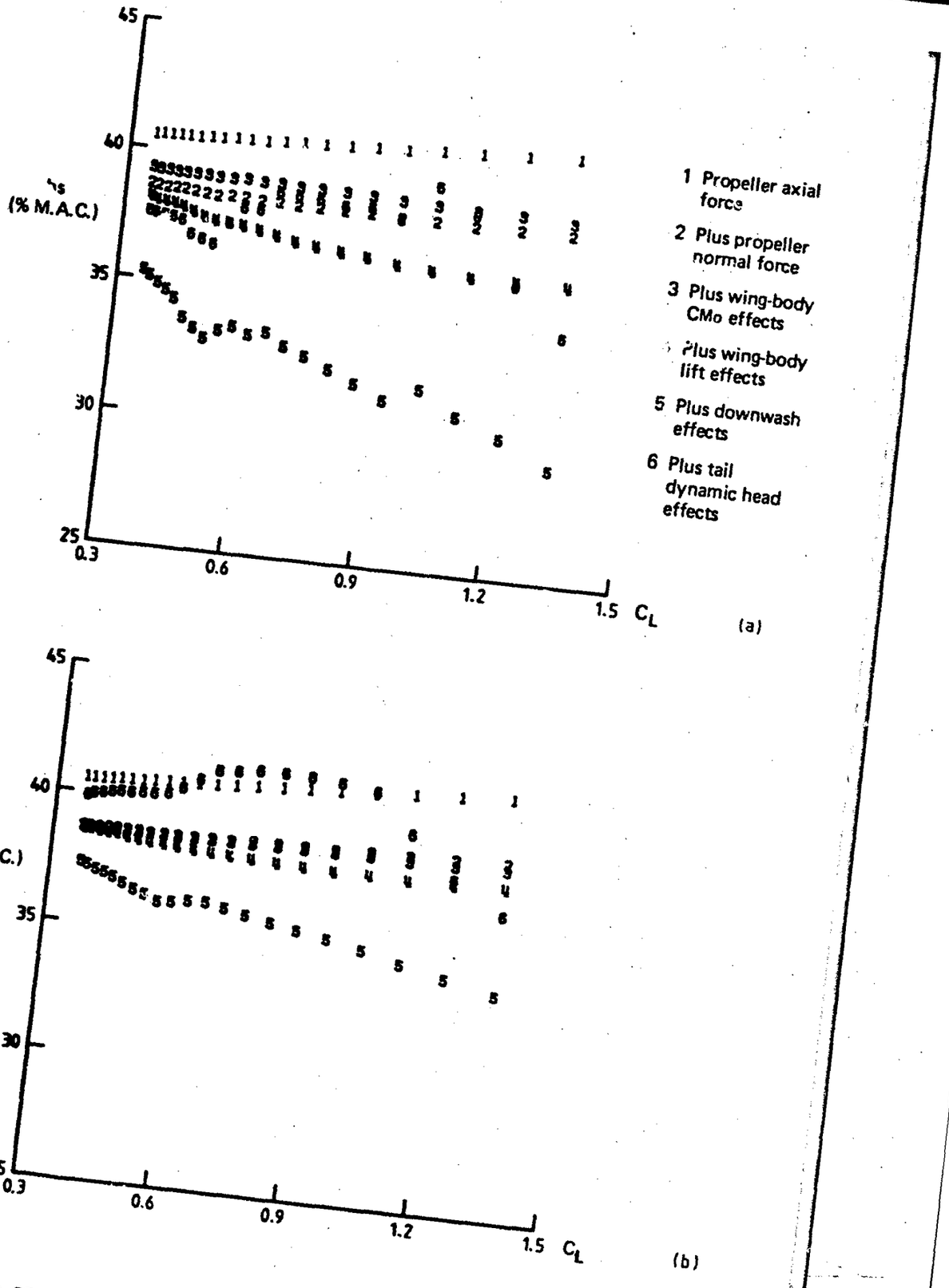

FIG. 25 ACCUMULATION OF POWER EFFECTS ON hs AND hn HIGH TAIL

bution in the slipstream differ from the idealised representation used in this Report. While the general trends indicated by the results are likely to exist in practice, the magnitude of the changes may not be as large as those predicted.

It is generally more convenient, and it is accepted practice, to consider the longitudinal tail position as part of the tail volume coefficient $\bar{V}$. In the absence of downwash and slipstream influences, increasing $\bar{V}$ by increasing tail arm or tailplane area, increases longitudinal stability. However, when the effects of power are included, this simple relation no longer exists.

Two cases will be considered. In Case A, $\bar{V}$ is fixed, while tail arm and tail area are varied accordingly. In Case B, tail area is fixed while tail arm is varied resulting in varying $\bar{V}$. In both cases, tailplane chord remains constant.

The change in stability for Case A with the "standard case" $\bar{V}$ of 0·49, and with tail arm varying $\pm$0·6 m is shown in Figures 26 and 27. As tail arm increases, the power-off h_n increases by 2%$\bar{c}$ as a result of reduced downwash gradient. With power on, the change in h_n, although large, is similar for long and short tail arms at low speeds. The composition of these effects follows the pattern described in Section 5 for the "standard case". At high speeds, the reduction in h_n with power, is 4%$\bar{c}$ greater for the short tail arm than for the long tail arm as shown in Figure 27*d*. The reduced effect of power with the long tail arm is due, firstly, to the more favourable downwash field and, secondly, because tailplane span is reduced with increasing tail arm for constant $\bar{V}$, a larger proportion of the tail is immersed in the slipstream. These benefits are not maintained at low speeds because the tail emerges from the slipstream, and for the long tail arm, this represents a larger proportion of the tail area, than for the short tail arm.

The change in stability for Case B is shown in Figures 28 and 29 in which tail area is fixed at the "standard case" value, and tail arm is varied $\pm$0·6 m giving a variation in $\bar{V}$ of 0·42 to 0·56. With power off, the long tail arm increases h_n by 7%$\bar{c}$ compared with the short tail arm. This is due to a combination of increased $\bar{V}$ and also to a more favourable downwash field. Comparison of Figures 28*d* and 29*d* shows that applying full power reduces h_n by 1%$\bar{c}$ at high speeds for both tail arms, but gives a 4%$\bar{c}$ greater reduction at low speeds for the long tail arm. The increase in $\bar{V}$ with the long tail arm, would be expected to magnify the reduction in stability, due to power effects at the tailplane. However, at high speeds, this is offset by the more favourable downwash field, while at low speeds, the large value of $\bar{V}$ magnifies the loss in stability due to the tailplane emerging from the slipstream.

In summary, increasing tail arm, with either fixed $\bar{V}$ or fixed tail area increases power-off stability. However, for the "standard case," the increases are not maintained at low speeds with power on, due to emergence of the tailplane from the slipstream. Although the value of h_n is increased at all speeds with increased tail arm, the variation of h_n with speed is also increased, and this can be a disadvantage, as discussed in Section 8.

Reference 16 describes wind tunnel tests on a model with various values of $\bar{V}$, tail arm and tailplane area. The results showed an unexpected increase in downwash gradient with increasing tail arm for the power on case. The cause of this result could not be explained, and is an illustration of an effect which would not be predicted by the current empirical design formulae.

6.4 Effect of Flap Deflection

The aerodynamic contributions due to the slotted flap shown in Figure 2*b* are calculated from the empirical formula given in Reference 6. The following effects have been represented:

(*a*) change in wing lift ΔC_{L_F}—the lift curve slope is assumed to be unchanged;

(*b*) change in wing pitching moment ΔC_{m_F}—the wing aerodynamic centre is assumed to be unchanged;

(*c*) change in wing drag ΔC_{D_F}—the change in induced drag factor has been ignored;

(*d*) change in downwash at the tailplane $\Delta\epsilon_F$ due to increased inboard wing loading.

The change in *trim* due to lowering the flap 20 deg. is shown in Figure 30*b* for the power-off case. The changes due to the contributions listed above are as follows:

ΔC_{m_F} is negative, because of increased lift at the rear of the wing, so up-elevator is required for trim. However, $\Delta\epsilon_F$ is positive and its effect is trimmed by a down-elevator movement. To maintain constant lift, aircraft incidence is reduced, which will reduce the nose-up pitching

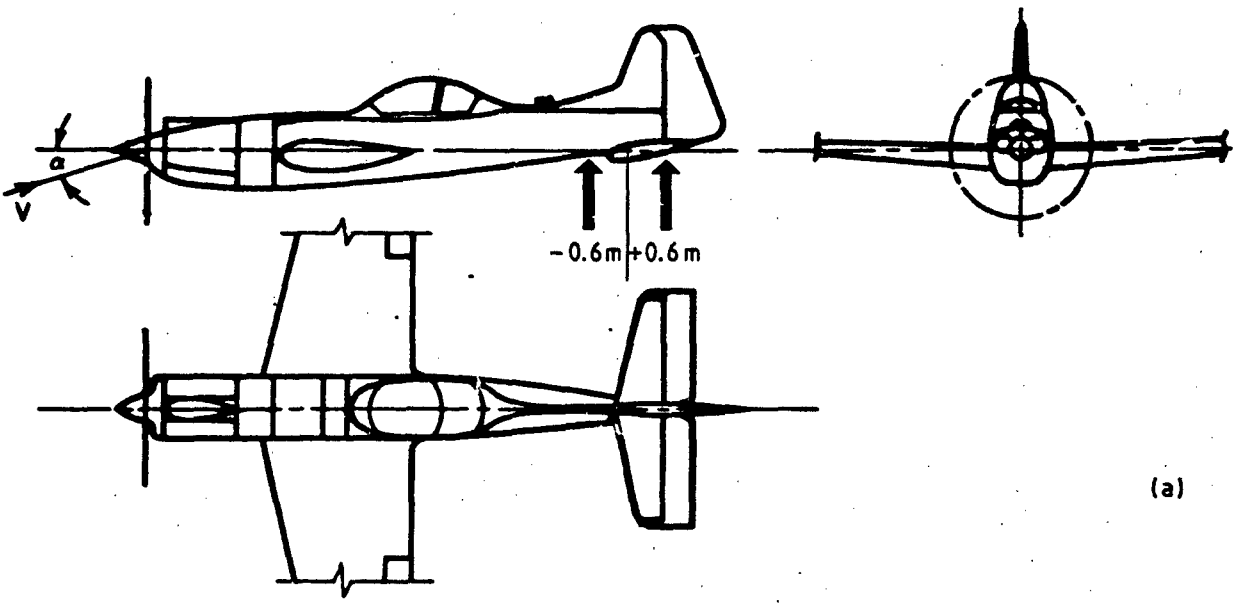

(a)

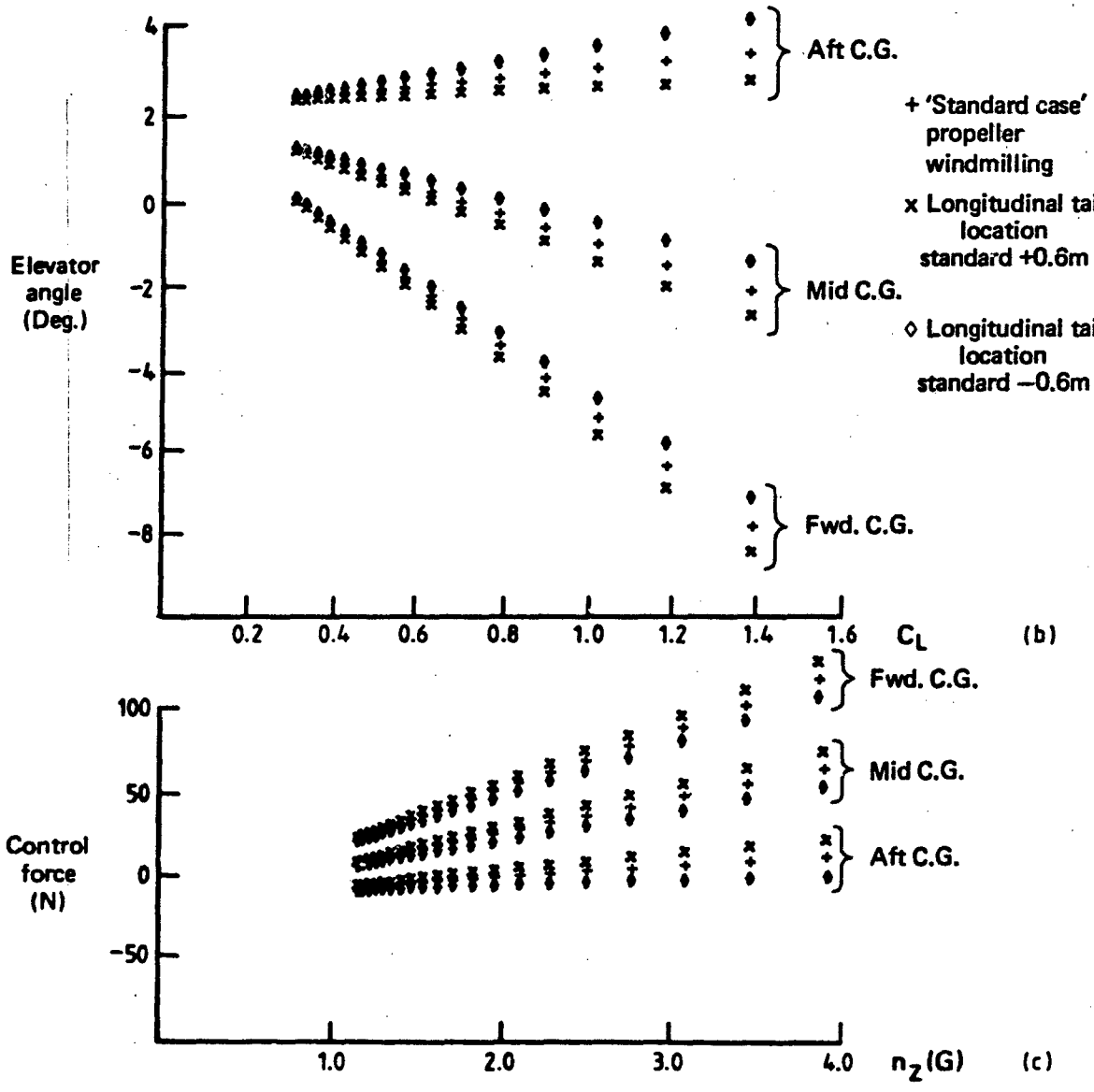

(b)

(c)

FIG. 26 EFFECT OF TAIL LONGITUDINAL POSITION: TAIL VOLUME COEFFICIENT ($\bar{V}$) CONSTANT (POWER-OFF)

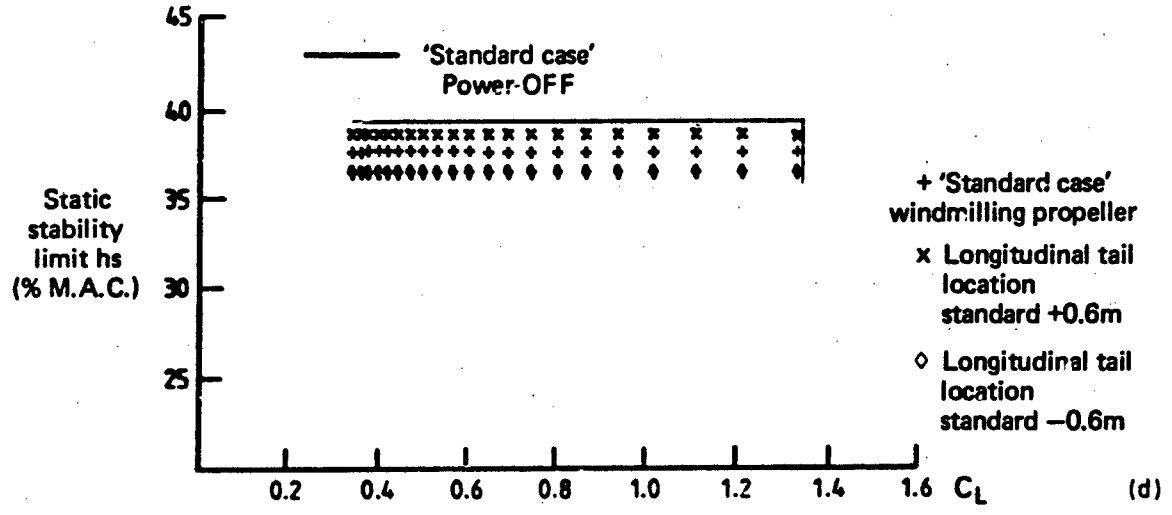

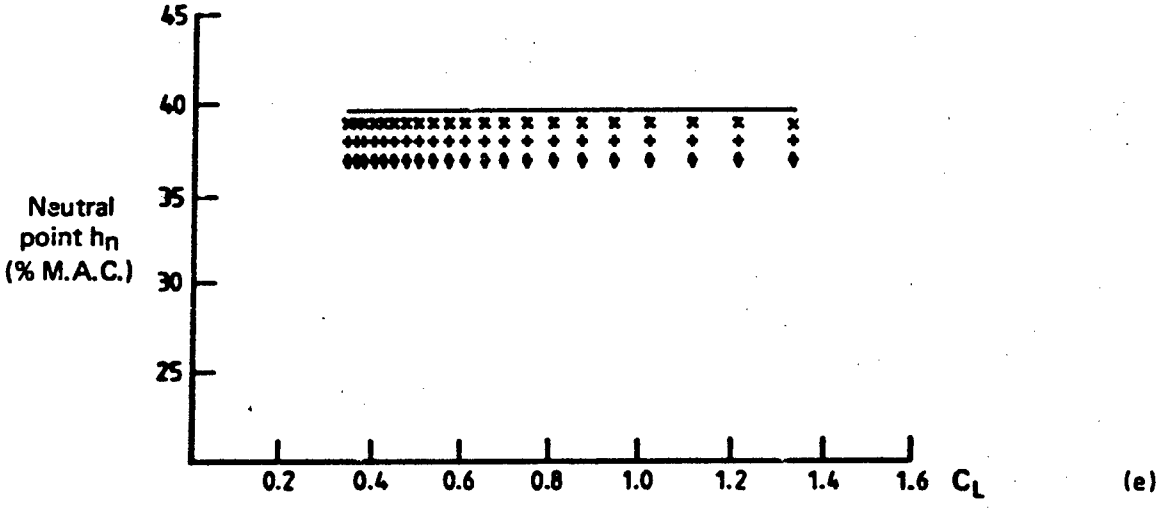

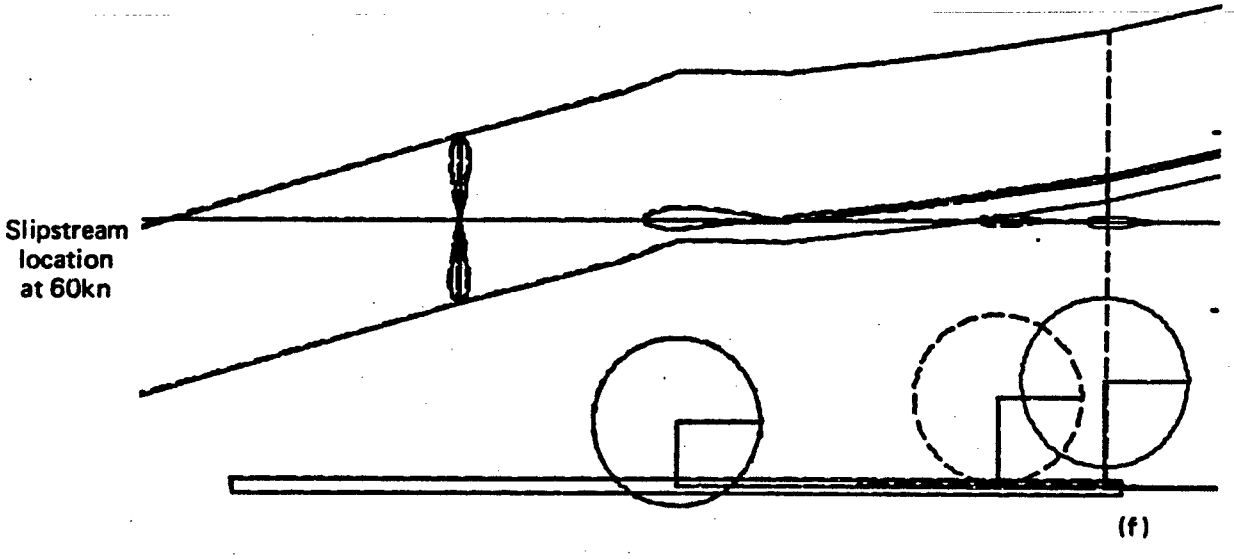

FIG. 26 EFFECT OF TAIL LONGITUDINAL POSITION: TAIL VOLUME COEFFICIENT $\bar{V}$ CONSTANT (POWER-OFF)

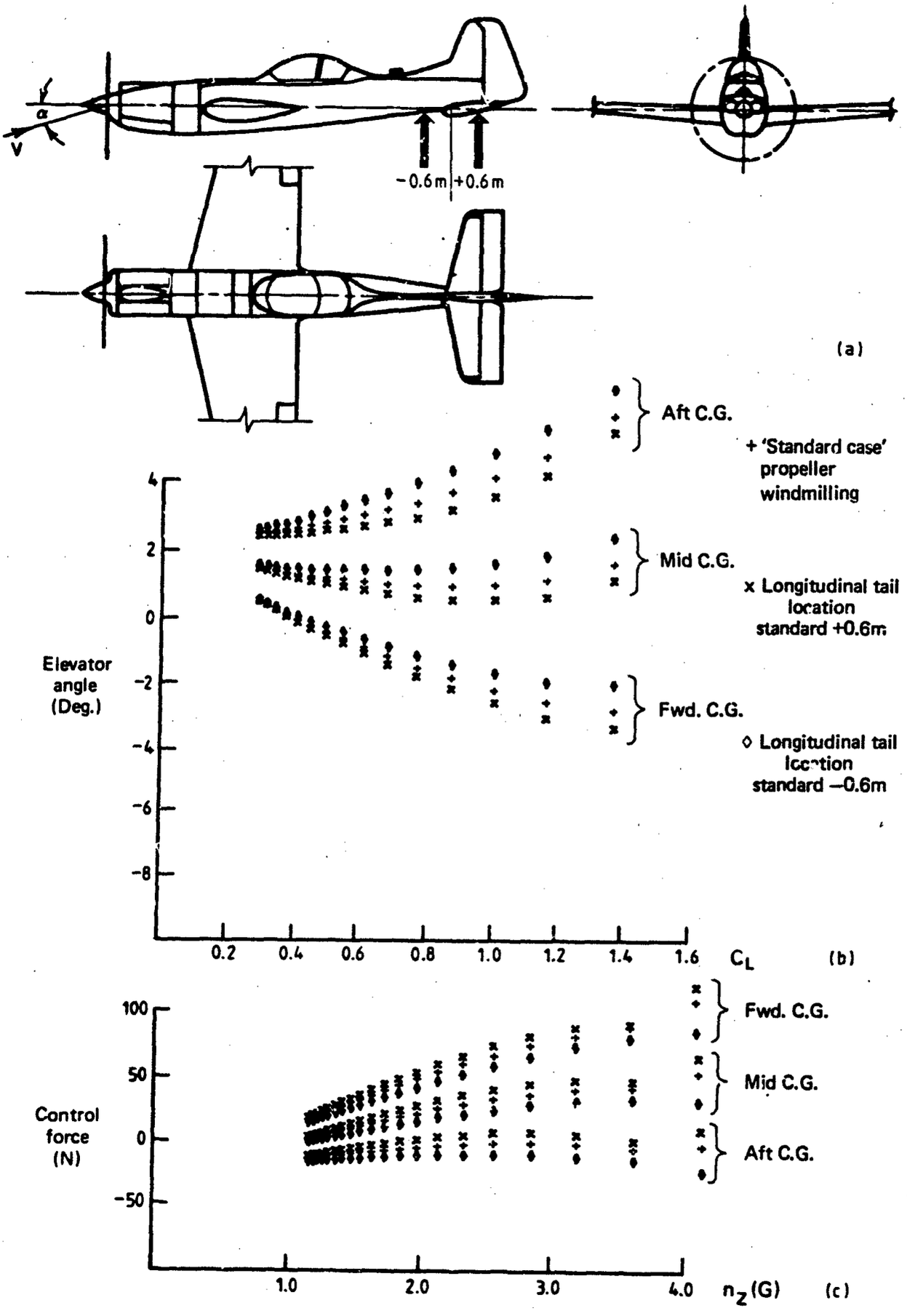

FIG. 27 EFFECT OF TAIL LONGINUDINAL POSITION: TAIL VOLUME COEFFICIENT ($\bar{V}$) CONSTANT (POWER-ON)

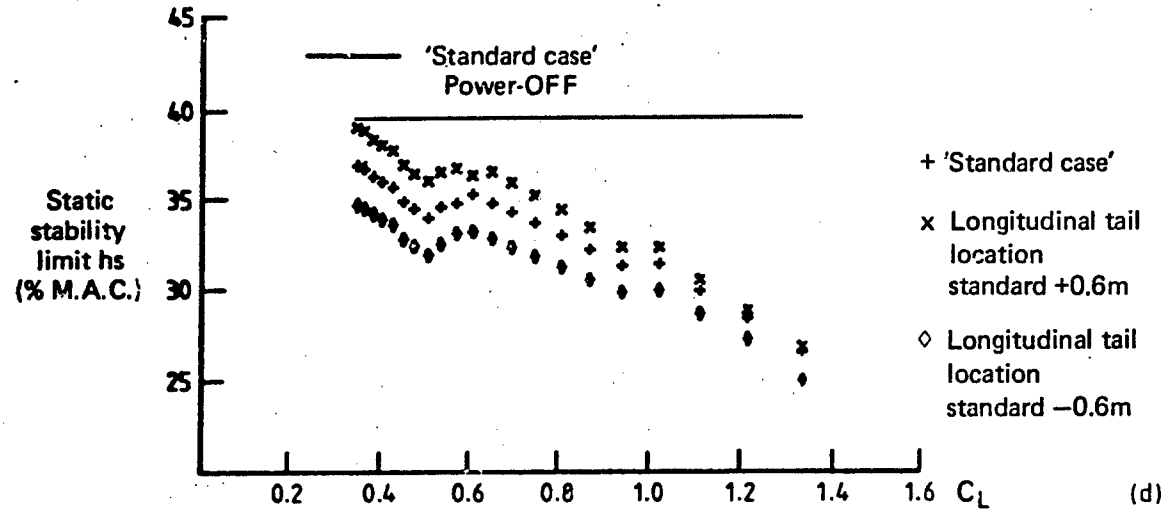

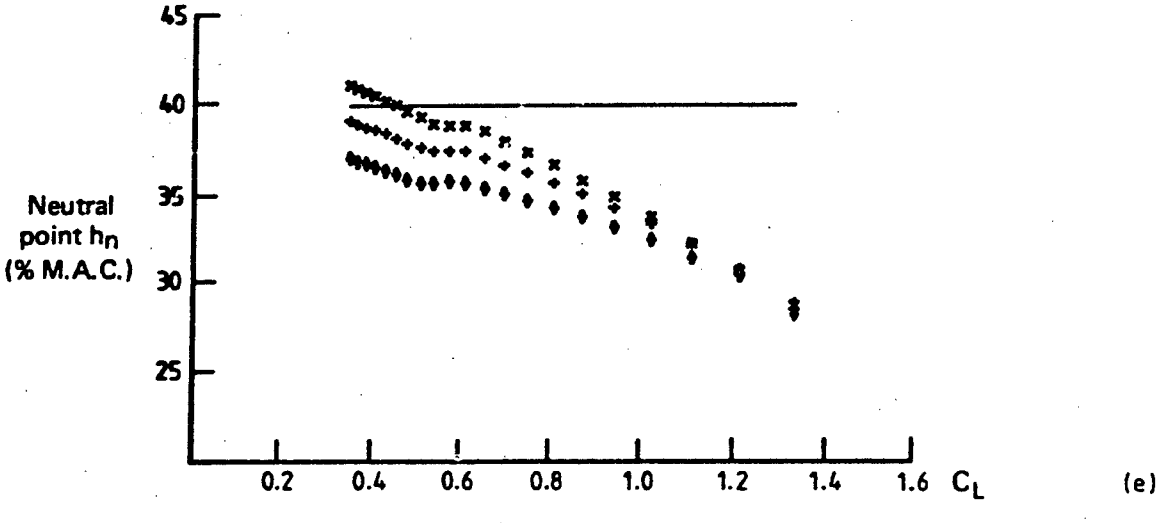

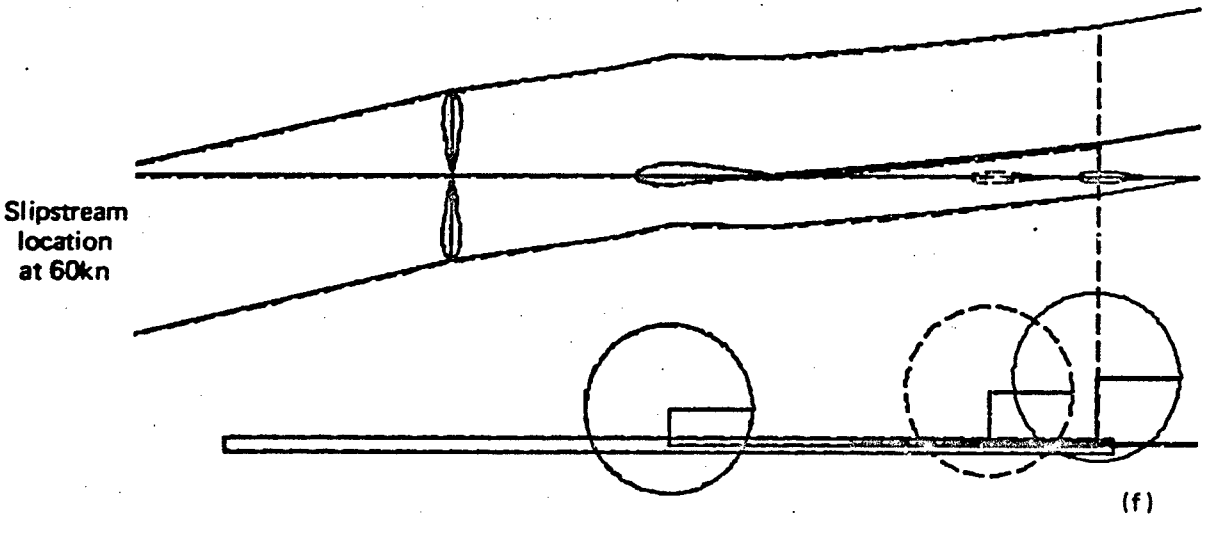

FIG. 27 EFFECT OF TAIL LONGITUDINAL POSITION: TAIL VOLUME COEFFICIENT $\bar{V}$ FIXED (POWER-ON)

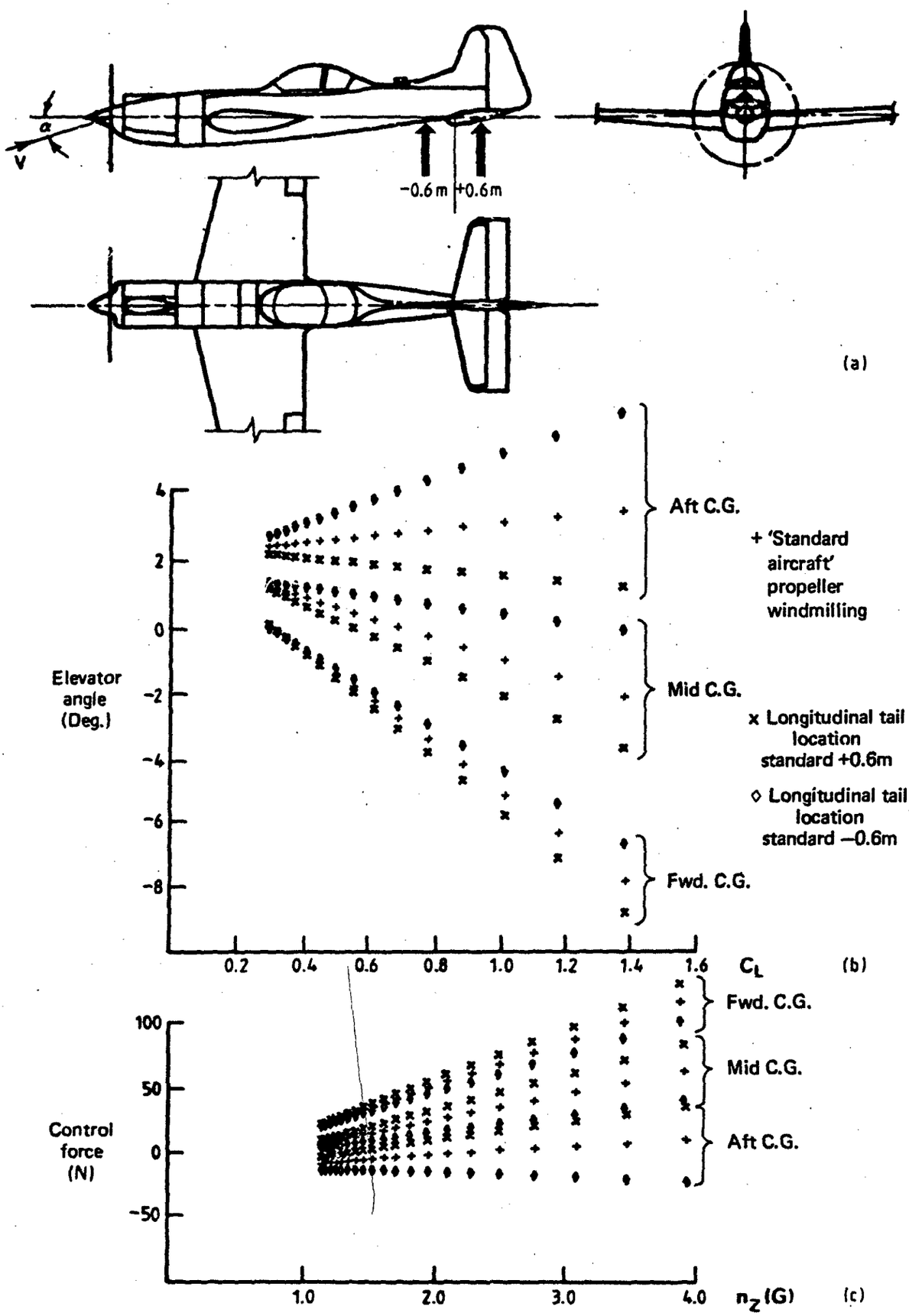

FIG. 28 EFFECT OF TAIL LONGITUDINAL POSITION: TAIL VOLUME COEFFICIENT $\bar{V}$ VARYING (POWER-OFF)

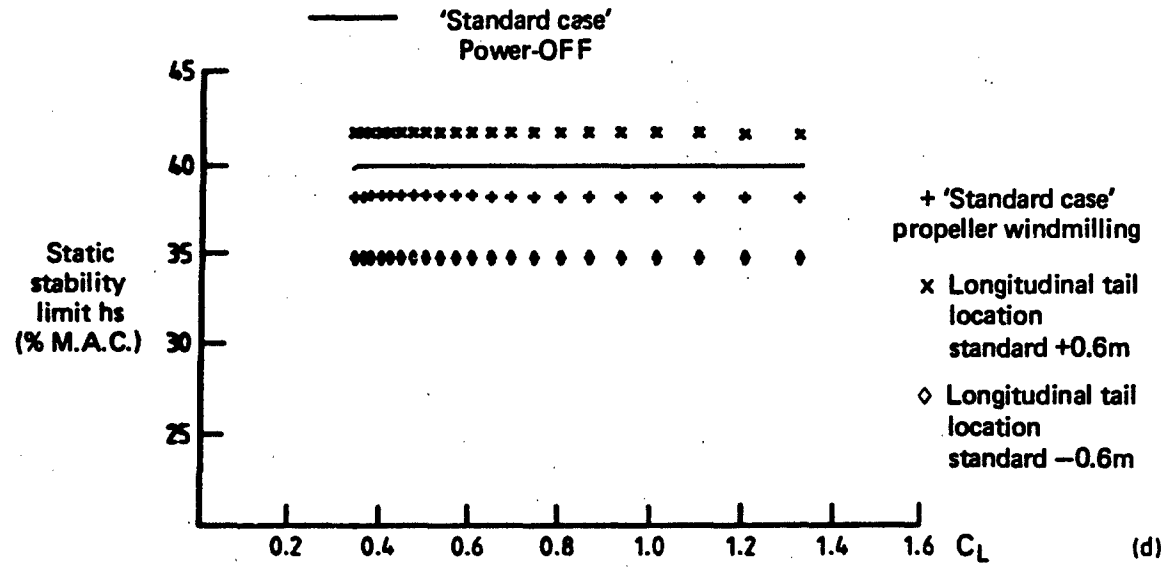

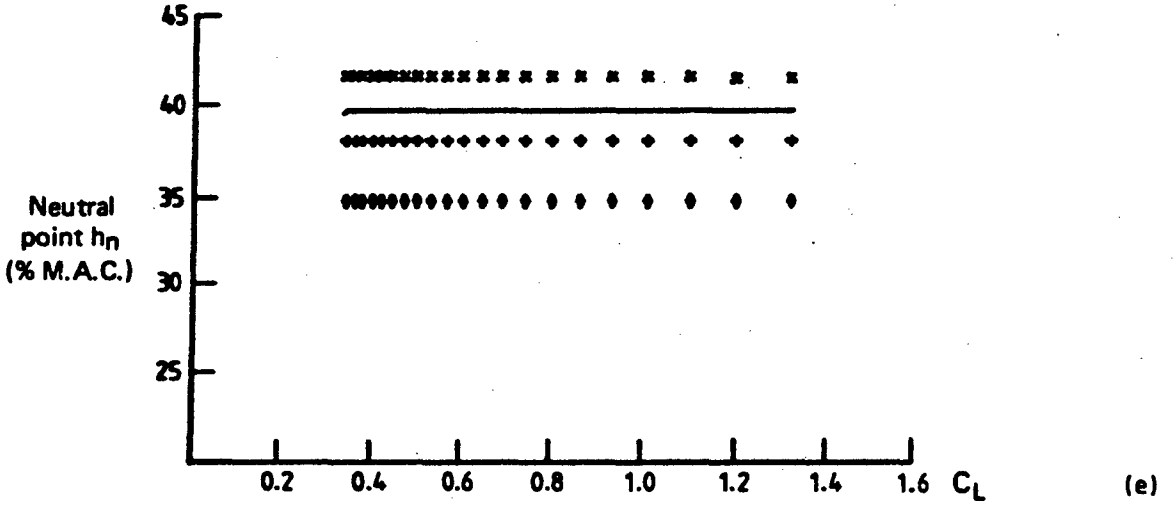

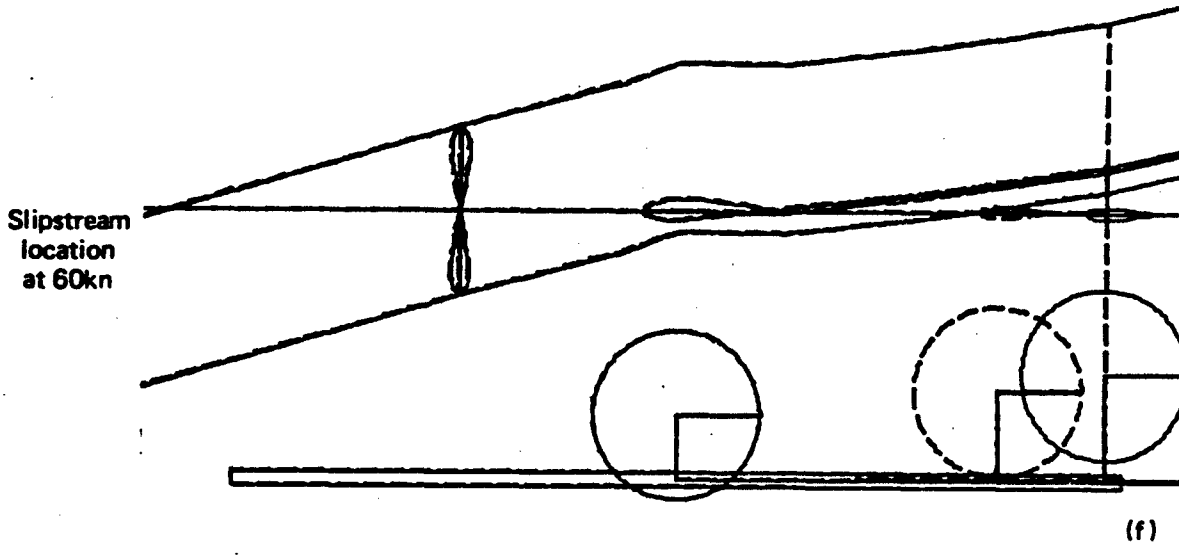

FIG. 28 EFFECT OF TAIL LONGITUDINAL POSITION: TAIL VOLUME COEFFICIENT ∇ VARYING (POWER-OFF)

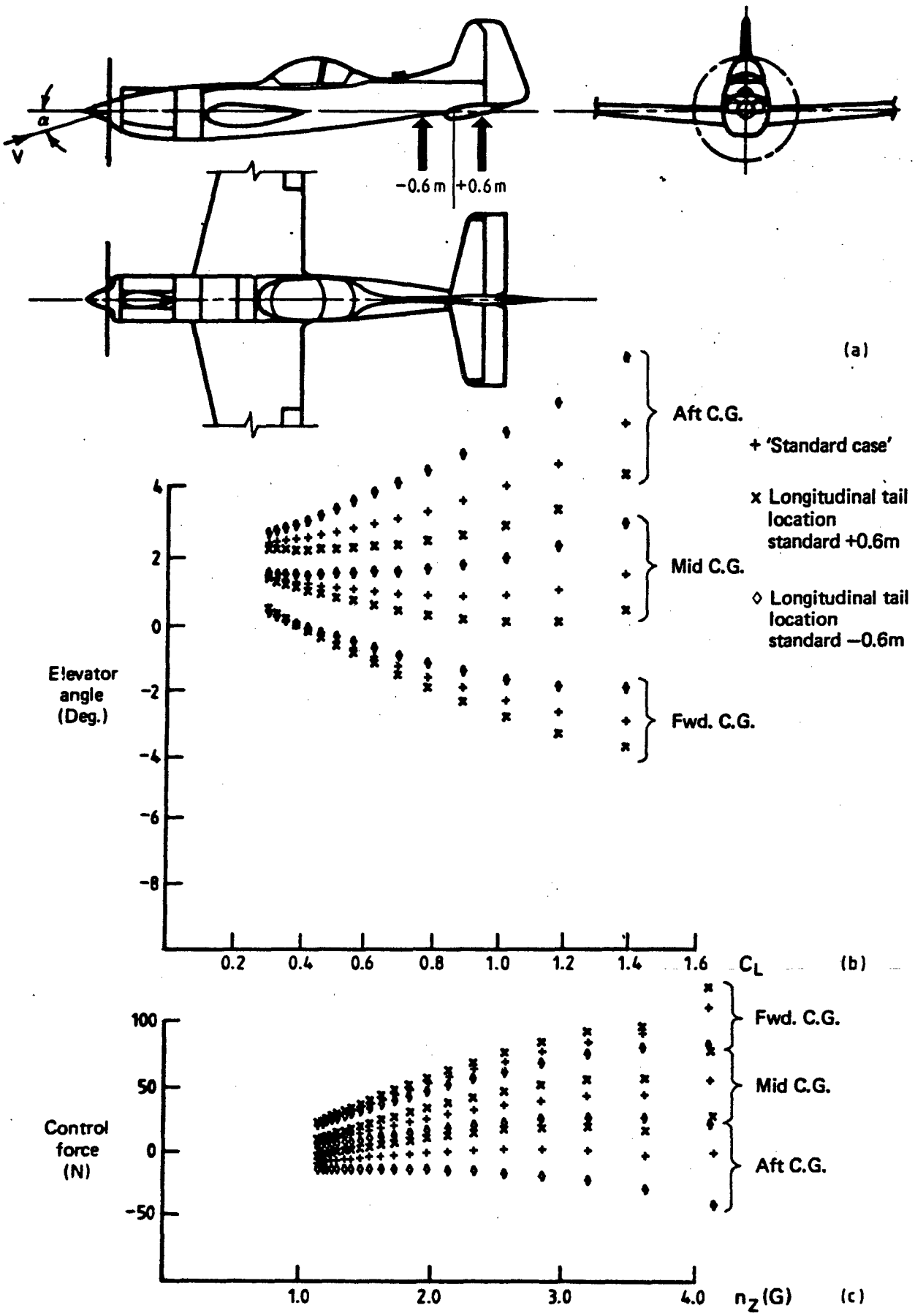

FIG. 29 EFFECT OF TAIL LONGITUDINAL POSITION: TAIL VOLUME COEFFICIENT VARYING (POWER-ON)

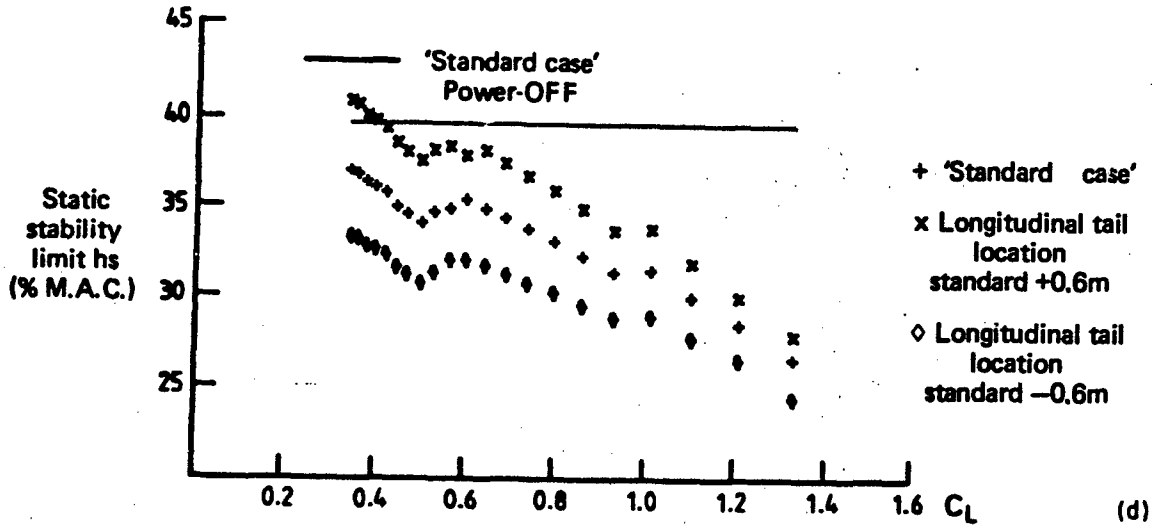

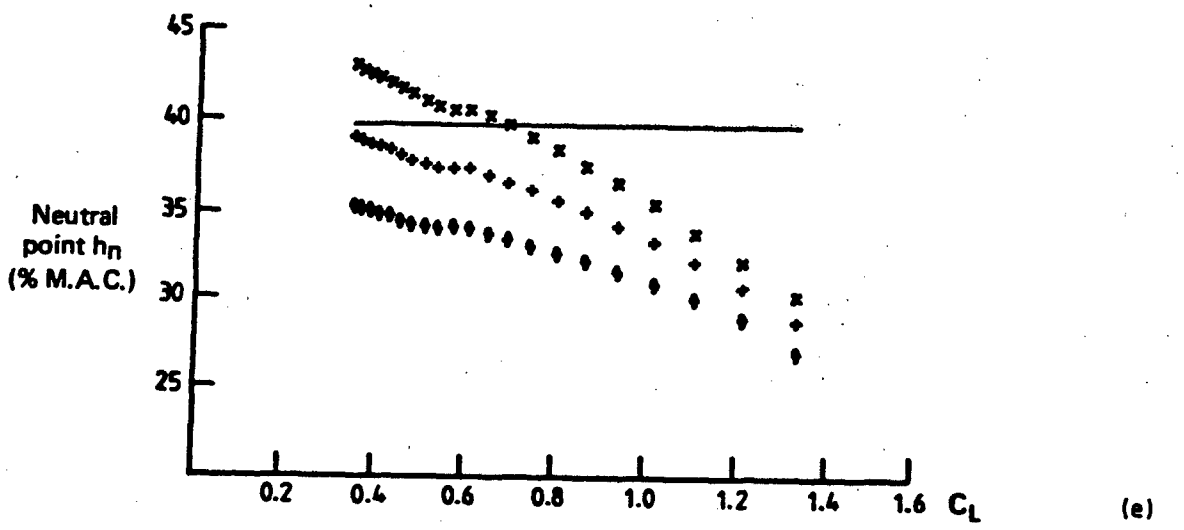

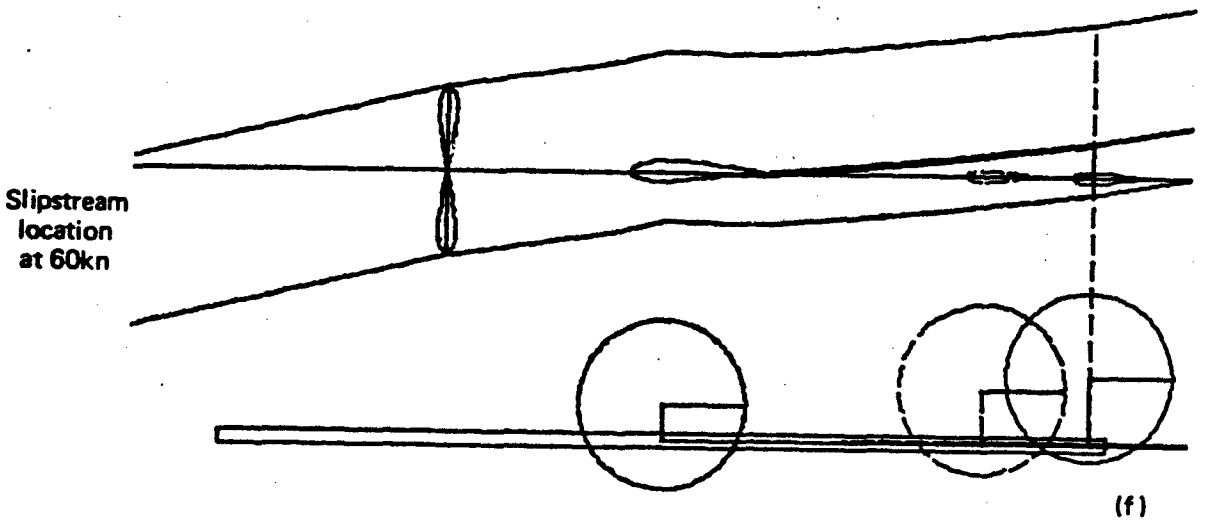

FIG. 29 EFFECT OF TAIL LONGITUDINAL POSITION: TAIL VOLUME COEFFICIENT VARYING (POWER-ON)

moment from the windmilling propeller. This will be trimmed by a small up-elevator change. The effect of ΔC_{D_F} depends on the vertical c.g. position, but is generally small compared with the other contributions.

The net trim change due to these individual effects is; an increase in down elevator of approximately 2 deg. (as shown in Fig. 30*b*), and a small push force on the control column of between 4 and 10 N (1 and 2 lbf) depending on the speed. These trim changes are approximately the same for all c.g. positions.

The change in *stability* due to deflecting the flaps 20 deg. with power off is very small, as shown in Figure 30*d*. This reduction is due to a change in the downwash gradient at the tailplane, caused by increased aerodynamic loading on the inboard portion of the wing and by a change in the tailplane location with respect to the wing wake, at a given C_L.

The change in *trim* due to lowering the flaps with power on is small, and is less than for the power-off case, as shown by comparing Figures 30*b* and 31*b*. The small net trim changes are the result of much larger changes due to individual power effects. ΔC_{m_P} is effectively increased due to increased dynamic head over the wing and body, and is trimmed by a large up-elevator movement. Opposing this change is a down-elevator movement. This is required to oppose the effects of increased downwash arising from the effect of slipstream on the flapped portion of the wing. In addition, the net download on the tailplane required for trimming in the flapped configurations, is magnified by the slipstream dynamic head and so, a further down-elevator movement is required for trim.

The change in stability due to lowering the flaps by 20 deg. with power on is large, as shown in Figure 21*d*. While the net change is similar in magnitude to the zero flap changes with power, the individual contributions to h_s, as shown in Figure 31*g*, are substantially different. With 20 deg. flap, the dynamic head effects at the tailplane are mostly destabilising as shown in Figure 31*g*, while with zero flap they are mostly stabilising, as shown in Figure 14*a*. The difference arises because, firstly, the tailplane carries a download with flaps deflected, and (as discussed in Section 5.5) the effects of power in these circumstances can be destabilising. Secondly, as incidence decreases, and speed increases to maintain rectilinear flight, and the tailplane emerges from the top of the slipstream. These destabilising effects are opposed by a large stabilising contribution due to the effects of power on ΔC_{m_F}, as shown by the change from curve 2 to curve 3 in Figure 31*g*, and by a smaller downwash effect compared with the zero flap case. The large stabilising contribution due to ΔC_{m_F} only affects h_s, as Figures 31*g* and 31*h* illustrate. Therefore, the "manoeuvrability" characteristics will be degraded more than the "static stability" characteristics, due to the effects of power with flaps deflected, as discussed in Section 8.

The effects of power with flaps deflected, illustrate the importance of the correct selection of tailplane location. For the "standard case" aircraft layout used in this study, the tailplane emerges from the bottom of the slipstream at low speed with zero flap, and emerges from the top of the slipstream at high speed with 20 deg. flap. In both cases stability is reduced considerably.

7. EFFECT OF POWER ON CONTROLS FREE STABILITY

For an aircraft with manual controls, the elevator hinge moment characteristics determine the angle to which the elevator will float if the controls are free, or alternatively, the control force, if the controls are restrained by the pilot. In the first condition, the longitudinal stability is modified.

The simple theory of "static stability" shows that the change in neutral point (h_n) due to freeing the controls is given by:

$$\Delta h_n = -\bar{V}\left(\frac{\partial C_{L_T}}{\partial \delta_e}\Big/\frac{\partial C_L}{\partial \alpha}\right)\left(\frac{\partial C_H}{\partial \alpha_T}\Big/\frac{\partial C_H}{\partial \delta_e}\right)\left(1-\frac{\partial \epsilon}{\partial \alpha}\right). \tag{21}$$

Compared with the development in Reference 1, Equation (21) neglects the effect of elevator on total aircraft lift and uses $\bar{V}$ based on the distance between wing and tailplane aerodynamic centres. The parameter $\partial C_H/\partial \alpha_T$ has particular significance since it can be modified readily in both magnitude and sign by the designer. A zero value gives zero change in h_n, while positive

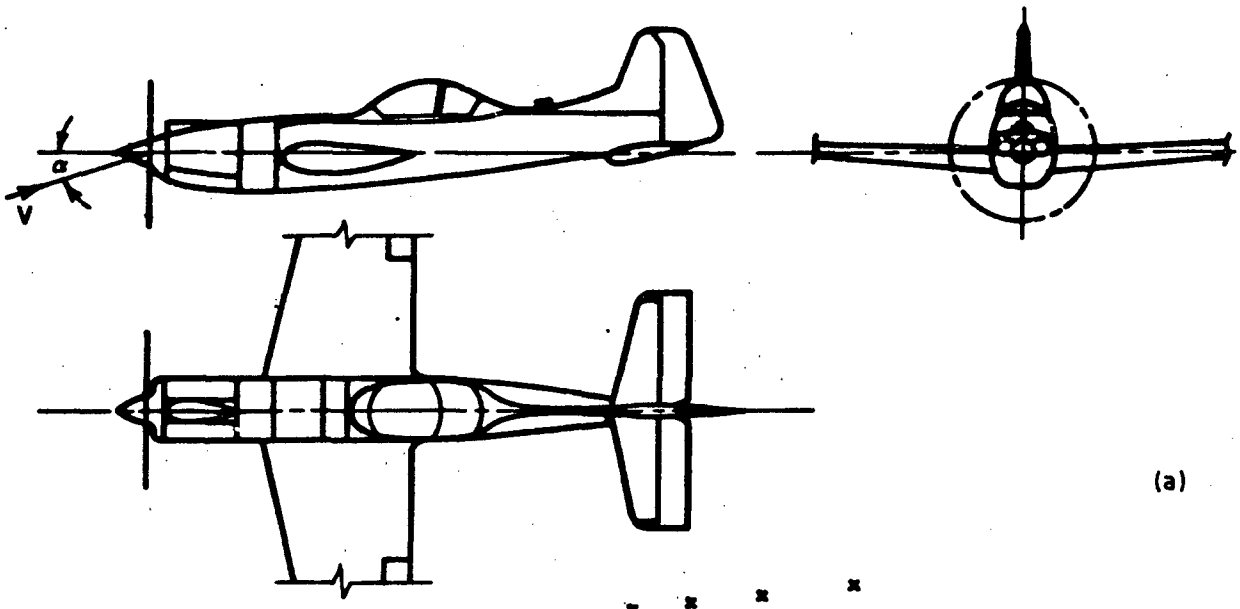

(a)

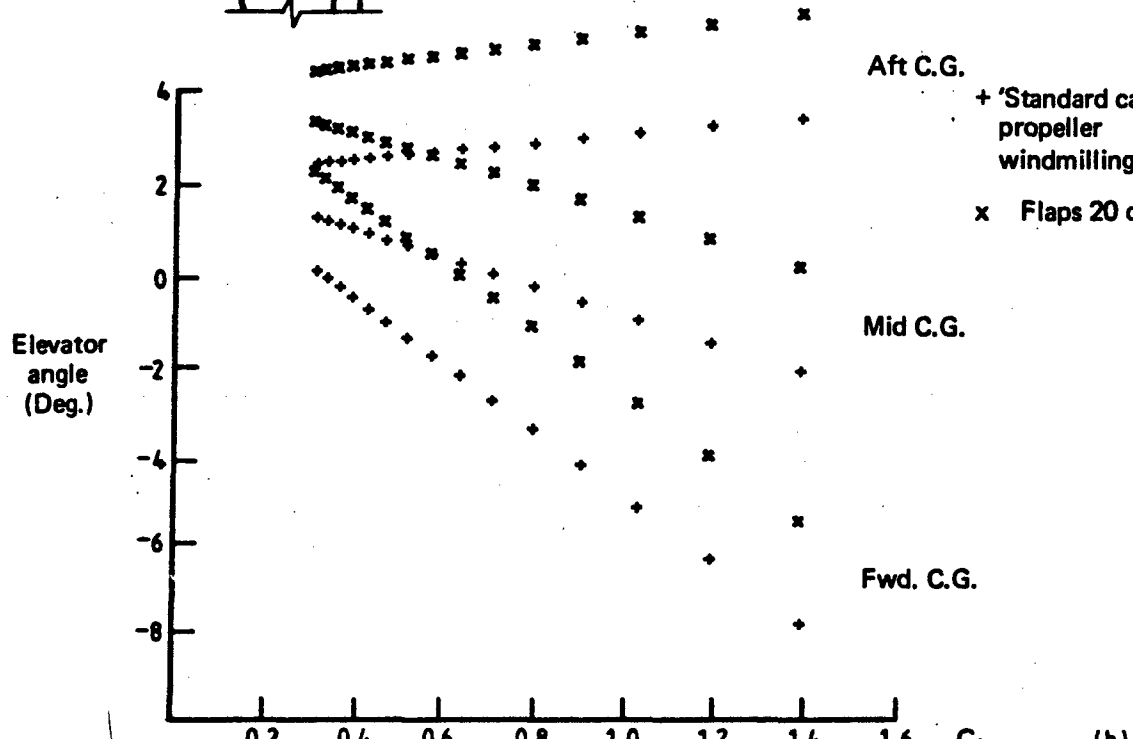

(b)

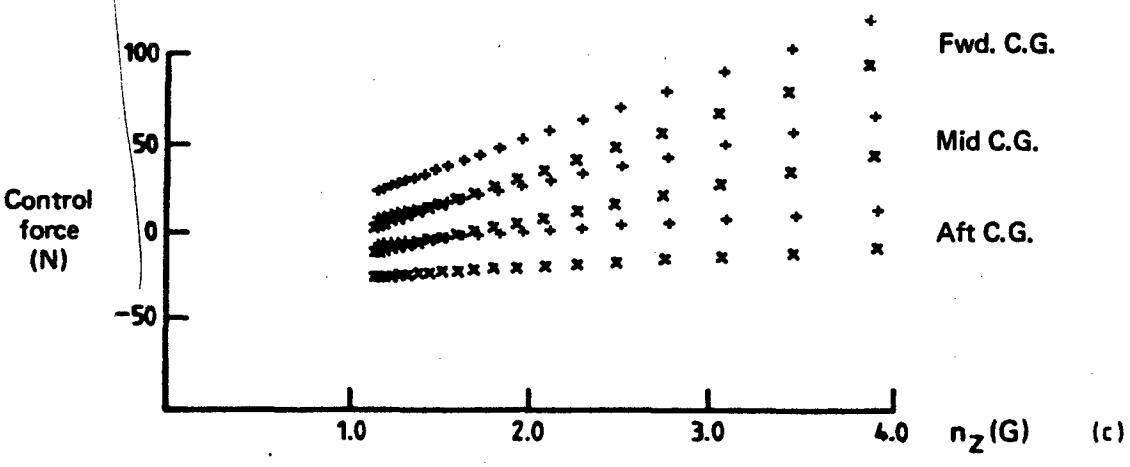

(c)

FIG. 30 EFFECT OF 20 DEG. FLAP DEFLECTION (POWER-OFF)

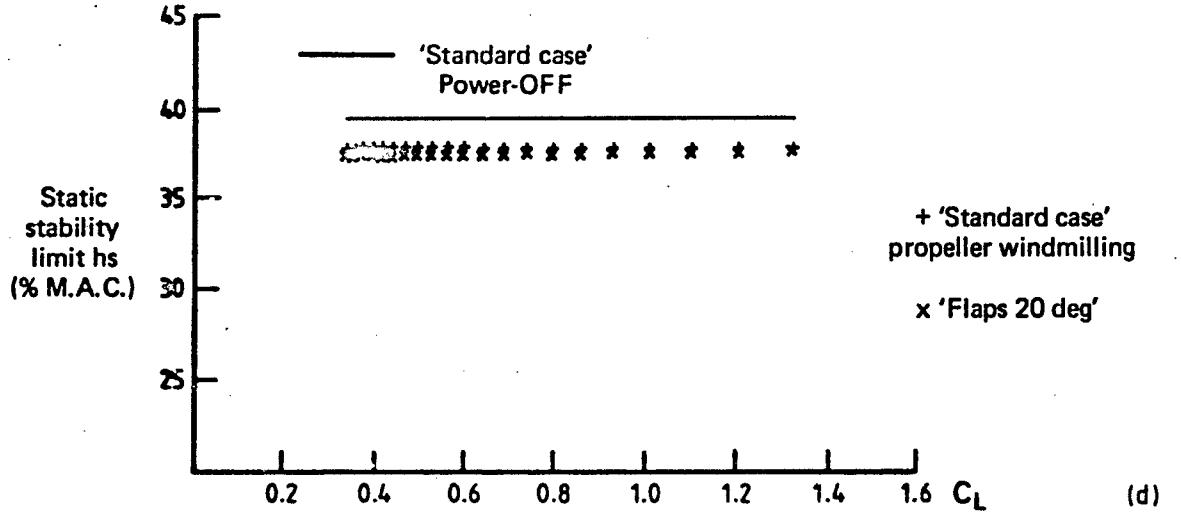

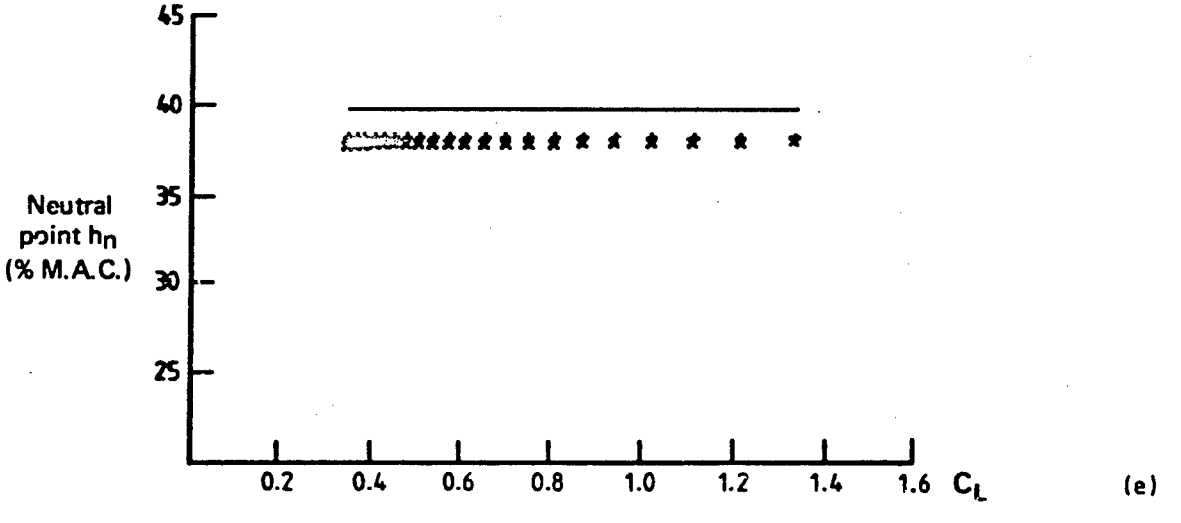

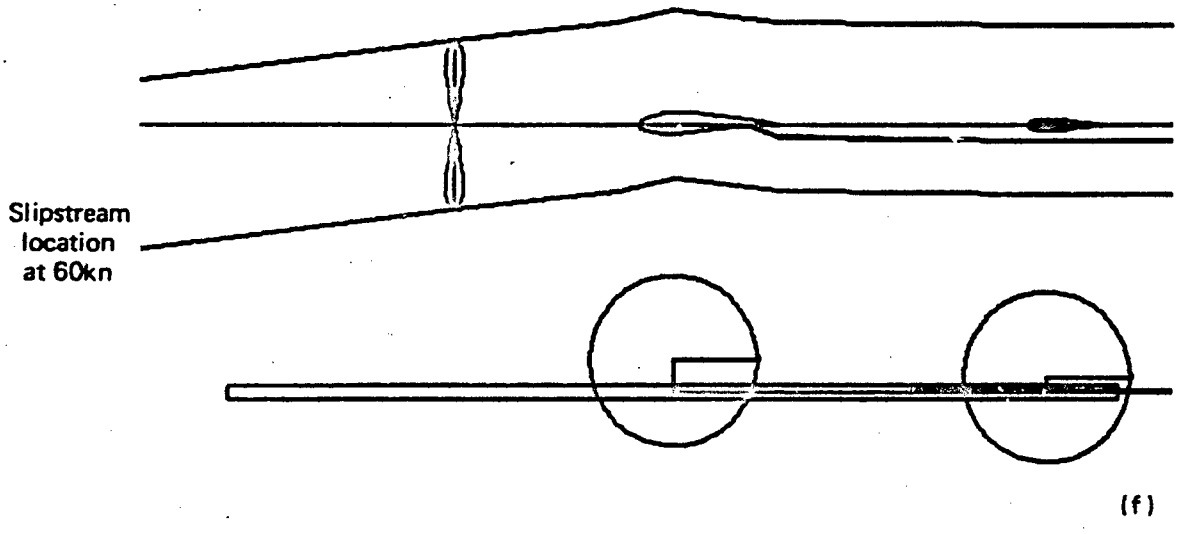

FIG. 30 EFFECT OF 20 DEG. FLAP DEFLECTION (POWER-OFF)

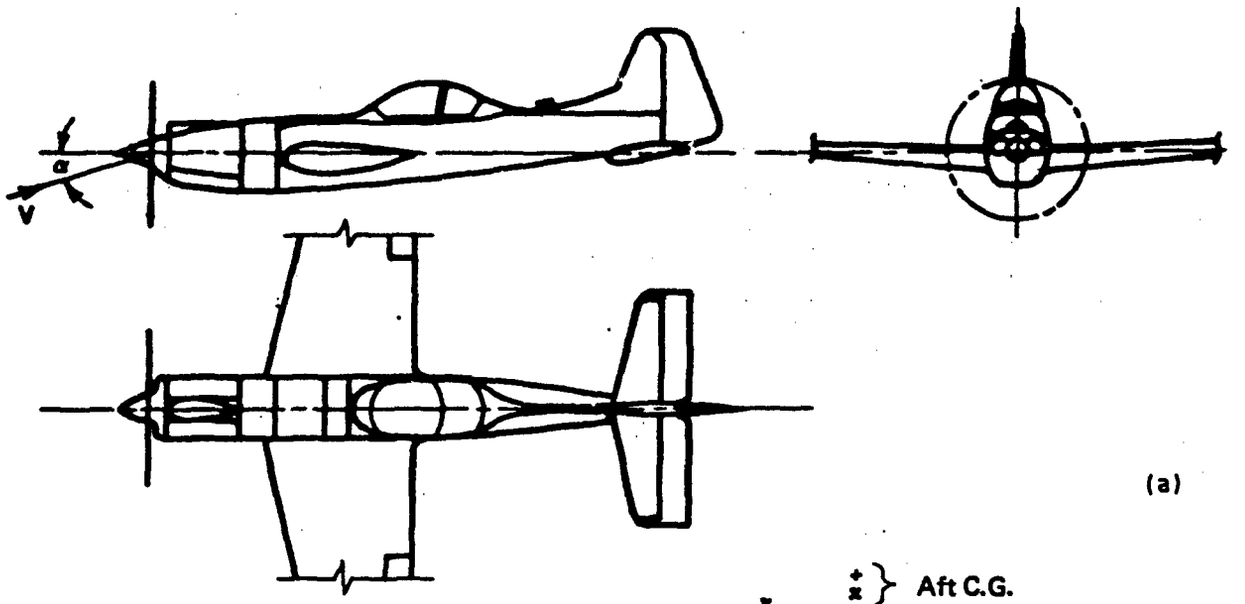

(a)

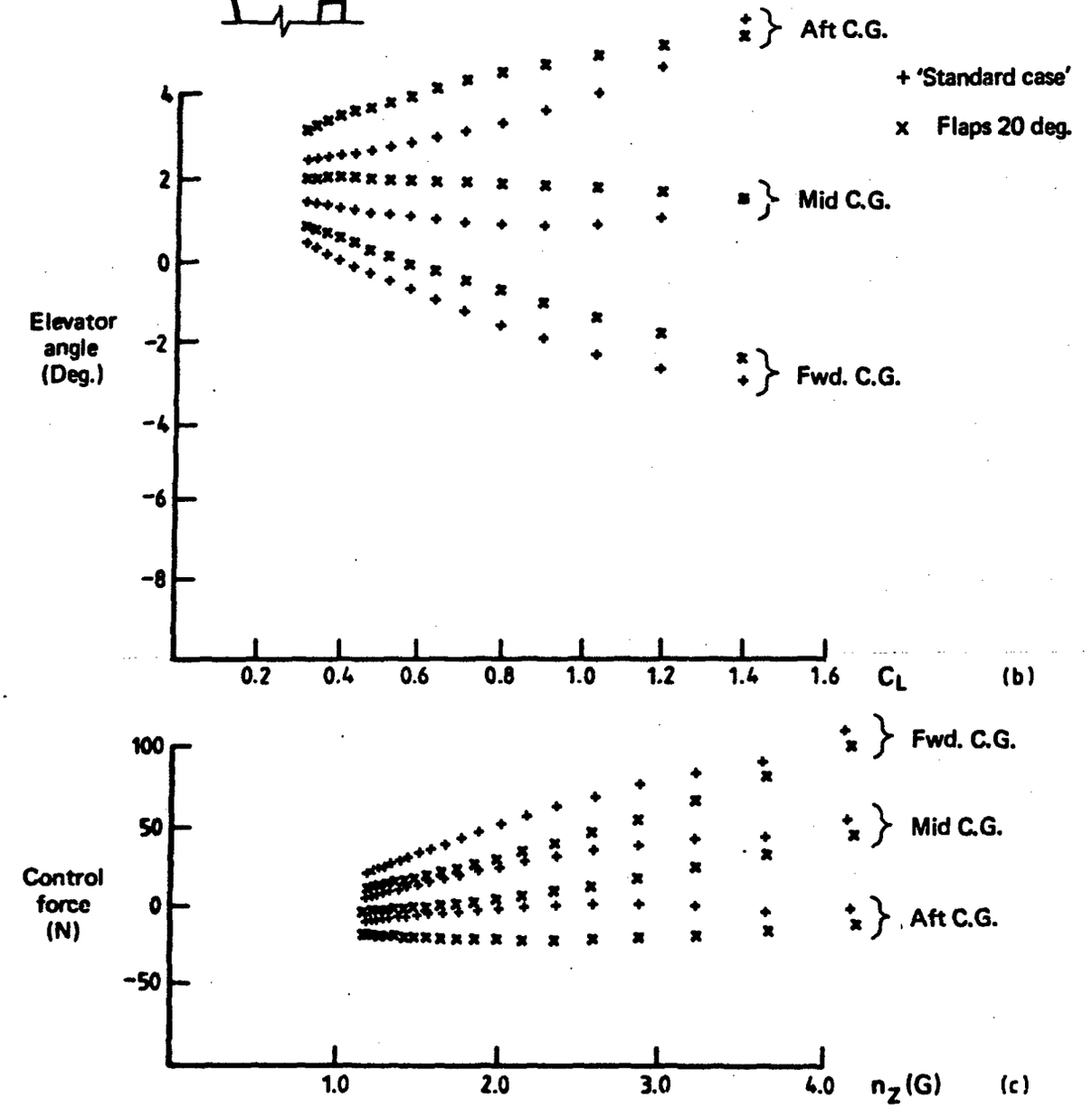

FIG. 31 EFFECT OF 20 DEG. FLAP DEFLECTION (POWER-ON)

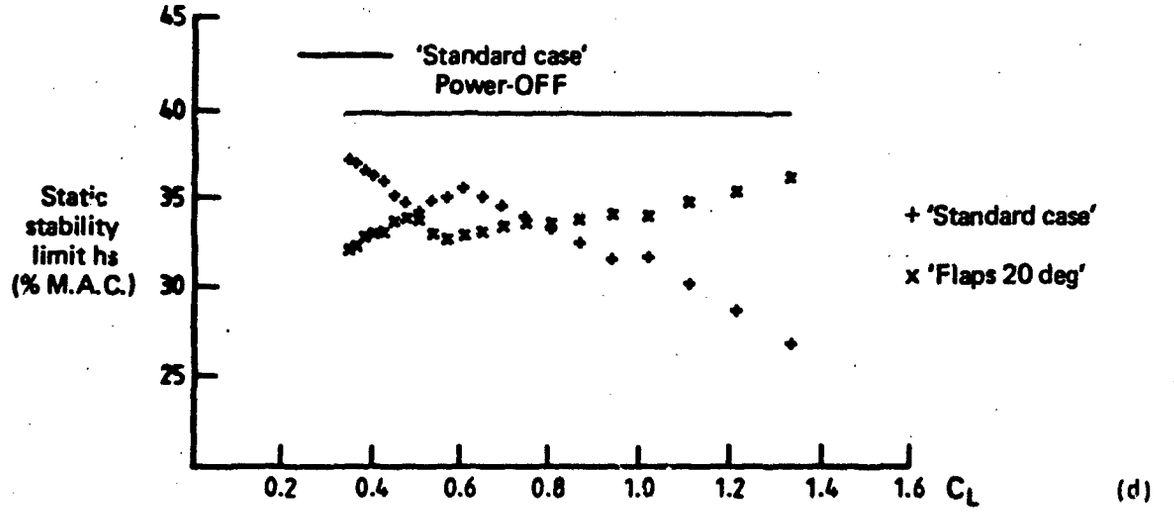

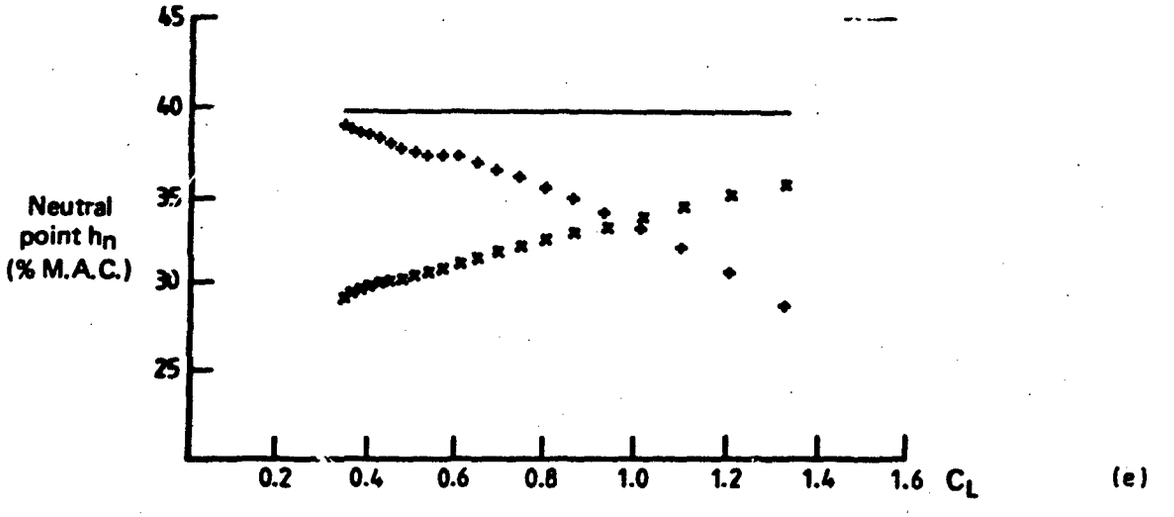

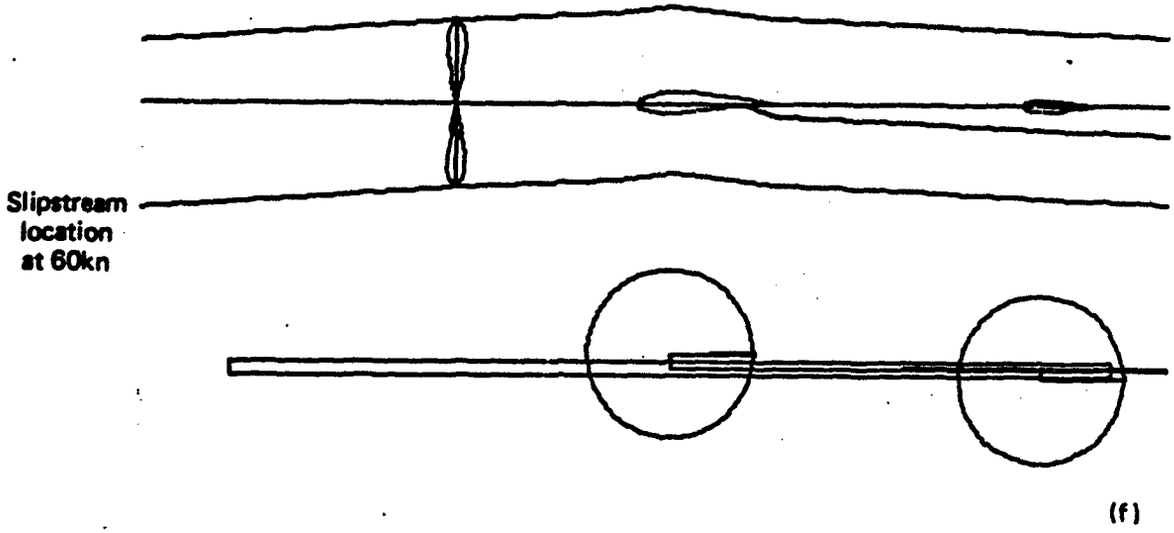

FIG. 31 EFFECT OF 20 DEG. FLAP DEFLECTION (POWER-ON)

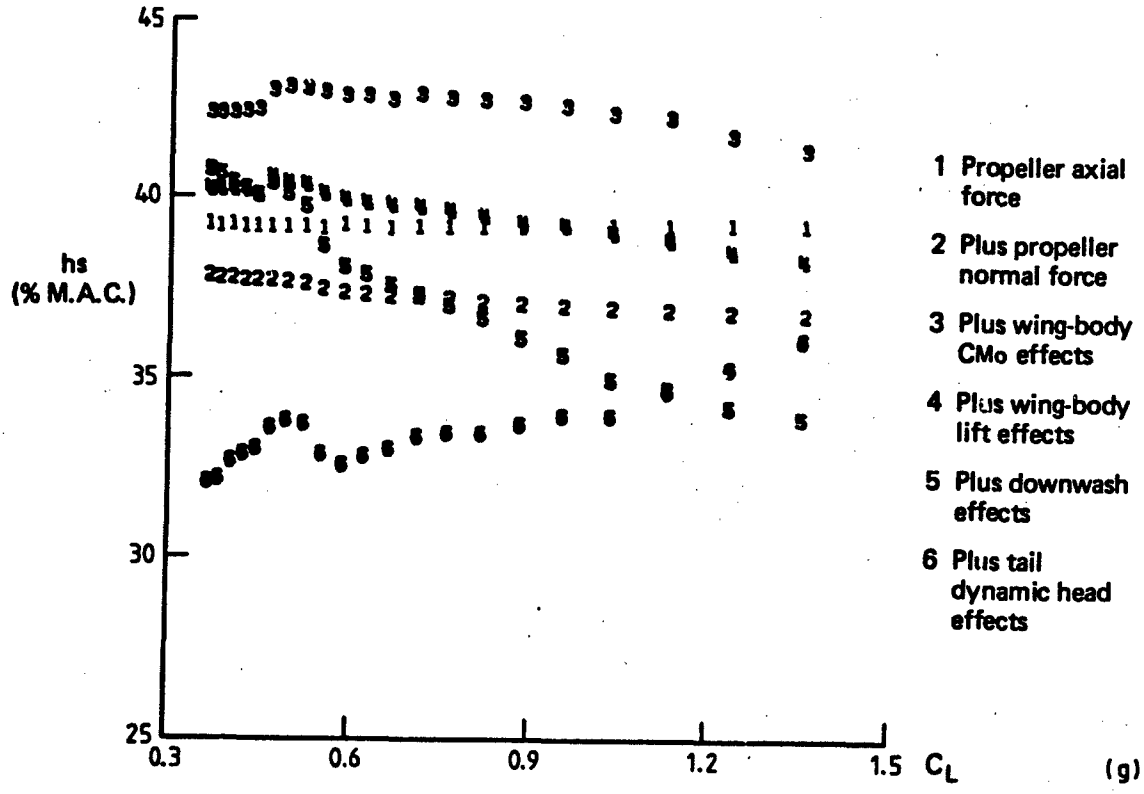

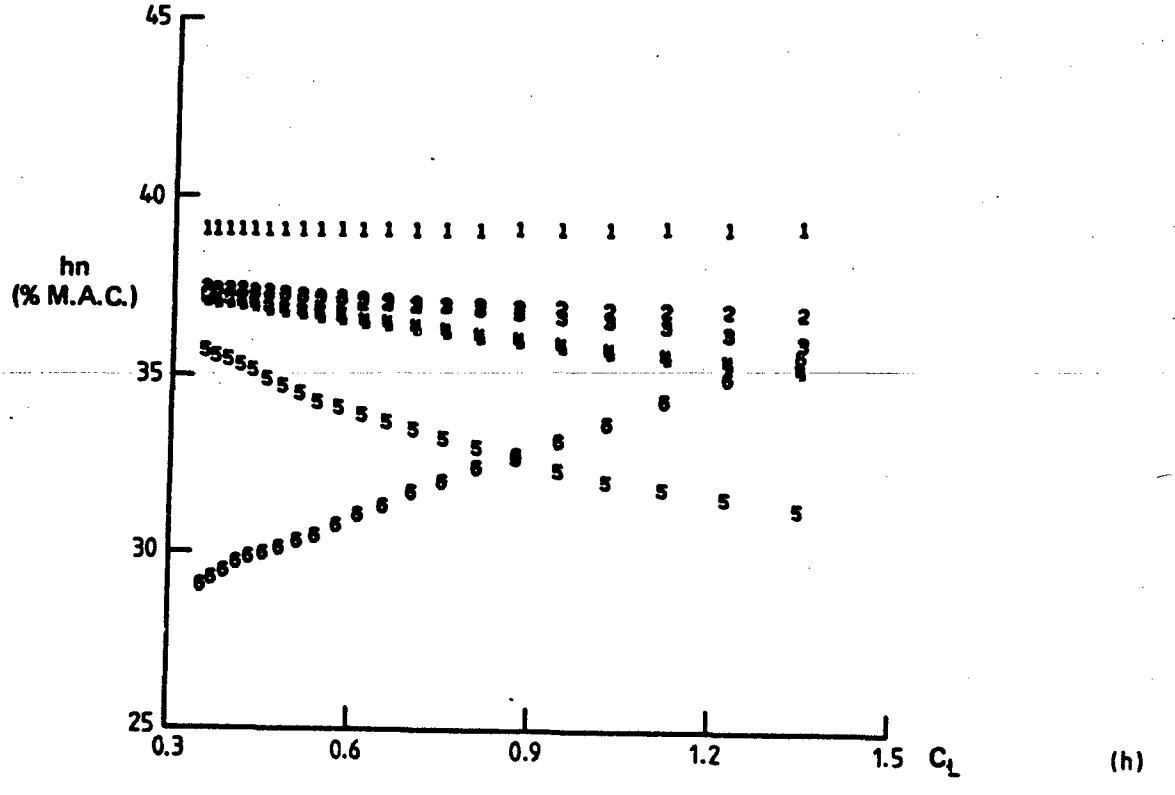

FIG. 31 ACCUMULATION OF POWER EFFECTS OF hs AND hn 20 DEG. FLAP DEFLECTION

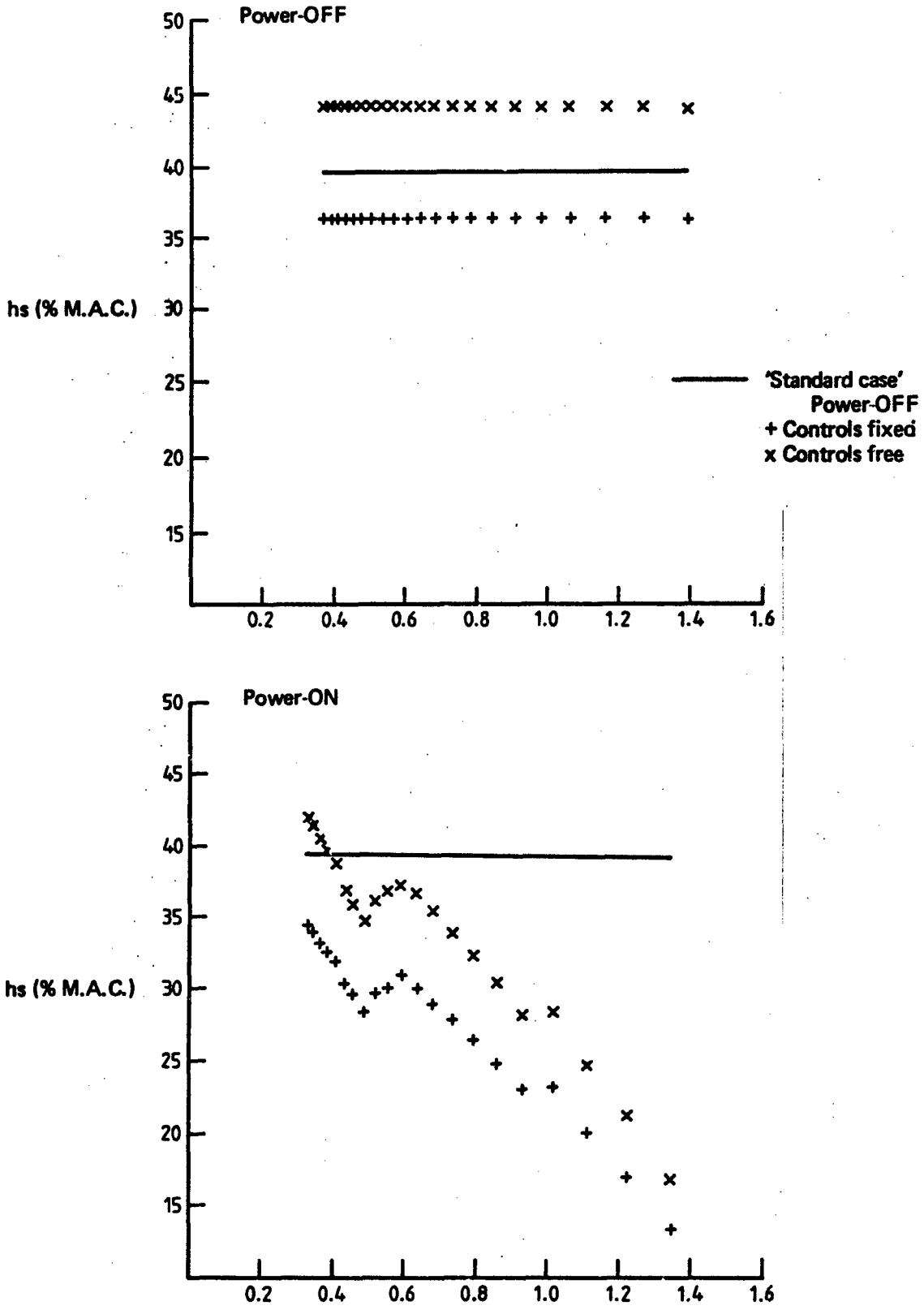

FIG. 32 EFFECT OF POWER ON hs CONTROLS FIXED AND CONTROLS FREE

and negative values lead to an increase and decrease in h_n respectively. When the controls are freed, the elevator floats to a position determined by the relative sizes of $\partial C_H/d\alpha_T$ and $\partial C_H/d\delta_e$. In the more general case, the hinge moments will be a function of aircraft velocity (V) due, for example, to slipstream effects. For the present study, it will be assumed, in the absence of contradictory information, that the change in hinge moment characteristics with speed is assumed to be proportional to the effective dynamic head ratio. Thus, all the coefficients of the hinge moment equation (Eqn. 19), will increase in the same proportion, and the float angle will be the same irrespective of thrust coefficient (C_T). Equation (21) shows that the only change to stability due to power, when the controls are freed, will arise from changes in the lift characteristics $\partial C_L/\partial\alpha$ and $\partial C_{L_T}/\partial\delta_e$ and in the downwash gradient $\partial\epsilon/d\alpha$. Figures 32*a* and 32*b* show the effect of power on h_3 with controls fixed and free, assuming $\partial C_H/\partial\alpha_T = 0{\cdot}135$. The increase in h_n is approximately $4\%\bar{c}$ both with power off and power on at most speeds. At low speeds, Δh_n is slightly less with power on, because of the reduction in tail effectiveness $\partial C_{L_T}/\partial\alpha_T$ as the tail emerges from the slipstream compared with the increase in wing–body lift curve slope $\partial C_L/\partial\alpha$.

When the controls are restrained, the control forces are proportional to the changes in hinge moment characteristics given in Equation (19). Although positive $\partial C_H/\partial\alpha_T$ increases the controls free stability, "manoeuvrability" requirements may limit the size of $\partial C_H/\partial\alpha_T$.

8. EFFECT OF POWER ON LONGITUDINAL MANOEUVRABILITY, DYNAMIC MODES AND RESPONSE TO CONTROLS

8.1 Longitudinal Manoeuvrability

The theory of longitudinal manoeuvrability is closely associated with "static stability", and has been given similar prominence in the study of flying qualities because it relates to two major handling qualities parameters, control force per g and control angle per g. These parameters are defined for trimmed flight in steady turns, or steady pull-ups at constant speed. Compared with conditions in trimmed rectilinear flight, considered under "static stability", the forces due to changes in speed are absent, but additional forces due to rate of pitch are present. The steady pitch rate produces a variation in local incidence along the aircraft which is a function of; pitch rate, distance from the aircraft c.g., and true air speed. For a low-speed aircraft of conventional layout, and having a nose-mounted propeller, the main changes in aerodynamic forces and moments are associated with changes in incidence at the tail and at the propeller. The incidence changes at the wing and body due to pitch rate are small and, in this study, have been neglected.

The effects of power on the aerodynamic forces at the propeller and tailplane induced by the pitch rate are the same as the steady effects described in Section 5. Because the induced incidence at the tailplane depends on the *true* speed of the airflow over the tailplane, the resulting aerodynamic force will be a function of altitude and also of slipstream velocity. For this study, slipstream velocity is calculated from the mean effective dynamic pressure at the tail.

From the theory of "manoeuvrability", it can be shown that control force per g is given by the equation:

$$P_{\delta_e}/n_z = -G_{\delta_e} S_{\delta_e} c_{\delta_e} \frac{W}{S_w} \frac{\partial C_H/\partial\delta_e}{\partial C_{L_T}/\partial\delta_e} \frac{1}{\bar{V}} \left(h_{n,\text{FREE}} - h + \bar{V} \frac{\overline{\partial C_{L_T}}}{\partial\alpha_T} \Big/ 2\mu_1 \right) \tag{22}$$

where $h_{n,\text{FREE}}$ is the neutral point with controls free and

$$\frac{\overline{\partial C_{L_T}}}{\partial\alpha_T} = \frac{\partial C_{L_T}}{\partial\alpha_T} - \frac{\partial C_{L_T}}{\partial\delta_e} \times \left(\frac{\partial C_H}{\partial\alpha_T} \Big/ \frac{\partial C_H}{\partial\delta_e} \right), \tag{23}$$

$$\mu_1 = W/gS_w\rho l_T. \tag{24}$$

Compared with the development in Reference 1, Equation (22) neglects the effect of elevator on total aircraft lift, and uses $\bar{V}$ based on the distance between wing and tailplane aerodynamic centres.

Equation (22) shows that control force per g is a function of c.g. position (h), the neutral point ($h_{n,\text{FREE}}$), wing loading (W/S_w), control gearing (G_{δ_e}), altitude, via the parameter μ_1, and the control characteristics $\partial C_L/\partial\alpha_T$, $\partial C_L/\partial\delta_e$, $\partial C_H/\partial\alpha_T$, $\partial C_H/\partial\delta_e$. However, it is independent

of the motion variables aircraft velocity (V) and incidence (α). When power effects are present, the aerodynamic forces become non-linear functions of both aircraft velocity (V) and incidence (α). As a result, control force per g becomes in general, a non-linear function of incidence, with different values at different aircraft velocities.

Airworthiness specifications require the control force per g to lie within a given range depending upon the aircraft type. In practice, it can be difficult for a designer to meet these requirements for all variations of c.g. position, wing loading, aircraft speed and power. In Figure 33, the variation of control force per g with speed is summarised for the "standard case", for a c.g. range of 10%$\bar{c}$, for zero and 6 km altitude with power off and power on. The aft c.g. is located at 25%$\bar{c}$, so that the aircraft is "statically stable" at 60 kn and above. For reference, a useful design aim for this type of aircraft is to provide a control force per g range of 3 to 8 lbf./g (13·3 to 35·6 N/g) within a c.g. range of 10%$\bar{c}$ throughout the flight envelope. Figure 33 shows that the maximum control force per g for the "standard case" occurs at sea-level, 120 kn with power off, and c.g. at the forward limit. In this condition, h_n is 14%$\bar{c}$ aft of the aft c.g. limit showing that the aircraft possesses large pitch stiffness. The minimum control force per g occurs at 6 km height, 60 kn speed, with power on and aft c.g. In this condition h_n is 3%$\bar{c}$ aft of the aft c.g. and so a small degree of pitch stiffness still exists. The control force per g range of 1·8 to 13·5 lbf./g (8 to 60 N/g) is outside the design guide at both limits. As illustrated in Figure 33, this large range of values results from the large change in pitch stiffness with speed for the "standard case".

The difference between h_s and h_n can also influence the control force per g range. For example, h_s may be increased without altering h_n by inclining the thrust axis, as described in Section 6.1, or by incorporating a "downspring" in the control circuit and so permitting the aft c.g. to be moved rearwards. In Figure 34 the control force per g values for the case with the thrust axis inclined downwards 5 deg. are summarised. If the aft c.g. is moved back to 30%$\bar{c}$, to take advantage of the increased "static stability", the minimum control force per g becomes negative at 6 km height, 60 kn speed, with power on and aft c.g. This is caused by a combination of negative pitch stiffness, i.e. h_n lying ahead of the aft c.g., and a low pitch-damping contribution, due to the emergence of the tailplane from the slipstream at low speeds. From these examples it can be seen that the variation in control force per g will be a minimum if, firstly, there are no changes in h_n with power and, secondly, if the minimum value of h_s is equal to this constant h_n.

As shown in Figures 31*d* and 31*e*, the effect of 20 deg. flaps is to reduce the power-on values of h_n more than h_s at high speeds. However, Figure 35 shows that the resulting control force per g range is smaller than for the zero flap case and hence more acceptable. This arises because the maximum value occurs with power off, and is not significantly altered by deflecting the flaps, while the minimum value is calculated using the most rearward c.g. position permitted in the zero flap case, i.e. 25%$\bar{c}$. With 20 deg. flap the aircraft would be statically stable at a c.g. of 32%c, but the associated pitch stiffness would be negative and the control force per g would become unacceptably small.

A further manoeuvrability requirement is that the variation of control force with g should be substantially linear. Figure 13*e* shows that the "standard case" layout with power on exhibits a marked reduction in control force gradient with g above 2·0g, and Figure 13*f* shows a similar reduction in control force per g at low speeds. Both effects occur as incidence increases and are due to the tailplane emerging from the slipstream.

Control force per g characteristics can be changed by changing control hinge-moment characteristics. However, consideration of hinge-moment characteristics, particularly in the presence of power effects, is outside the scope of this Report.

Results for the effect of power on control *deflection* per g have not been presented in this Report, since, in general, this parameter has far less influence on flying qualities than control force per g. It is mainly of importance to the designer in providing adequate control authority for trimming and manoeuvring.

8.2 Longitudinal Dynamic Modes

The longitudinal motion of a stable low-speed conventional aircraft following a disturbance is characterised by two modes of motion, the phugoid and the short period. According to the basic linear theory of aircraft stability, the existence of "static stability" ensures that the phugoid

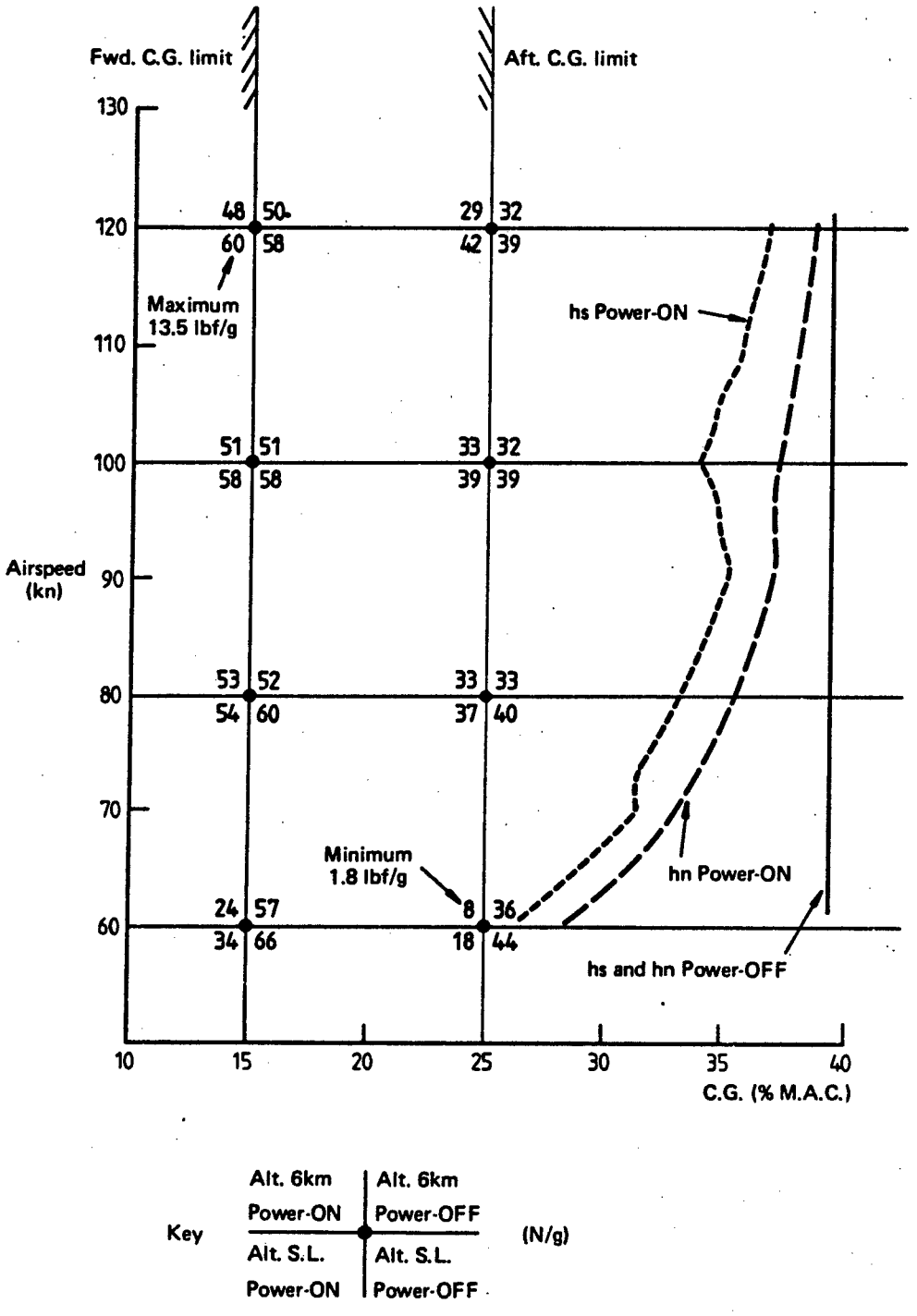

FIG. 33 CONTROL FORCE PER 'g': 'STANDARD CASE'

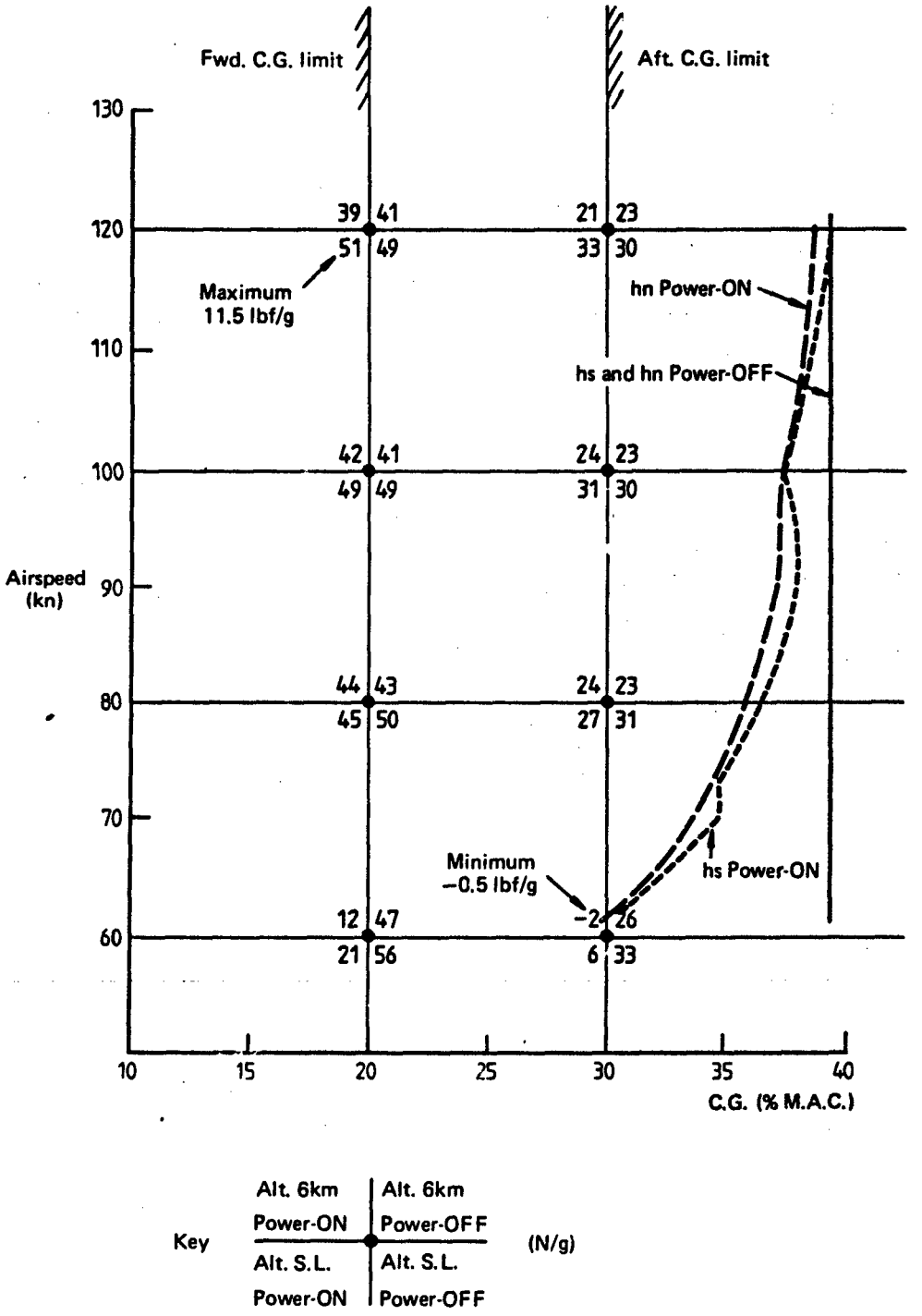

FIG. 34 CONTROL FORCE PER 'g': THRUST AXIS INCLINED – 5 DEG.

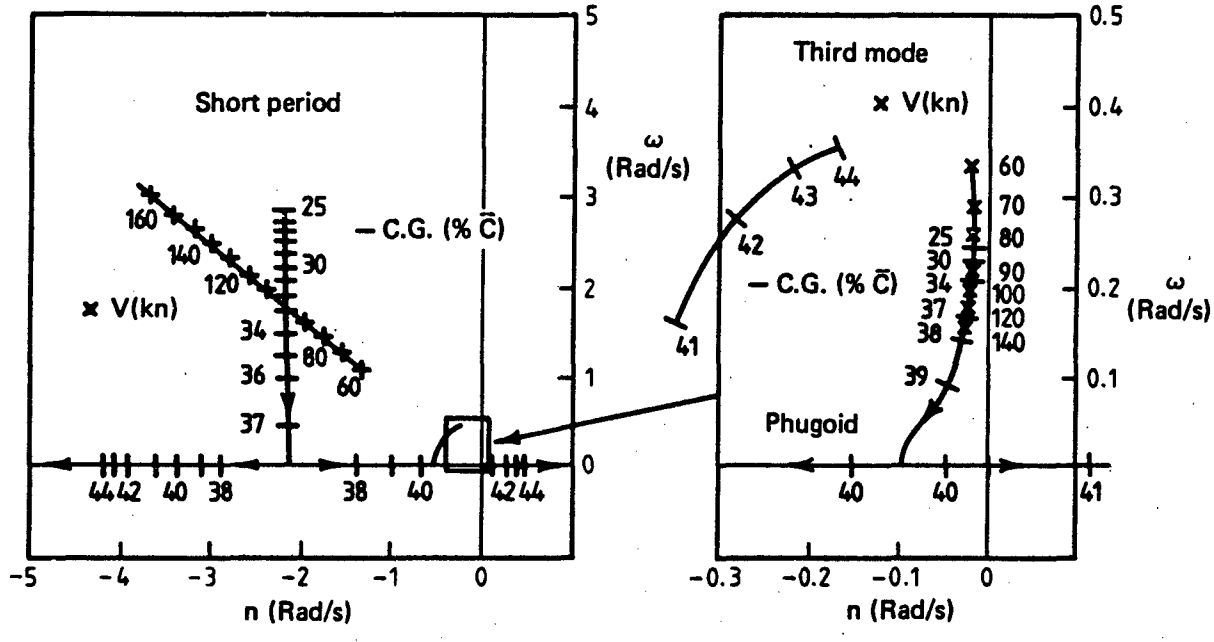

(a) Effect of C.G. and speed 'Standard case' (Power-OFF)

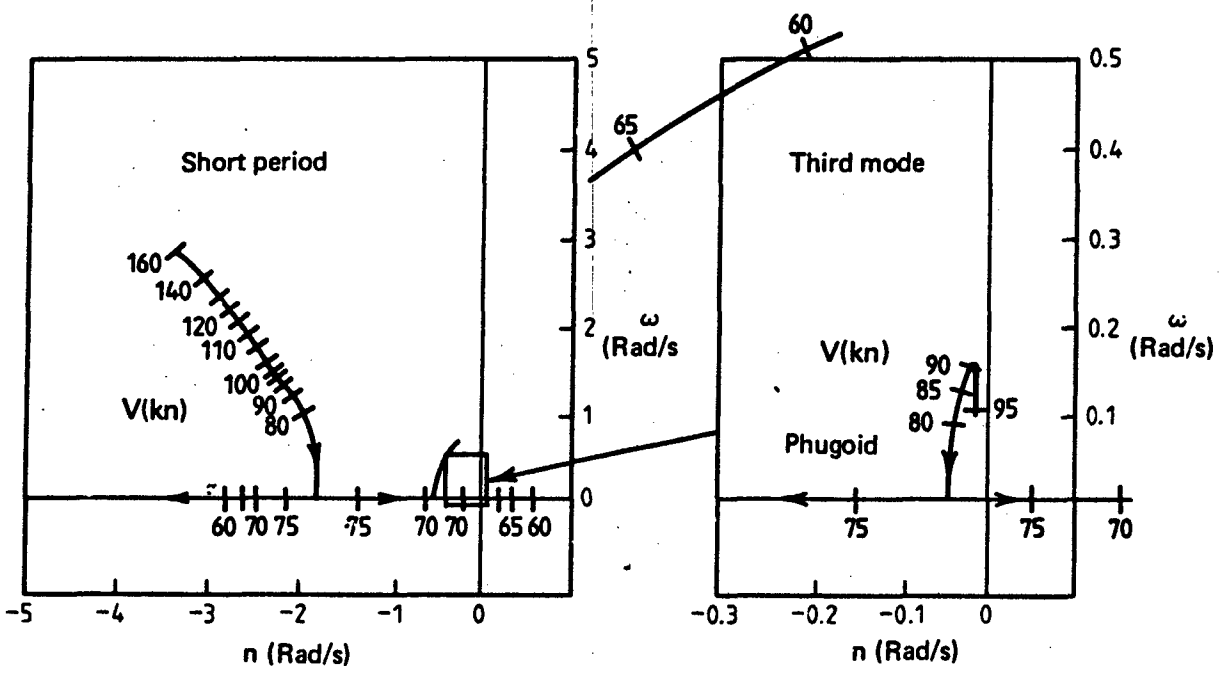

(b) Effect of speed 'Standard case' (Power-ON) Mid C.G.

FIG. 36 EFFECT OF POWER ON LONGITUDINAL DYNAMIC MODES: ROOT LOCUS PLOTS

is stable, and for the type of aircraft considered in this study, also ensures that the short period mode is stable and well damped. The close link between the "static stability" condition and longitudinal stability arises because the stiffness derivatives C_{m_α} and C_{m_V}, which determine the neutral point (h_n) and the static stability limit (h_s), are also dominant terms in the linear longitudinal dynamic equations. Consequently the effect of power on "static stability" parameters h_n and h_s will be reflected in the characteristics of dynamic modes.

Figure 36*b* shows the locus of the eigenvalues of the longitudinal modes as speed is varied for the "standard case" with power on. A mid c.g. has been selected which illustrates both stable and unstable conditions. For comparison, Figure 36*a* shows the eigenvalue loci for the power-off case in which the "static stability" limit (h_s) is approximately constant. Two loci are shown: one with a fixed speed of 100 kn and varying c.g., the other with a fixed mid c.g. of 32·3%$\bar{c}$ and varying speed. The first locus illustrates the effect of changing pitch stiffness, and the second locus illustrates the effect of changing speed. Since the speed derivatives C_{m_V} and C_{L_V} are zero with power off, the variations with speed are due to trim conditions C_{L_e} and C_{D_e} and in particular, for the short period motion, they indicate the dimensionalising of essentially constant non-dimensional eigenvalues. At high speeds, the power-on locus for the short period mode displays the characteristics due to speed changes. As speed reduces, the power effects cause changes in the pitch stiffness so that the locus displays the characteristics illustrated for the changes in c.g. position, with power off. Similarly, the phugoid locus, power on, displays the characteristics associated with both speed and c.g. changes. It is shown in Section 9.4.6 of Reference 1 that the phugoid mode becomes unstable when the c.g. is at the static stability limit (h_s). This occurs, as shown in Figure 13*c*, for the power-on case with mid c.g. when the speed lies between 75 and 80 kn. Below 70 kn the plots show that the phugoid is replaced by a divergence and a "third mode" resulting from the convergent branch of the original phugoid and one of the real modes which was formed when the short period oscillation disappeared between 75 and 80 kn. At the point of neutral stability, the neutral point (h_n) is still aft of the c.g. position indicating that the aircraft still possesses a small amount of pitch stiffness. As discussed in Section 2, this occurs because the stability depends on pitch stiffness, represented by h_n, and also the speed derivatives C_{m_V} and C_{L_V}; for the "standard case", C_{m_V} is negative and hence destabilising.

Figure 37 shows the root locus plots for the case with flaps deflected 20 deg. With power off, the short period and phugoid characteristics are similar to the zero flap case, as would be expected from the plots of h_s in Figure 30*d*. With power on, although the aircraft remains stable at all speeds, i.e. h_s is aft of the mid c.g., the pitch stiffness becomes negative above 95 kn as shown in Figures 31*d* and 31*e*; this results in two real convergent modes instead of a heavily damped short period oscillation. Therefore, although the configuration is stable, the longitudinal response may be unsatisfactory as discussed in Section 8.3.

8.3 Longitudinal Response to Controls

The short-period oscillation frequency is an important factor in determining the longitudinal response to elevator control inputs. In Figure 38, the short period frequency for a mid c.g. is compared with current Flying Qualities Requirements from Reference 4. The boundaries shown in the figure are for constant values of the term $\omega_{n_{sp}}^2/n_{z_\alpha}$ which is equivalent to the control anticipation parameter CAP $= \dot{q}_0/n_{z_{ss}}$ described in Chapter 12.8 of Reference 1. The use of this parameter is based on the proposition that, in order to make precise adjustments to flight path, the pilot makes use of initial pitch response information. Figure 38 shows that with power off and mid c.g. the "standard case" aircraft has satisfactory response characteristics. With power on, the characteristics are satisfactory except below 75 kn, where, as shown in Figure 13*b*, the pitch stiffness is very low or negative. These low-speed cases would, as discussed in Section 8.2, also be unacceptable from stability considerations. In Figure 39, the short period frequency requirements are shown for the case with flaps deflected 20 deg. In this configuration, although the motion is stable with power on, at a mid c.g. of 32·3%$\bar{c}$, the response characteristics are unacceptable at all but the lowest speeds, due to low or negative pitch stiffness, as indicated by h_n in Figure 31*d*. As mentioned in the Introduction, considerations of longitudinal response for manually-controlled aircraft should also include the ratio of initial control force to steady normal acceleration in a rapid manoeuvre. This ratio depends strongly on the hinge-moment derivatives. A study of this problem is outside the general scope of this Report.

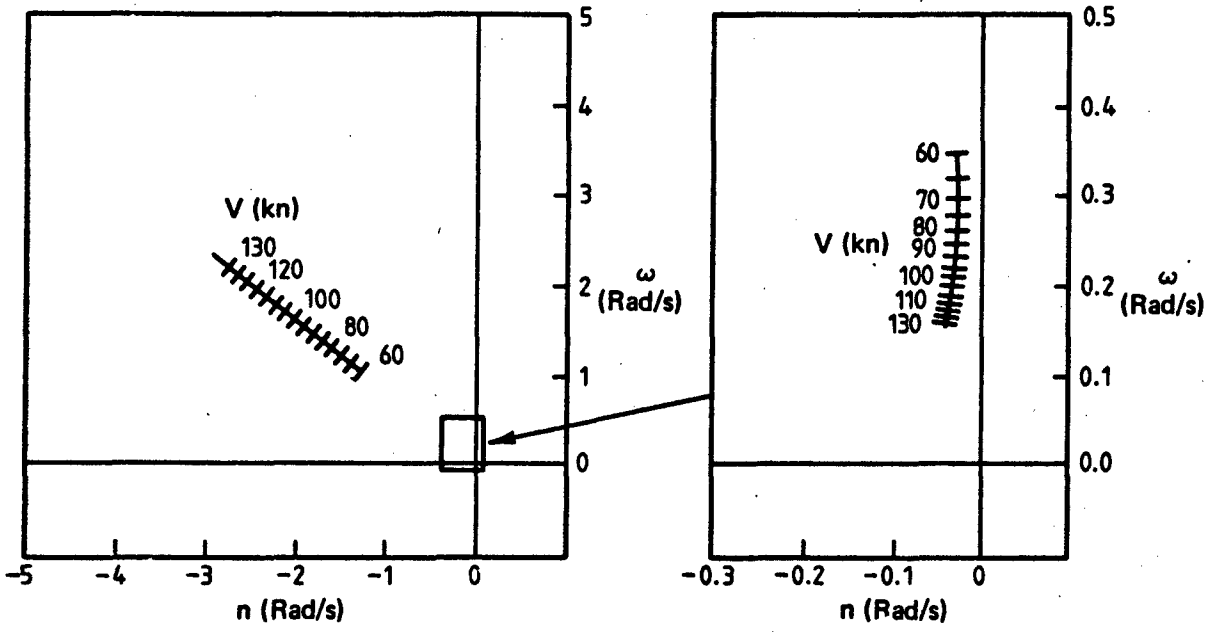

(a) Effect of speed (Power-OFF) Flaps 20 deg. Mid C.G.

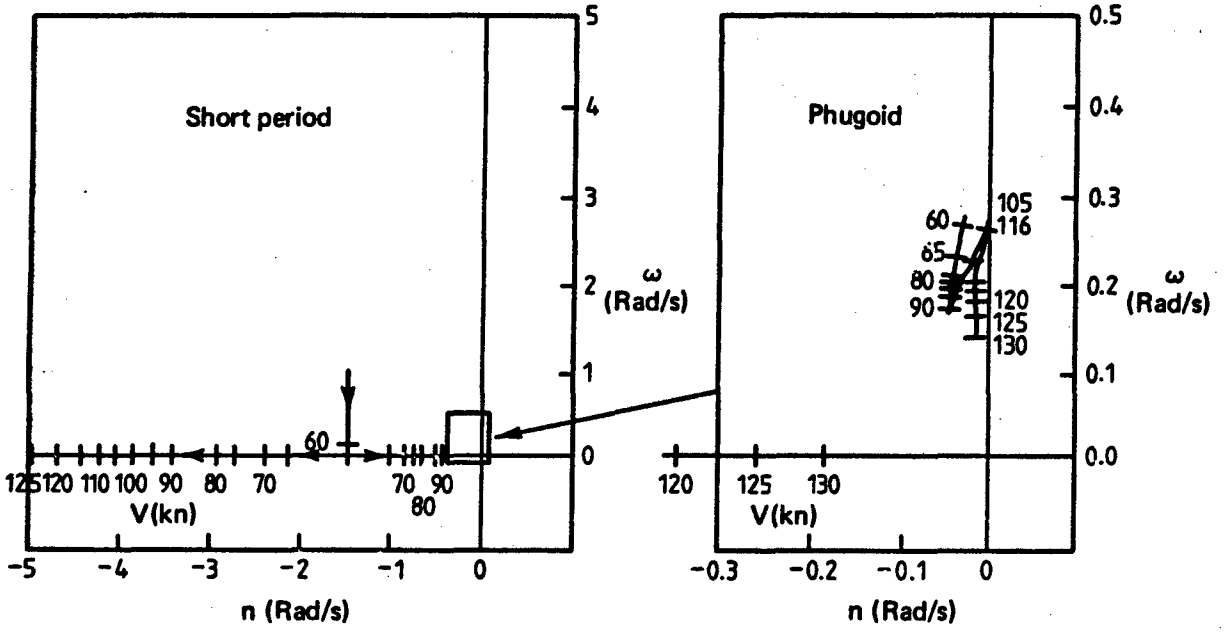

(b) Effect of speed (Power-ON) Flaps 20 deg. Mid C.G.

FIG. 37 EFFECT OF POWER ON LONGITUDINAL DYNAMIC MODES
ROOT LOCUS PLOTS

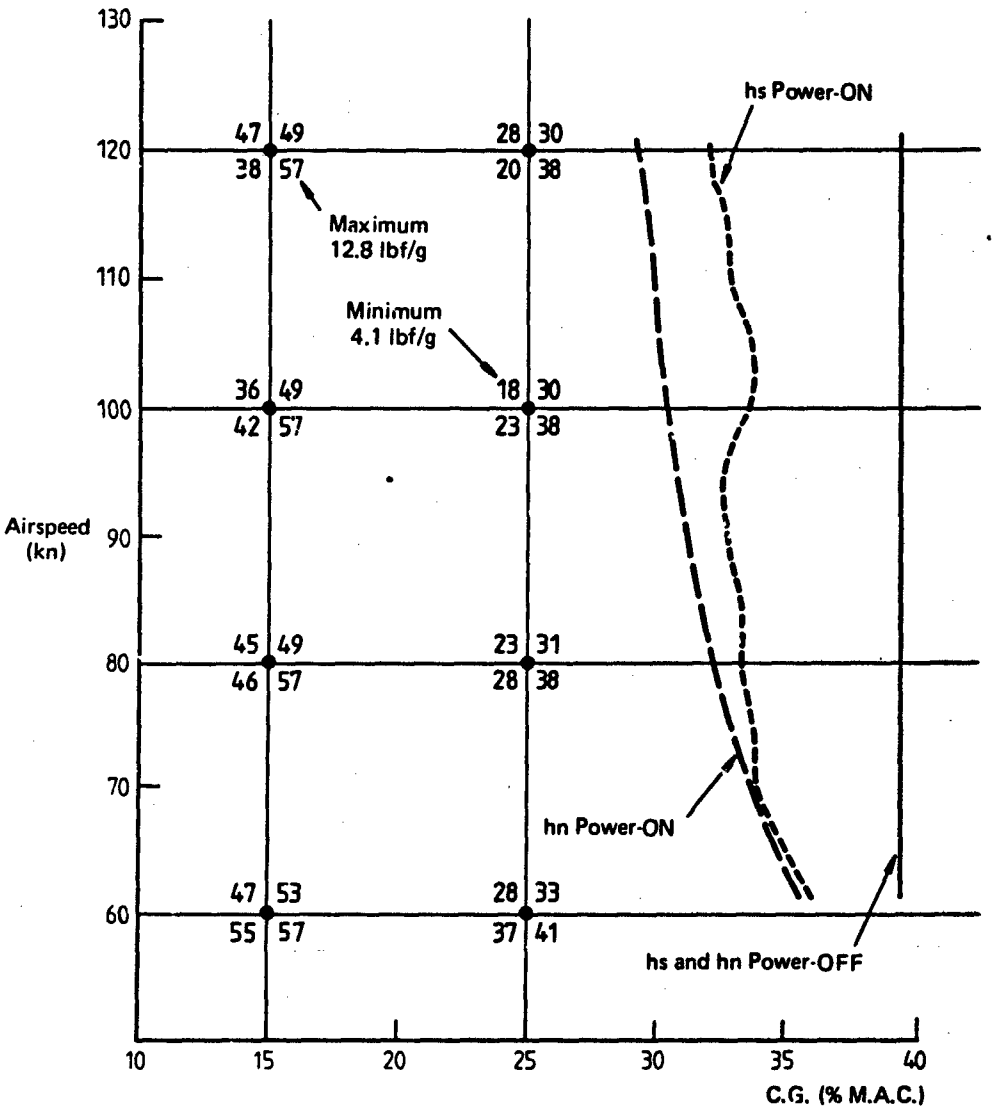

Key

Alt. 6km Power-ON	Alt. 6 km Power-OFF
Alt. S.L. Power-ON	Alt. S.L. Power-OFF

(N/g)

FIG. 35 CONTROL FORCE PER 'g': FLAPS 20 DEG.

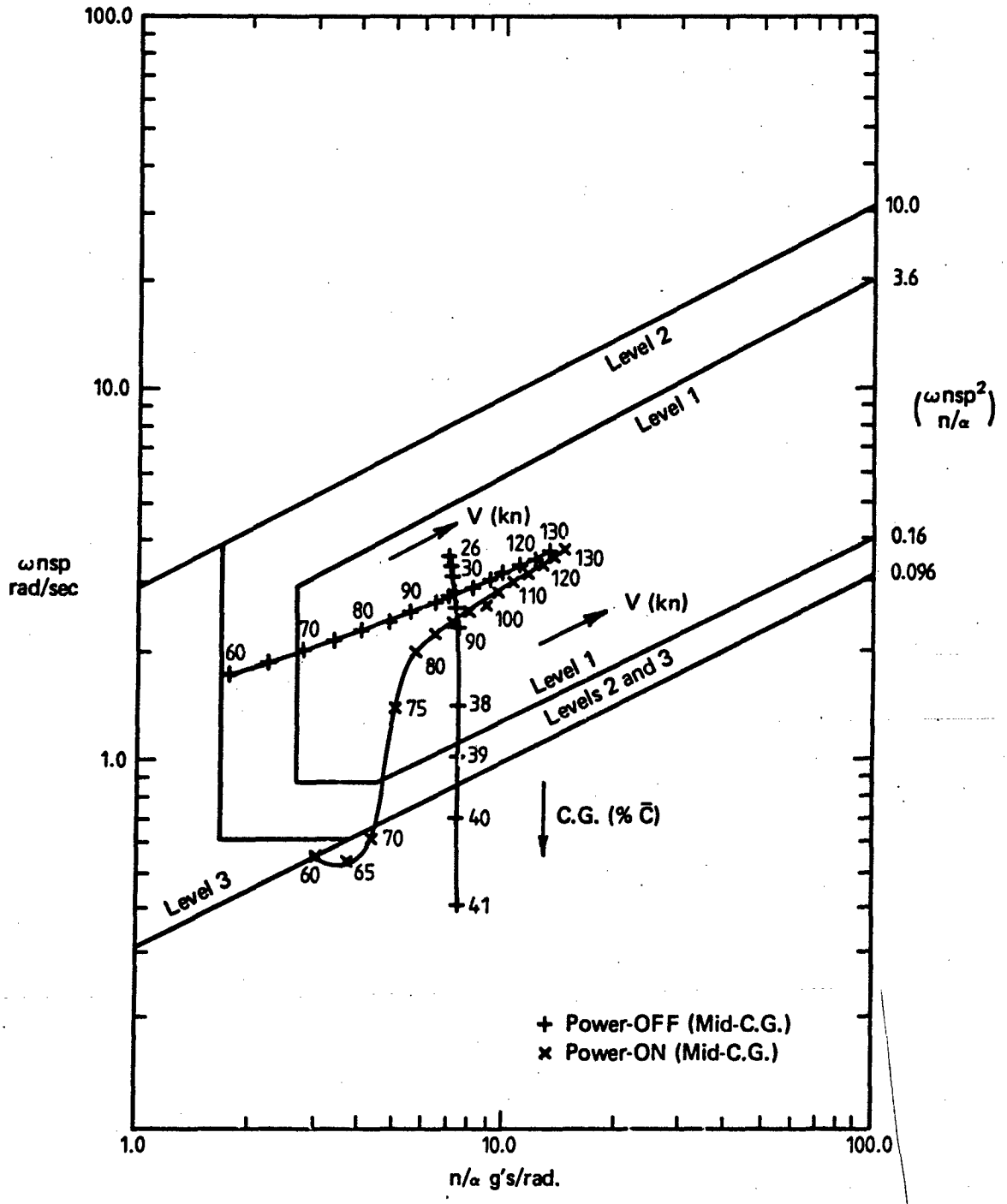

FIG. 38 SHORT PERIOD FREQUENCY REQUIREMENTS – MID C.G. RESULTS. REFERENCE MIL-8785C. CLASS 1 AIRCRAFT TERMINAL FLIGHT PHASE

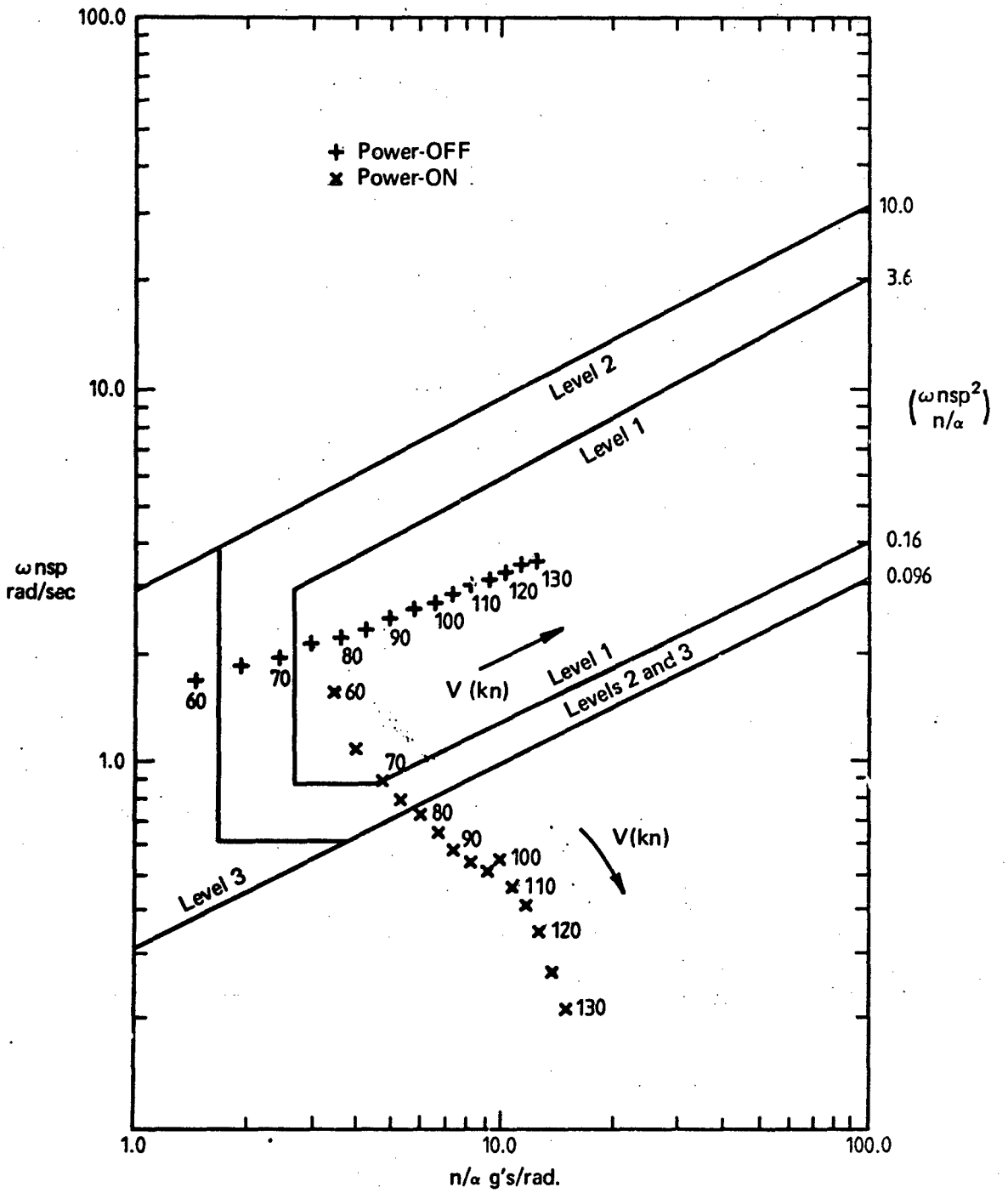

FIG. 39 SHORT PERIOD FREQUENCY REQUIREMENTS – MID C.G. FLAPS 20 DEG. REFERENCE MIL-8785C. CLASS 1 AIRCRAFT TERMINAL FLIGHT PHASE

9. POWER EFFECTS ON A SINGLE-ENGINE PROPELLER-DRIVEN AIRCRAFT WITH TYPICAL LAYOUT

Many recently designed single-engine propeller-driven aircraft have the wing and tailplane located below and above the engine thrust line respectively, as typified by the layout in Figure 1. The low wing is generally chosen to give a short undercarriage design, a simple wing-to-fuselage attachment, and a wing carry-through box which avoids the cockpit. Aerodynamic and stability considerations generally have much lower priority. The tail location is also influenced by structural requirements such as rear fuselage upsweep and attachment, but aerodynamic and stability characteristics are also important. In addition, where spin recovery is required, the relative positions of the fin and tailplane can be very important. While structural requirements generally lead to a vertical location of the tailplane above the thrust line, the exact position may be established by aerodynamic characteristics observed from wind tunnel test programmes. To provide a comparison with the "standard case" layout used in this study, which exhibited large power effects, the trim and stability characteristics have been calculated for the layout given in Figure 1, with wing aerodynamic centre 0·26 m below the thrust line, vertical c.g. 0·05 m below the thrust line and tailplane 0·55 m above the thrust line.

Figures 40*b* and 40*c* show that, with power off and flaps zero, there is a reduction in the static stability limit (h_s) with C_L. This is the net effect of a reduction in stability due to the low wing (as discussed in Section 6.2), and a slight increase in stability due to a more favourable downwash gradient at the tailplane (as discussed in Section 6.3). Compared with the "standard case", the power-off values of h_s and h_n vary from zero at high speed, to 3%$\bar{c}$ less as speed reduces to 60 kn.

In contrast with the "standard case", the net effects of power are stabilising for most of the speed range, as shown in Figure 42*c*. This is due primarily to a large stabilising contribution from the effect of dynamic head at the tailplane in the manner described in Section 6.3. While the stability of the aircraft with power on differs little from the power-off case, Figure 41*b* shows that the variation of trim curve slope with c.g. is considerably less than for the power-off case. This example shows that, in general, stability is not directly related to c.g. position, as assumed in simple "static stability" theory, and highlights the danger of using this theory to analyse trim curves when power effects are present.

With flaps deflected 20 deg., the power-off values of h_s and h_n (Fig. 42*c*), are approximately 1%$\bar{c}$ further aft than for the zero flap case, due to reduced downwash at the tailplane. With power on and flaps deflected 20 deg., the aircraft becomes unstable at speeds below 80 kn for all except the forward c.g. considered, as shown in Figures 43*b* and 43*c*. This condition is an example of the destabilising effect of tail dynamic pressure when acting on a tailplane carrying a download, as discussed in Section 5.6. The download is required to trim the nose-down pitching moment arising from the effect of power on the wing and body with flaps deflected. As speed reduces and incidence increases to maintain rectilinear flight, the dynamic pressure ratio in the slipstream increases, and also the tailplane begins to enter the slipstream from above, as shown in Figure 43*d*. The resulting increase in dynamic pressure at the tailplane increases tailplane download and produces a nose-up moment which exceeds the usual restoring moment due to increasing tailplane incidence. As c.g. is moved forward, pitch stiffness increases; however, the tailplane download required for trim also increases, such that the total change in pitching moment becomes almost independent of c.g. position.

As previously discussed, the representation of propeller slipstream in this Report is greatly simplified compared with actual conditions, and this possibly may exaggerate the instability discussed above. Nevertheless, the example clearly illustrates an effect that is possible, given large tailplane downloads for trim and large engine power at low speeds.

The control force per g values with flaps deflected 20 deg. are shown in Figure 45 for speeds above 80 kn. Below 80 kn, the aircraft is unstable at all but the forward c.g., as previously discussed. For the speed range considered, the values of control for per g are similar to those with zero flap even though the pitch stiffness indicated by h_n is smaller. The control force per g is maintained because, as incidence and g increase, an increasing tail upload is required. Therefore, as the tailplane enters the slipstream, the pitch stiffness and pitch damping are increased beyond their 1g values.

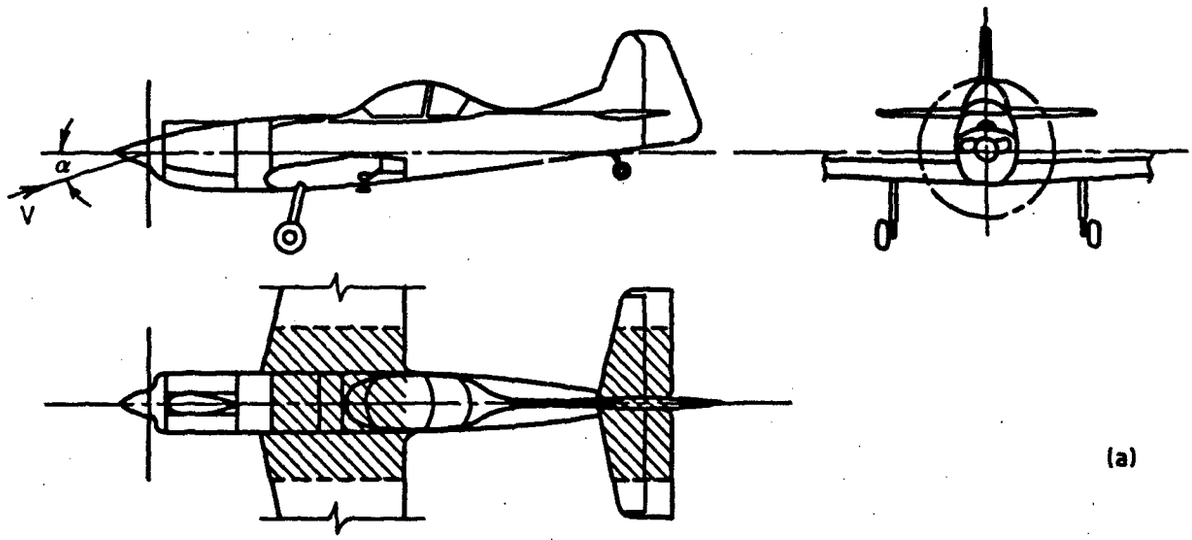

(a)

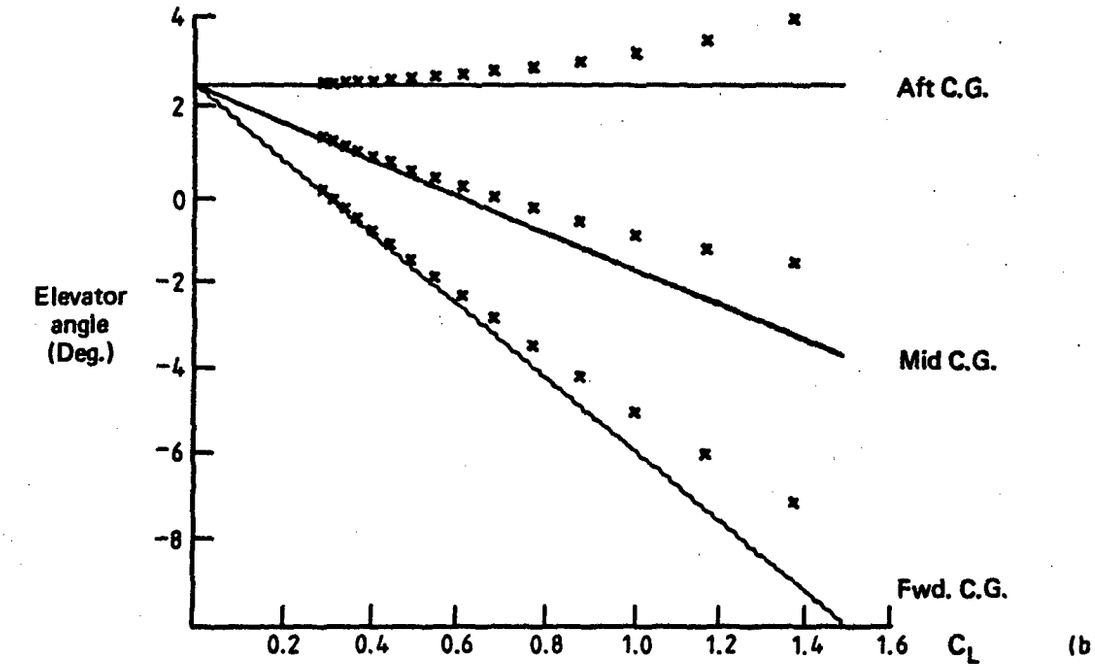

(b)

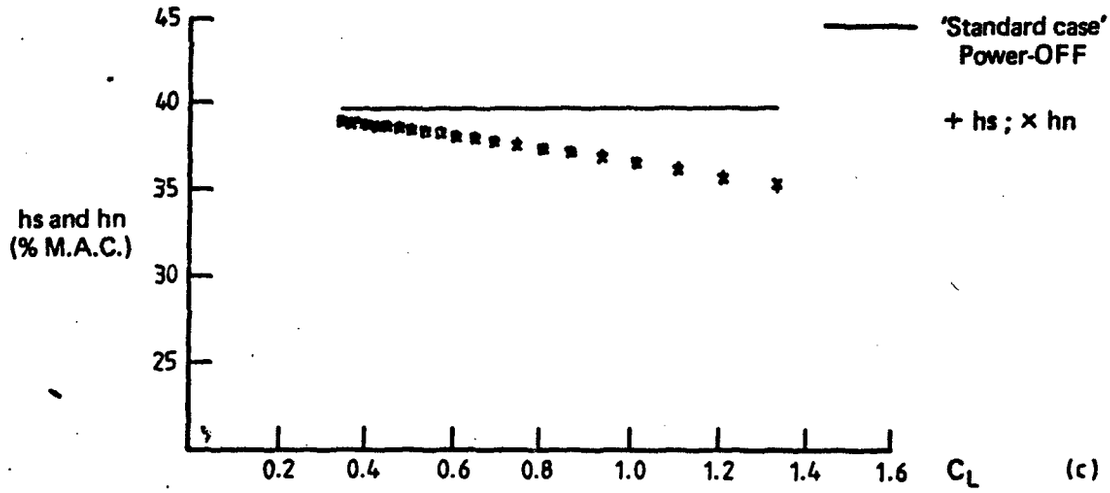

(c)

FIG. 40 TRIM AND STABILITY CHARACTERISTICS FOR A TYPICAL AIRCRAFT LAYOUT
POWER-OFF FLAPS ZERO

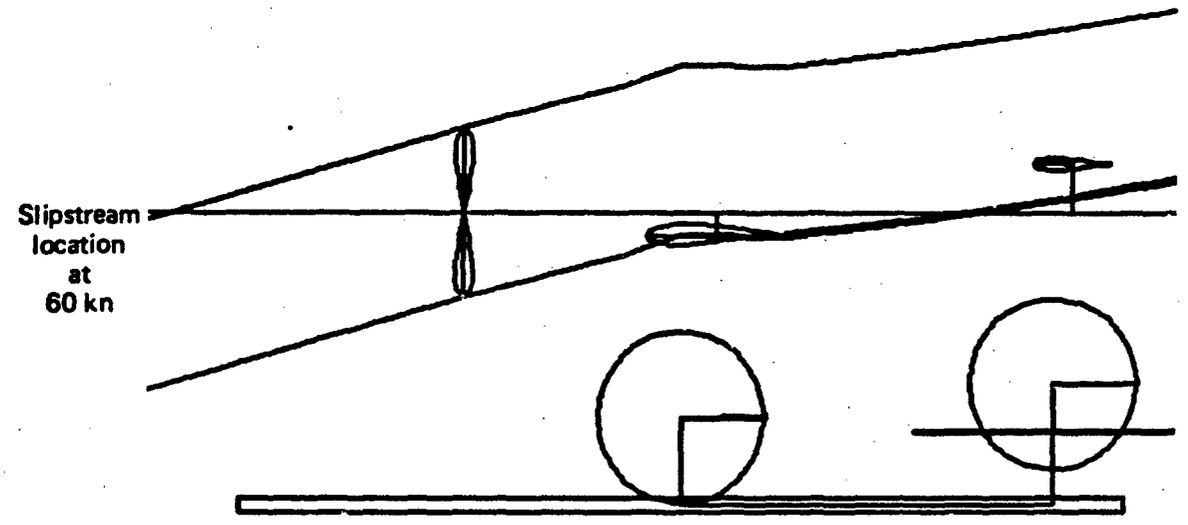

(d)

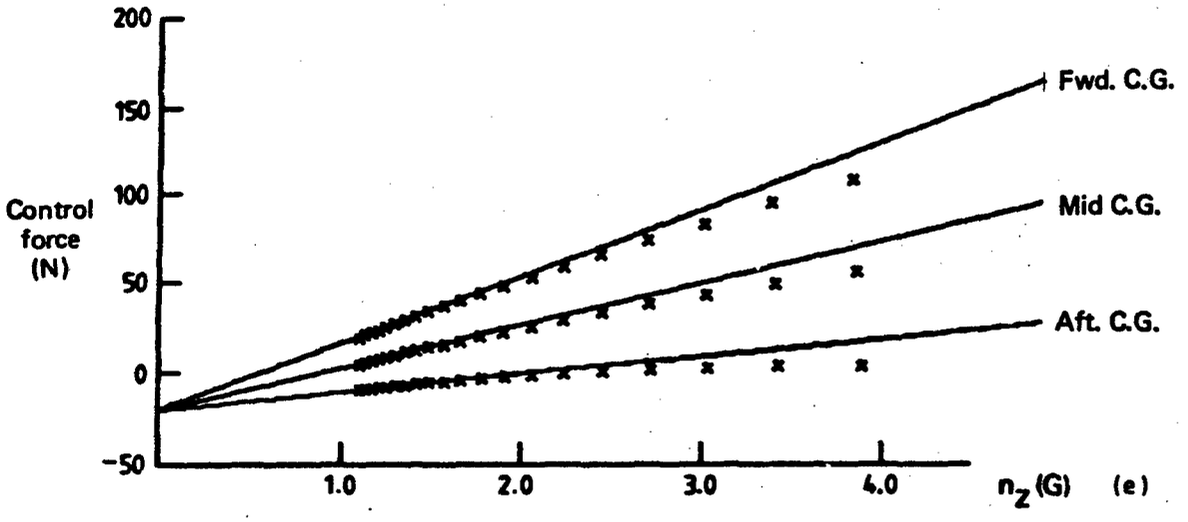

(e)

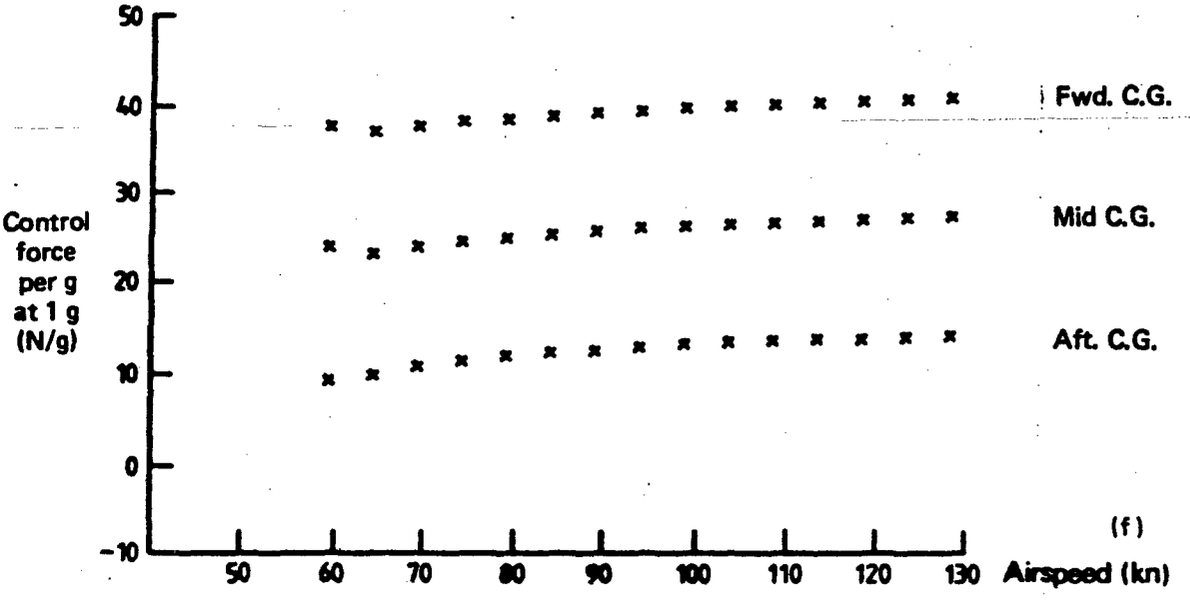

(f)

FIG. 40 TRIM AND STABILITY CHARACTERISTICS FOR A TYPICAL AIRCRAFT LAYOUT POWER-OFF FLAPS ZERO

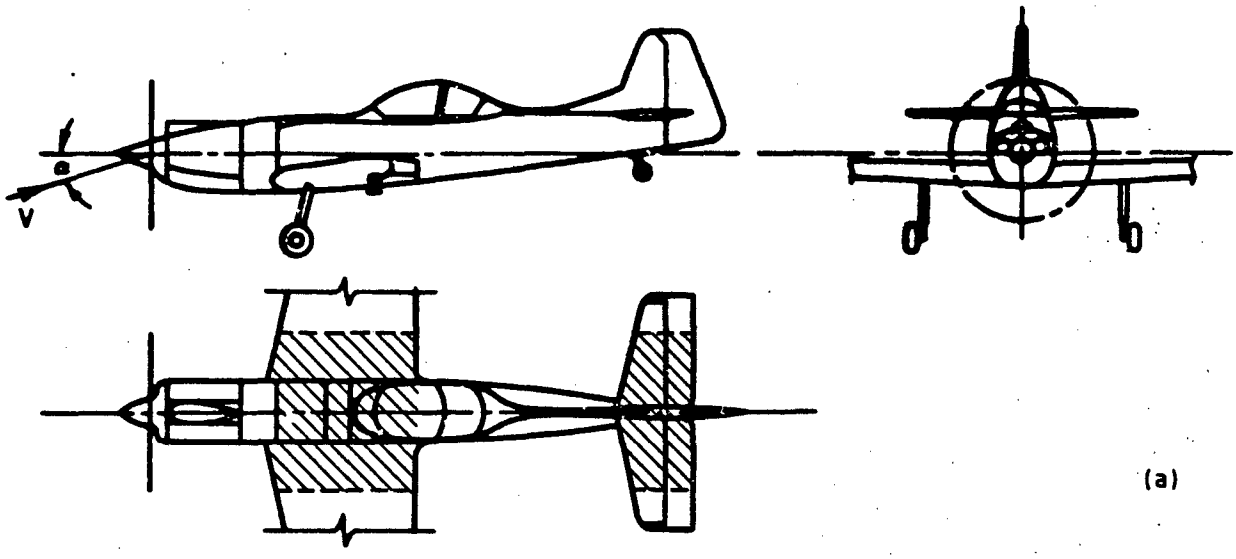

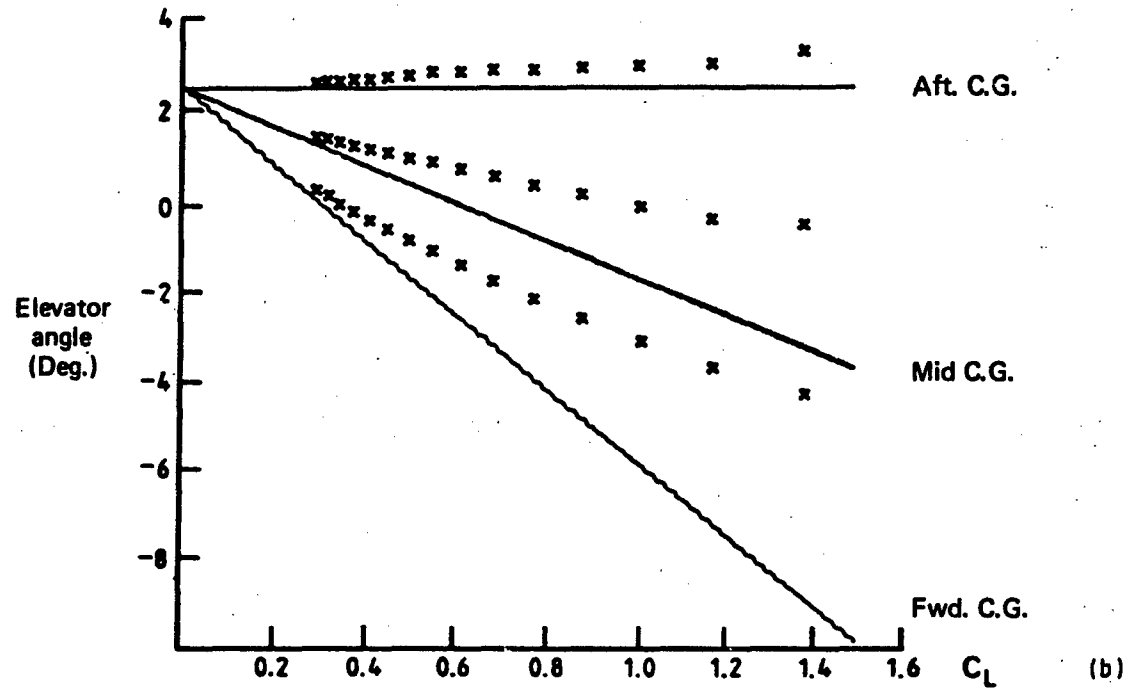

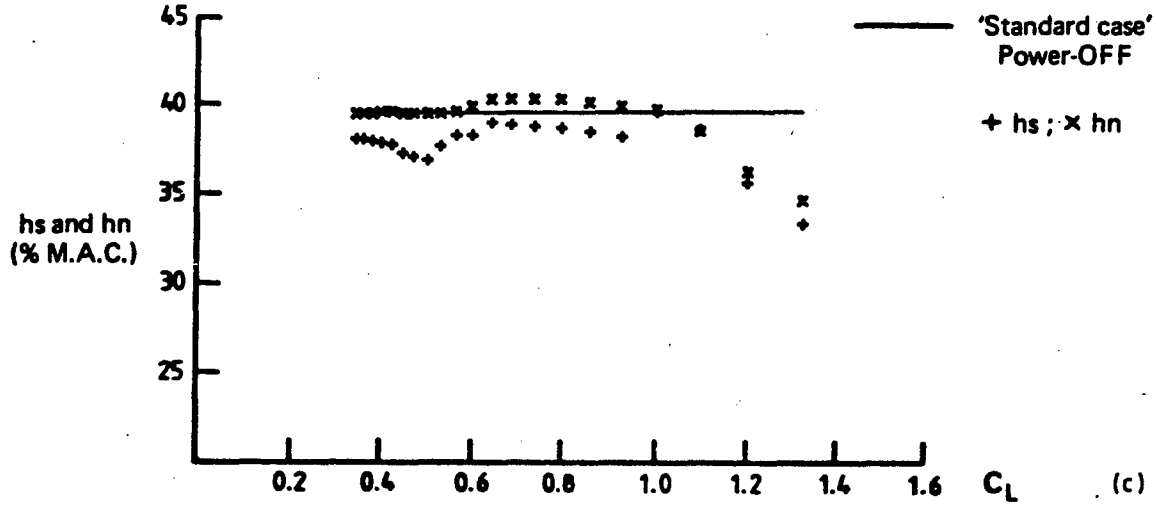

FIG. 41 TRIM AND STABILITY CHARACTERISTICS FOR A TYPICAL AIRCRAFT LAYOUT POWER-ON FLAPS ZERO

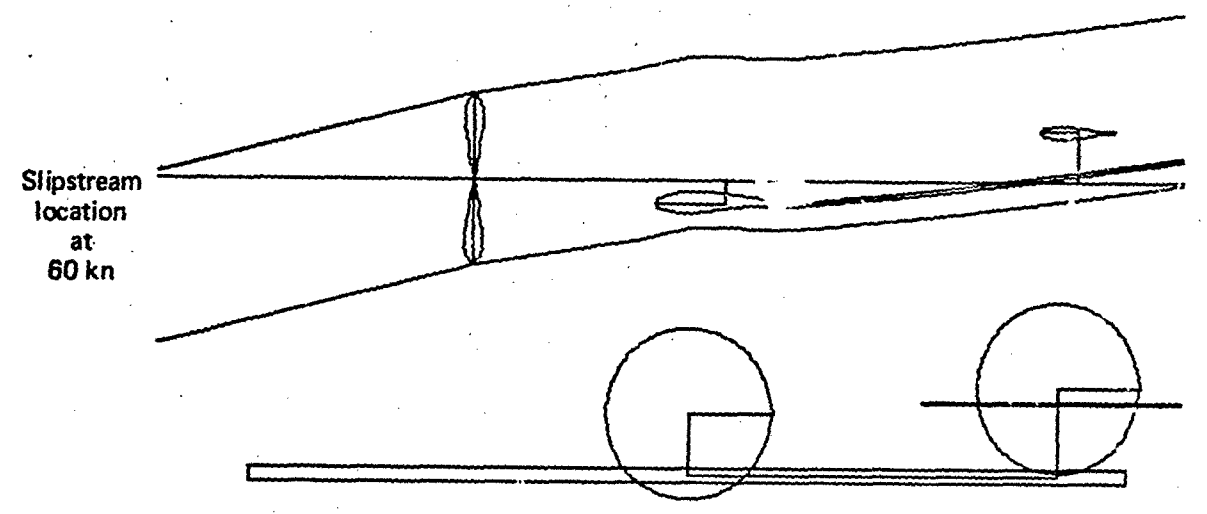

(d)

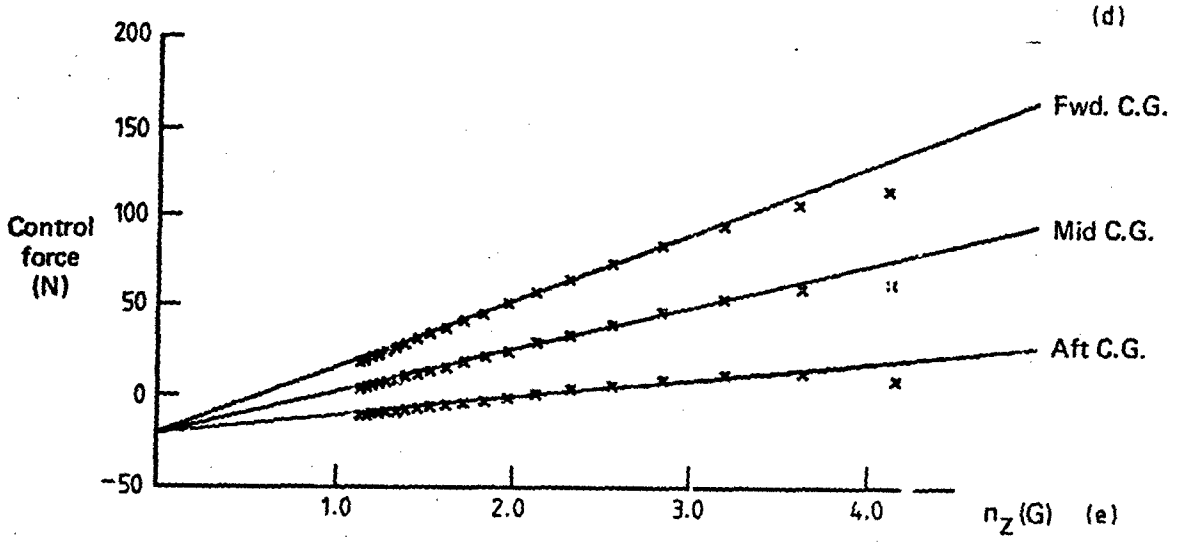

(e)

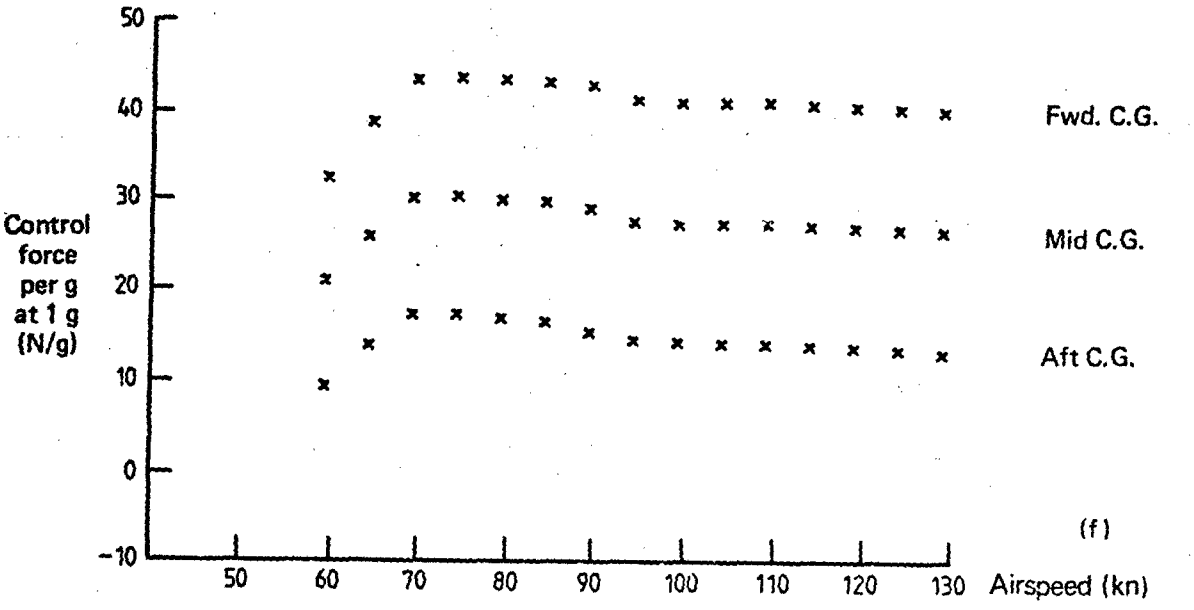

(f)

FIG. 41 TRIM AND STABILITY CHARACTERISTICS FOR A TYPICAL AIRCRAFT LAYOUT
POWER-ON FLAPS ZERO

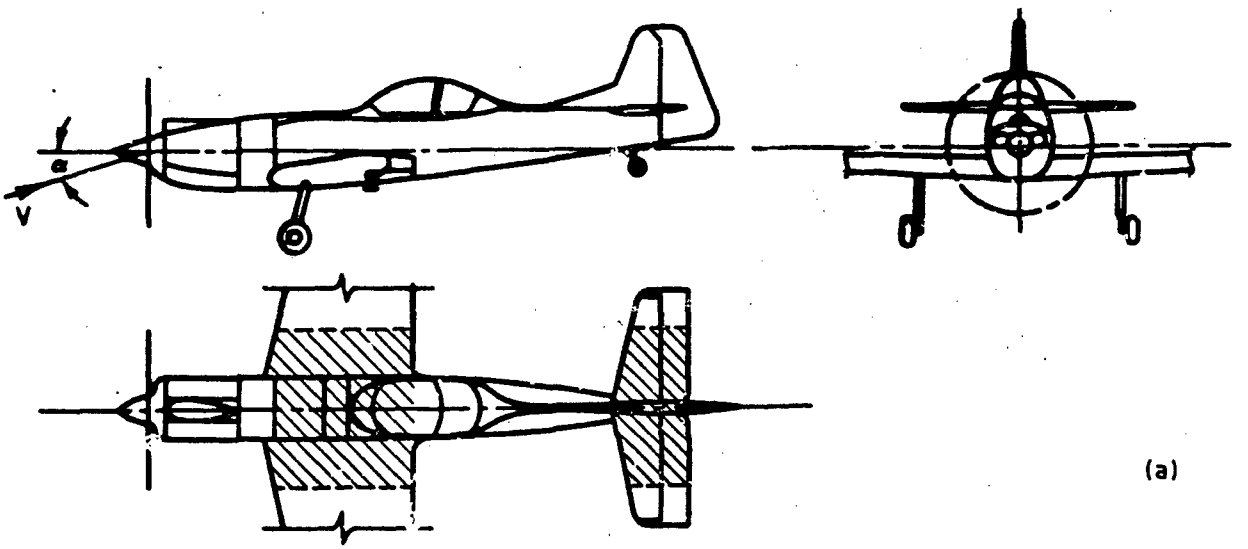

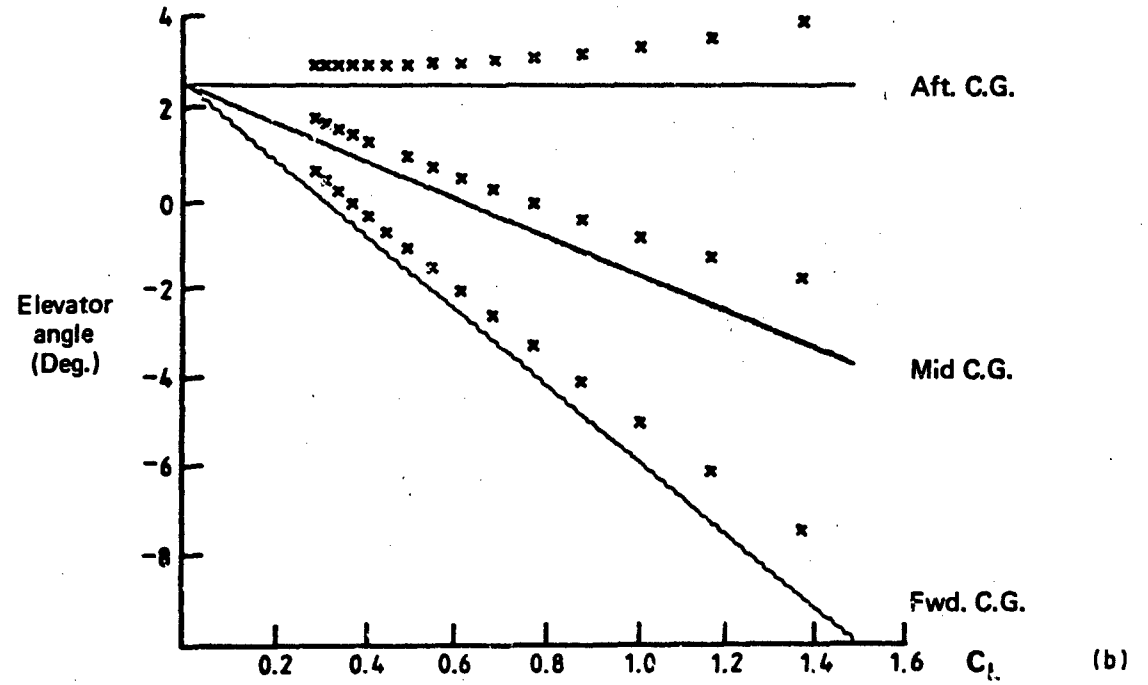

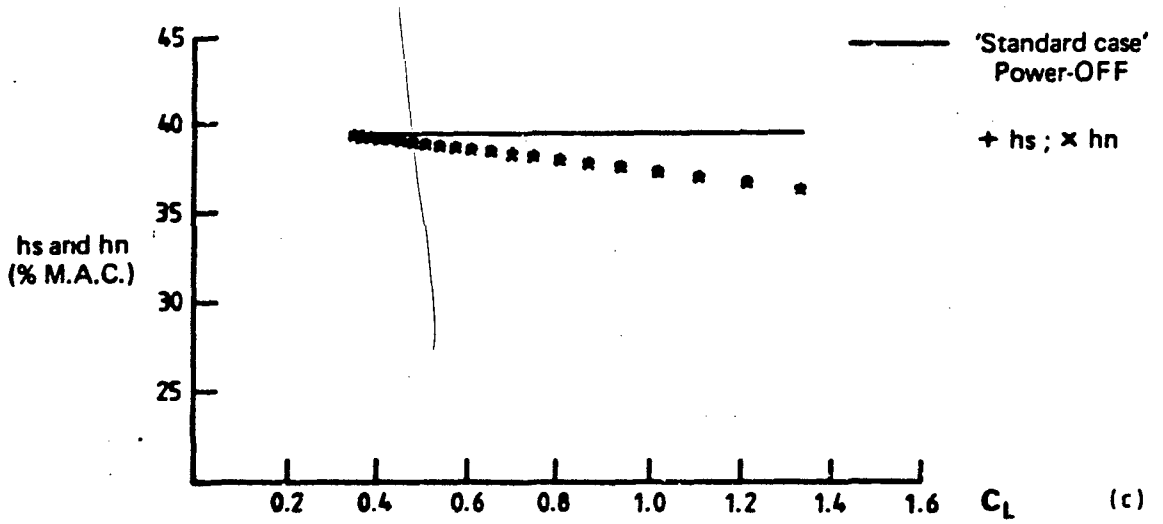

FIG. 42 TRIM AND STABILITY CHARACTERISTICS FOR A TYPICAL AIRCRAFT LAYOUT POWER-OFF FLAPS 20 DEG.

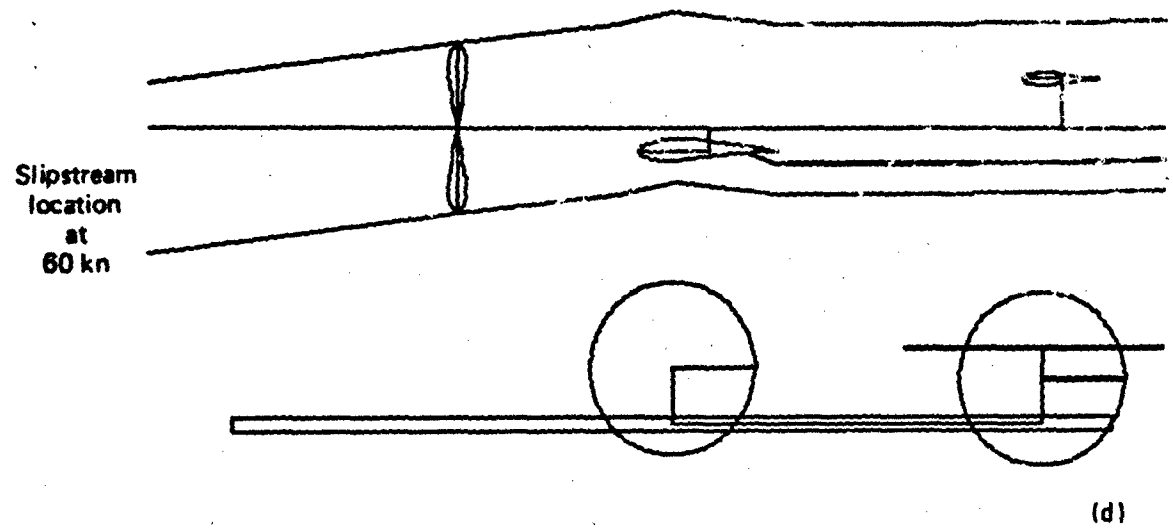
Slipstream
location
at
60 kn

(d)

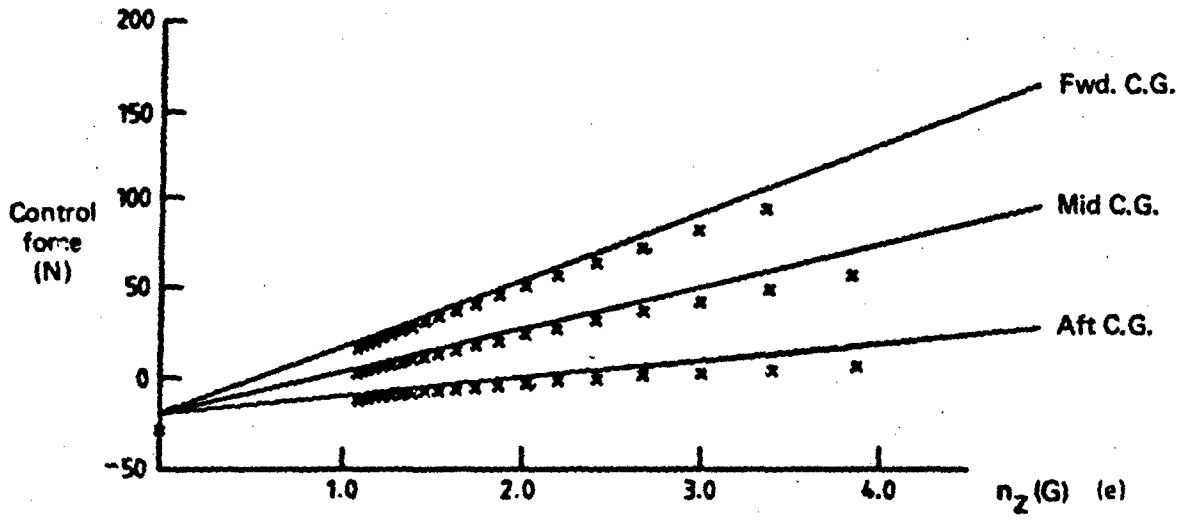
Control
force
(N)
200
150
100
50
0
-50
1.0
2.0
3.0
4.0
n_z (G)
Fwd. C.G.
Mid C.G.
Aft C.G.

(e)

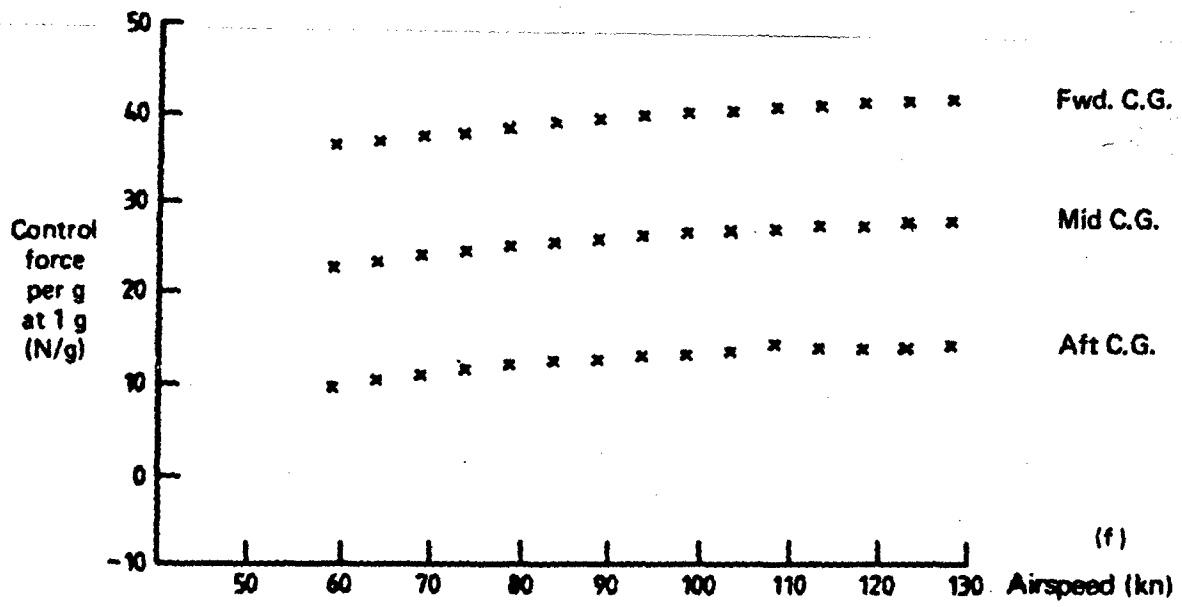
Control
force
per g
at 1 g
(N/g)
50
40
30
20
10
0
-10
50
60
70
80
90
100
110
120
130
Airspeed (kn)
Fwd. C.G.
Mid C.G.
Aft C.G.

(f)

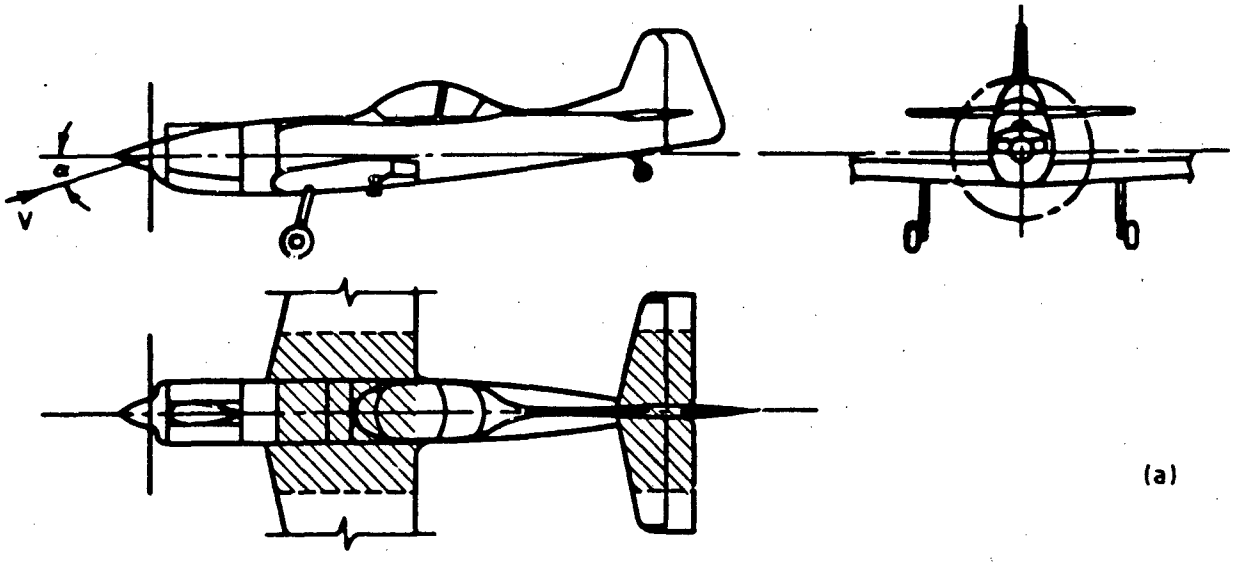
V
α

(a)

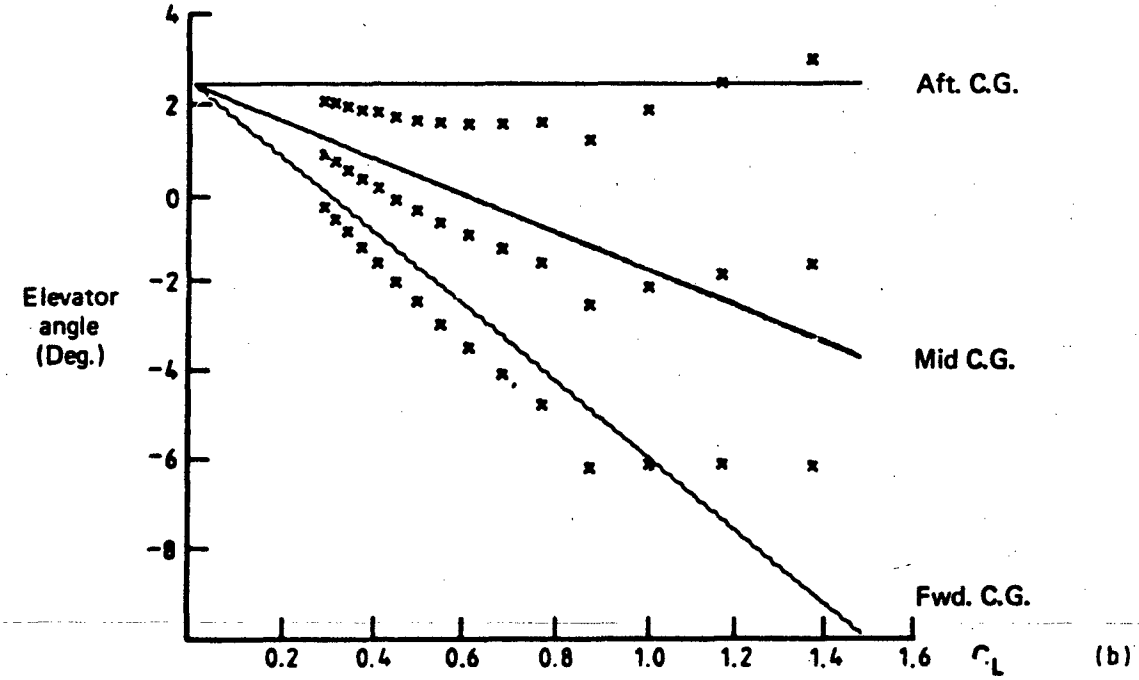
Elevator angle (Deg.)
4
2
0
-2
-4
-6
-8
Aft. C.G.
Mid C.G.
Fwd. C.G.
0.2
0.4
0.6
0.8
1.0
1.2
1.4
1.6
C_L

(b)

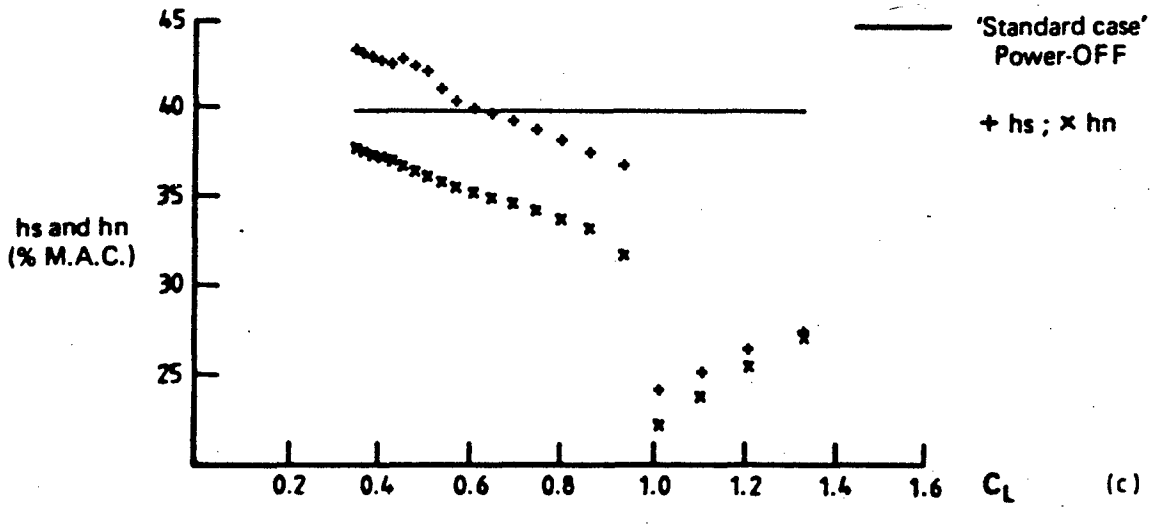
hs and hn (% M.A.C.)
45
40
35
30
25
'Standard case' Power-OFF
+ hs ; × hn
0.2
0.4
0.6
0.8
1.0
1.2
1.4
1.6
C_L

(c)

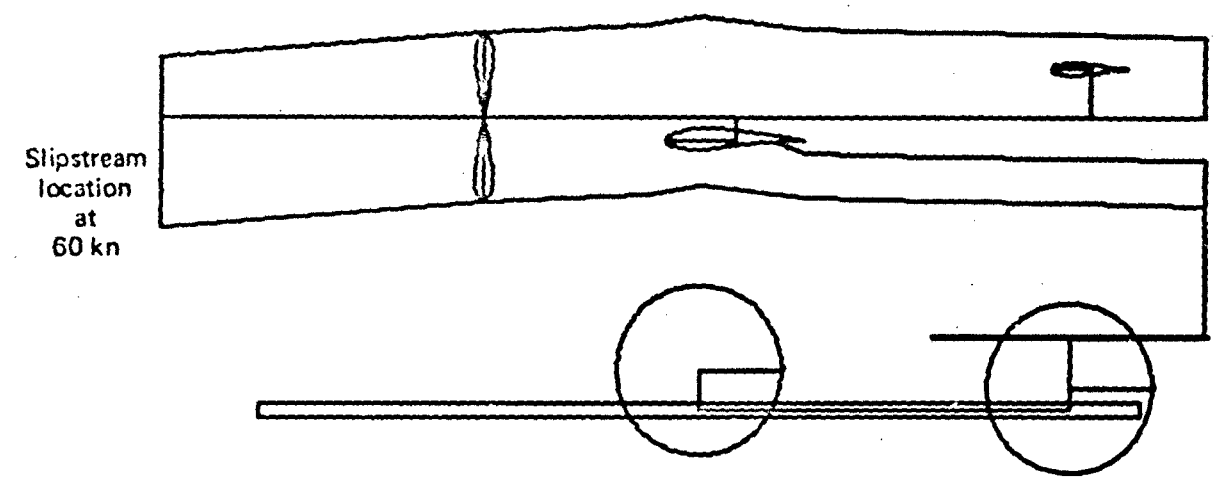

(d)

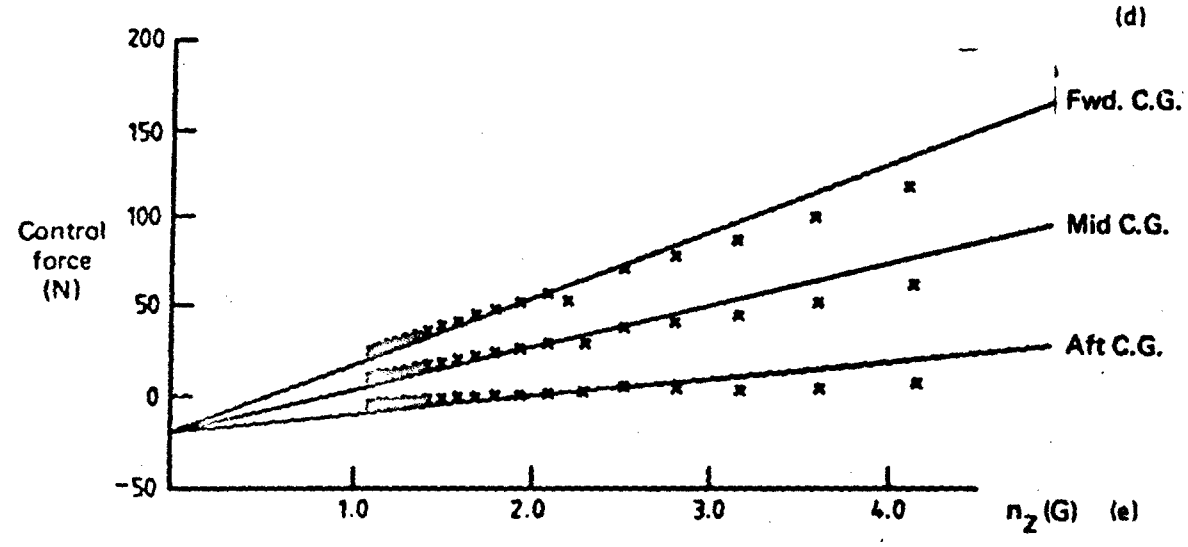

(e)

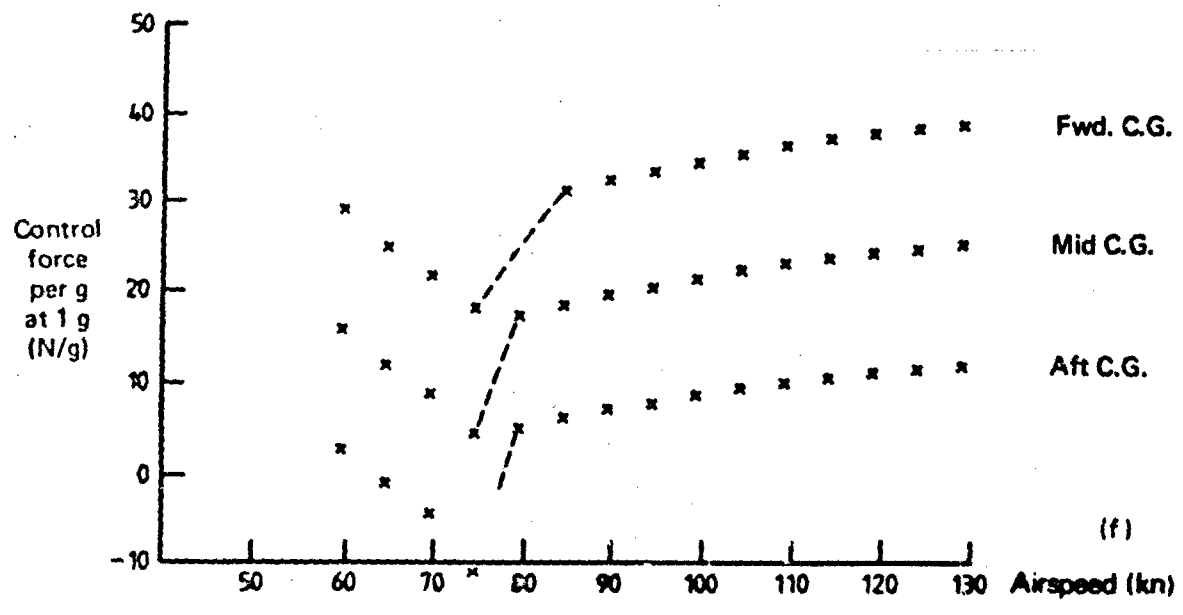

(f)

FIG. 42 TRIM AND STABILITY CHARACTERISTICS FOR A TWIN

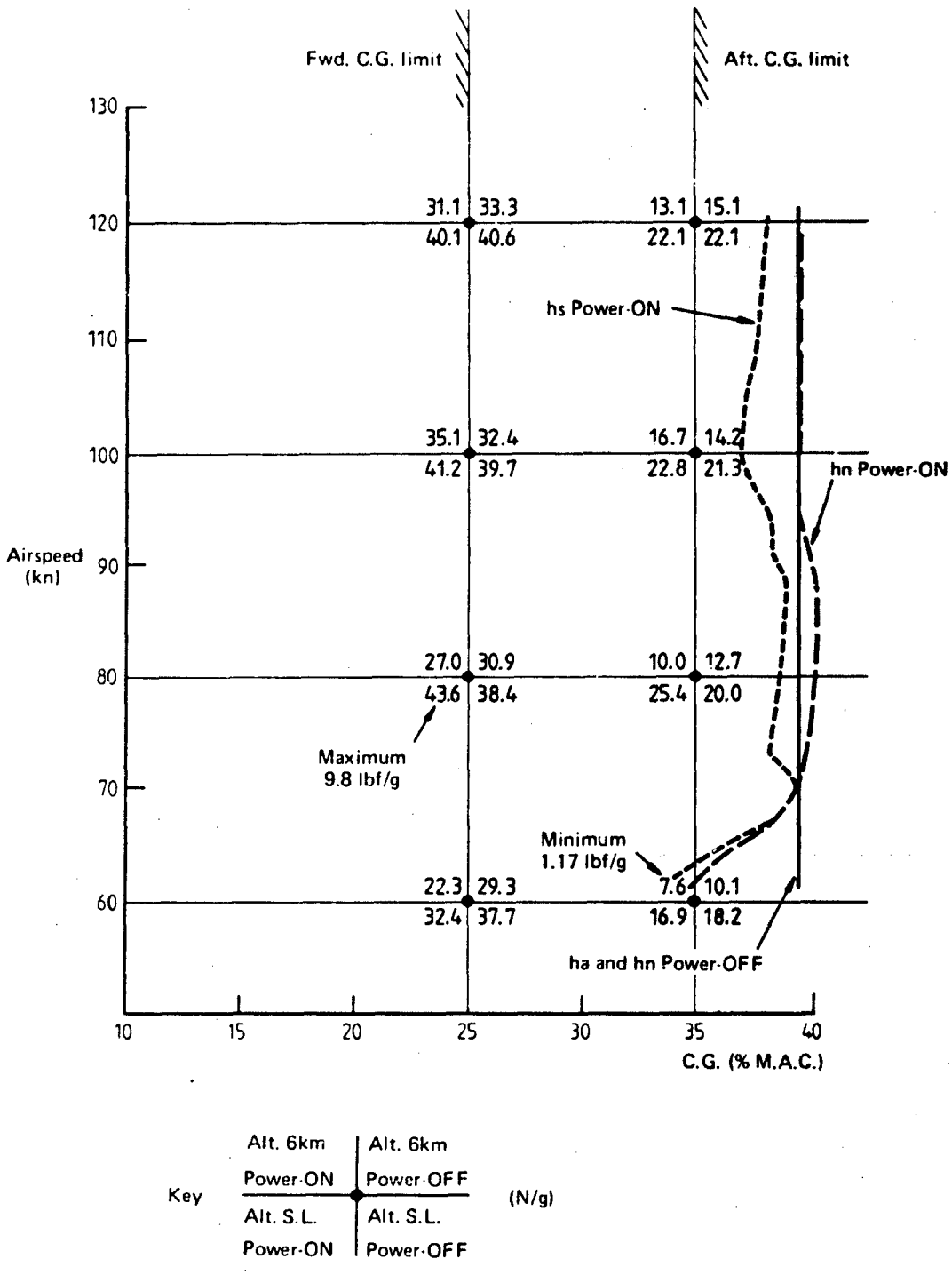

FIG. 44 CONTROL FORCE PER 'g': TYPICAL AIRCRAFT LAYOUT
FLAPS ZERO

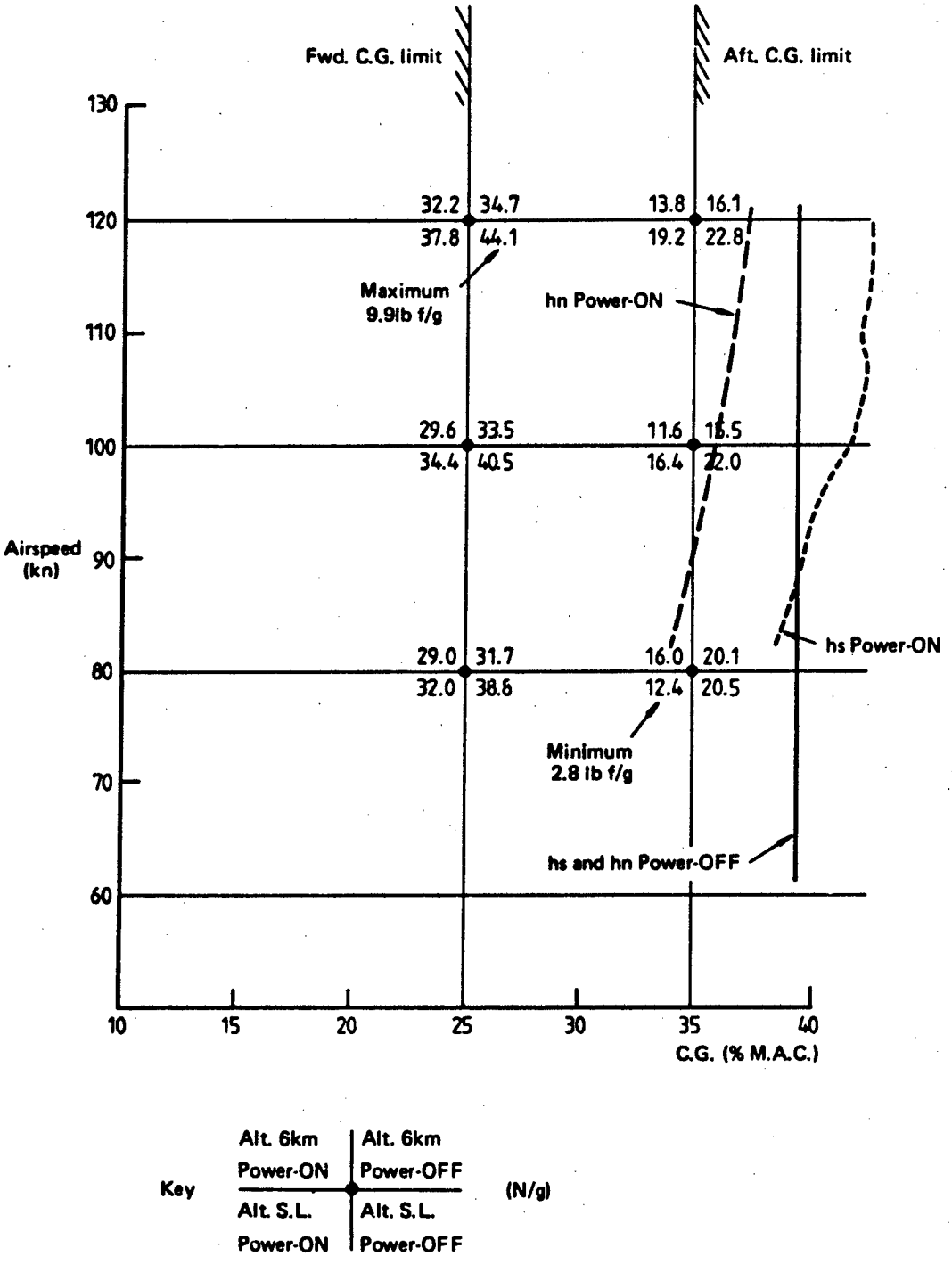

FIG. 45 CONTROL FORCE PER 'g': TYPICAL AIRCRAFT LAYOUT
FLAPS 20 DEG.

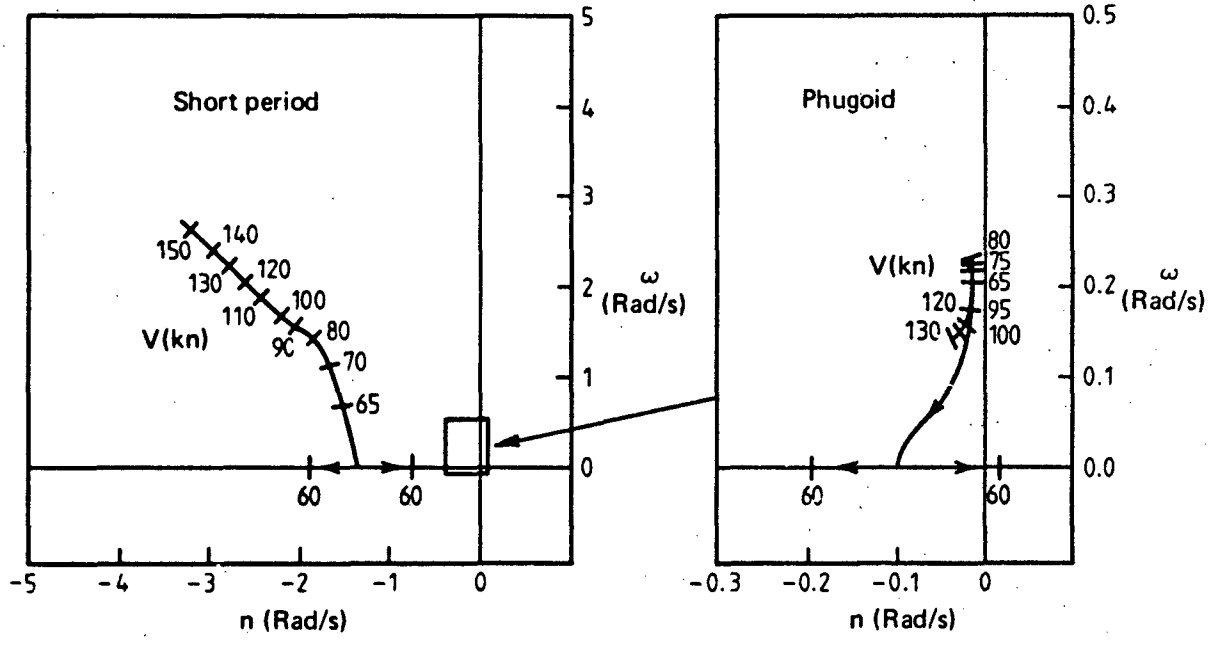

(a) Effect of speed 'Typical layout' (Power-ON), Flaps 0 deg. Mid C.G.

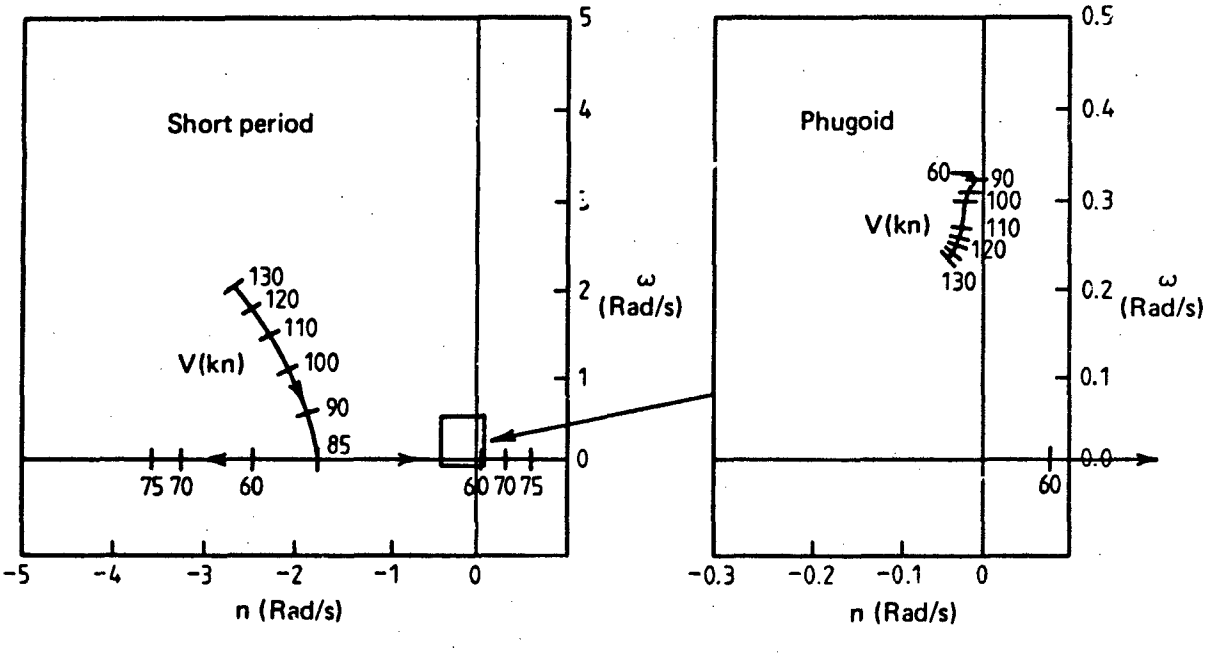

(b) Effect of speed 'Typical layout' (Power-ON), Flaps 20 deg. Mid C.G.

FIG. 46 EFFECT OF POWER AND FLAPS ON LONGITUDINAL DYNAMIC MODES ROOT LOCUS PLOTS

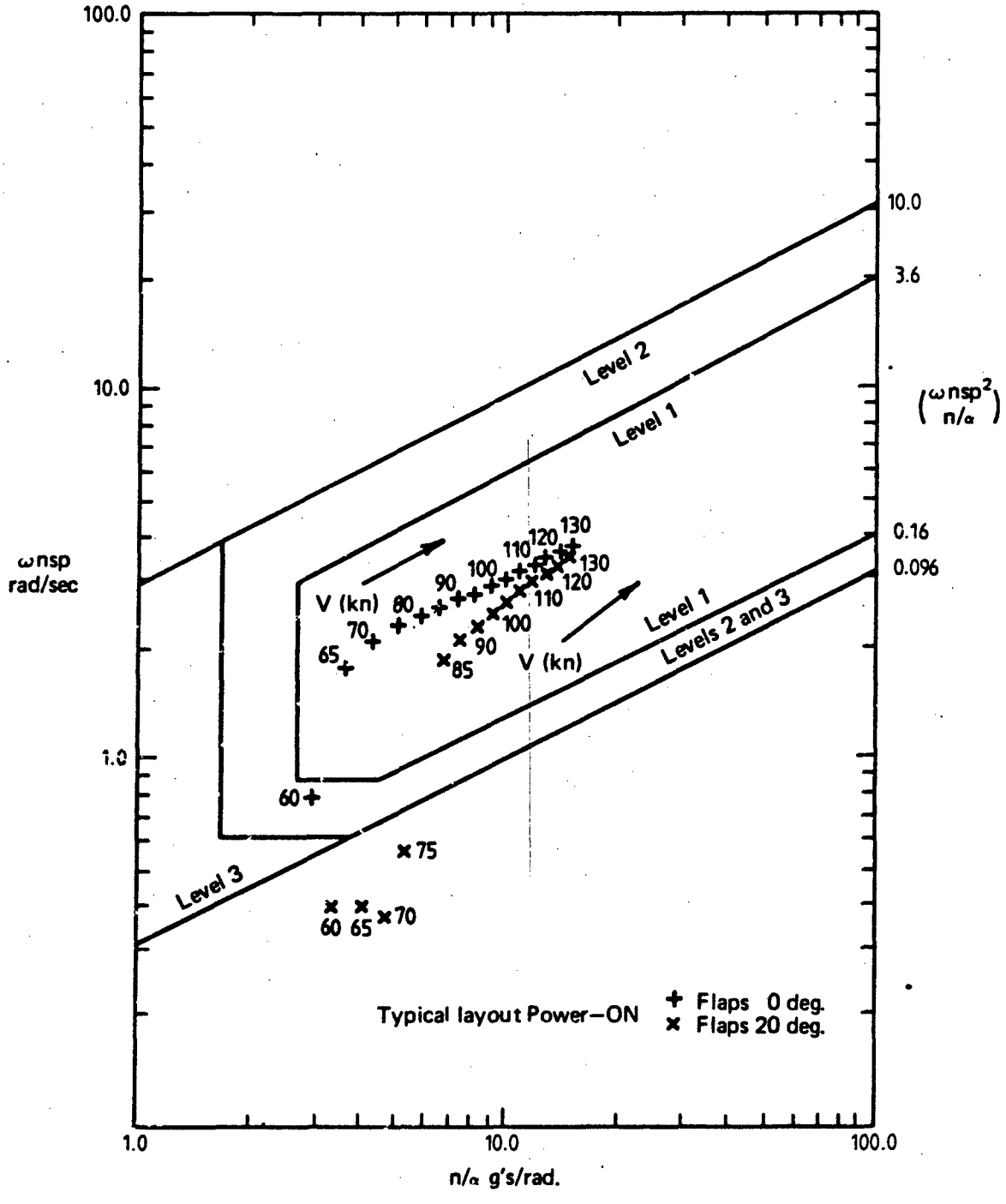

FIG. 47 SHORT PERIOD FREQUENCY REQUIREMENTS – MID C.G. RESULTS
REFERENCE MIL-8785C. CLASS 1 AIRCRAFT TERMINAL FLIGHT PHASE

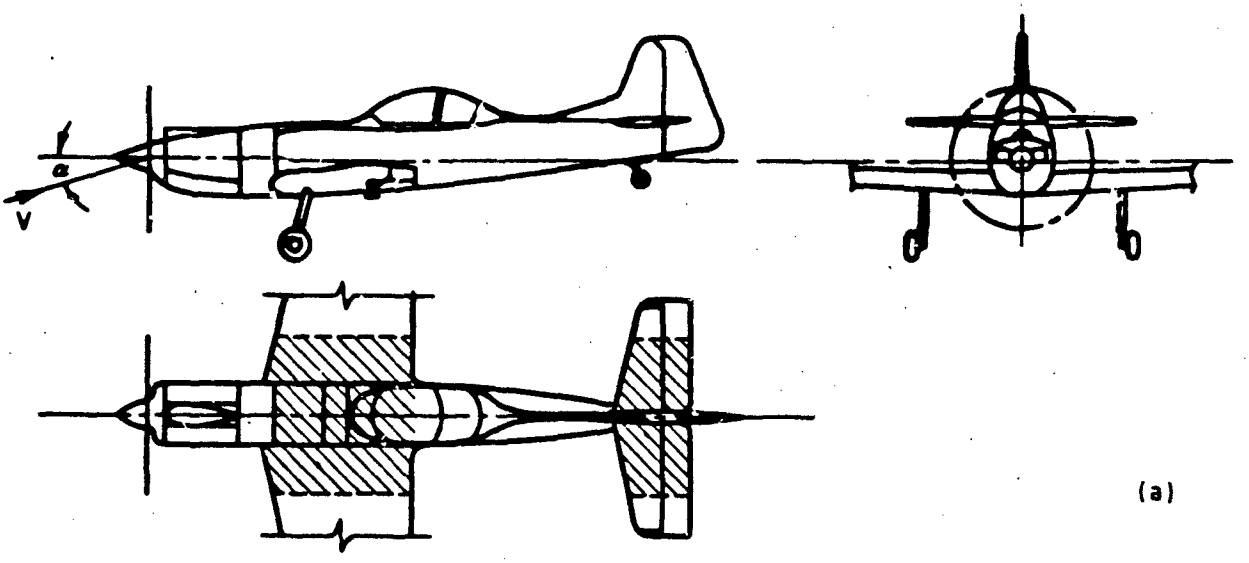
a
V

(a)

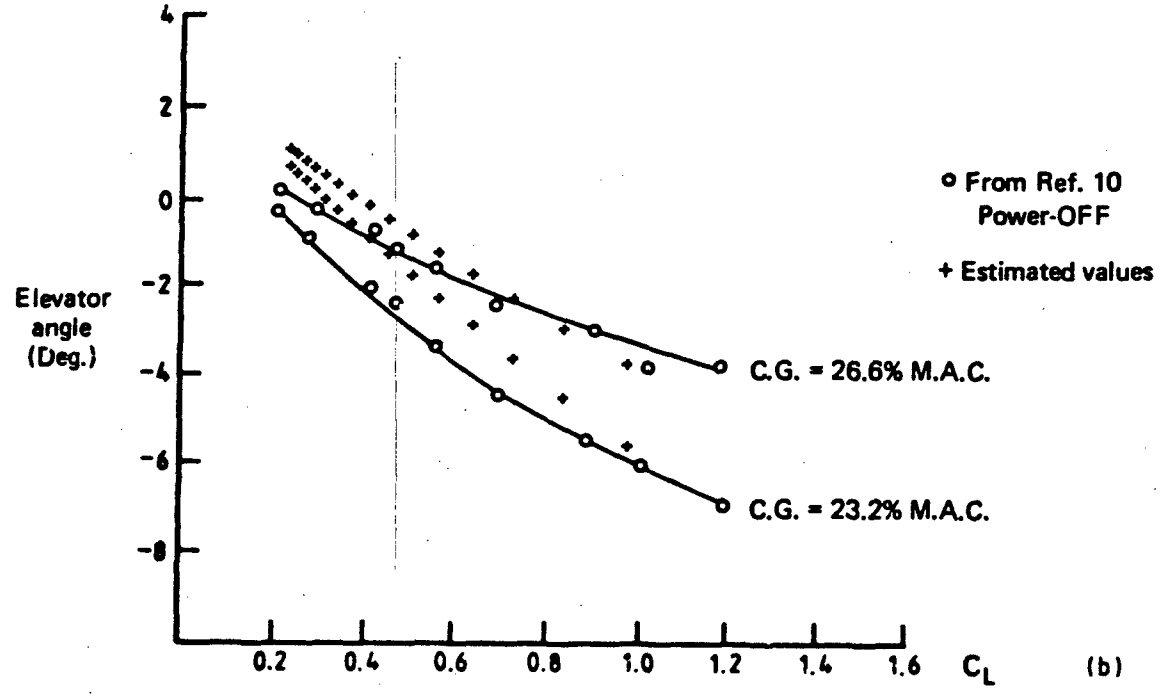
Elevator angle (Deg.)
4
2
0
-2
-4
-6
-8
0.2
0.4
0.6
0.8
1.0
1.2
1.4
1.6
C_L
o From Ref. 10 Power-OFF
+ Estimated values
C.G. = 26.6% M.A.C.
C.G. = 23.2% M.A.C.

(b)

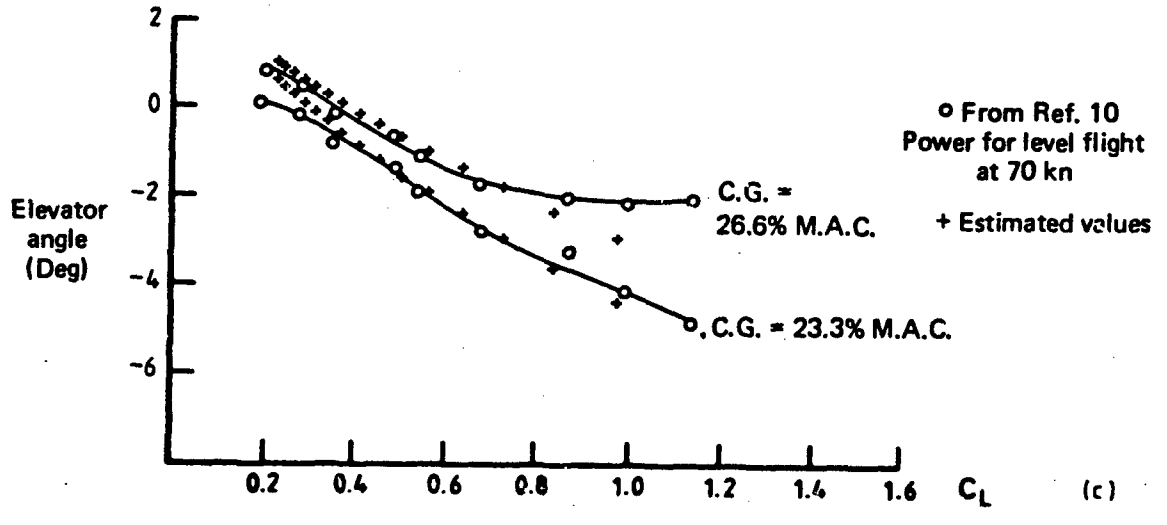
Elevator angle (Deg)
2
0
-2
-4
-6
0.2
0.4
0.6
0.8
1.0
1.2
1.4
1.6
C_L
o From Ref. 10 Power for level flight at 70 kn
+ Estimated values
C.G. = 26.6% M.A.C.
C.G. = 23.3% M.A.C.

(c)

Figures 46*a* and 47 show that the dynamic mode characteristics for the mid c.g. position are satisfactory for the typical layout with zero flap. Figure 46*b* shows that, with flaps deflected 20 deg., the low-speed instability (described above) varies such that, the divergent mode becomes more unstable as speed increases from 60 kn to 80 kn. This divergence disappears above 80 kn. The phugoid mode remains an oscillation throughout these changes, although it almost becomes a divergent oscillation at 90 kn.

Above 95 kn the short period frequency requirements are satisfactory, as shown in Figure 47. Below 85 kn the values have little meaning since the linear mode analysis is unrealistic, due to the large non-linear changes in aerodynamic characteristics at these speeds.

The task of investigating the accuracy of the estimated power effects from Reference 6 against flight measurements is not addressed in this study. However, since flight measurements are available for the aircraft shown in Figure 1, a comparison of estimated and measured trim curves is included in Figures 48*b* and 48*c*. While this limited comparison shows reasonable agreement, a far more comprehensive range of test conditions would be required to determine the accuracy of the estimated equations.

10. REVIEW OF RESEARCH ON THE EFFECTS OF POWER ON PROPELLER-DRIVEN AIRCRAFT

Because the propeller proved to be a key element in achieving the first power-driven flight in 1903, and is still used as the main method of producing thrust on low-speed aircraft, the effects of propellers on aircraft stability and control have been the topic of much research. During the 1930s and 1940s, engine horsepowers increased rapidly to meet the needs of small high-performance military aircraft and larger military and civil aircraft. At this time the effect of power on aircraft stability and control was a major area of research in the national research agencies of Germany, Britain and the USA. With the advent of the jet engine and of swept wings, the research emphasis rapidly moved away from propeller aircraft in the late 1940s and early 1950s. Research interest in propeller effects has only recently revived with the development of V/STOL aircraft and with developments in numerical analysis methods.

The fundamental purpose of the propeller is to provide thrust and considerable theoretical and experimental research was carried out at an early stage on the performance of propellers. However, a number of investigations concerning propeller characteristics other than thrust, also appeared in the technical literature at a relatively early date. Some remarkable flight measurements of slipstream dynamic head at the tail of an aircraft were made in 1917 [Ref. 18] and interesting calculations were made of the "Behaviour of the Slip-stream on a Phugoid Oscillation" in 1918 [Ref. 19], and on the influence of slipstream on the longitudinal damping derivatives in 1923 [Ref. 20]. As knowledge accumulated, it was realized that the net effect of power on aircraft stability and control was the result of a large number of individual effects which, in certain cases varied markedly with small changes in layout and configuration. As engine horsepower increased, the effect of power on aircraft handling became a major design consideration, and a desperate need arose for reliable design estimation methods. Although much research has been carried out and substantial progress has been made in particular areas, the need for reliable design estimation methods still exists today.

A purely theoretical attack on the problem was, and still is, impractical because of the complex nature of the phenomena involved and because of the large interference between different effects. The general approach taken in the past has been to combine a relatively crude elementary theoretical analysis of the important elements of the problem with empirial data obtained from experiment. This approach is typified by the important reports by Bryant and McMillan [Ref. 21] in 1938; Gates [Ref. 22], 1939; Millikan [Ref. 23], 1940; Falkner *et al.* [Ref. 24], 1941; and later by Weil and Steeman [Ref. 25], 1948 and Priestly [Ref. 26], 1953. The estimation methods adopted for use in Datcom [Ref. 6] and used in this study are similar to those used in Reference 25. A completely empirical approach was used by Morris and Morrall [Ref. 27] in 1953 but its applicability is restricted to a limited range of aircraft configurations. The developments throughout these reports were almost entirely in the updating of empirical data, based on the considerable amount of wind tunnel research that was being carried out. The elementary theoretical analysis remained virtually unaltered.

A theoretical treatment of the forces acting on a propeller inclined to the free-stream was made by Harris [Ref. 28] in 1918 and Glauert [Ref. 29] in 1919. Glauert's expression for propeller normal force was shown to give good agreement with measurements by Lesley [Ref. 30] in 1937 and was used in the methods presented by Millikan [Ref. 23]. Later, Ribner developed formulae for propeller side force coefficients based on the geometry of the propeller blades. The results are presented in charts in Reference 31 for different propeller designs and for different numbers of blades. These charts are used in the methods of Reference 25 and also in Datcom [Ref. 6]. Additional wind tunnel measurements on propeller normal force are given in Reference 11.

A theoretical treatment of the problem of the wing in the propeller slipstream is very difficult. An early classical treatment of the problem was published by Koning [Ref. 32] in 1935. However, this approach was considered to be too complicated for practical applications, particularly when extended to include large thrusts. An early attempt to provide a practical rule for design estimation was made by Bradfield [Ref. 33] in 1928 in which a method of calculating the increase in lift coefficient due to slipstream was proposed. An extension of the work of Reference 33 was made by Smelt and Davies [Ref. 12] in 1937 in which a more rigorous estimate of slipstream velocity was made and the effects of an inclined airscrew were determined. The resulting methods were used for the analysis of propeller power effects given in References 21, 23 and 26. In Reference 25 an approximation to the Smelt and Davies equations was used to simplify them. The calculation of slipstream velocity by Smelt and Davies is particularly interesting in that it shows that the flow equations of motion for the slipstream can be approximated such that Euler's equation is satisfied by a potential function which is in fact the slipstream pressure. The potential can be obtained by covering the surface of the propeller disc with doublets and the velocity distribution is obtained directly using Bernoulli's equation. This solution was presented previously by Koning in full in Reference 32 and has more general applications as shown in References 34 and 35. More recently, the development of computational aerodynamic methods and the development of powered lift STOL aircraft has attracted renewed interest in this area. Various approaches to the problem are being made (e.g. Refs. 36 and 37) including extensions of Koning's method (e.g. Refs. 38 and 39). These developments offer hope that satisfactory theoretical estimates of the effect of propeller slipstream on wing characteristics can be made for particular configurations including the presence of the fuselage.

As shown in Section 5 the largest changes in longitudinal stability due to power are generally those associated with the effects of power on downwash and dynamic head at the tail. These effects pose an extremely difficult theoretical problem and even the empirical methods which are adopted cannot be relied upon to give accurate results. A number of attempts have been made to establish empirical design formulae. In Reference 25, the results of wind tunnel tests on several models of single-engine fighter aircraft were analysed to give formulae for the prediction of downwash, stabilator effectiveness and elevator effectiveness with power. While the empirical formulae were shown to fit the test results with small variability, and reasonable accuracy was demonstrated in one application of the formulae, the general level of accuracy and range of applicability was not demonstrated. A similar approach had been adopted by Bradfield [Ref. 40] in 1939 covering a wide range of models. This information was augmented in 1950 by Spence [Ref. 41] with data from a range of more recent aircraft model tests. Spence concluded that

> "It is felt unlikely that any useful generalisation can be based on the present data. Further attempts at a mathematical attack are desirable; any future experimental work should be of a systematic nature."

A more systematic approach had been started by Hills and Kirk [Ref. 42] in 1941 but does not appear to have been continued. In the formulae developed in Reference 25, the propeller diameter and tail position were taken into account, but the exact locus and shape of the slipstream was not determined or used in the formulae. As discussed in Section 3, the prediction methods used in Datcom [Ref. 6] do take into account slipstream location, although the assumptions are made that the slipstream is circular with diameter equal to that of the propeller disc and that the effect on dynamic head decreases with distance from the slipstream centreline. The limited experimental data available in the research literature on slipstream profiles, for example Reference 18 from 1917 and References 43 and 44 from German tests in 1938 and Reference 21 in 1949, show that these assumptions are substantial simplifications. This is also clear from more recent, but less detailed, tests carried out on full-scale models of light single-engined aircraft models in the

Langley full-scale wind tunnel (e.g. Refs. 45, 58 and 59). These measurements show that downstream of the propeller, the slipstream shape becomes distorted, the dynamic pressure is markedly non-uniform and the slipstream location is displaced and modified by the presence of the wing and body. As a result, the lift on a tailplane situated behind propellers depends strongly on tailplane location. The prediction of the slipstream at the tailplane of an aircraft represents a complex computational problem which has yet to be tackled. The problem involves the interaction of the propeller flow with a number of lifting surfaces for a substantial distance downstream. The empirical design estimates of Reference 25 or Reference 6 give information on the mean effectiveness of the tailplane with slipstream, but this information is not sufficiently accurate to allow the determination of the optimum tailplane location; for this level of detail, powered wind tunnel tests are required for the particular design under consideration. Because the changes in downwash and dynamic head at the tail are generally the most dominant power effects, improved methods are needed for their estimation.

There is a considerable number of wind tunnel research reports of studies carried out by the NACA and RAE in the 1940s on powered models. Most of the models were of contemporary military aircraft, although some had more general characteristics. A small number of flight test reports on power effects also exists for the same period. This collection of reports provides a useful compendium of the effects of power and configuration on longitudinal stability. As previously mentioned, the knowledge obtained has far outstripped complementary theoretical methods of analysis. It is probable that aircraft manufacturers have a similar collection of wind tunnel and flight test information on propeller power effects and may have more reliable estimation methods for particular classes of aircraft. However, estimation methods with general application and good accuracy do not exist in the open literature.

A good summary of the effects of power in terms of aircraft flying qualities is provided by Phillips [Ref. 46], 1948. A discussion of some of the individual effects of power is contained in References 21, 23, 14, 24, 47 and 25. Reference 25, in particular, separates the power effects into components, a separation which is followed in this Report. References 48, 22, 26, 23 and 21 present extensions to the longitudinal stability equations to include power effects.

Comprehensive wind tunnel investigations on powered models of single-engined aircraft are reported in References 49, 50, 51 and 52. Reference 49 presents the contribution to aircraft neutral point (h_n) of individual power effects. Particular power effects are studied in the following reports.

Reference 53 deals with propeller normal force, Reference 47 deals with thrust setting angle, and in Reference 16 the effect of tail length with power is studied. In References 44, 45 and 60 consideration is given to the effects of power on the airflow at the tailplane, and rare plots of slipstream total head and flow direction are presented. References 54, 55, 56 and 57 present flight test measurements on the effects of power on longitudinal stability. References 55 and 57 give information on thrust setting angle and Reference 56 also gives some rare flight-measured data on slipstream total head and flow direction. More recently, a number of investigations (such as Refs. 58 and 59) have been carried out on full-scale models in the Langley full-scale wind tunnel. These reports provide useful information on the effects of power on the total aircraft, but they contain little information on the individual contributions to the net effects measured. Complementary to the references discussed, there is a similar list of research reports dealing with the effects of power on lateral and directional aircraft characteristics. In many cases the same models have been used for both areas of investigation.

11. CONCLUSIONS

A survey has been made of research literature on the effects of power on the longitudinal flying qualities of propeller-driven aircraft. From this survey, the status and source of current design estimation methods were identified. This design information was used to calculate and illustrate the effects of power, of aircraft layout, and of configuration on longitudinal flying qualities. As a result of the study the following conclusions were reached:

- The most complete set of design estimation methods currently available in the published literature for the prediction of power effects on conventional low-speed aircraft is contained in Datcom [Ref. 6].

- These methods are almost entirely empirical and mostly represent the status of design information available in the 1940s.
- In certain areas, such as the effect of slipstream on wing lift, numerical solutions are being developed which offer the prospect of improved accuracy.
- The net effect of power is developed as a resultant of six major contributions which vary in character from those which are predominantly incidence-dependent to those which are predominantly speed-dependent. These effects can be non-linear and are not necessarily independent.
- It is shown in the Report that the effect on stability of the incidence-dependent terms is conveniently described by the neutral point (h_n), while the combined incidence- and speed-dependent terms can be described by the static stability limit (h_s) as proposed by Etkin in Reference 1.
- Some power effects are relatively independent of aircraft layout, while others are particularly sensitive to it, such that the net effects can be very large for one aircraft and small for another.
- For the "standard case" aircraft layout considered in the study, in which the thrust axis, the wing, and the tailplane are at the same height, the majority of power effects are destabilising and increased with decreasing speed.
- The largest power effects are those associated with downwash and with dynamic head at the tailplane and these can change significantly when flaps are deflected. Consequently the location of the tailplane with respect to the slipstream stands out as an important design parameter.
- The substantial effect of wing height on stability, both with power off and power on has been demonstrated, to emphasize its important influence.
- It is shown that the design technique of inclining the thrust axis to provide a nose-down thrust moment arm produces an increase in stability which is primarily a speed effect. This technique is similar to the use of a downspring in the control circuit, in that the "static stability" can be increased while "manoeuvrability" and short period response remain unaltered.
- In general, increasing tail arm, with either fixed $\bar{V}$ or fixed tail area, increases power-off stability. With power on, this increase was not sustained at low speeds for the "standard case" aircraft layout, due to emergence of the tailplane from the slipstream.
- Deflecting the flaps is shown to make substantial changes to individual power effects. For the "standard case" layout considered, the net effects of power with flaps deflected 20 deg. are little different in magnitude from the zero flaps configuration, but the composition of these effects differs considerably.
- Power effects are also demonstrated for an aircraft layout typical of modern designs, having the wing and tailplane located respectively below and above the thrust line. Calculations show that the layout results in improved stability characteristics with zero flaps compared with the "standard case", due to a more favourable effect of dynamic head at the tailplane. With flaps 20 deg., a flight condition was demonstrated in which the combination of power and flaps produces an instability which is almost independent of c.g. position. A further study is proposed on this topic.
- It is shown that the c.g. range may be limited by control force per g requirements if the power effects are large. This limitation arises if the variation of the neutral point (h_n) with speed and configuration is large and can be exacerbated if the difference between h_s and h_n is also large.
- In general the effects of power on "static stability" and "manoeuvrability" are also reflected in the longitudinal response characteristics. However, a situation has been demonstrated in which the longitudinal response would be unacceptable even though the aircraft is stable.
- The literature review is summarised at the end of the Report. This review shows that a large amount of wind tunnel research has been carried out on propeller power effects from the early days of powered flight. The results are characterised by their diversity, and attempts to find a basis for correlating the results from different configurations have had limited success. This experience highlights the limitations of general empirical design methods and emphasises the need for more robust theoretical and numerical analysis methods. In addition, there is a need for more comprehensive test data. Both the calculations in this Report and the research literature show that the effect of slipstream on tailplane lift is one of the largest and also most sensitive power effects. Unfortunately this is an area in which there is a paucity of design information. The literature contains few examples of comprehensive wind tunnel measurements of the slipstream characteristics at the tailplane and little work has

been done on relating these measurements to tailplane lift. Similarly, while some flight measurements have been made to determine the effects of power, these have not been sufficiently detailed to allow individual effects to be identified nor has a thorough correlation with wind tunnel results been made.

Finally, it is concluded from the information presented in this Report and from the survey of research literature that the quality of the design information available for predicting the effects of power on highly-powered propeller-driven aircraft is deficient compared with the methods used in other areas of aerodynamic design.

REFERENCES

1. Etkin, B. E.: *Dynamics of Aerodynamic Flight*. John Wiley and Sons Inc., 1972.
2. Bryan, G. H.: *Stability in Aviation*. Macmillan, 1911.
3. Gates, S. B., and Lyon, H. M.: "A Continuation of Longitudinal Stability and Control Analysis. Part I—General Theory." R & M 2027, 1944.
4. Anon.: "Flying Qualities of Piloted Airplanes." MIL-F-8785C, November 1980.
5. Gates, S. B., and Lyon, H. M.: "A Continuation of Longitudinal Stability and Control Analysis. Part II—Interpretation of Flight Control." R & M 2028, 1944.
6. Hoak, D. F. (Project Engineer): "U.S.A.F. Stability and Control Datcom." Flight Control Division, AFFDL, Wright-Patterson AFB, June 1977 (Revision).
7. Haines, A. B., MacDougall, M. A., and Monaghan, B. A.: "Charts for the Determination of the Performance of a Propeller Under Static, Take-Off, Climbing and Cruising Conditions." R & M 2086, March 1946.
8. Fletcher, C. A. J.: "'POWITT'- A Program for Solving Non-Linear Algebraic Equations." WRE-TN-1431 (WR & D), June 1975.
9. Anon.: "Competition Aerobatic Aircraft Specification." Flight Invert Ltd., Cranfield Institute of Technology, June 1976.
10. Martin, C. A., and Ward, R. E.: "Cranfield A1. The First Fifty Flights." C. of A. Memo 7703, Cranfield Institute of Technology, April 1977.
11. Walker, N. K., and Levack, I.: "Wind Tunnel Measurements of the Forces of Inclined Propellers." RAE Report Aero 2024, 1945.
12. Hills, R. and Kirk, F. N.: "Note on the Effect of Slipstream on the Downwash Angle Behind a High Lift Wing." RAE Report No. B.A. 1671, May 1941.
13. Smelt, B. A., and Davies, H.: "Estimation of Increase in Lift Due to Slipstream." R & M 788, February 1937.
14. Francis, R. M., and Pringle, G. E.: "Notes on Longitudinal Stability at Low Speeds." R & M 1833, 1938.
15. Wimpenny, J. C.: "Stability and Control in Aircraft Design." *Journal of the Royal Aeronautical Society* 58, May 1954.
16. Johnson, H. S.: "Wind Tunnel Investigation of Effects of Tail Length on the Longitudinal Stability Characteristics of a Single-Engine Low-Wing Airplane Model." NACA TN No. 1766, 1948.
17. Phillips, W. H.: "An Investigation of Additional Requirements for Satisfactory Elevator Control Characteristics." NACA TN No. 1060, June 1946.
18. Anon.: "Exploration of the Airspeed in the Airscrew Slipstream of a Tractor Machine." R & M 438, 1917.
19. Anon.: "Behaviour of the Slipstream on a Phugoid Oscillation." R & M 464, July 1918.
20. Simmons, L. F. G., and Ower, E.: "An Investigation of the Influence of Downwash on the Rotary Derivative Mq. Part II—The Effect of the Airscrew Slipstream." R & M 883, 1923.

21. Bryant, L. W., and McMillan, G. A.: "The Longitudinal Stability of a Twin-Engined Monoplane with Airscrews Running." R & M 2310, 1949.

22. Gates, S. B.: "An Analysis of Static Longitudinal Stability in Relation to Trim and Control Force." R & M 2132, 1939.

23. Millikan, C. B.: "The Influence of Running Propellers on Airplane Characteristics." *Journal of the Aeronautical Sciences* 7, No. 3, January 1940.

24. Falkner, V. M., Nixon, H. L., and Sweeting, N. E.: "An Experimental Investigation of the Effect of Airscrews on the Longitudinal Stability of a Twin Engined Monoplane." Aero Dept NPL, A.R.C. Rep. No. 5026, R & M 2070, March 1941.

25. Weil, J., and Sleeman, C.: "Prediction of the Effects of Propeller Operation on the Static Longitudinal Stability of Single Engine Tractor Monoplanes with Flaps Retracted." NACA TN 1722, October 1948.

26. Priesty, E. A General Treatment of Static Longtitudinal Stability with Propellers, with Application to Single-Engined Aircraft. R & M 2732. 1953.

27. Morris, D. E., and Morrall, J. C.: "The Effect of Slipstream on the Longitudinal Stability of Multi-Engined Aircraft." R & M 2701, 1953.

28. Harris, R. G.: "Forces on a Propeller Due to Sideslip." R & M 427, February 1918.

29. Glauert, H.: "Stability Derivatives of an Airscrew." R & M 642, October 1919.

30. Lesley, E. P., Worley, G. F., and Moy, S.: "Air Propellers in Yaw." NACA Tech. Rep. 597, 1937.

31. Ribner, H. S.: "Notes on the Propeller and Slipstream in Relation to Stability." NACA ARR No. L4I12a, 1944.

32. Koning, C.: "Influence of the Propeller on Other Parts of the Airplane." *Aerodynamic Theory*, Vol. IV. Edited by W. F. Durand. 1963.

33. Bradfield, F. B.: "Preliminary Tests on the Effects on the Lift of a Wing of the Position of the Airscrews Relative to It." R & M 1212, 1928.

34. Riemann-Webes.: *Differential Gleichungen Dep Physik*, Vol. 1, Chapter XIV. Braunschweig 1925.

35. Abrahams Becker: *Cl. sical Electricity and Magnetism.*

36. Lan, C. E.: "A Quasi-Vortex-Lattice Method in Thin Wing Theory." *Journal of Aircraft* **11**, No. 9, September 1974.

37. Kleinstein, G. and Liu, C. H.: "Application of Airfoil Theory for Non-Uniform Streams to Wing–Propeller Interaction." *Journal of Aircraft* **9**, No. 2, February 1972.

38. Shollenberger, C. A.: "Three Dimensional Wing/Jet Interaction Analysis Including Jet Distortion Influences." *Journal of Aircraft* **12**, 706–13, September 1975.

39. Squire, M. A., and Chester, W.: "Calculation of the Effect of Slipstream on Lift and Induced Drag." R & M 2668, 1950.

40. Bradfield, F. B.: "Slipstream Effect on the Downwash and Velocity at the Tailplane." R & M 1488, 1932.

41. Spence, A.: "Effect of Propeller Thrust on Downwash and Velocity at Tailplane." ARC CP, 21, 1950.

42. Hills, R. and Kirk, F. N.: "Note on the Effect of Slipstream on the Downwash Angle Behind a High Lift Wing." RAE Rept. No. BA 1671, May 1941.

43. Stuper, J.: "Effect of Propeller Slipstream on Wing and Tail." NACA Tech. Memo. No. 874, 1938.

44. Muttray: "Investigations on the Downwash Behind a Tapered Wing with Fuselage and Propeller." NACA TM 876, 1938.

45. Shivers, J. P., Fink, M. P., and Ware, G. M.: "Full Scale Wind Tunnel Investigation of the Static Longitudinal and Lateral Characteristics of a Light Single-Engine Low Wing Airplane." NASA TN D-5857, 1970.

46. Phillips, W. H.: "Appreciation and Prediction of Flying Qualities." NACA TN 1670, 1948.

47. Goett, H. J., and Delany, N. K.: "Effect of Tilt of the Propeller Axis on the Longitudinal Stability. Characteristics of Single Engine Airplanes." NACA Rep. No. 744, 1944.

48. Donlan, C. J.: "Some Theoretical Considerations of Longitudinal Stability in Power-On Flight with Special Reference to Wind Tunnel Testing." NACA ARR AA/12/8, 1942.

49. Harper, C. W., and Bradford, H. W.: "A Comparison of the Effects of Four-Blade Dual- and Single-Rotation Propellers on the Stability and Control Characteristics of a High Powered Single-Engine Airplane." NACA WR ARR 4F17, 1944.

50. Hagerman, J. R.: "Wind Tunnel Investigation of the Effects of Power and Flaps on the Static Longitudinal Stability and Control Characteristics of a Single-Engine High-Wing Airplane Model." NACA TN No. 1339, July 1947.

51. Wallace, A., Rossi, P. F., and Wells, E. G.: "Wind Tunnel Investigations of the Effects of Power and Flaps on the Static Longitudinal Stability Characteristics of a Single-Engine Low-Wing Airplane Model." NACA TN No. 1239, 1947.

52. Lees, J. H., and Davies, H.: "Wind Tunnel Tests on the Effects of Extreme Slipstream on Single and Twin-Engined Monoplanes with Split or Slotted Flaps." R & M 1797, 1937.

53. Hufton, P. A.: "The Effect of the Lift Component of the Propeller on the Stability of the Spitfire." RAE Tech. Note No. Aero 991, 1942.

54. White, M. D.: "Effect of Power on the Stick-Fixed Neutral Points of Several Single Engine Monoplanes as Determined in Flight." NACA WR. C.B. L4H01, 1944.

55. Goranson, R. F.: "Flight Tests of an SB2C-3 Airplane with a Production and Tilted Propeller Axis." NACA WR MR No. L5E19A, 1945.

56. Steisz, W.: "Effect of the Direction of Rotation of the Airscrews on the Longitudinal Stability of Twin-Engined Aircraft." Air Ministry Translation No. 853, 1938.

57. Rathert, G. A.: "Flight Investigation of the Effects on Airplane Static Longitudinal Stability of a Bungee and Engine Tilt Modification." NACA TN 1260, May 1947.

58, Fink, M. P., Freeman, D. C., and Greer, H. D.: "Full-Scale Wind Tunnel Investigation of the Longitudinal and Lateral Characteristics of a Light Single-Engine Airplane." NASA TN D-5700, March 1970.

59. Greer, H. D., Shivers, J. P., and Fink, M. P.: "Wind Tunnel Investigation of Static Longitudinal and Lateral Characteristics of a Full-Scale Mockup of a Light Single-Engine High Wing Airplane." NASA TN D-7149, 1973.

60. Katzoff, S.: "Longitudinal Stability and Control with Special Reference to Slipstream Effects." NACA Report 690, 1940.

DISTRIBUTION

AUSTRALIA

DEPARTMENT OF DEFENCE

Central Office

Chief Defence Scientist
Deputy Chief Defence Scientist
Superintendent, Science and Technology Programmes
Controller, Projects and Analytical Studies
} (1 copy)

Defence Science Representative (UK) (Doc. Data sheet only)
Counsellor, Defence Science (USA) (Doc. Data sheet only)
Defence Central Library
Document Exchange Centre, DISB (17 copies)
Joint Intelligence Organisation
Librarian H Block, Victoria Barracks, Melbourne
Director-General—Army Development (NSO) (4 copies)
Defence Industry and Material Policy, FAS

Navy Office

Navy Scientific Adviser
RAN Aircraft Maintenance and Flight Trials Unit
Directorate of Naval Aircraft Engineering
Directorate of Naval Aviation Policy

Army Office

Army Scientific Adviser
Engineering Development Establishment, Library
Royal Military College, Library
US Army Research, Development and Standardisation Group

Air Force Office

Air Force Scientific Adviser
Aircraft Research and Development Unit
    Scientific Flight Group
    Library
Technical Division Library
Director-General Aircraft Engineering—Air Force
Director-General Operational Requirements—Air Force
HQ Operational Command (SMAINTSG)
HQ Support Command (SENGSO)
RAAF Academy, Point Cook

Central Studies Establishment

Information Centre

DEPARTMENT OF DEFENCE SUPPORT

Aeronautical Research Laboratories

Director
Library
Superintendent—Aerodynamics
Divisional File—Aerodynamics

Author: C. A. Martin
D. A. Secomb
R. A. Feik
J. S. Drobik
B. G. Gunn

Materials Research Laboratories
Director/Library

Defence Research Centre
Library

RAN Research Laboratory
Library

Government Aircraft Factories
Manager
Library
Mr. P. Hughes
Mr. D. Pilkington

DEPARTMENT OF AVIATION
Library
Flying Operations and Airworthiness Division

STATUTORY AND STATE AUTHORITIES AND INDUSTRY
Trans-Australia Airlines, Library
Qantas Airways Limited
SEC of Victoria, Herman Research Laboratory, Library
Ansett Airlines of Australia, Library
Commonwealth Aircraft Corporation
Library
Mr. J. Caterson
Hawker de Havilland Aust. Pty. Ltd., Bankstown, Library
Rolls-Royce of Australia Pty. Ltd., Mr. C. G. A. Bailey
Australian Aircraft Consortium, General Manager

UNIVERSITIES AND COLLEGES

Adelaide	Barr Smith Library
	Professor of Mechanical Engineering
Flinders	Library
Latrobe	Library
Melbourne	Engineering Library
Monash	Hargrave Library
Newcastle	Library
Sydney	Engineering Library
New South Wales	Physical Sciences Library
	Professor R. A. A. Bryant, Mechanical Engineering
Queensland	Library
Tasmania	Engineering Library
Western Australia	Library
	Associate Professor J. A. Cole, Mechanical Engineering
RMIT	Library
	Mr. E. Stokes, Civil and Aeronautical Engineering

CANADA

International Civil Aviation Organization, Library
Canadair Limited, Mr. R. E. Ward
NRC
Aeronautical and Mechanical Engineering, Library
Division of Mechanical Engineering, Director

Universities

Toronto — Institute for Aerospace Studies

FRANCE

ONERA, Library

GERMANY

Fachinformationszentrum: Energie, Physik, Mathematik GmbH
DFVLR (Braunschweig)

INDIA

Defence Ministry, Aero Development Establishment, Library
Gas Turbine Research Establishment, Director
Hindustan Aeronautics Ltd., Library
National Aeronautical Laboratory, Information Centre

ISRAEL

Technion-Israel Institute of Technology, Professor J. Singer

ITALY

Ing. Guilio Cesare Valdonio, Aermacchi
Professor Ing. Guiseppe Gabrielli

JAPAN

Institute of Space and Astronautical Science, Library

NETHERLANDS

National Aerospace Laboratory (NLR), Library

Universities

Delft University of Technology — Library
Mr. J. A. Mulder

NEW ZEALAND

Defence Scientific Establishment, Library
Transport Ministry, Airworthiness Branch, Library
RNZAF, Vice-Consul (Defence Liaison)

Universities

Canterbury — Library
Professor D. Stevenson, Mechanical Engineering

SWEDEN

Aeronautical Research Institute, Library
Swedish National Defense Research Institute (FOA)

SWITZERLAND

Armament Technology and Procurement Group
F+W (Swiss Federal Aircraft Factory)

UNITED KINGDOM

CAARC, Secretary (NPL)
Royal Aircraft Establishment
Bedford, Library
Commonwealth Air Transport Council Secretariat
Civil Aviation Authority, Mr. Darrol Stinton
National Gas Turbine Establishment
Director, Pyestock North
British Library, Lending Division
CAARC Co-ordinator, Structures
Aircraft Research Association, Library
GEC Gas Turbines Ltd., Managing Director
Rolls-Royce Ltd.
Aero Division Bristol, Library
British Aerospace
Warton Division, Library
Hatfield—Chester Division, Library
Kingston—Brough Division, Library
British Hovercraft Corporation Ltd., Library
Short Brothers Ltd., Technical Library

Universities and Colleges

Bristol	Engineering Library
Cambridge	Library, Engineering Department
	Whittle Library
London	Professor G. J. Hancock, Aero Engineering
Manchester	Professor, Applied Mathematics
	Professor N. Johannesen, Fluid Mechanics
Nottingham	Science Library
Southampton	Library
Liverpool	Fluid Mechanics Division, Dr. J. C. Gibbings
Strathclyde	Library
Cranfield Inst. of Technology	Library
Imperial College	Aeronautics Library

UNITED STATES OF AMERICA

NASA Scientific and Technical Information Facility
Applied Mechanics Reviews
Beech Aircraft Corp., VP Research and Development
Cessna Aircraft Company, Chief Engineer
Lockheed—California Company
McDonnell Aircraft Company, Library
Piper Aircraft Corp., Director of Engineering
Systems Technology Inc., Mr. I. J. Ashkenas
Air Force Flight Dynamics Laboratory, Mr. J. E. Jenkins

Universties and Colleges

Johns Hopkins	Professor S. Corrsin, Engineering
Princeton	Professor G. L. Mellor. Mechanics
Massachusetts Inst. of Technology	MIT Libraries
George Washington	Joint Institute for Advancement of Flight Studies, Dr. V. Klein

Spares (20 copies)

Total (175 copies)

Department of Defence

DOCUMENT CONTROL DATA

1. a. AR No.	1. b. Establishment No.	2. Document Date	3. Task No.
AR-002-925	ARL-AERO-REPORT-157	February 1983	DST 82/030

4. Title
POWER EFFECTS ON THE LONGITUDINAL CHARACTERISTICS OF SINGLE-ENGINE PROPELLER-DRIVEN AIRCRAFT

5. Security
a. document: Unclassified
b. title: U. c. abstract: U.

6. No. Pages
44

7. No. Refs
60

8. Author(s)
C. A. Martin

9. Downgrading Instructions
—

10. Corporate Author and Address
Aeronautical Research Laboratories,

P.O. Box 4331, MELBOURNE, Vic. 3001.

11. Authority (as appropriate)
a. Sponsor c. Downgrading
b. Security d. Approval
—

12. Secondary Distribution (of this document)
Approved for public release.

Overseas enquirers outside stated limitations should be referred through ASDIS, Defence Information Services, Branch, Department of Defence, Campbell Park, CANBERRA, ACT 2601.

13. a. This document may be ANNOUNCED in catalogues and awareness services available to . . .
No limitations

13. b. Citation for other purposes (i.e. casual announcement) may be (select) unrestricted (as for 13a.

14. Descriptors

Propellers	Longitudinal stability
Aircraft engines	Aircraft engine power
Flight characteristics	Flying qualities

15. COSATI Group
0103

16. Abstract
The effects of power on the longitudinal flying qualities of a single-engine propeller-driven aircraft have been investigated. The net effect is developed as the resultant of six major contributions which, in this study, have been estimated from the USAF Stability and Control Datcom. These contributions are not independent and in general are non-linear functions of both incidence and speed. It is shown that the effect on stability of the incidence-dependent terms is conveniently described by the neutral point (h_n) while the combined incidence and speed terms can be described by the static stability limit (h_s). The effects of each power contribution on the longitudinal static and dynamic characteristics of a basic aircraft layout, termed the "standard case" have been illustrated both individually and collectively. The influence of aircraft layout and configuration has also been demonstrated with both power-off and power-on. It is shown that net power effects are sensitive to aircraft layout and can change appreciably when flaps are deflected. An instability is demonstrated which is due to power and flap effects and which is almost

This page is to be used to record information which is required by the Establishment for its own use but which will not be added to the DISTIS data base unless specifically requested.

16. Abstract (Contd)

independent of c.g. position. The power effects for an aircraft layout typical of modern designs are also illustrated. The study is completed by a survey of research on propeller power effects which draws attention to the large amount of wind tunnel research which has been carried out from the early days of powered flight. The sources of many of the estimation methods in Datcom are identified and discussed. From the survey and from the information presented in this Report it is concluded that there exists a need for more robust theoretical and numerical design methods for most of the power effects considered and also for more comprehensive wind tunnel and flight test data regarding the effect of slipstream on tailplane lift.

17. Imprint

Aeronautical Research Laboratories, Melbourne

18. Document Series and Number	19. Cost Code	20. Type of Report and Period Covered
Aerodynamics Report 157	52 7730	—

21. Computer Programs Used

—

22. Establishment File Ref(s)

—